ALMA MATER STUDIORUM
UNIVERSITÀ DI BOLOGNA

DOTTORATO DI RICERCA IN

SCIENZE DELLA TERRA, DELLA VITA E DELL'AMBIENTE

Ciclo 37

Settore Concorsuale: 04/A3 - GEOLOGIA APPLICATA, GEOGRAFIA FISICA E GEOMORFOLOGIA

Settore Scientifico Disciplinare: GEO/05 - GEOLOGIA APPLICATA

QUANTIFYING THE EFFECTS OF GLOBAL WARMING ON SPRING DISCHARGE AND ASSESSING FUTURE DISCHARGE TRENDS ALONG THE APENNINES (ITALY)

Presentata da: Tommaso Casati

Coordinatore Dottorato

Barbara Cavalazzi

Supervisore

Alessandro Gargini

Co-supervisori

Antonio Navarra

Maria Filippini

Esame finale anno 2025

Abstract

Global warming affects atmospheric and oceanic energy budgets, modifying the Earth's water cycle. Groundwater is the primary component of fresh water within the planet's hydrosphere, and it represents a vital and accessible resource, serving ecological, environmental, and societal needs. In countries where springs are a predominant water source, such as Italy, their protection, along with the assessment of their resilience to climate-induced changes in recharge, is crucial for ensuring water supply and preserving ecosystems. The Mediterranean region is a climate change hotspot, already experiencing a decline in recharge and an increase in the frequency and severity of droughts. Along the Apennine chain (Italy), situated at the heart of the Mediterranean region, significant climate impacts have been observed over the past few decades. It thus becomes important to estimate discharge scenarios to support water companies by providing sufficient time to plan and implement mitigation measures to address forthcoming water crises.

This PhD project presents a century-long analysis of discharge patterns from key springs located along the Apennines, aiming to quantify the long-term effects of climate change and forecast future scenarios. The study employed multiple approaches, tailored to the nature of the data, and focused on a select number of springs chosen based on the availability of long-term hydrological discharge records extending back at least 60 years.

The first approach involved a combination of experimental and historical analyses to evaluate the long-term effects of climate change on the flow rate of Nadìa Spring (Northern Apennines), which discharges from a fractured calcarenitic aquifer, as well as its resilience to such changes. The spring demonstrated an exceptional capacity to sustain base flow even during prolonged drought periods. Such resilience was attributed to a combination of factors, including a large groundwater reservoir, a network of faults and fractures, and karst dissolution processes. The second approach employed a multiregression analysis to investigate the relationship between recharge-related parameters and the discharge of Sanità Spring (Southern Apennines, karst aquifer) and Ermicciolo Spring (Amiata Mountain, volcanic aquifer), aiming to forecast long-term spring flow for the period 2040-2070. Projected meteorological scenarios from a Regional Circulation Model were used alongside the regression coefficients to estimate discharge trends. Finally, the third approach applied a machine learning method, Long Short-Term Memory, to the same springs, Sanità and Ermicciolo, to predict discharge over both short- and long-term futures. In addition to these three springs, which were the primary focus of the analyses, four other springs were also investigated, with particular attention given to the effects of climate change on their flow rates over multi-decadal timescales.

The methodological approaches adopted in this PhD thesis, together with the results, provide a quantitative rather than merely descriptive understanding of the relationship between climate drivers and spring flow rate. Furthermore, they enable the projection of discharge scenarios and the subsequent evaluation of future groundwater availability along the Apennines.

Contents

Chapter 1:

Introduction

1.1. Preface

This PhD thesis derives from an interdisciplinary collaboration between hydrogeology and atmospheric physics, supported scientifically by Professor Antonio Navarra, President of the Euro-Mediterranean Center on Climate Change (CMCC). This collaboration has been essential in linking the study of spring discharge dynamics with past and future climate trends. Furthermore, the PhD project is part of the PON programme, which emphasises technology transfer to benefit stakeholders. In this context, the research is primarily supported by Acquedotto Pugliese S.p.A., the main stakeholder of the project and the largest water utility company in Italy, where the candidate also undertook a period of internship.

The present chapter introduces the primary topics addressed throughout this PhD project. Firstly, an overview of the globally changing climate, particularly in the Mediterranean area, will be presented in Section 1.2, with emphasis on its impact on the groundwater component of the hydrosphere (Section 1.2.1). This discussion will delve into specific issues, focusing in detail on droughts and spring discharge along the Apennines (Section 1.2.2).
Next, Section 1.3 will provide insights into the springs analysed during this PhD research, focusing on their geological and hydrogeological settings (Section 1.3.1), as well as the rationale behind their selection compared to other springs initially considered for analysis (Section 1.3.2). Subsequently, the broader implications of negative projections and their societal impacts for the investigated areas along the Apennines are discussed in Section 1.3.3.
Lastly, Section 1.4 outlines the fundamental scientific questions underpinning this PhD project, followed by a comprehensive overview of the thesis structure, serving as a brief guide to the subsequent chapters.

1.2. Global warming

Until the early 1800s, humanity was unaware of the role the atmosphere played in making the planet habitable. The first to formulate hypotheses on this matter was the French natural philosopher Joseph Fourier in the 1820s. Fourier (1824) wondered why the Earth, which should have been much colder given its distance from the Sun, had temperatures capable of supporting life. He proposed several hypotheses, including the idea that the Earth's atmosphere might trap a portion of solar radiation, for unknown reasons, thereby increasing the planet's temperature. In a reprint of his 1824 work, Fourier (1827) compared the effect of the Earth's atmosphere to that of 'a pane of glass covering a bowl', making this the first hypothesis of what we now call the greenhouse effect.

The fundamental relationship between carbon dioxide and climate was first understood and explained several decades later by a Swedish chemist, Svante Arrhenius (1896), who demonstrated that global temperature changes as a function of increasing CO_2 levels. At that time, there were no instruments capable of measuring the amount of carbon dioxide in Earth's atmosphere, but Arrhenius estimated that if CO_2 level had increased to double that present at the time, the Earth's temperature would have risen drastically.

Nowadays, it is widely acknowledged that global warming is having an increasing impact on our planet. One of the main scientific priorities today is to predict global and regional climate changes associated with global warming (Navarra and Philander, 2016), which is driven by the rapid, human-induced rise in emissions of carbon dioxide, other greenhouse gases (GHGs), and aerosols, along with changes in land use. The governments of the world, in 1988, have thus established the Intergovernmental Panel on Climate Change (IPCC) to evaluate periodically the available scientific and technical data, and to coordinate the research efforts of scientific teams working on this issue. In other words, it was determined that the United Nations body would be responsible for assessing the effects of climate change. In its Sixth Assessment Report (AR6), the IPCC (2023) concluded that human activities, primarily through GHG emissions, have unequivocally caused global warming, with global surface temperatures rising to 1.1 °C above 1850-1900 levels during the period 2011-2020. Since then, global GHG emissions have continued to rise steadily, significantly impacting the atmospheric water and energy budgets, and they are projected to continue doing so in the future. The rising frequency, intensity, and/or duration of droughts and heat stress linked to climate change (Allen et al., 2010) might profoundly reshape the biosphere and hydrosphere in numerous regions.

Heatwaves, extreme precipitation, droughts, and floods are among the most common extreme events posing risks and causing damage to society. The majority of these events are linked to two parameters: air temperature and precipitation (Scoccimarro and Navarra, 2022). Alexander et al.

(2006) conducted a study on global changes in daily extremes of temperature and precipitation, which revealed over 70% of the globally surveyed land area has shown a significant decrease in the annual occurrence of cold days and nights (defined as when temperatures fall below the long-term 10th percentile), alongside a significant increase in warm ones (when temperatures exceed the long-term 90th percentile; Fig. 1.1).

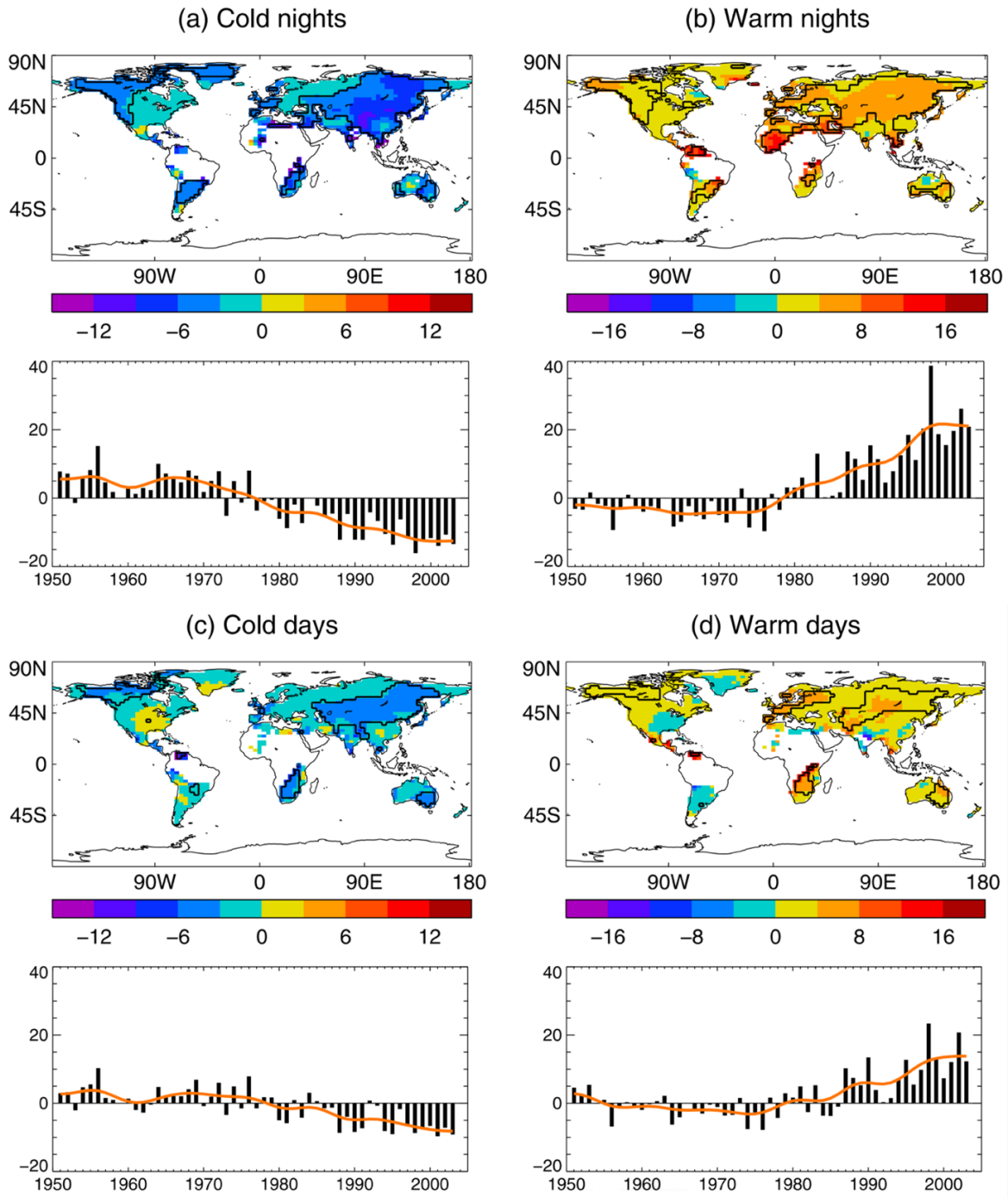

Fig. 1.1. Trends (in days per decade, shown as maps) and annual time series anomalies relative to 1961-1990 mean values (shown as plots) for annual series of percentile temperature for 1951-2003 for (a) cold nights, (b) warm nights, (c) cold days, and (d) warm days. Trends were calculated only for the grid boxes with sufficient data (at least 40 yr of data and the last year is no earlier than 1999) (Alexander et al., 2006).

Mediterranean-type climates (Csa and Csb, Fig. 1.2) according to the Köppen-Geiger classification (Kottek et al., 2006) are among the areas of the planet most exposed to droughts. These climates, classified as warm temperate, are characterised by dry summers and mild, rainy winters. In the Mediterranean region, the sea plays a crucial role in shaping the climate, since it absorbs heat during the summer and gradually releases it throughout the winter months.

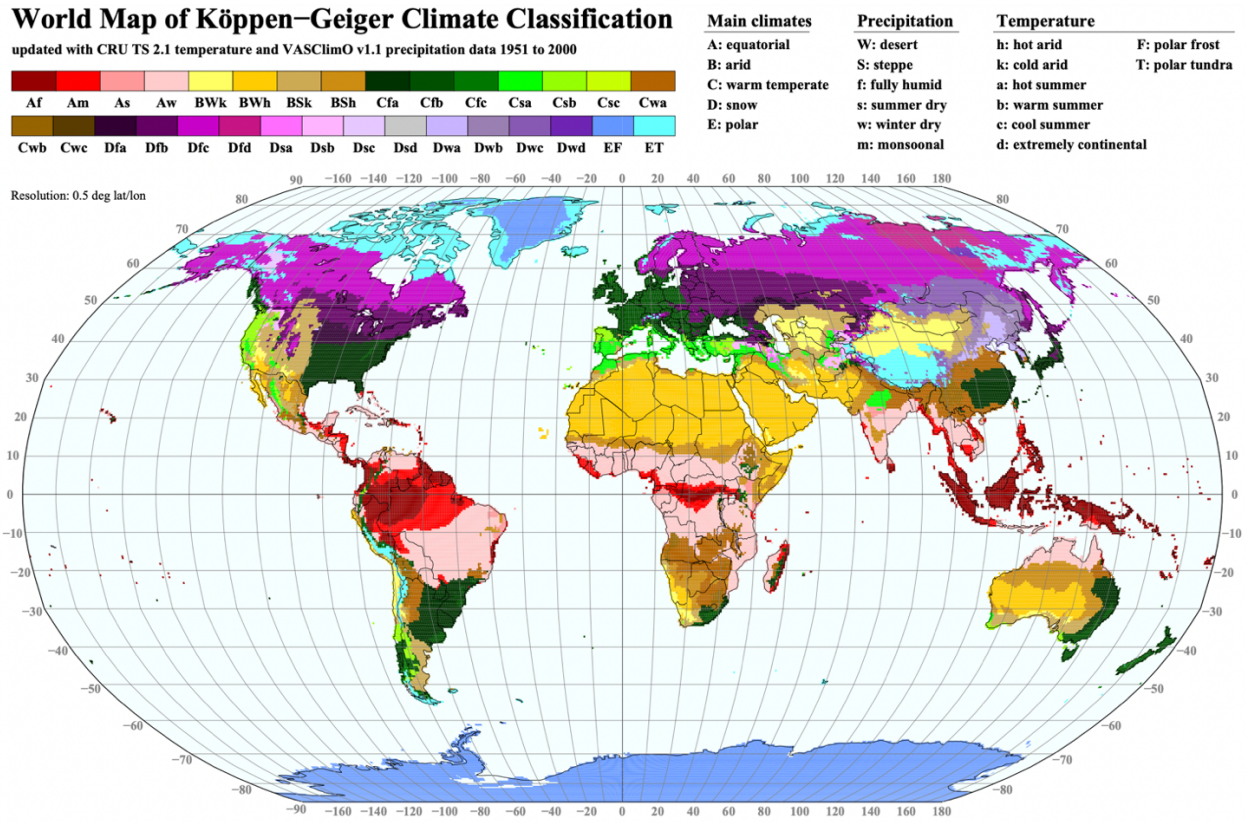

Fig. 1.2. World Map of Köppen-Geiger climate classification updated with mean monthly temperature and precipitation data for 1951-2000 on a regular 0.5-degree latitude/longitude grid (Kottek et al., 2006).

In addition to the classic Mediterranean region, which extends between Southern Europe (including Anatolia and the Near East) and the northwestern coast of Africa, the Csa and Csb type climate can also be found along the western coast of the United States (Scanlon et al., 2012), in central Chile (Garreaud et al., 2017), at the southern tip of South Africa (Blake et al., 2010), and along the southwestern coast of Australia (Alilou et al., 2022) (Fig. 1.2). These climatic zones are located slightly north or south of the Tropics. This geographical location is the reason why Mediterranean-type climates are often recognized as subtropical (Troll and Paffen, 1963). Mediterranean climate zones are ranked among the regions of the globe most affected by global warming (Van Loon et al., 2014).

In particular, the Mediterranean region is considered a highly critical zone for climate change due to a significant decrease in recharge and an increase in the frequency and severity of droughts over the last two to three decades. The Regional Climate Change Index (RCCI), developed by

Giorgi (2006), indicates that the Mediterranean and Northeastern European regions emerge as the primary Hot-Spots (Fig. 1.3), followed by high latitude northern hemisphere regions and by Central America.

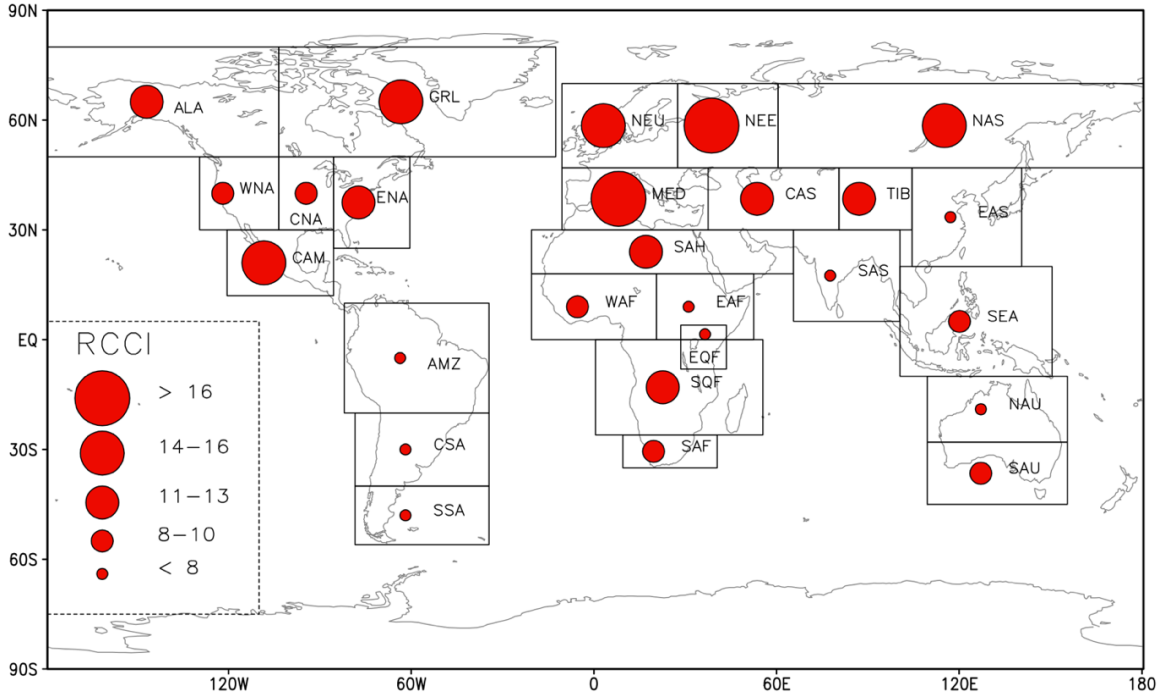

Fig. 1.3. Regional Climate Change Index over 26 land regions of the World calculated from 20 coupled Atmosphere/Ocean General Circulation Models (AOGCMs) and 3 IPCC emission scenarios (Giorgi, 2006).

Future climate projections for the Mediterranean region (Giorgi and Lionello, 2008) indicate a significant reduction in precipitation, particularly during the summer season, except for northern Mediterranean areas (e.g., the Alps) during winter, and a marked warming, peaking always in the summer months. Inter-annual variability is expected to increase, especially in summer, which, combined with the overall warming, would result in a higher frequency of extreme heat events. The strength and consistency of the climate change signals produced also by more recent climate models (Essa et al., 2023; Mirgol et al., 2024) confirm that the Mediterranean region may be particularly vulnerable to global change.

1.2.1. Climate change effects on groundwater

Approximately 70% of the Earth's surface is covered by water, with 97.5% being saltwater and only 2.5% classified as freshwater (Oksana and Dmytro, 2021). Thinking about freshwater often suggests images of flowing rivers and clear lakes, but nearly all the world's liquid freshwater (97-99%; Stone et al., 2019), which is not frozen and locked away in ice caps and glaciers, exists as groundwater. Groundwater is indeed an almost universally available source of high-quality freshwater. On a global scale, groundwater accounts for about one third of all freshwater

extractions, providing an estimated 42%, 36%, and 27% of the water utilized for agricultural, domestic, and industrial purposes, respectively (Döll et al., 2012). In numerous ecosystems, natural groundwater discharges support baseflow to rivers, lakes, and wetlands during periods of low or no precipitation. Despite the crucial role groundwater plays in supporting human wellbeing and aquatic ecosystems, the limited number of studies examining the link between climate and groundwater has significantly hindered the capacity of the IPCC to evaluate the interactions between groundwater and climate change (Taylor et al., 2013).

Recent scientific data indicate that many of the world's major groundwater reservoirs are being depleted (Wada, 2016), resulting in reduced streamflow, the drying up of springs and wetlands, loss of vegetation, water-level declines in wells, and land subsidence. Another significant threat to groundwater, particularly for karst aquifers (Kalhor et al., 2019), is pollution caused by human activities, leading to the infiltration of chemicals and different types of waste into the subsurface. This contamination, exacerbated by climate change through altered recharge patterns and extreme events, deteriorates groundwater quality and poses risks to both human and ecological health (Balaram et al., 2023). Coastal aquifers, which form the interface between oceanic and terrestrial hydrological systems, are critically important as they provide a water source for over one billion people (Small and Nicholls, 2003) living in coastal regions. The extent of seawater intrusion into these aquifers is another major issue affecting groundwater, and it depends on various factors such as coastal topography, reduced recharge rates, groundwater abstraction from coastal areas, and sea level rise (Ferguson and Gleeson, 2012).

Global warming affects the energy balance of atmosphere and oceans, leading to alterations in the Earth's water cycle with consequent changes to precipitation typologies and regimes, with extreme regional variability of the effects (Caloiero et al., 2018). Patterns of precipitation change are indeed more spatially and temporally variable than temperature change (Kundzewicz and Döll, 2009). The more steady but significantly high rise in air temperatures leads to a substantial increase in evapotranspiration, thereby reducing the effectiveness of precipitation in recharging aquifers (Cardell et al., 2020). The continuous modification of land use and land cover for regional development in the context of a changing climate has also resulted in an alarming decrease in groundwater levels. First, the expansion of irrigated agriculture leads to excessive groundwater pumping, depleting aquifers. Second, land surfaces are often sealed with impervious materials, reducing aquifer recharge (Halder et al., 2024). Climate variability and change further impact groundwater systems directly by altering recharge patterns and indirectly through changes in land use and global processes (Taylor et al., 2013).

The Mediterranean region is expected to undergo significant changes that will impact the sustainability, quantity, quality, and management of freshwater (García-Ruiz et al., 2011). Future scenarios for water resources in this climate zone suggest:

1. A progressive decline in groundwater storage (GWS) (Fig. 1.4), leading to a significant decrease in average spring discharge and streamflow.
2. Changes in key river regime characteristics, including an earlier reduction in high flows from faster snowmelt in the spring season, and more severe low flows in summer.
3. Alterations in surface reservoir inputs and management, with reduced discharges released from dams and a resulting increase in pumping from wells to satisfy the water demands for irrigation and urban areas.
4. Hydrological and population shifts in coastal areas, especially in delta zones, affected by water depletion, groundwater reduction, and saline water intrusion.

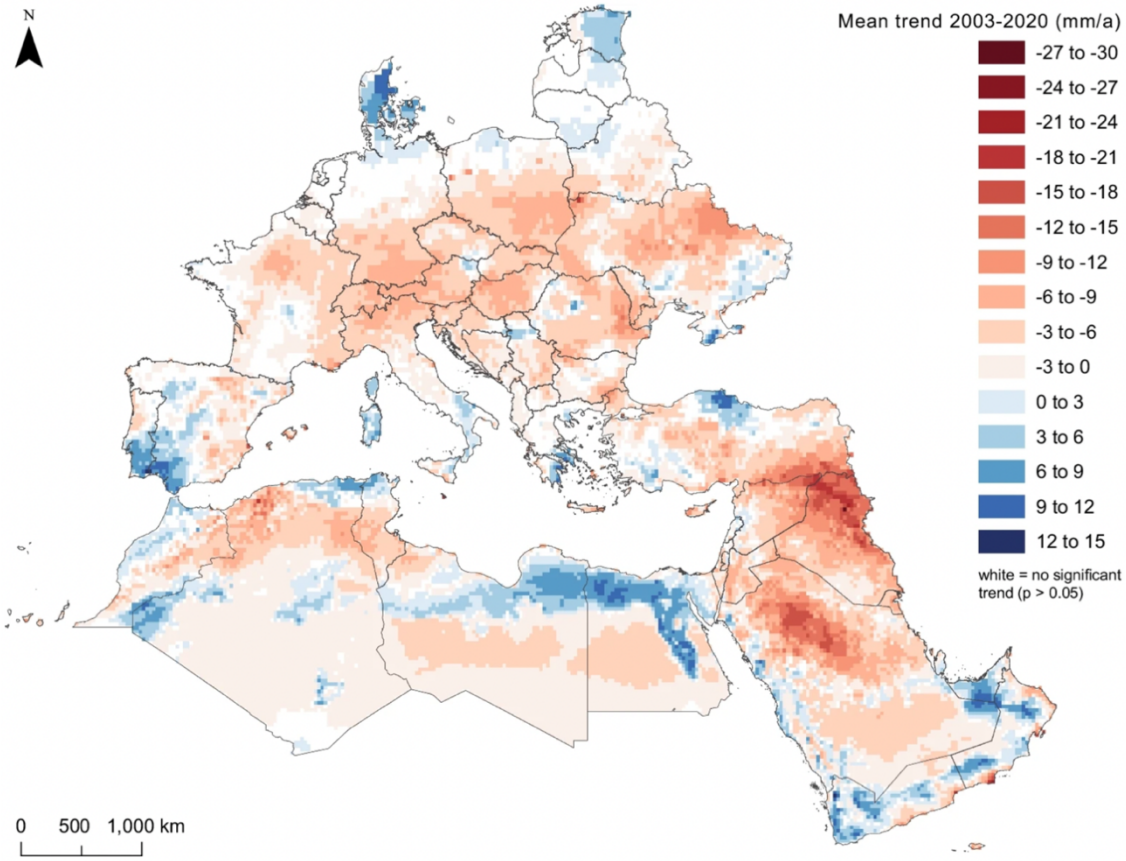

Fig. 1.4. Mean annual trend of GRACE-derived GWS in the Euro-Mediterranean region for the 2003-2020 period, based on the detection of gravity anomalies. A negative trend over the period is equivalent to a decrease in groundwater resources, while positive trends indicate an increase (Xanke and Liesch, 2022).

Significant impacts on groundwater availability have been observed along the Apennine chain in Italy, a major European mountain range, as well as in the rest of the Mediterranean basin, primarily due to the increased frequency and duration of droughts in recent decades. These impacts on freshwater resources are especially critical given that groundwater across the Italian peninsula constitutes the primary source of drinking water for many regions. Major urban centres, including Rome and Naples, depend on springs for public aqueduct supply (ISPRA, 2020).

Therefore, a significant and prolonged reduction in groundwater availability, extending over several years and manifested through decreased springs discharge and lower piezometric levels in aqueduct wells, could have profound societal consequences in the future.

1.2.2. Impacts on spring discharge along the Apennines

Spring discharge is an important water supply source, critical for communities and ecological systems dependent on groundwater resources. In Italy, the vast majority of freshwater used for public water supply is drawn from groundwater, which alone accounts for roughly 84.7% (of which 48.5% is from wells and 36.2% from springs) of all water extracted (Gandelli, 2022). Among the countries currently part of the European Union (EU), Italy ranks as the nation withdrawing the highest annual per capita volume of groundwater (Fig. 1.5), with over 130 m^3 per person per year (56 from springs). This water is used to meet the daily needs of the population as well as those of small businesses, hotels, services, commercial activities, production, agriculture, and industry directly connected to the urban network, in addition to public demands (such as schools, government offices, hospitals, public fountains, etc.) (Istat, 2022).

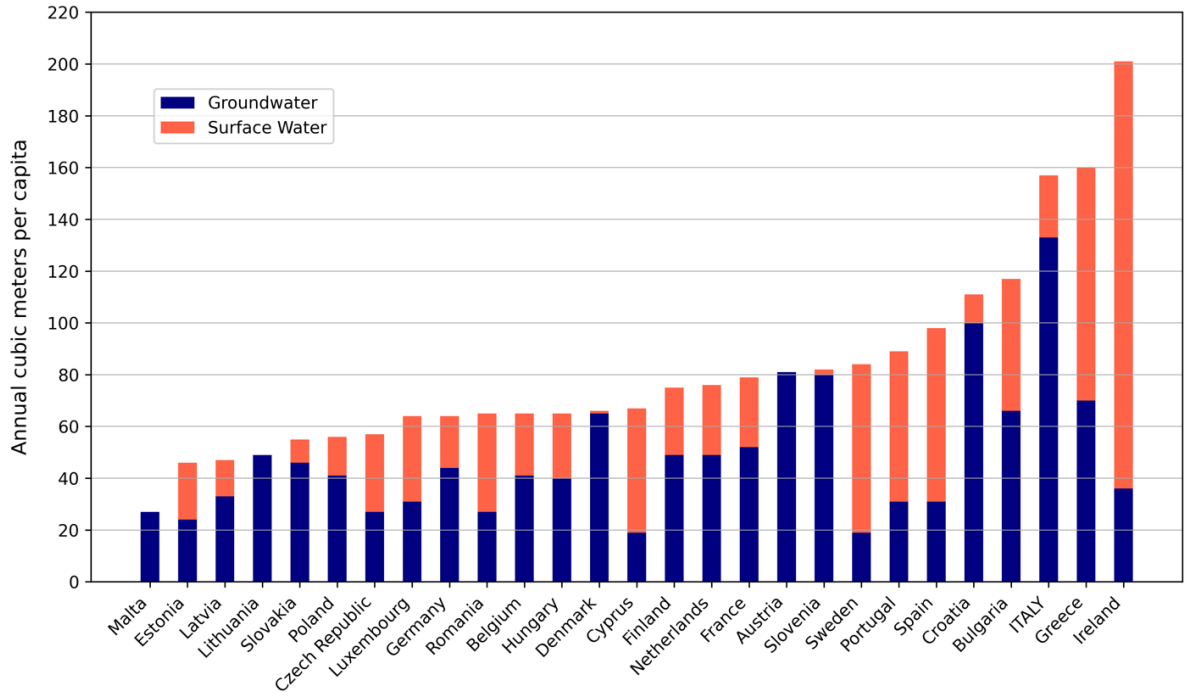

Fig. 1.5. Freshwater withdrawals for drinking purposes in the 27 EU countries in 2022. Groundwater withdrawals (from wells and springs) are indicated in blue, while surface water withdrawals (from artificial reservoirs, surface watercourses, and natural lakes) are shown in orange (Istat, 2022, modified).

The crucial role of springs in public water supply across Italy is illustrated in Fig. 1.5, and proves to be particularly indispensable along the Alps, the Apennines, and in mountainous areas more generally, where aqueduct wells are less prevalent. Mountain springs typically provide high-

quality water, in contrast to wells predominantly located in urbanised or industrialised lowland and coastal areas (Nicholson et al., 2018; Simsek et al., 2008). Therefore, shortages in groundwater recharge, altering spring outflows, can significantly impact society, especially during prolonged drought periods, which are becoming increasingly frequent (Alilou et al., 2022). Affected by both regional and local climate fluctuations, the seasonal and annual variability of spring discharge reflects a climate memory signal that is notably influenced when drought patterns arise within evolving climate conditions (Diodato et al., 2022), a phenomenon currently impacting the Mediterranean climate. Indeed, the effects of climate change on groundwater resources along the Apennine chain have been particularly severe in recent decades.

In the Southern Apennines, the duration and intensity of droughts have increased, particularly since the late 1980s (Fiorillo and Guadagno, 2012; Fiorillo et al., 2015), with groundwater storage decreasing accordingly, impacting numerous springs located on the Matese Massif and the Picentini Mountains (Fiorillo et al., 2021), the Lauria Mountains (Canora et al., 2019), the Pollino Massif (Grimaldi et al., 2008), and, more broadly, along the entire Southern Apennine area (Allocca et al., 2014). The continuous decline in spring discharge across such a wide region reflects the groundwater system's response to climate change over the past decades. The regulatory groundwater reserves of karst aquifers — which are the predominant aquifer type in the Southern Apennines — play a crucial role in sustaining significant karst spring outflows even after prolonged multi-year droughts, thereby defining the productivity and resilience of these hydrogeological systems (Diodato et al., 2022).

In Central Italy, population growth, tourism, and climate change have led to the frequent over-exploitation of alluvial lowland aquifers. Consequently, water managers are increasingly focusing on mountain regions, especially in the Central Apennines, featuring extensive karst aquifers (e.g., the Majella Massif), to identify groundwater resources for drinking purposes (Tazioli et al., 2020). Indeed, water from local aquifers and scattered spring discharge could help mitigate water scarcity and the overexploitation of larger water distribution networks, exacerbated by drought periods linked to climate change (Di Curzio et al., 2021). However, negative effects related to climate change have been observed on both the quantity (Di Nunno et al., 2021; Magi et al., 2019; Sappa et al., 2019) and quality (Barbieri et al., 2021; Sappa et al., 2019) of spring discharge in the Central Apennines. Two primary reasons for the reduction in spring discharge in this area are the shorter duration of snow on the ground (accelerated snowmelt) and the significant reduction in total snowfall (Gentilucci and Pambianchi, 2022; Petitta et al., 2022), factors primarily linked to the steady and continuous increase in air temperature.

In the Northern Apennines, water for drinking and industrial purposes is provided from hundreds of low-yield springs with short groundwater flow paths, developed primarily within fractured sedimentary rock units, which are abundant in this part of the Apennines (Filippini et al., 2024).

This type of hydrogeological setting does not provide the high discharge rates (greater than 1 m^3/s) typical of carbonate aquifers; rather, it produces spring water that closely follows meteoric recharge patterns (Cervi et al., 2018), resulting in low-flow periods concentrated in summer and early autumn (without multi-annual time lags sometimes observed in the large karst massifs of the Central and Southern Apennines). Consequently, spring outflow can be highly sensitive to reductions in recharge, especially during prolonged drought periods, which can cause serious water management issues. Negative trends in spring discharge have also been observed in the Northern Apennines, particularly in the Monte Fumaiolo area, located in the southeastern Emilia-Romagna Region near the border with Tuscany (Di Matteo et al., 2016), as well as in the Tuscan-Emilian Apennines on the Adriatic side (Filippini et al., 2024; Petronici et al., 2019).

1.3. Investigated springs along the Apennines

1.3.1. Geological and hydrogeological setting

The Apennines are an extensive mountain range with a NW-SE orientation, which can be divided into the Northern, Central, and Southern sectors (Fig. 1.6). The complex tectonic history of the Apenninic chain can be summarized in three main phases: an initial extensional phase, followed by a compressional phase, and finally, a renewed phase of extension (Boccaletti et al., 1971; Carmignani and Kligfield, 1990).

In the Early Jurassic, the break-up of the Pangea supercontinent occurred, leading to the fracturing of the Tethys carbonate platform. These extensional movements also facilitated the opening of the Liguria-Piedmont (LP) Ocean, which resulted in the separation of the European plate and the Sardinian-Corsican block from the African plate and Adria, a 'microplate' also referred to as the 'Promontory of Africa' (Channell and Horváth, 1976). The second major tectonic phase began during the transition from the Lower to Upper Cretaceous, when the expansion of the LP Ocean ended, and the African plate, reversing its direction, started moving north-westward, leading to the closure of the ocean (Boccaletti et al., 1982). In the Late Eocene to Miocene, as the last portion of the LP Ocean's oceanic crust was subducted, the collision between the European continental margin (including the Sardinian-Corsican block) and the Adriatic margin began; this collision marks the onset of the Apennine orogeny (Molli, 2008). The third and final phase of the Apennines' tectonic history is characterised by extension, which began in the Late Oligocene-Miocene in the Tyrrhenian area, while compression was still ongoing in the chain, and continues to the present day (Carmignani et al., 1994). The extensional tectonics have resulted in a progressive thinning and subsequent fracturing of the crust along the Tyrrhenian margin of the Apennines. The succession of these tectonic phases has led to the formation of several lithological units, marked by diverse features across the Apennines sectors (Fig. 1.6).

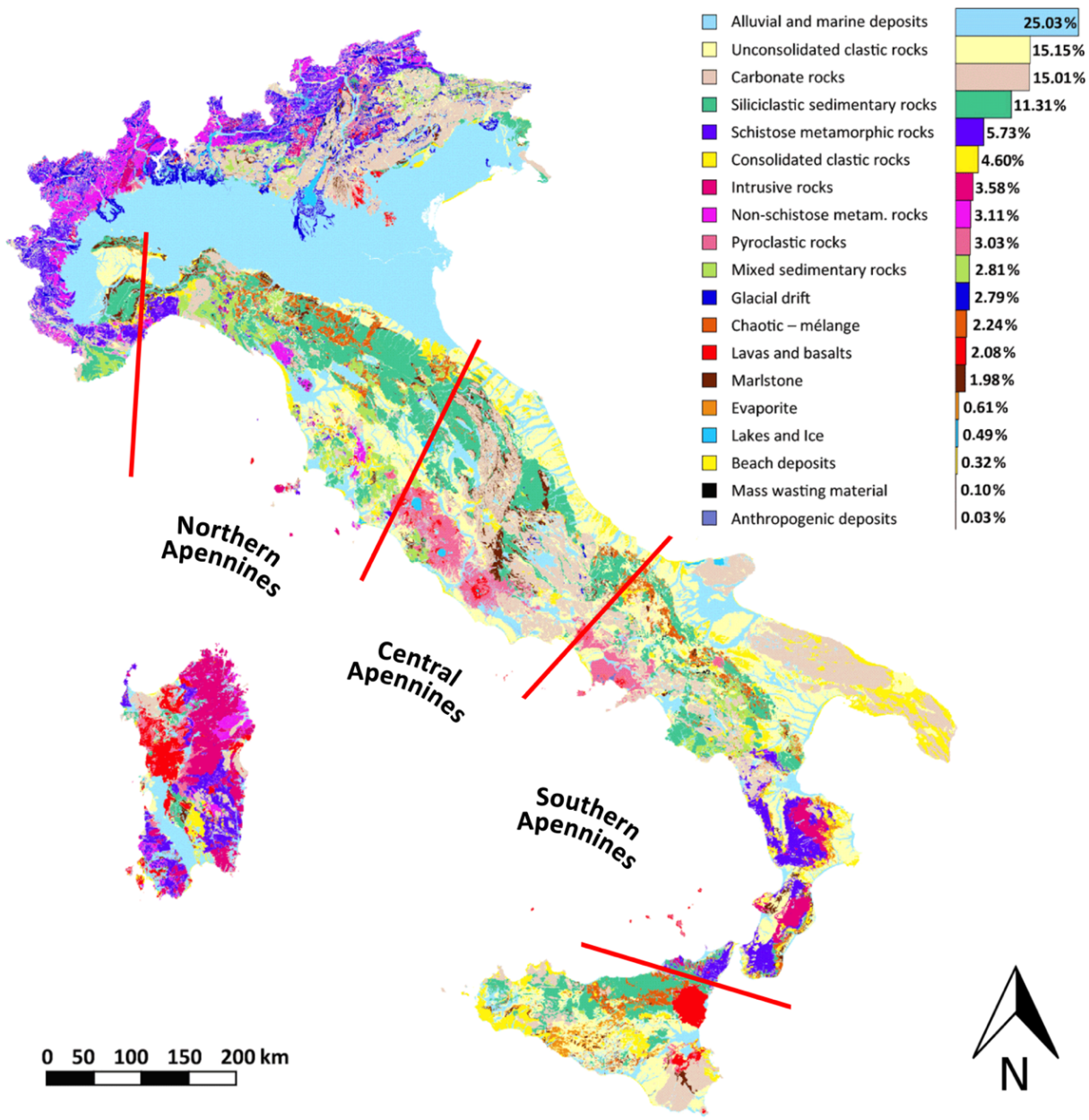

Fig. 1.6. Map of Italy showing 19 lithological classes. The extended name and percentage distribution of each class is indicated in the bar chart located in the top-right corner (Bucci et al., 2022, modified).

In the Northern Apennines, turbiditic sequences are predominant, resulting from deep-sea sedimentation during the first extensional phase, while the Central Apennines are dominated by widespread carbonate platforms, which were uplifted during the collision phase (Cosentino et al., 2010; Marroni et al., 1992). The Southern Apennines, on the other hand, exhibit a more complex interplay of various geological formations, with significant nappes resulting from the thrusting processes (Patacca and Scandone, 2007). Moreover, the post-orogenic extensional phase that has affected, and continues to affect, the Tyrrhenian margin of Central and Southern Italy has been characterised by Plio-Quaternary back-arc volcanism, which has given rise to multiple volcanic edifices and eruptive fissures (Acocella and Funiciello, 2006).

The numerous tectonic, magmatic, and sedimentary environments that existed during the evolution of the Apennine orogen account for the wide range of lithological formations found across the Apennines. This diversity is also reflected in the various hydrogeological settings along the mountain range, which include different types of aquifers such as sedimentary carbonate, sedimentary siliciclastic, crystalline metamorphic, volcanic, and fluvio-lacustrine intramontane. However, most of the groundwater in the Apennine chain is stored in carbonate karst aquifers (De Vita et al., 2012; Petitta and Tallini, 2002). Nevertheless, aquifers with significant yield can also be found in volcanic and arenitic settings (Doveri et al., 2012; Filippini et al., 2024).

As previously mentioned, this PhD project presents a century-long analysis of discharge patterns along the Apennines. To identify springs with extensive discharge datasets, the research initially focused on the monographs "*Le Sorgenti Italiane*" (Italian Springs), compiled by the Hydrographic Service between the 1920s and 1960s, covering the central-southern Italian regions of Abruzzo, Basilicata, Calabria, Campania, Lazio, Molise, Puglia, Sardinia, and Sicily. For this PhD thesis, given the focus on the Apennine chain, Puglia Region and the two island regions, Sardinia and Sicily, were excluded, as shown in Fig. 1.7.

Region \ Meinzer class	II	III	IV	V
Abruzzo	4	9	27	102
Basilicata	2	27	102	466
Calabria	0	54	335	4015
Campania	24	44	248	678
Lazio	13	24	84	111
Molise	6	16	57	210

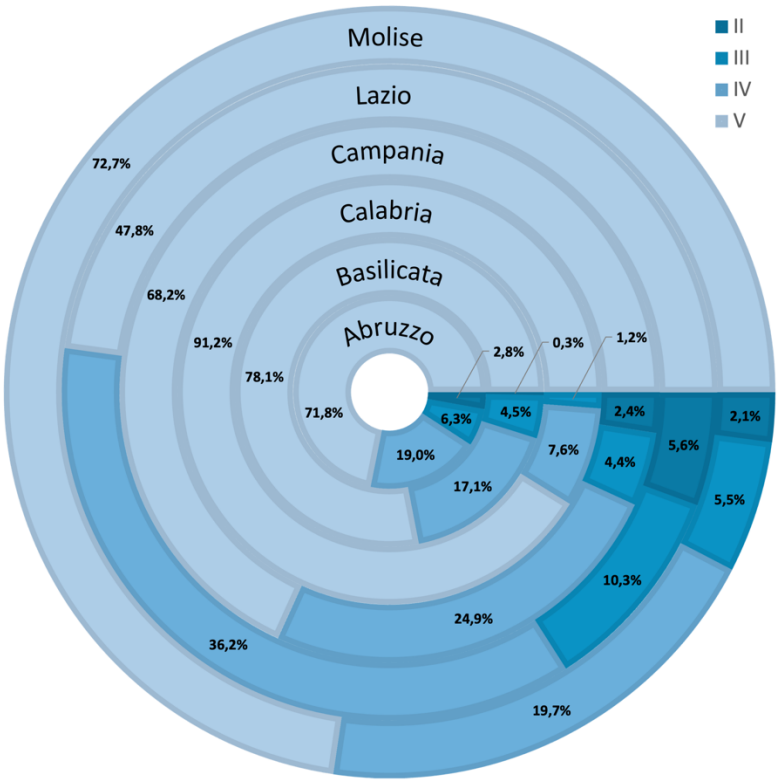

Fig. 1.7. Summary statistics of the number of springs in the Italian regions of Abruzzo, Basilicata, Calabria, Campania, Lazio, and Molise, categorised by Meinzer class II (1000-9999.99 L/s), III (100-999.99 L/s), IV (10-99.99 L/s), and V (1-9.99 L/s). No springs in Meinzer class I (≥ 10000 L/s) are present in any of these six regions. On the left, a summary table displays the number of springs per class for each region; on the right, a pie chart illustrates the corresponding percentages of springs per class for each region.

Additionally, since the aim was to identify significant springs monitored over long periods, the focus was placed on springs of Meinzer class V or higher, given the greater likelihood of long-term monitoring. Following an in-depth review of these monographs during the initial months of research, the selection was further narrowed to Meinzer class II springs, owing to their already considerable number (49 across the six regions, Fig. 1.7). After an extensive bibliographic and online review to identify springs of similar significance in the Central and Northern Apennines, few springs with potentially long discharge records were identified. Subsequently, the relevant local authorities responsible for managing all the selected springs were contacted. Following a well-thought-out selection process, primarily based on the availability of extensive historical datasets, only seven springs were identified as potentially suitable for study in this PhD project. These springs are listed below, arranged from north to south (Fig. 1.8):

- Nadìa Spring (Northern Apennines).
- Cannucceto Spring (Northern Apennines).
- Ermicciolo Spring (Amiata Volcano - Central Italy).
- Verde Spring (Central Apennines).
- Serino Spring group (Southern Apennines).
- Cassano Irpino Spring group (Southern Apennines).
- Sanità Spring (Southern Apennines).

Nadìa Spring is situated in the Emilia-Romagna Region, specifically in the municipality of Montese (Modena), at an elevation of 555 m above sea level (asl) (44°19'09'' N; 10°58'14'' E), nearby the main divide of the Northern Apennines belt between the valleys of the Reno and Panaro Rivers. The spring, managed by the public water supply company Gruppo Hera S.p.A., is uptaken by a 75 m long draining tunnel built between 1917 and 1920 (Vecchi, 1920), and it represents one of the most productive springs in the Northern Apennines. The aquifer is a fractured sedimentary arenite, composed of medium- to fine-grained calcareous sands (Amorosi, 1997), with karst-like corrosion phenomena. Regarding the discharge data, monthly values are available for the period between January 1915 and October 1918, during which accurate total flow rate monitoring was carried out as a preliminary step to the excavation of the drainage tunnel. More recent measures of the withdrawn fraction of the spring flow (excluding overflow) have been continuously collected by the water company since 2017. However, contemporary total discharge data are only available for the period between December 2020 and March 2023, as reported by Filippini et al. (2024), thanks to monitoring conducted by the Hydrogeology Group of the BiGeA Department at the University of Bologna, which also involved this PhD project. Considering all available monitoring periods, Nadìa Spring exhibited a minimum mean monthly total discharge of 42 L/s and a maximum of 140 L/s, placing it within the fourth (IV) class of Meinzer's quantitative spring discharge classification (1923).

Fig. 1.8. Topographic and bathymetric map of Italy showing the location of the analysed springs along the Apennines (base map derived from Gaba, 2009 [licensed under GFDL/CC-BY-SA]; modified).

Cannucceto Spring is located in the Tuscany Region, near the border with the Emilia-Romagna Region, in the municipality of Scarperia, at an elevation of 915 m asl (44°04'44" N; 11°18'15" E). The spring is situated on the southern slope of Monte Gazzaro (Northern Apennines), situated along the main divide between the Arno River basin (to the south) and the Reno River basin (to the north). Cannucceto Spring is exploited by the mineral water bottling company Acqua Panna (Nestlé Waters group) and stands as the most important spring among those within the mining concession. The spring is tapped by a small intake structure built in the groundwater emergence area. The aquifer is sedimentary arenitic, consisting of siliciclastic turbidites with a relatively high Arenite/Pelite ratio, and sandstone layers composed of coarse- to medium-sized sand grains (Bettelli et al., 2005). The permeability is primarily controlled by faults and fractures, or by

discontinuities caused by layering, which facilitate the interconnection of the various arenitic layers. Concerning the discharge data, daily values have been available since January 1979, and since the early 2000s, data with a temporal resolution of five seconds have also been recorded. Cannucceto Spring has historically been characterised by a minimum discharge of 0.55 L/s during the low-flow period and a maximum of approximately 21 L/s, placing it within the sixth (VI) class of Meinzer's classification (1923).

Ermicciolo Spring is also situated in the Tuscany Region, in the municipality of Castiglione d'Orcia, at an elevation of 1020 m asl (42°55'26" N; 11°38'29" E). The spring is located on Mount Amiata, an extinct volcano whose evolution is associated with the magmatism linked to the most recent Apenninic post-orogenic extensional phase (Frondini et al., 2009). For this reason, although Mount Amiata is approximately 100 km to the south-west of the main Northern Apennine divide, it can be associated with the internal extensional sector of the Apennine chain. Ermicciolo Spring is managed by the water company Acquedotto del Fiora (ACEA S.p.A. group) and is exploited it through an 80-meter-long drainage tunnel constructed between 1908 and 1914 on the northern slope of the volcanic aquifer complex, which is primarily composed of ignimbrites and trachytes (Doveri et al., 2012). Regarding spring discharge, total flow rate data of at least monthly frequency are available from 1939 to the present day, with a six-year gap in acquisition from 1990 to 1995. Originally, discharge monitoring was performed manually using a thin-wall weir, whereas since the 1990s, a pressure transducer hydrometer has been installed for automatic measurements. The average discharge of Ermicciolo Spring fluctuates between roughly 90 L/s and 210 L/s. It is noticeable that since the mid-1970s, the Meinzer class of the spring has dropped from the third (III) to the fourth (IV) class, as the spring has started recording flow rates below 100 L/s during the low-flow period.

Verde Spring is located in the Abruzzo Region, within the municipality of Fara San Martino, at an elevation of 415 m asl (42°05'30" N; 14°12'08" E). The spring discharges on the eastern side of the Majella Massif (Central Apennines), one of the main carbonate reliefs in Central Italy, covering an outcrop area of 273 km² (Chiaudani et al., 2019). Verde Spring is managed by the water company Società Abruzzese per il Servizio Idrico S.p.A. (SASI), which uptakes the water through two drainage tunnels with a combined length of approximately 4 km, constructed between the late 1920s and early 1930s. From a geological perspective, the aquifer consists of a thick (~2 km) sequence of carbonate karstified formations (Nanni and Rusi, 2003). Concerning the discharge data, we have daily values available from January 1938 to December 2005; however, spring flow rate monitoring is still being carried out today by automated water level stations with calibrated flow sections. Verde Spring is characterised by a minimum discharge during the low-flow period of about 900 L/s and a historical maximum of 6170 L/s, placing it within the third (III) class of Meinzer's quantitative classification.

Cassano Irpino Spring group is located in the Campania Region, within the municipality of the same name, at an elevation of 476 m asl (40°52'12" N; 15°01'54" E). The springs emerge on the eastern side of the Terminio-Tuoro Massif, which is part of the Picentini Mountains karst system (Southern Apennines). Cassano Irpino Spring group, consisting of Bagno della Regina, Peschiera, Pollentina, and Prete Springs (Fiorillo and Guadagno, 2012), is managed by the water company Acquedotto Pugliese S.p.A. (AQP), which taps the spring group through intake structures and drainage mats constructed between the 1950s and the 1960s. From a geological perspective, the aquifer is primarily composed of limestone and calcareous-dolomitic rocks marked by karst phenomena (Corniello et al., 2010). In the discharge border area, groundwater flows out by a superimposed permeability threshold, under pressure through a lower permeability fractured arenitic cover (Coppola et al., 1989). Regarding the discharge data, mean monthly values are available for the period 1965 to 1979, while from 1980 onward, data have been recorded on a daily basis. Cassano Irpino Spring group exhibits a minimum discharge during the low-flow period of about 1400 L/s and a historical maximum of 5510 L/s, classifying it within the second (II) class of Meinzer's quantitative classification.

Serino Spring group is also located in the Campania Region, within the municipality of the same name, at an elevation of approximately 352 m asl (40°52'49" N; 14°51'40" E). Managed by the water company Acqua Bene Comune, it serves as the main source of aqueduct water supply for the city of Naples, along with the Gari Spring, located in the Simbruini Mountains in southern Lazio. Serino Spring group is situated on the western slope of the Terminio-Tuoro Massif (Southern Apennines) and consists of Urcioli Spring and Acquaro-Pelosi Spring, which are tapped through drainage channels and mats built at the end of the 19th century. In this case as well, the discharge area is characterised by upward-directed groundwater flow (Fiorillo et al., 2018), and the geological setting is also the same. The Terminio-Tuoro Massif appears to be fragmented by a hydrogeological divide, as resulted by a tracer test conducted in 1979 by Celico and Russo (1981), involving the injection of Uranine into the “Bocca del Dragone”, a karst sinkhole located within the main endorheic basin – a polje – of the massif, known as “Piana del Dragone”. The tracer revealed a connection between the sinkhole and Cassano Irpino Spring group (where the fluorescent tracer arrived after a few days), but not with those of Serino group, where the tracer was not detected. Concerning the whole spring discharge of the group, monthly flow rate data are available from 1962, with only two small gaps in the historical dataset in 1976 and 1999. The total average discharge of Serino Spring group fluctuates between 1100 L/s and 3500 L/s, also placing it within the second (II) class of Meinzer's classification.

Sanità Spring is also located in the Campania Region, specifically in the municipality of Caposele, at an elevation of roughly 420 m asl (40°48'58" N; 15°13'13" E). The spring is situated on the eastern side of the Cervialto Massif, which, along with the Terminio-Tuoro Massif, is the other

major carbonate relief of the Picentini Mountains karst system (Southern Apennines). Sanità Spring is managed by the water company Acquedotto Pugliese S.p.A., which uptakes the spring through a surface drainage system located at the base of the massif's slope. This system is characterised by several niches excavated along the discharge front at the beginning of the twentieth century. The karst aquifer consists of a series of limestone and limestone-dolomite formations (Leone et al., 2021), with a thickness reaching up to 3000 m. Regarding discharge data collection, this spring has a unique century-long historical dataset, with at least monthly data available from 1920. Originally, the flow rate was quantified using a hydrometric reel along the main channel, with a monitoring frequency of twice a month. In 1927, Venturi tubes were installed to make the monitoring system more efficient (Fiorillo et al., 2021), which was further improved in 1980 when data acquisition became daily. Throughout the entire monitoring period, Sanità Spring exhibits a discharge ranging from approximately 3300 L/s to 5400 L/s, classifying it within the second (II) class of Meinzer's spring discharge classification (1923).

1.3.2. Selected and excluded springs

During the data collection phase, historical discharge data for all seven of the springs were acquired, thanks to scientific collaboration agreements with the water managing authorities. However, in the analysis phase, it was decided to restrict the research to only a few of these springs: Nadìa, Ermicciolo and Sanità. The main criterion for the exclusion of the other springs is related to the limited length of the historical dataset or the absence of accurate historical discharge data dating back to the early 20th century (century-long data), even if collected occasionally or only in certain years (as in the case of Nadìa Spring). Firstly, it must be considered that at least 30 years of data are required to detect and appreciate a climate trend (Livezey et al., 2007), and consequently at least 60 years of data are necessary to determine whether flow rate or meteorological trends are changing due to climatic forcing. Secondly, to appreciate the long-term discharge relationship with recharge-related data, it is indispensable to base the analysis on secular historical records (Chen et al., 2004; Leone et al., 2021), which can then be projected into the long-term future to forecast spring discharge.

The importance of considering very long historical datasets can be highlighted by the following observation. Figs. 1.9 and 1.10 compare the hydrographs of Cannucceto Spring (excluded from the analysis) and Ermicciolo Spring. For Cannucceto, where flow rate data are only available from January 1979 onwards, the discharge appears to have gradually increased, as indicated by the linear trend line showing a gentle positive slope (or, at most, no trend).

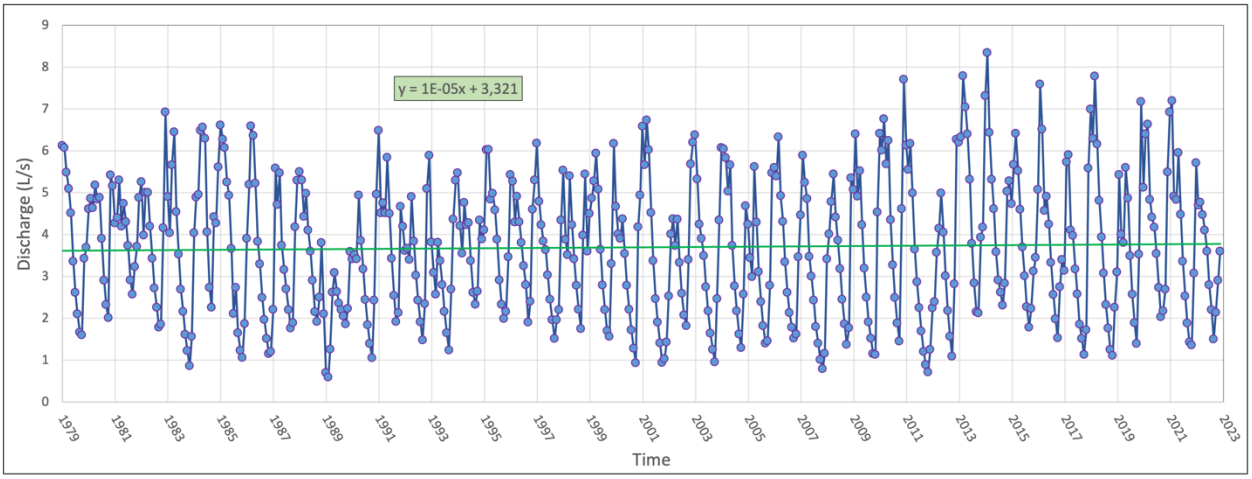

Fig. 1.9. Mean monthly discharge of Cannucceto Spring. The labels on the x-axis indicate January of each respective year. The positive slope of the linear trend line (shown in green) indicates a subtle increase in discharge over the entire historical record of the spring.

However, when looking at the same period for Ermicciolo (Fig. 1.10), which is geographically the closest, among those studied, to Cannucceto Spring with a near-century-long historical record available, the trend from January 1979 to the present also shows an increase in discharge. However, when the full dataset, starting in January 1939, is considered, it becomes evident that the spring's discharge has significantly decreased relative to historical levels. Therefore, it cannot be definitively determined whether, or to what extent, Cannucceto Spring has been impacted by long-term climate change. Focusing solely on recent discharge datasets (spanning no more than 30 to 50 years) may lead to misleading and unrepresentative conclusions regarding trends and impacts associated with global warming.

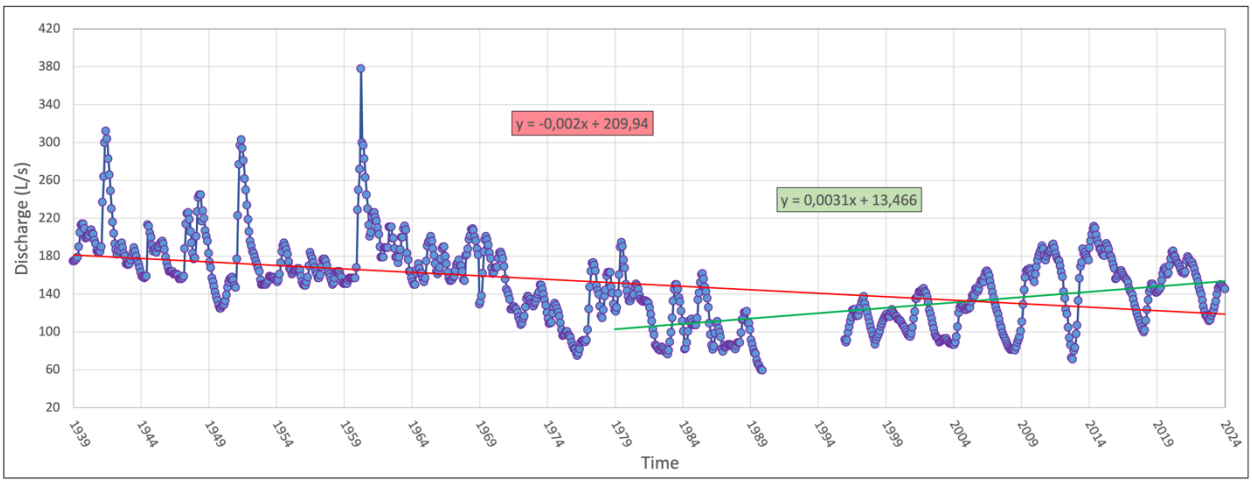

Fig. 1.10. Mean monthly discharge of Ermicciolo Spring. The labels on the x-axis indicate January of each respective year. The red linear trend line refers to the complete historical record, while the green one refers only to the period from 1979 to the present. The respective slopes indicate a positive trend in discharge over the past 45 years but a significantly negative trend when considering the full time series.

Verde Spring was excluded from the analysis for two reasons: firstly, discharge data are available only up until 2005; secondly, there is a four wells field located in the discharge area, which affects the spring flow. Given the inability to precisely quantify the effects of the well field on the spring, due to the variable pumping rates of the wells, it was not possible to determine whether, or to what extent, the spring has been impacted by global warming.

Cassano Irpino and Serino Spring groups, both discharging from the Terminio-Tuoro Massif, were excluded from the analysis because the Dragone Plain, the polje representing the main endorheic basin of the massif (Pagnozzi et al., 2019), is highly anthropized, with cultivated farmland, livestock grazing activities, and various commercial undertakings. Consequently, in this plain, located in the municipality of Volturara Irpina, there are unquantifiable withdrawals from pumping wells. Therefore, as in the case of Verde Spring, it was not possible to accurately determine the extent to which the spring discharge of Cassano Irpino and Serino Spring groups has been influenced by climate change.

Despite their exclusion from the subsequent in-depth analyses, the discharge datasets for Verde Spring and Cassano Irpino and Serino spring groups have still proven useful. Using a multi-decadal approach, they allowed for the evaluation of discharge decline, even though based on a shorter time span (approximately 60 years, still a significant and rare attribute). The results of these multi-decadal flow rate analyses will be presented at the end of Chapter 3.

1.3.3. Societal implications of ongoing and future negative spring discharge

In all study areas, and more generally along the entire Apennine range (as highlighted in Section 1.2.2), springs are experiencing reductions in discharge. This, as previously explained, is primarily due to the more frequent and severe occurrence of droughts, which have a wide range of consequences on water supply systems. As spring discharge declines, aqueducts increasingly struggle to meet the water demands of local populations, especially during summer months when tourism peaks, further straining groundwater resources.

Several towns located in the Bologna and Modena Apennines (Northern Apennines), which rely on spring water and small wells for their public water supply, experienced severe droughts in recent years. In response to critical shortages, emergency measures such as water trucks were promptly deployed. For instance, during the severally dry summer of 2021, approximately 650 water truck deliveries were required in some municipalities supplied by the Gruppo Hera water company, including Montese, where Nadìa Spring is located. In the following summer (2022), during a similar drought event, around 570 water truck deliveries were needed. On average, nearly 10,000 m^3 of water were supplied in this manner per season (UniBo and RER for Gruppo Hera, 2023). Considering the projected increasing trends in air temperature across the entire

Mediterranean area (IPCC, 2023), these findings underscore the potential for concerning and prolonged water shortages in that part of the Northern Apennines in the future.

In the Central Apennines, the recent situation is even more critical. In the summer of 2024, the Abruzzo Region faced a severe water crisis; to maintain adequate flow and pressure in the public water supply network managed by the SASI water company, it became necessary, starting in July, to implement nightly aqueduct outages across several municipalities (Il Manifesto, 2024). The main springs of the Gran Sasso and Majella Massifs, including Verde Spring, also experienced substantial reductions in flow that summer, primarily due to the lack of winter and spring rainfall and snowfall. In the Molise Region, meanwhile, the primary water sources saw their flows nearly halved. The main spring of the "Riofreddo" drainage tunnel, in the municipality of Bojano, which had provided approximately 3,500 L/s in 2023, was reduced to an average of only 1,700 L/s by July 2024, while Sant'Onofrio Spring, an important spring draining the Montagnola di Frosolone (Tozzi et al., 1999), significantly declined from 120 L/s to 70 L/s. Other minor springs in Molise also displayed unsatisfactory levels. Additionally, the hydraulic head of the region's main well fields dropped of approximately 8 m (Il Messaggero, 2024). In certain areas of the Central Apennines, water companies were indeed forced to implement emergency measures, primarily through severe water rationing.

Recent studies in the Southern Apennines have highlighted the need for accurate estimates of future aqueduct spring discharge to improve decision support systems for the exploitation of groundwater resources (Diodato et al., 2017). Indeed, the significant and prolonged water scarcity period occurred in the Southern Apennines in recent years has had very negative consequences on spring discharge (Diodato et al., 2022). Sanità Spring and Cassano Irpino Spring group, which drain the Cervialto and Terminio-Tuoro Massifs respectively, are essential water sources for much of Southern Italy. Since the 1930s, water from these two springs has been conveyed through a 450 km-long gravity-driven network of tunnels and bridges from the Campania Region to the southernmost part of Puglia (Fiorillo, 2009), as well as to part of the Basilicata Region. The AQP water company, responsible for supplying water from these springs, was compelled to initiate pressure reductions across the network in October 2024 as an adaptation measure to the ongoing drought, leading to outages in vast areas of Southern Italy (Acquedotto Pugliese S.p.A., 2024). AQP sources approximately 55% of its water from five surface reservoirs (Sinni, Pertusillo, Conza, Occhito, and Locone), which also supply water for irrigation; 33% from the Sanità and Cassano Irpino Springs; and the remaining 12% from around 180 wells, primarily located in southern Puglia and used exclusively for drinking purposes. This mix of sources is distributed in several interconnected water supply aqueduct schemes across four regions (Campania, Basilicata, Puglia, and part of Molise), allowing AQP to offset shortages in one

scheme with resources from another (Acquedotto Pugliese S.p.A., 2024). However, the recent widespread water crisis of 2024 has affected all supply areas, leading to a significant drawdown in wells, severe dewatering in reservoirs, and a marked decrease in the discharge of Sanità and Cassano Irpino Springs.

The recurring drought crises present a significant challenge to water companies and authorities, necessitating various measures as part of adaptation strategies to address water scarcity across the Apennines, such as:

(**i**) The construction of new surface water reservoirs, strongly advocated by politicians and water managers, which, however, presents critical issues regarding environmental sustainability, including extensive land consumption, hydrogeological risks, reservoir siltation, and water loss through evaporation exacerbated by global warming.

(**ii**) The installation of new well fields in groundwater reserve areas or deeper sections of major aquifers, which could help mitigate seasonal declines in shallower or coastal aquifers.

(**iii**) Enhancing adaptation through the establishment of robust interconnections between different sources and watersheds, as exemplified by AQP, which allows for the seasonal transfer of substantial quantities of water from surplus regions, including on an interregional scale, to those facing water shortages.

(**iv**) Reducing pipe leakage rates, estimated in Italy at an average loss of 42.4% of distributed aqueduct water (Fig. 1.11; Istat, 2022), with local losses exceeding 60% of withdrawn resources in some areas. This is largely due to the aged infrastructure, as roughly 60% of the network was installed over 30 years ago, and 25% now exceeds 50 years in age (Gandelli, 2022).

(**v**) Educating the public on water conservation in daily activities is crucial, such as turning off taps while brushing teeth, which can save around 15 L per person per day. Additionally, adopting dietary habits that involve less water-intensive foods, such as reducing meat and certain fruit consumption, and paying closer attention to sustainable lifestyle choices can make a significant impact. Italy's per capita daily water consumption is 220 L, compared to the European average of 165 L (Corriere della Sera, 2023), primarily attributed to avoidable waste.

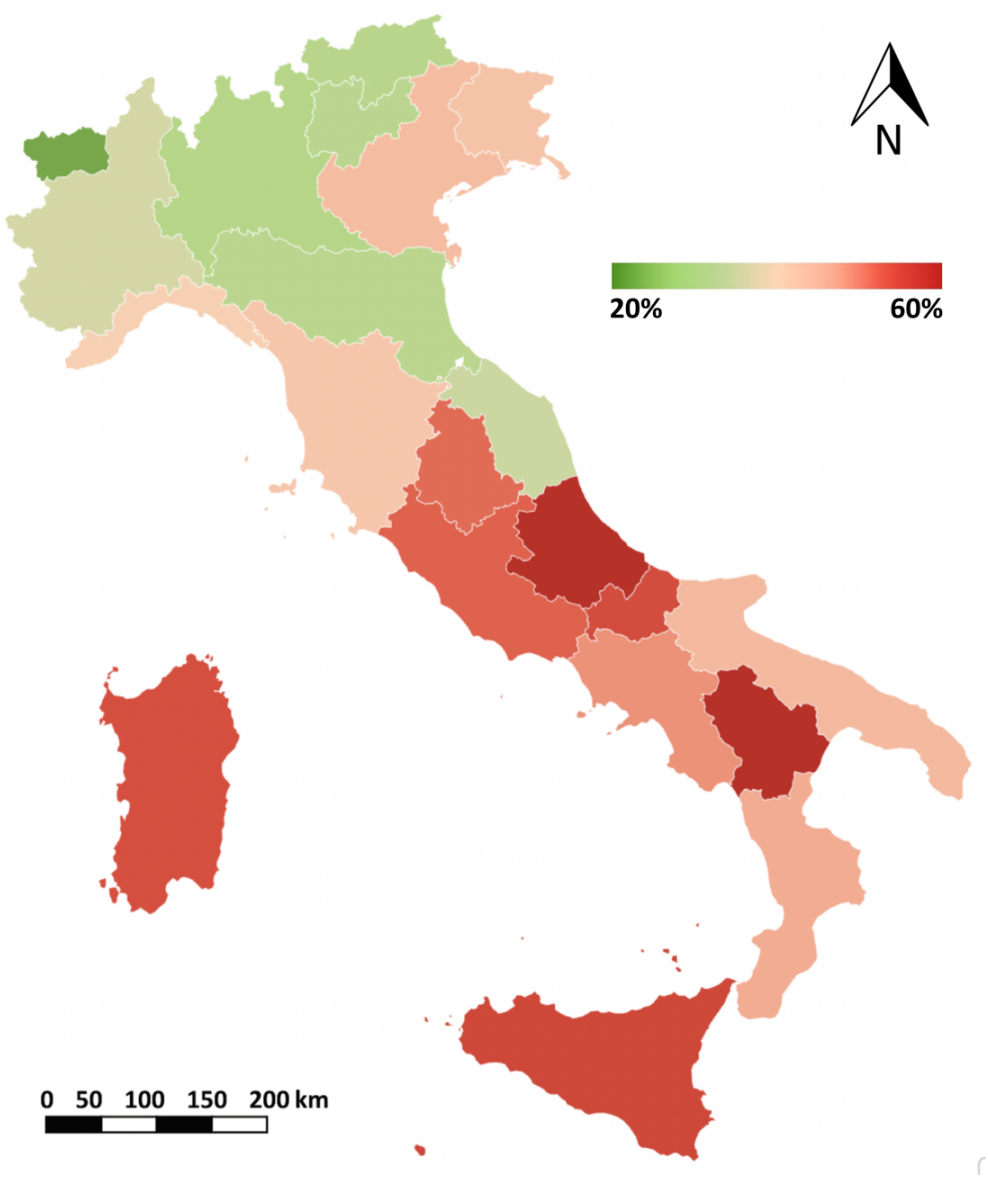

Fig. 1.11. Water supply network losses in Italy by region (Gandelli, 2022, modified).

Independent of the adaptation measures to address droughts, estimating future spring discharge patterns is a fundamental asset for water companies and authorities, enabling them to plan the necessary actions to mitigate water scarcity.

1.4. Research questions and outline

In the previous sections, the impacts of climate change on spring discharge have been discussed as a complex and significant challenge for modern society. Despite broad knowledge about hydrogeological processes associated with aquifer recharge, the relationship between spring discharge and meteorological variables, and the effects of global warming on groundwater quality and availability, a notable gap remains in the literature regarding both the quantitative

impacts on spring flow and future projections of these discharge reductions, particularly for long-term scenarios. Such long-term perspectives may be essential for planning and implementing large-scale infrastructure projects to address incumbent water crises. Moreover, understanding the impacts of climate changes on the historical flow of springs also enables identification of those that are more resilient to these changes.

The primary challenges in this research involve collecting century-long historical discharge datasets and understanding long-term relationships between recharge-related parameters and spring flow rate to enable projections and assessments of future spring discharge. These challenges encompass some of the central issues and essential research questions addressed in this PhD project, which will be briefly introduced in this section and explored in detail in subsequent chapters, considering the ongoing decline in spring discharge observed nearly everywhere along the Apennine Mountain range in Italy.

The springs located along the Apennines have experienced notable and consistent reductions in discharge throughout recent decades, primarily attributed to the continuous rise in air temperature, which has led to increased evapotranspiration and accelerated snowmelt in mountainous areas, thereby resulting in reduced aquifer recharge. A marked acceleration in the downward trend of spring discharge was recorded between the 1980s and 1990s, when most hydrographs of the main Apennine springs showed a severe period of low flow, with subsequent high-flow phases featuring peak discharges significantly lower than historical values. Until recently, water companies managed to address drought issues through various temporary mitigation measures, such as increasing withdrawals from surface water systems (which are more prone to stress during droughts) or drilling new aqueduct wells. However, since the severe drought of 2017, water scarcity problems have further intensified along the entire Apennine chain, mainly due to the decrease in spring discharge, prompting water authorities to also implement water rationing measures.

For this reason, the main objectives of this PhD project have focused, first and foremost, on understanding the impacts of climate changes on the historical discharge of springs, also aiming to assess their degree of resilience. Secondly, through various types of analyses, efforts were made to estimate the long-term future discharge of some main springs in order to support water companies in planning the necessary mitigation measures to address recurring droughts.

Question 1 - *What is the impact of global warming on spring discharge along the Apennines, and to what extent is it feasible to assess the resilience of springs to climate change?*

Question 2 - *Is it possible to estimate the long-term future discharge of springs based on long-term recharge-discharge relationships?*

The **first research question** will be thoroughly addressed in Chapter 2, which focuses on the hydrogeological assessment of Nadìa Spring, located in the Northern Apennines. The spring was the subject of a research paper published in Science of the Total Environment, co-authored with other researchers and supported by contributions from this PhD project. The study focused on the analysis of century-long historical discharge patterns in comparison with contemporary data, as well as the characterization of the spring's resilience to climate change. Additional, issues related to this research question, particularly concerning the impacts of climate change on historical discharge, will be examined in Chapter 3.

The **second research question** will be explored in detail in Chapters 3 and 4, which focus on Ermicciolo Spring (Amiata Mountain, Central Italy) and Sanità Spring (Cervialto Massif, Southern Apennines). Two distinct methodological approaches were applied to historical discharge time series to examine the relationship between meteorological variables and spring discharge: Multiregression Statistical Analysis (MSA) and Long Short-Term Memory (LSTM) machine learning. These relationships were then combined with future climate projections to estimate the long-term discharge of the investigated springs.

Finally, Chapter 5 will summarise the findings of this **research**, highlighting their significance, and will briefly outline potential directions for future studies and perspectives in the field.

1.5. References

Acocella, V., Funiciello, R., 2006. Transverse systems along the extensional Tyrrhenian margin of central Italy and their influence on volcanism. Tectonics, 25(2), TC2003.

Acquedotto Pugliese S.p.A., 2024. Siccità, riduzioni di pressione su tutta la rete per affrontare la crisi idrica. Comunicato Stampa - Comunicazione e Media, Bari, 21 October 2024.

Alexander, L.V., Zhang, X., Peterson, T.C., Caesar, J., Gleason, B., Klein Tank, A.M.G., Haylock, M., Collins, D., Trewin, B., Rahimzadeh, F., Tagipour, A., Rupa Kumar, K., Revadekar, J., Griffiths, G., Vincent, L., Stephenson, D.B., Burn, J., Aguilar, E., Brunet, M., Taylor, M., New, M., Zhai, P., Rusticucci, M., Vazquez-Aguirre, J.L., 2006. Global observed changes in daily climate extremes of temperature and precipitation. Journal of Geophysical Research Atmospheres, 111(5), D05109.

Alilou, H., Oldham, C., McFarlane, D., Hipsey, M.R., 2022. A structured framework to interpret hydro-climatic and water quality trends in Mediterranean climate zones. Journal of Hydrology, 614, 128512.

Allen, C.D., Macalady, A.K., Chenchouni, H., Bachelet, D., McDowell, N., Vennetier, M., Kitzberger, T., Rigling, A., Breshears, D.D., Hogg, E.H., Gonzalez, P., Fensham, R., 2010. Forest Ecology and Management, 259(4), pp. 660-684.

Allocca, V., Manna, F., De Vita, P., 2014. Estimating annual groundwater recharge coefficient for karst aquifers of the Southern Apennines (Italy). Hydrology and Earth System Sciences, 18(2), 803-817.

Amorosi, A., 1997. Miocene shallow-water deposits of the northern Apennines: a stratigraphic marker across a dominantly turbidite foreland-basin succession. Geologie en Mijnbouw, Netherlands Journal of Geosciences, 75, 295-307.

Arrhenius, S., 1896. On the Influence of Carbonic Acid in the Air upon the Temperature of the Ground. Philosophical Magazine and Journal of Science, 5(41), 237-276.

Balaram, V., Copia, L., Kumar, U.S., Miller, J., Chidambaram, S., 2023. Pollution of water resources and application of ICP-MS techniques for monitoring and management—A comprehensive review. Geosystems and Geoenvironment, 2(4), 100210.

Barbieri, M., Barberio, M.D., Banzato, F., Billi, A., Boschetti, T., Franchini, S., Gori, F., Petitta, M., 2023. Climate change and its effect on groundwater quality. Environmental Geochemistry and Health, 45(4), 1133-1144.

Bettelli, G., Boccaletti, M., Cibin, U., Panini, F., Poccianti, C., Rosselli, S., Sani, F., Catanzariti, R., Fioroni, C., Fornaciari, E., Fregni, P., Di Giulio, A., Benvenuti, M., Gasperini, P., Martelli, L., 2005. Note Illustrative della Carta Geologica d'Italia alla scala 1:50.000. Foglio 252 - Barberino di Mugello. A cura di Regione Toscana, ISPRA.

Blake, D., Mlisa, A., Hartnady, C., 2010. Large scale quantification of aquifer storage and volumes from the Peninsula and Skurweberg Formations in the southwestern Cape. Water SA, Cape Town, 36(2), 177-184.

Boccaletti, M., Elter, P., Guazzone, G., 1971. Plate Tectonic Models for the Development of the Western Alps and Northern Apennines. Nature Physical Science, 234, 108-111.

Boccaletti, M., Conedera, C., Dainelli, P., Gočev, P., 1982. The recent (Miocene-Quaternary) regmatic system of the western Mediterranean Region: A New Model of Ensialic Geodynamic Evolution, in a Context of Plastic/Rigid Deformation. Journal of Petroleum Geology, 5(1), 31-49.

Bucci, F., Santangelo, M., Fongo, L., Alvioli, M., Cardinali, M., Melelli, L., Marchesini, I., 2022. A new digital lithological map of Italy at the 1:100000 scale for geomechanical modelling. Earth System Science Data, 14(9), 4129-4151.

Caloiero, T., Caloiero, P., Frustaci, F., 2018. Long-term precipitation trend analysis in Europe and in the Mediterranean basin. Water and Environment Journal, 32, 433-445.

Canora, F., Rizzo, G., Panariello, S., Sdao, F., 2019. Hydrogeology and hydrogeochemistry of the lauria mountains northern sector groundwater resources (basilicata, italy). Geofluids, 1-16.

Cardell, M.F., Amengual, A., Romero, R., Ramis, C., 2020. Future extremes of temperature and precipitation in Europe derived from a combination of dynamical and statistical approaches. International Journal of Climatology, 40(11), 4800-4827.

Carmignani, L., Kligfield, R., 1990. Crustal extension in the northern Apennines: The transition from compression to extension in the Alpi Apuane Core Complex. Tectonics, 9(6), 1275-1303.

Carmignani, L., Decandia, F.A., Fantozzi, P.L., Lazzarotto, A., Liotta, D., Meccheri, M., 1994. Tertiary extensional tectonics in Tuscany (Northern Apennines, Italy). Tectonophysics, 238(1-4), 295-310, 313-315.

Celico, P., Russo, D., 1981. Studi idrogeologici sulla Piana del Dragone (Avellino). Bollettino della Società dei Naturalisti, 90, 37-50.

Cervi, F., Petronici, F., Castellarin, A., Marcaccio, M., Bertolini, A., Borgatti, L., 2018. Climate-change potential effects on the hydrological regime of freshwater springs in the Italian Northern Apennines. Science of the Total Environment, 622-623, 337-348.

Channell, J.E.T., Horváth, F., 1976. The African/Adriatic promontory as a palaeogeographical premise for alpine orogeny and plate movements in the Carpatho-Balkan region. Tectonophysics, 35(1-3), 71-101.

Chen, Z., Grasby, S.E., Osadetz, K.G., 2004. Relation between climate variability and groundwater levels in the upper carbonate aquifer, southern Manitoba, Canada. Journal of Hydrology, 290(1-2), 43-62.

Chiaudani, A., Di Curzio, D., Rusi, S., 2019. The snow and rainfall impact on the Verde Spring behavior: A statistical approach on hydrodynamic and hydrochemical daily time-series. Science of the Total Environment, 689, 481-493.

Coppola, L., Cotecchia, V., Lattanzio, M., Salvemini, A., Tadolini, T., Ventrella, N.A., 1989. Il gruppo di sorgenti di Cassano Irpino: regime idrologico ed analisi strutturale del bacino di alimentazione. Geologia Applicata e Idrogeologia, 24, 227-260.

Corniello, A., Ducci, D., Aquino, A., 2010. Hydrogeological map of the Monti Picentini Regional Park (Southern Italy) at 1: 50,000 scale. Bollettino di Geofisica Teorica ed Applicata, 51(4), 325-343, ISSN: 0006-6729.

Corriere della Sera, 2023. Acqua, italiani tra i più spreconi in Europa ma iniziano a cambiare le abitudini, [https://www.corriere.it/economia/consumi/23_marzo_21/acqua-italiani-piu-spreconi-europa-ma-iniziano-cambiare-abitudini-38103aaa-c7da-11ed-b48b-1072850ccecb.shtml]. Alessia Conzonato, Corriere della Sera, 'L'Economia - Risparmi, Mercati, Imprese', Milano, 21 March 2023.

Cosentino, D., Cipollari, P., Marsili, P., Scrocca, D., 2010. Geology of the central Apennines: A regional review. Journal of the Virtual Explorer, 36.

De Vita, P., Allocca, V., Manna, F., Fabbrocino, S., 2012. Coupled decadal variability of the North Atlantic Oscillation, regional rainfall and karst spring discharges in the Campania region (Southern Italy). Hydrology and Earth System Sciences, 16(5), 1389-1399.

Di Curzio, D., Rusi, S., Di Giovanni, A., Ferretti, E., 2021. Evaluation of groundwater resources in minor plio-pleistocene arenaceous aquifers in central Italy. Hydrology, 8(3), 121.

Di Matteo, L., Dragoni, W., Maccari, D., Piacentini, S.M., 2016. A contribution to the definition of the ongoing climate change and its impacts on the water resources: The case of Monte Fumaiolo (Central Italy). Rendiconti Online Societa Geologica Italiana, 41, 46-49.

Di Nunno, F., Granata, F., Gargano, R., de Marinis, G., 2021. Prediction of spring flows using nonlinear autoregressive exogenous (NARX) neural network models. Environmental Monitoring and Assessment, 193(6), 350.

Diodato, N., Bellocchi, G., Fiorillo, F., Ventafridda, G., 2017. Case study for investigating groundwater and the future of mountain spring discharges in Southern Italy. Journal of Mountain Science, 14(9), 1791-1800.

Diodato, N., Ljungqvist, F.C., Fiorillo, F., Esposito, L., Ventafridda, G., Bellocchi, G., 2022. Climatic fingerprint of spring discharge depletion in the southern Italian Apennines from 1601 to 2020 CE. Environmental Research Communications, 4(12), 125011.

Döll, P., Hoffmann-Dobrev, H., Portmann, F.T., Siebert, S., Eicker, A., Rodell, M., Strassberg, G., Scanlon, B.R., 2012. Impact of water withdrawals from groundwater and surface water on continental water storage variations. Journal of Geodynamics, 59-60, 143-156.

Doveri, M., Nisi, B., Cerrina Feroni, A., Ellero, A., Menichini, M., Lelli, M., Masetti, G., Da Prato, S., Principe, C., Raco, B., 2012. Geological, hydrodynamic and geochemical features of the volcanic aquifer of Monte Amiata (Tuscany, central Italy): an overview. Acta Vulcanologica, 23, 51-72.

Essa, Y.H., Hirschi, M., Thiery, W., El-Kenawy, A.M., Yang, C., 2023. Drought characteristics in Mediterranean under future climate change. npj Climate and Atmospheric Science, 6(1), 133.

Ferguson, G., Gleeson, T., 2012. Vulnerability of coastal aquifers to groundwater use and climate change. Nature Climate Change 2, 342-345.

Filippini, M., Segadelli, S., Dinelli, E., Failoni, M., Stumpp, C., Vignaroli, G., Casati, T., Tiboni, B., Gargini, A., 2024. Hydrogeological assessment of a major spring discharging from a calcarenitic aquifer with implications on resilience to climate change. Science of The Total Environment, 913, ISSN 0048-9697.

Fiorillo, F., 2009. Spring hydrographs as indicators of droughts in a karst environment. Journal of Hydrology, 373, 290-301.

Fiorillo, F., Guadagno, F.M., 2012. Long karst spring discharge time series and droughts occurrence in Southern Italy. Environmental Earth Sciences, 65(8), 2273-2283.

Fiorillo, F., Petitta, M., Preziosi, E., Rusi, S., Esposito, L., Tallini, M., 2015. Long-term trend and fluctuations of karst spring discharge in a Mediterranean area (central-southern Italy). Environmental Earth Sciences, 74(1), 153-172.

Fiorillo, F., Esposito, L., Pagnozzi, M., Ciarcia, S., Testa, G., 2018. Karst springs of Apennines typified by upwelling flux. Acque Sotterranee - Italian Journal of Groundwater, 7(4), 21-30.

Fiorillo, F., Leone, G., Pagnozzi, M., Esposito, L., 2021. Long-term trends in karst spring discharge and relation to climate factors and changes. Hydrogeology Journal, 29(1), 347-377.

Fourier, J.B.J., 1824. Remarques générales sur les temperatures du globe terrestre et des espaces planétaires. Annales de Chimie et de Physique (Paris), deuxième série, 27, 136-167.

Fourier, J.B.J., 1827. Mémoire sur les températures du globe terrestre et des espaces planétaires. Mémoires de l'Académie des Sciences, deuxième série, 7, 569-604.

Frondini, F., Caliro, S., Cardellini, C., Chiodini, G., Morgantini, N., 2009. Carbon dioxide degassing and thermal energy release in the Monte Amiata volcanic-geothermal area (Italy). Applied Geochemistry, 24(5), 860-875.

Gaba E., 2009 (licensed under GFDL/CC-BY-SA). Italy topographic map. Sources of data: SRTM30 Plus, NGDC World Data Bank II, UN Cartographic section, and regions boundaries created from File.svg by NordNordWest.

Gandelli, S., 2022. La rete idrica italiana è un colabrodo: il 36% dell'acqua viene persa lungo il tragitto [Italy's water supply network is highly inefficient, with 36% of water lost along its distribution routes]. Fonti d'acqua dolce, Geopop.

García-Ruiz, J.M., López-Moreno, J.I., Vicente-Serrano, S.M., Lasanta-Martínez, T., Beguería, S., 2011. Mediterranean water resources in a global change scenario. Earth-Science Reviews, 105(3-4), 121-139.

Garreaud, R.D., Alvarez-Garreton, C., Barichivich, J., Pablo Boisier, J., Christie, D., Galleguillos, M., LeQuesne, C., McPhee, J., Zambrano-Bigiarini, M., 2017. The 2010-2015 megadrought in central Chile: Impacts on regional hydroclimate and vegetation. Hydrology and Earth System Sciences, 21(12), 6307-6327.

Gentilucci, M., Pambianchi, G., 2022. Prediction of Snowmelt Days Using Binary Logistic Regression in the Umbria-Marche Apennines (Central Italy). Water (Switzerland), 14(9), 1495.

Giorgi, F., 2006. Climate change hot-spots. Geophysical Research Letters, 33, L08707.

Giorgi, F., Lionello, P., 2008. Climate change projections for the Mediterranean region. Global and Planetary Change, 63(2-3), 90-104.

Grimaldi, S., Leone, D., Summa, G., 2008. Studio sui caratteri idrogeologici, idrogeochimici e quantitativi della principale sorgente del massiccio del M.te Pollino: Sorgente del Mercure (Basilicata, Italia Meridionale) [Hydrogeological, hydrogeochemical and quantitave features of the main spring of the mount Pollino massif: The Mercure Spring (Baslicata, Southern Italy)]. Rendiconti Online Societa Geologica Italiana, 3(2), 458-459.

Halder, S., Sahoo, S., Hazra, T., Debsarkar, A., 2024. Studies on Impacts of Land Use/Land Cover Changes on Groundwater Resources: A Critical Review. Environmental Science and Engineering, Part F2387, 143-170.

Il Manifesto, 2024. Siccità e condutture colabrodo, l'Abruzzo in emergenza idrica, [https://ilmanifesto.it/siccita-e-condutture-colabrodo-labruzzo-in-emergenza-idrica]. Serena Giannico, Il Manifesto, Chieti, 21 July 2024.

Il Messaggero, 2024. Emergenza idrica, sorgenti al collasso. Tavolo in Prefettura, [https://www.primopianomolise.it/attualita/136823/emergenza-idrica-sorgenti-al-collasso-tavolo-in-prefettura/]. 'Primo Piano Molise' in Il Manifesto, Campobasso, 10 July 2024.

IPCC, 2023. Climate Change 2023: Synthesis Report. Contribution of Working Groups I, II and III to the Sixth Assessment Report of the Intergovernmental Panel on Climate Change [Core Writing Team, H. Lee and J. Romero (eds.)]. Geneva, Switzerland, 35-115.

ISPRA, 2020. Le risorse idriche nel contesto geologico del territorio italiano. Disponibilità, grandi dighe, rischi geologici, opportunità. Istituto Superiore per la Protezione e la Ricerca Ambientale, Rapporti 323/2020, ISBN 978-88-448-1011-5.

Istat, 2022. Le statistiche dell'Istat sull'acqua, anni 2019-2022. Statistiche Report, Istituto nazionale di STATistica, 21-3-22. https://www.istat.it/it/files/2022/03/REPORTACQUA2022.pdf.

Kalhor, K., Ghasemizadeh, R., Rajic, L., Alshawabkeh, A., 2019. Assessment of groundwater quality and remediation in karst aquifers: A review. Groundwater for Sustainable Development, 8, 104-121.

Kottek, M., Grieser, J., Beck, C., Rudolf, B., Rubel, F., 2006. World map of the Köppen-Geiger climate classification updated. Meteorologische Zeitschrift, 15(3), 259-263.

Kundzewicz, Z.W., Döll, P., 2009. Will groundwater ease freshwater stress under climate change? Hydrological Sciences Journal, 54, 665-675.

Leone, G., Pagnozzi, M., Catani, V., Ventafridda, G., Esposito, L., Fiorillo, F., 2021. A hundred years of Sanità Spring discharge measurements: trends and statistics for understanding water resource availability under climate change. Stochastic Environmental Research and Risk Assessment, 35(2), 345-370.

Livezey, R.E., Vinnikov, K.Y., Timofeyeva, M.M., Tinker, R., van den Dool, H.M., 2007. Estimation and extrapolation of climate normals and climatic trends. Journal of Applied Meteorology and Climatology, 46(11), 1759-1776.

Magi, F., Doveri, M., Menichini, M., Minissale, A., Vaselli, O., 2019. Groundwater response to local climate variability: hydrogeological and isotopic evidences from the Mt. Amiata volcanic aquifer (Tuscany, central Italy). Rendiconti Lincei, 30(1), 125-136.

Marroni, M., Monechi, S., Perilli, N., Principi, G., Treves, B., 1992. Late Cretaceous flysch deposits of the Northern Apennines, Italy: age of inception of orogenesis-controlled sedimentation. Cretaceous Research, 13(5-6), 487-504.

Meinzer, O.E., 1923. Outline of groundwater hydrology with definitions. In: US Geological Survey Water-Supply Paper. 494, 48-54.

Mirgol, B., Dieppois, B., Northey, J., Eden, J., Jarlan, L., Khabba, S., Le Page, M., Mahe, G., 2024. Future changes in agrometeorological extremes in the southern Mediterranean region: When and where will they affect croplands and wheatlands? Agricultural and Forest Meteorology, 358.

Molli, G., 2008. Northern Apennine-Corsica orogenic system: An updated overview. Geological Society Special Publication, 298, 413-442.

Nanni, T., Rusi, S., 2003. Idrogeologia del massiccio carbonatico della montagna della Majella (Appennino centrale) [Hydrogeology of the Montagna della Majella carbonate massif (Central Apennines - Italy)]. Bollettino della Società Geologica Italiana, 122, 173-202.

Navarra, A., Philander, G., 2016. Weathering global climate change. World Scientific Series on Asia-Pacific Weather and Climate, 7, 305-312.

Nicholson, K.N., Neumann, K., Dowling, C., Gruver, J., Sherman, H., Sharma, S., 2018. An Assessment of Drinking Water Sources in Sagarmatha National Park (Mt Everest Region), Nepal. Mountain research and development, 38(4), 353-363.

Oksana, T., Dmytro, G., 2021. Earth's Water Distribution. In: Leal Filho, W., Azul, A.M., Brandli, L., Lange Salvia, A., Wall, T. (Eds), Clean Water and Sanitation. Encyclopedia of the UN Sustainable Development Goals. Springer, Cham, Switzerland.

Pagnozzi, M., Fiorillo, F., Esposito, L., Leone, G., 2019. Hydrological features of endorheic areas in southern Italy. Italian Journal of Engineering Geology and Environment, Special Issue 1, 85-91.

Patacca, E., Scandone, P., 2007. Geology of the Southern Apennines. Bollettino della Società Geologica Italiana, Supplemento, 7, 75-119.

Petitta, M., Tallini, M., 2002. Groundwater hydrodinamic of the Gran Sasso Massif (Abruzzi): New hydrological, hydrogeological and hydrochemical surveys (1994-2001). Bollettino della Societa Geologica Italiana, 121(3), 343-363.

Petitta, M., Banzato, F., Lorenzi, V., Matani, E., Sbarbati, C., 2022. Determining recharge distribution in fractured carbonate aquifers in central Italy using environmental isotopes: snowpack cover as an indicator for future availability of groundwater resources. Hydrogeology Journal, 30(5), 1619-1636.

Petronici, F., Pujades, E., Jurado, A., Marcaccio, M., Borgatti, L., 2019. Numerical modelling of the Mulino Delle Vene Aquifer (Northern Italy) as a tool for predicting the hydrogeological system behavior under different recharge conditions. Water (Switzerland), 11(12), 2505.

Sappa, G., Ferranti, F., Iacurto, S., De Filippi, F.M., 2018. Effects of climate change on groundwater feeding the Mazzoccolo and Capodacqua di Spigno Springs (Central Italy): First quantitative assessments. International Multidisciplinary Scientific GeoConference Surveying Geology and Mining Ecology Management, SGEM, 18(3.1), 219-226.

Sappa, G., De Filippi, F.M., Ferranti, F., Iacurto, S., 2019. Environmental issues and anthropic pressures in coastal aquifers: A case study in Southern Latium Region. Acque Sotterranee - Italian Journal of Groundwater, 8, 47-51.

Scanlon, B.R., Faunt, C.C., Longuevergne, L., Reedy, R.C., Alley, W.M., McGuire, V.L., McMahon, P.B., 2012. Groundwater depletion and sustainability of irrigation in the US High Plains and Central Valley. Proceedings of the National Academy of Sciences of the United States of America, 109(24), 9320-9325.

Scoccimarro, E., Navarra, A., 2022. Precipitation and temperature extremes in a changing climate. Hydrometeorological Extreme Events and Public Health, Chapter 2, 3-25. John Wiley & Sons, Inc., New York, United States of America.

Simsek, C., Elci, A., Gunduz, O., Erdogan, B., 2008. Hydrogeological and hydrogeochemical characterization of a karstic mountain region. Environmental Geology, 54, 291-308.

Small, C., Nicholls, R.J., 2003. A global analysis of human settlement in coastal zones. Journal of Coastal Research, 19, 584-599.

Stone, A., Lanzoni, M., Smedley, P., 2019. Groundwater resources: past, present, and future. In: Dadson, S.J., Garrick, D.E., Penning-Rowsell, E.C., Hall, J.W., Hope, R., Hughes, J. (Eds.), Water Science, Policy, and Management: A Global Challenge, 29-54. John Wiley & Sons, Inc., New York, United States of America.

Taylor, R.G., Scanlon, B., Döll, P., Rodell, M., Van Beek, R., Wada, Y., Longuevergne, L., Leblanc, M., Famiglietti, J.S., Edmunds, M., Konikow, L., Green, T.R., Chen, J., Taniguchi, M., Bierkens, M.F.P., Macdonald, A., Fan, Y., Maxwell, R.M., Yechieli, Y., Gurdak, J.J., Allen, D.M., Shamsudduha, M., Hiscock, K., Yeh, P.J.-F., Holman, I., Treidel, H., 2013. Ground water and climate change. Nature Climate Change, 3(4), 322-329.

Tazioli, A., Colombani, N., Palpacelli, S., Mastrocicco, M., Nanni, T., 2020. Monitoring and modelling interactions between the montagna dei fiori aquifer and the castellano stream (Central Apennines, Italy). Water (Switzerland), 12(4), 973.

Tozzi, M., De Corso, S., Antonucci, A., Di Luzio, E., Lenci, F., Scrocca, D., 1999. Assetto geologico della Montagnola di Frosolone. Geologica Romana, 35, 89-109.

Troll, C., Paffen, K.H., 1963. Jahreszeitenklimate der Erde. In: Rodenwaldt, E., Jusak, H.J. (Hrsg): Weltkarten zur Klimakunde, 7-28, Berlin.

UniBo and RER for Gruppo Hera, 2023. Progettazione idrogeologica, basata su indagini in situ, monitoraggio e modellazione numerica, di scenari di ottimizzazione/potenziamento della captazione di acque sotterranee nei punti di prelievo hera di Tolè (Comune di Vergato) e Arpolli (Comuni di Gaggio Montano e Montese) e di analisi della vulnerabilità idrogeologica del sistema sorgentizio Acquaretto-Vergatello (Comune di Castel d'Aiano). Final Report by UniBo and RER (Regione Emilia-Romagna) for the Scientific Collaboration with Gruppo Hera, authored by: Gargini, A., Filippini, M., Landi, L., Casati, T., Segadelli, S., 31 January 2023.

Van Loon, A.F., Tijdeman, E., Wanders, N., Van Lanen, H.A.J., Teuling, A.J., Uijlenhoet, R., 2014. How climate seasonality modifies drought duration and deficit. Journal of Geophysical Research, 119(8), 4640-4656.

Vecchi, A., 1920. La sorgente di Rosola e la sua derivazione per l'acquedotto modenese (the Rosola spring and its uptake for the Modena aqueduct). In: Italian, Giornale del Genio Civile. Genio Civile, Rome.

Wada, Y., 2016. Modeling Groundwater Depletion at Regional and Global Scales: Present State and Future Prospects. Surveys in Geophysics, 37, 419-451.

Xanke, J., Liesch, T., 2022. Quantification and possible causes of declining groundwater resources in the Euro-Mediterranean region from 2003 to 2020. Hydrogeology Journal, 30, 379-400.

Chapter 2:

Hydrogeological assessment of a major spring discharging from a calcarenitic aquifer with implications on resilience to climate change

2.1. Preface

The first research question of this PhD project, which primarily aims to quantify the long-term effects of climate change on spring discharge, also involves estimating the resilience of Nadìa Spring to climate change. Among the investigated springs, Nadìa Spring is particularly notable. Comparing the average discharge from 100 years ago to the present day, there has been a significant decline (on average roughly 40%), yet the spring remains the primary contributor to discharge in the Bologna and Modena Apennines. It continues to play a critical role in the public water supply managed by Gruppo Hera S.p.A., still providing approximately 50 L/s during the low-flow season, a remarkable quantity compared to many smaller neighbouring springs. Why is it so resilient to climate change? What factors contribute to a spring's resilience to climatic variations? As a complementary task to this PhD project and closely aligned with the analysis of the climate change effects on spring discharge, I participated in research focused on the resilience of Nadìa Spring, coordinated by my co-supervisor, Maria Filippini.

This chapter summarises and presents the multidisciplinary approach employed to study Nadìa Spring. In the final section of the chapter, following the article references, a detailed discussion on the frequency and severity of droughts in the Emilia-Romagna Apennines will be included, highlighting the substantial reduction in spring discharge to which they have contributed over the past century. The chapter consists primarily of a paper edited in the journal *Science of the Total Environment*: Filippini, M.[1], Segadelli, S.[2], Dinelli, E.[1], Failoni, M.[1], Stumpp, C.[3], Vignaroli, G.[1], Casati, T.[1], Tiboni, B.[1], Gargini, A.[1], 2024. Hydrogeological assessment of a major spring discharging from a calcarenitic aquifer with implications on resilience to climate change, STOTEN, 913, 169770, ISSN 00489697, https://doi.org/10.1016/j.scitotenv.2023.169770.

[1] Department of Biological, Geological, and Environmental Sciences - BiGeA, Alma Mater Studiorum University of Bologna, via Zamboni 67, 40126, Bologna, Italy
[2] Geological, Seismic and Soil Service, Emilia-Romagna Region Administration, Viale della Fiera 8, 40127, Bologna, Italy
[3] Department of Water, Atmosphere and Environment, University of Natural Resources and Life Sciences, Muthgasse 18, 1190, Vienna, Austria

2.2. Highlights, Graphical abstract, and Keywords

- Spring yield is due to geometrical and structural reasons, instabilities, dissolution.
- Dual porosity (quick-flow conduits and diffuse fractures) impacts the spring behavior.
- Resilient to climate change, Nadìa maintains stable discharge and water composition.
- Historical hydrographs reveal evolving behavior and increased interdecadal resilience.
- The study serves as a valuable assessment-model for similar water discharge points.

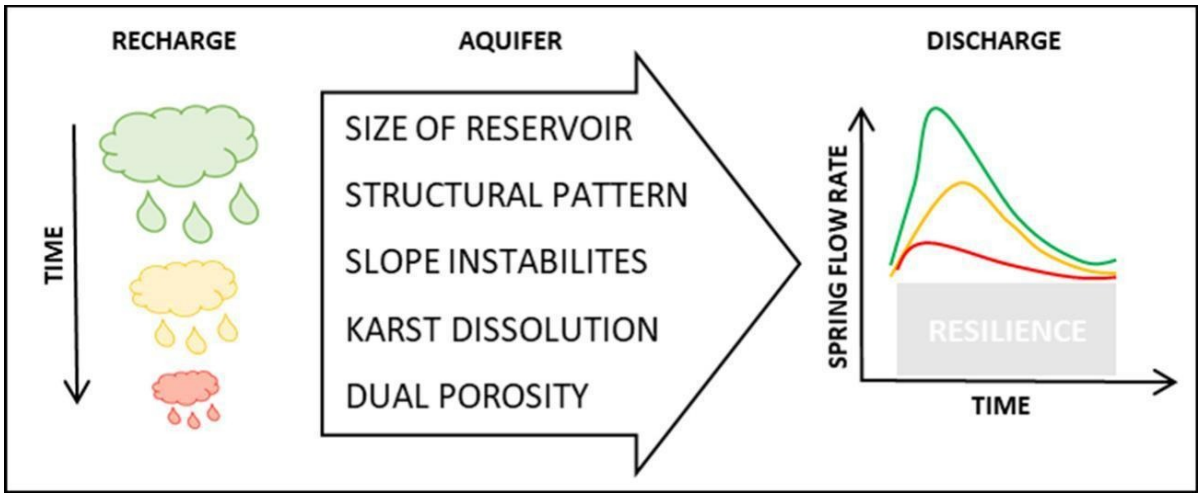

Spring discharge, Recharge decrease, Resilience, Fractured aquifer, Northern Apennines

2.3. Abstract

Groundwater is a vital source of freshwater, serving ecological, environmental, and societal needs. In regions with springs as a predominant source, such as the Northern Apennines (Italy), resilience of these springs to climate-induced recharge changes is crucial for water supply and ecosystem preservation. In this study, Nadìa Spring in the Northern Apennines is examined through an unprecedented array of multidisciplinary analyses to understand its resilience and unique characteristics. The Nadìa Spring's exceptional response, characterized by a sustained base flow even in the face of drought, is attributed to a combination of factors including a substantial groundwater reservoir, a complex network of faults/fractures, slope instabilities, and karst dissolution. The investigation reveals a dual porosity system in the aquifer, consisting of fast-flow conduits and a diffuse fracture network. While fast-flow conduits contribute to rapid responses during high-flow conditions, the diffuse system becomes predominant during low-flow periods. This dual porosity structure helps the spring maintain a consistent base flow in the face of climate-induced recharge fluctuations. The study shows that Nadìa Spring exhibits remarkable resilience to year-to-year variations in recharge, as evidenced by stable minimum discharge

values. While the spring has undergone a decline in discharge over the past century due to long-term climate change, it is becoming more resilient over interdecadal timescales due to transition to a diffuse drainage system that mitigates the impact of reduced recharge. The availability of a century-long spring discharge monitoring was a crucial piece of information for understanding the spring's discharge response and drawing conclusions about its long-term resilience to recharge fluctuations. Continuing long-term monitoring and research in the future will be essential to validate and expand upon these findings in the context of changing climatic conditions. This research serves as a model for assessing strategic groundwater discharge points in geological settings similar to the Northern Apennines.

2.4. Introduction

Groundwater is a primary source of freshwater and provides essential ecosystem services by supporting ecological and environmental flows, as well as sustaining Groundwater Dependent Ecosystems (GDEs; Cantonati et al., 2020; Stevens et al., 2022). Moreover, it plays a pivotal part in meeting societal needs, serving as a fundamental supply for drinking, agricultural and industrial purposes (Abderrahman, 2005; Tsur, 1990). Groundwater is progressively gaining significance as a strategic asset during periods of drought, as it boasts substantial reserves within suitable geological settings (Grönwall and Oduro-Kwarteng, 2018; Kruse and Eslamian, 2017) and appears to withstand the impacts of climate change better than surface water (Liesch and Wunsch, 2019; Taylor et al., 2013).

Groundwater exploitation predominantly occurs through well extraction or through the uptake of natural springs discharge. The latter approach is prevalent in mountainous regions, where springs generally offer high-quality, gravity-fed water due to minimal anthropogenic impacts on the groundwater system compared to urbanized/industrialized lowland or coastal areas (Nicholson et al., 2018; Simsek et al., 2008). However, the anticipated decrease of discharge, stemming from reduced recharge due to global warming and alterations in seasonal patterns of solid and liquid precipitation (Amanambu et al., 2020; Atawneh et al., 2021; Caloiero et al., 2018; Dore, 2005; Kundzewicz and Doli, 2009; Riedel and Weber, 2020; Tambe et al., 2012; Weissinger et al., 2016), can yield supply-related challenges in these regions. As such, it becomes essential to identify springs resilient to recharge decrease.

Resilience is defined in recent hydrogeological literature as “the ability of the system to maintain groundwater reserves in spite of major disturbances” (Sharma and Sharma, 2006), or as “the adaptive capacity of a system to a change generated by external pressures while maintaining certain vital functions” (Herrera-Franco et al., 2020). The discharge resilience to drought-induced recharge decrease is the capacity of a spring system to sustain its flow during periods of low

recharge by releasing groundwater stored during intermittent periods of higher recharge, while avoiding irreversible depletion of the spring reservoir.

The resilience of a hydrogeological system can be studied by examining both how the groundwater responds to specific stresses and the characteristics of the geological medium that affect resilience (Cuthbert et al., 2019; De la Hera-Portillo et al., 2020). Most previous studies on groundwater resilience have focused on trend analyses of aquifer recharge, groundwater storage, hydraulic heads, and discharge, while relatively few studies have considered different aquifer characteristics such as lithology and permeability, saturated thickness and transmissivity, or geometrical properties of the fracture network (Zeydalinejad, 2023).

When examining groundwater resilience to climate-related stresses, both long-term (decadal) climate change trends, and short-term (less than one year) stresses must be taken into account (MacDonald et al., 2011). Some authors have focused on analyzing the millennium-scale resilience of discharge, e.g. the fossil aquifers recharged during the last glaciation that now represent vast groundwater reservoirs no longer being replenished or with a direct recharge lower than 5 mm/yr (Ram et al., 2020; Sultan et al., 2019). However, the acceleration of water crises in the first glimpse of this millenium demands an analysis on shorter timescales, spanning centuries or decades, tied to resource management challenges. Yet, monitoring data are often unavailable for such time-spans, as already highlighted by Liesch and Wunsch (2019) regarding hydraulic heads. Research that investigates the effects of recharge changes on spring discharge using extensive historical datasets is rare and often restricted to large karst aquifers (e.g., Fiorillo et al., 2021). Indeed, these aquifers have long been of interest due to their socio-economic relevance related to high water yields (Ford and Williams, 2007; Kresic and Stevanovic, 2010) unfortunately associated to a high vulnerability to climate changes and pollution (Butscher and Huggenberger, 2009; Campanale et al., 2022; Kačaroğlu, 1999; Mimi and Assi, 2009).

Other types of aquifers, such as those in fractured sedimentary or hard-rock strata, are less studied compared to karst, having a lower permeability and a limited storage capacity (Lachassagne, 2008; Lachassagne et al., 2011; Mézquita González et al., 2021). In mountainous regions dominated by these aquifers, springs are generally highly vulnerable to discharge decrease during drought periods due to a limited extension of the associated groundwater flow systems with constrained underground pathways and rapid loading and unloading. An example is the Northern Apennines belt (Italy), where the supply of drinking water derives from numerous low-yield springs fed by sedimentary fractured aquifers that renew stored groundwater almost completely every hydrological year (Cervi et al., 2018; Gargini et al., 2008; Petronici et al., 2019; Segadelli et al., 2021). In this setting, identifying strategic resources with peculiar resilience to recharge decreases becomes crucial to manage recurring water shortage crises. Indeed, these crises often lead to conflicts between the demand for drinking water, which may necessitate

supplementary supply measures such as water tankers, and the preservation of GDEs (e.g., Cantonati et al., 2016).

Here, we investigated Nadìa Spring (Emilia Romagna Region, Northern Apennines), which stands out as a peculiarly substantial resource compared to other springs within the same context. Through a comprehensive array of analyses—including geological, hydrogeological, geochemical, isotopic, and tracer tests—tour study pursues several objectives: (1) unraveling the connection between recharge dynamics and discharge patterns across various time scales; (2) assessing the resilience of the spring discharge in response to past and anticipated recharge fluctuations; and (3) demonstrating the potential of integrated multidisciplinary analyses to identify recharge-discharge dynamics associated with spring resilience. To our knowledge, such an extensive set of analyses has not been previously employed in investigating strategic spring resources. Therefore, this study serves as a paradigm, offering insights into the definition of key evaluation tools and indicators for assessing spring resilience amid declining recharge in analogous geological settings.

2.5. Geological and hydrogeological setting

Nadìa Spring is situated in the Emilia Romagna Region (Italy) at an elevation of 555 m above sea level (asl) (44°19’09” N; 10°58’14” E), nearby the morphologic divide of the Northern Apennines belt between the valleys of the Reno and Panaro Rivers (Fig. 2.1a). The Northern Apennines are a Neogene fold-thrust belt that formed from the continental collision between Adria micro-plate (part of African plate) and the Eurasia plate beginning ~35 Ma (Boccaletti et al., 2011; Carminati and Doglioni, 2012; Vai and Martini, 2001). The sector of the chain between the Reno and Panaro Rivers is affected by km-long fault systems with both Apennine (NW-SE) and anti-Apennine (SW-NE) trends (Balocchi, 2014; Stendardi et al., 2023).

The main feature of the area is a complex NE-SW-trending fault zone, approximately 25-30 km long, named the Val Lavino Structural System (VLSS) (Fig. 2.1a). The faults of the VLSS are mainly oriented N30°-40° (Capitani, 1997), and they display left-lateral strike-slip kinematics with evidence of a transpressive component. These faults involve and deform all the structural-stratigraphic array of units of the Northern Apennines, including the Epiligurian Domain (ED), a wedge-top basin formed atop an accretionary wedge progressively evolving into a fold-and-thrust belt (Conti et al., 2020). The ED consists mainly of large sandstone-dominated slabs or plates averaging between 5 and 30 km^2 and deposited on top of allochtonous Ligurian and Subligurian nappe units made of clay-rich lithotypes (Cibin et al., 2001).

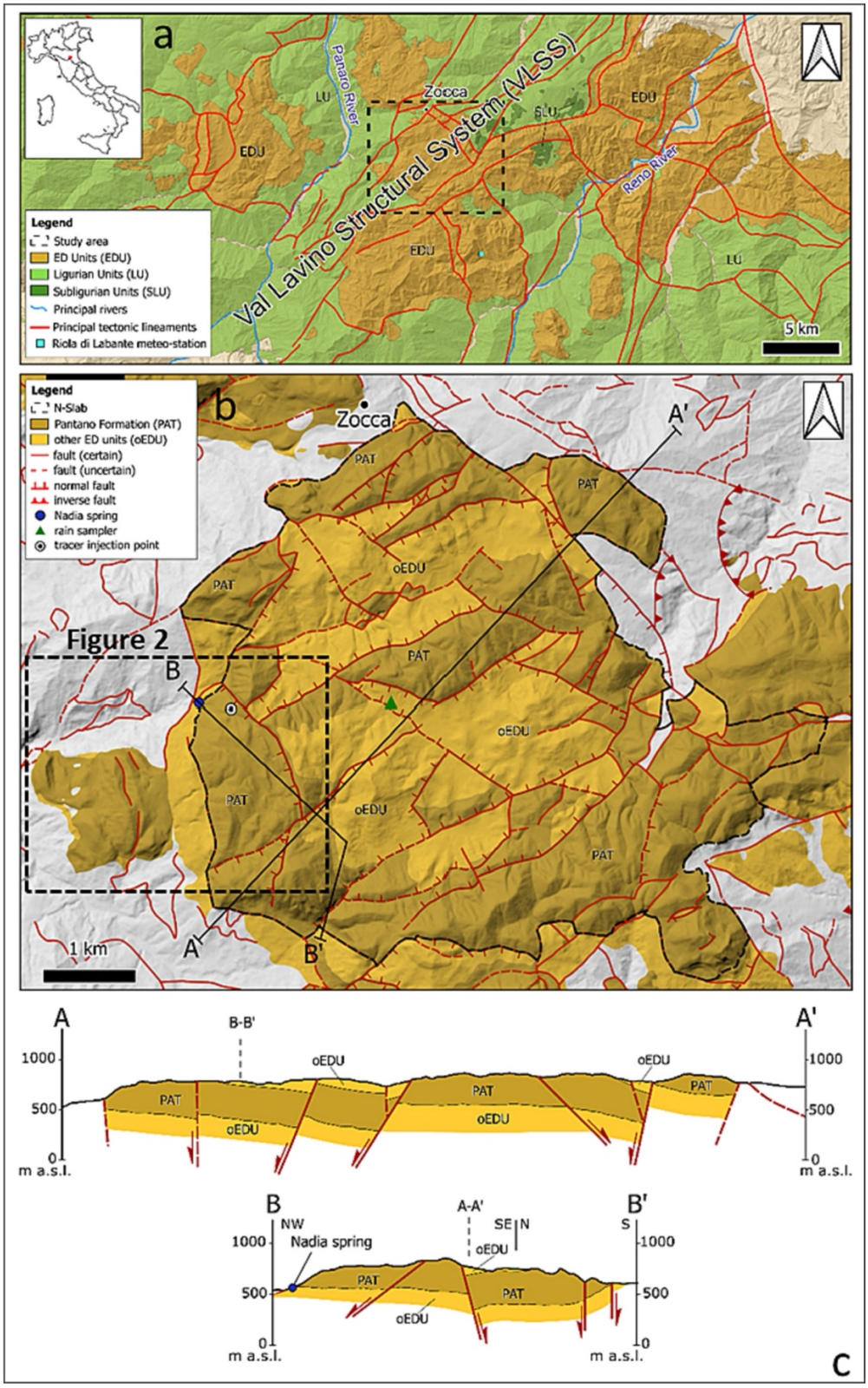

Fig. 2.1. Map of the research area: (a) geological setting of the Northern Apennines sector between the Panaro and the Reno rivers, with indication of the meteorological station of Riola di Labante; (b) geological setting of the N slab. The tracer injection point and the rain sampler for water isotopes are marked on the map. Black lines represent the traces of AA and BB geological cross sections, while the location of Fig. 2 (Fig. 2.2) is indicated by a dashed black line; (c) AA and BB geological cross sections of the N slab.

Nadìa Spring discharges at the western edge of an ED slab, referred to as “N slab”, which covers an area of 25.6 km^2 (Fig. 2.1b) with topographic elevation between 576 and 916 m asl (average elevation of 768 m asl). The N slab is tabular and gently monoclinalic (Fig. 2.1c), with bedding dipping between 10° and 40° to the east. Both anti-Apennine and Apennine strike faults affected the slab, showing strike-slip (left- and right-lateral, respectively) and subordinate normal kinematics. Balocchi (2014) interprets these faults as resulting from a “simple left shear” mechanism that induced an anticlockwise rotation of the structures. Subsequently, during a post-orogenic extensional event, these structures would have been reactivated as normal faults, forming structural highs and depressions resulting in a blocky pattern of the N slab.

The main aquifer of the N slab is the Pantano Formation (PAT), primarily composed of medium- to fine-grained calcareous sands deposited in a shallow marine environment between the upper Burdigalian and lower Langhian (Lower to Middle Miocene; Amorosi, 1997; Amorosi and Spadafora, 1995). PAT outcrops extensively over a 300 km^2 area in the Apennine reliefs southwest of Bologna and Reggio Emilia, representing one of the most productive groundwater reservoirs in the Northern Apennines and hosts several major springs in the region (Petronici et al., 2019). Unpublished borehole hydraulic filed tests performed by the authors in the PAT aquifer lithology few km far from the N-slab, indicate an aquifer transmissivity in the range of 0.001 and 0.004 m^2/s and a specific yield of 3.4%. The average groundwater saturated thickness of PAT in the N slab is approximately 190 m. Within the slab, various groundwater flow systems transfer direct recharge from precipitation to several discharge outlets, some of which are totally or partially up-taken by the local water supply company. Nadìa Spring stands as the largest discharge point in the slab, with an average discharge not lower than 40 L/s in the low-flow season, corresponding to IV class following Meinzer (1923). Meinzer classes ranging from V to VII characterize the other springs of the slab, corresponding to the most common classes in the Northern Apennines belt (Gargini et al., 2008).

The typical pattern of springs discharge in the sub-mediterranean area of the Northern Apennines is characterized by a peak during the spring season, following a rainy and snowy period from November to April (recharge season). An absolute discharge low is usually registered at the end of the hot and dry summer period of July-September (recession season) (Cervi et al., 2015; Gargini et al., 2008; Segadelli et al., 2021; Segadelli et al., 2017). However, increasingly frequent and intense droughts have occurred in the study area since the start of the XXI century, with a cycle of approximately five years (Peña-Angulo et al., 2022; Rakovec et al., 2022; Riedel and Weber, 2020). The most recent droughts were in years 2017 and 2022 when a significant decrease in precipitation was registered during the recharge season in association to a substantial increase of average annual temperature (ARPAE, 2018; ARPAE, 2023). These droughts

caused significant reduction of aquifer recharge that reflected in turn on a discharge decrease in many Northern Apennines springs, especially during the summer recession season, when the drinking water reaches a peak due to seasonal tourism.

2.6. Methods

2.6.1. Structural and geomorphological investigations

A geomorphological and structural field survey, integrated with publicly available aerial photographs (https://geoportale.regione.emilia-romagna.it/approfondimenti/database-topografico-regionale), was carried out in the N slab to identify and analyse those geological elements that may control the stratigraphic-structural setting of the N-slab and, consequently, the hydrogeological response of Nadìa Spring. The survey focused on structures affecting the ED domain, which more effectively register brittle deformation. The observed structural elements were divided in stratigraphic bedding, faults, and fractures/veins. The fault data were statistically analysed to obtain their main orientations. Moreover, continuous cores were drilled approximately 7 km south from Nadìa Spring within the same aquifer lithology as the N slab, as part of a separate research endeavour. Using acoustic and optical televiewer logs conducted along the uncased boreholes, it was possible to observe the distribution and size of open fractures. Details on coring and televiewer logging are in the Supplementary Material (SM).

2.6.2. Spring discharge

2.6.2.1. Discharge monitoring

Nadìa Spring is tapped through a slanting drainage tunnel 75 m long built between 1917 and 1920 (Vecchi, 1920). The tunnel has a concrete lining with openings on the walls allowing direct drainage of groundwater from the fracture's network of the aquifer. Part of the spring discharge is withdrawn by the local aqueduct company through a pumping system, which lifts water to main distribution tanks located at higher altitudes. The remaining discharge overflows in an open ditch outside the tunnel entrance that conveys water to a nearby stream. The flow rate withdrawn by the aqueduct is continuously monitored since 2017 through an electromagnetic flowmeter installed on the discharge pipe of the pumping system. The pumping flow rate varies every few hours, typically ranging from 20 to 50 L/s depending on the water demand from the aqueduct network. When the pumping rate is decreased, any excess discharge is released into the overflow ditch. The overflow discharge was monitored between December 2020 and March 2023. In detail, a pressure transducer (Hobo Onset water level data logger, U20L-04 model) was installed in the ditch to measure the water stage every 15 min. The relatively short 15-min

monitoring frequency was chosen since possible short-term responses of spring discharge to recharge events were unknown prior to this study and needed verification. An additional transducer placed outside of the water was used for atmospheric pressure compensation. Due to malfunctioning of the transducers, two significant registration gaps occurred from March 26th to April 3rd, 2021, and from May 29th to June 19th, 2022. To establish a rating curve for the channel, eight flow rate measurements were performed in various discharge conditions using an Acoustic Doppler Velocimeter (Flowtracker, SonTek/YSI Inc).

Due to random asynchronies between the two datasets, the sum of the withdrawn and overflow discharges was eventually calculated on daily averages and the resulting daily sums were further smoothed using a 5-day moving average in order to avoid false peaks.

2.6.2.2. Historical discharge data

Monthly monitoring of spring discharge was performed between January 1915 and October 1918, before the excavation of the tapping tunnel, through a thin plate contracted weir installed in a natural streambed originating at the spring outlet (Vecchi, 1920). The monthly amount of rainfall was monitored during the same time span at a meteorological station named “Montese” (920 m asl). This was the active station closest to the study area during the time-span covered by the historical monitoring. The historical data are shown in the SM.

This historical dataset of spring discharge, exceptionally rare in the global literature due to its century-long time span, allowed a unique comparison between the contemporary (2020−2022) and historical (1914-1918) spring hydrographs. The comparison focused on the spring's hydrodynamic response throughout each hydrologic year and on the evolution of discharge variability from past to present.

2.6.2.3. Recession analysis

The hydrologic recession of a spring refers to the final stage of the depletion limb of the hydrograph where discharge is solely contributed by groundwater from the aquifer with no perturbation induced by active direct recharge or fast-flow from the surface. This stage provides valuable information about a combination of intrinsic aquifer features, encompassing transmissive capacity (i.e. hydraulic conductivity) and storage capacity (i.e. storativity and size of the reservoir) (e.g. Azeez et al., 2015; Tague and Grant, 2004). The recession curves of the monitored hydrologic years 2020-21, 2021-22 and of the historic ones 1914-15, 1915-16, 1916-17, 1917-18 were analysed using the Maillet model (Maillet, 1905) which represents a linear approximation of the nonlinear quadratic spring reservoir depletion model proposed by

Boussinesq (1904). According to Maillet, the relationship between groundwater discharge and time follows the exponential decay of Eq. (2.1) in the absence of external influences, such as active recharge from precipitation, groundwater abstraction, or evapotranspiration affecting the saturated zone:

$$Q_t = Q_0 \, e^{-\alpha t} \qquad [2.1]$$

where Q_t and Q_0 are the flow rates (L^3/T) at time t (T) and at the beginning of the base-flow recession, respectively, and α is a constant (T^{-1}) representing storage lag-time. α is known as the "Maillet recession coefficient" and it is related to the time required to halve the recession discharge ($t_{0.5}$) as shown in Eq. 2.2:

$$\alpha = -[(\ln 0.5)/t_{0.5}] \qquad [2.2]$$

From a mathematical perspective, Eq. (2.1) has been described as the most convenient model for analysing spring recession in different geological settings, including karst (Cerino Abdin et al., 2021; Dewandel et al., 2003; Medici et al., 2023). Despite its simplicity, Eq. (2.1) has previously been shown to accurately represent the recession response of most Northern Apennines springs (Gargini et al., 2008; Segadelli et al., 2021).

For the six hydrographs analysed in this study, the recession curve was selected as the final linear segment of the depletion limb on a semi-log plot (i.e. Log Q VS time), resulting in varying starting times and durations among different years.

2.6.3. Hydrochemistry and water isotopes

High-frequency automatic groundwater sampling was performed between January 2022 and February 2023 using a programmable *ISCO series 3700* sampler. A total of 384 samples were collected every 12 or 24 h in 500 mL polypropylene bottles. The collection was interrupted for a total of 57 days distributed along the sampling period due to temporary malfunctioning of the sampler. Specific electrical conductivity (EC, compensated at 20 °C) and pH were measured in each sample with a HACH-HQ30D probe. 38 samples were selected within the period from January 19th, 2022, to November 23rd, 2022, for the analysis of major cations (Na^+, K^+, Ca^{2+}, Mg^{2+}). The samples were selected following a regular time step of approximately 7 days. Cations were analyzed by ICP-OES (Inductively Coupled Plasma – Optical Emission Spectroscopy) using an Agilent series 5800. The analysis was performed on filtered (0.45 μm) and acidified aliquots at the laboratory of the "Centro Ricerche Energia, Ambiente, Mare" located in Marina di Ravenna.

Seven additional groundwater samplings were performed at Nadìa Spring in June and November 2011, May and September 2014, May and August 2017, May and October 2021, for the analysis

of major cations and anions. The first six samples were collected and analysed in the Laboratories of Regional Environmental Protection Agency (ARPAE) following standardized procedures. The last two samples were collected for this study by filling a 250 mL bottle stored at 4 °C until analysis. The analysis was conducted in Laboratory of the GruppoHERA water company following the standard methods EPA 300.11997 and APAT-CNR-IRSA 29/2003 (sections 2010, 2090, 3010, 3020).

Four samplings were performed in February, June, September 2021, and January 2022 for stable water isotope analysis ($\delta^{18}O$ and $\delta^{2}H$). Samples were taken in 250 mL PET bottles from Nadìa Spring and from a rain sampler installed in the recharge area of the spring at an elevation of 752 m asl, for cumulated monthly rainfall collection (Fig. 2.1b). The analysis was performed using a laser-based isotope analyser (Picarro L2140-i) at the University of Natural Resources and Life Sciences, Vienna, Austria. Each sample was measured up to nine times and referenced using internal standards. These standards (deionized Baltic Sea water (−6.31 ‰ for $\delta^{18}O$ and − 45.8 ‰ for $\delta^{2}H$) and tap water (−11.16‰ for $\delta^{18}O$ and − 75.6‰ for $\delta^{2}H$)) are twice a year calibrated against international standards. The isotope ratios were given in the δ notation in ‰ relative to the Vienna-Standard Mean Ocean Water (V-SMOW).

2.6.4. Analysis of the recharge-discharge time lag

A number of discharge indicators, namely spring discharge (Q), EC, pH, total concentration of major cations (TCC), were exploited to investigate the time lag between the main recharge inputs (represented by the main precipitation events) and the consequent discharge output at the spring. The values of the indicators were derived from the monitoring described in 2.6.2.1 Discharge monitoring, 2.6.3 Hydrochemistry and water isotopes. TCC represents the sum of cation concentrations (meq/L) and is considered a proxy of groundwater salinity. As such, it is expected to be inversely correlated to the degree of dilution induced by the arrival of newly infiltrated water from precipitation. Daily precipitation data were acquired from a meteorological station managed by the Regional Agency for Prevention, Environment and Energy (ARPAE), namely “Riola di Labante” (Fig. 2.1a). The station was selected as the most representative of the Nadìa Spring recharge basin based on its location and altitude (623 m asl).

The analysis was conducted separately on two monitoring periods characterized by different hydrological regimes (as suggested by the results of Section 2.7.2): (1) the hydrologic year 2020-21 (data available from December 2020 to October 2021), characterized by higher spring discharges; (2) the hydrologic years 2021-2022 and 2022-2023 (data from November 2021 to March 2023), characterized by lower discharges. The two periods will be identified hereafter as

"high-flow period" and "low-flow period", respectively. The monitoring of Q covers both the high-flow and low-flow periods whereas EC, pH and TCC are only available for the low-flow period. The cumulative precipitation over 5 days was tentatively correlated, by means of bi-variate analysis, with the average values of Q, EC and pH in the same 5 days. Cumulative precipitations lower than 25 mm were eliminated from the dataset since it was proven, through an iterative trial and error series of correlation with different threshold values, that these would not have significant effects on spring discharge. Due to a low number of snowfall events during the 2020-23 monitoring period, it was not possible to perform a separate analysis on the effect of liquid versus solid precipitation (see further details in the SM). The discharge indicators were progressively shifted forward in time from 0 to 90 days, using a five-day increment. The five-day increment was chosen in order to smooth the roughness and intrinsic measuring uncertainties associated to the daily acquisition. For each time lag increment, the degree of linear correlation between recharge and discharge indicators was quantified by the coefficient of determination R^2 (see the correlation graphs in the SM). Two R^2 thresholds will be used to describe the time-lag analysis, corresponding to 0.6 and 0.3. These thresholds serve a primarily qualitative purpose, supporting the categorization of correlations into three groups: strong correlations ($R^2 > 0.6$), weaker correlations ($0.6 < R^2 < 0.3$), and the absence of correlation ($R^2 < 0.3$). When analysing the correlation between precipitation and Q, a $R^2 > 0.6$ suggests a clear association between these variables, likely reflecting the occurrence of preferential flow paths, such as open fractures or conduits, connecting the recharge area to the discharge point. As the correlation weakens, it might indicate a shift towards a more diffuse drainage network, resulting in a less defined signal of spring discharge in response to recharge events. Conversely, when examining EC or pH, a strong or weak inverse correlation with precipitation would indicate the arrival of newly infiltrated water. An absence of correlation, on the other hand, suggests that a discharge increase at the spring is driven by pressure transfer from the recharge area to the discharge point, i.e., increase of the hydraulic head in the recharge area with a subsequent increase of the hydraulic gradient in the aquifer.

During the timespan covered by TCC analysis, a comparison was performed between dilution events, i.e., variations of the parameter compared to its averaged value along the monitoring interval and five-day cumulative precipitation > 25 mm, in order to search for identifiable recharge-dilution time lags.

2.6.5. Artificial tracer test

On January 10th, 2023, a tracer test was performed involving the injection of 50 g of Uranine into a hole corresponding to an enlarged vertical fracture oriented NW-SE, aligned to the principal

system of extensional fractures affecting the PAT Formation (Stendardi et al., 2023). The hole had previously been identified as a karst morphology by local speleological associations (Lucci and Rossi, 2011). It is located at an altitude of 721 m asl, 166 m higher than the spring, at a planar linear distance of 313 m (Fig. 2.1b). Uranine was injected by pouring in 1.5 L at a solution of 33 g/L. In order to ensure the effective migration of the tracer through the unsaturated portion of the aquifer, estimated to be thicker than 120 m at the injection point, the solution was simultaneously introduced with 8000 L of water from a tanker truck. The truck was positioned 470 m from the injection point at an altitude 42 m higher. A series of connected hoses facilitated the gravity-driven transport of water to the injection site through a wooded area hardly accessible by vehicles. Precipitation amounted to 13.6 mm on the day before the injection, and to 1.8 mm on the day of the injection.

The arrival of the tracer was monitored at Nadìa Spring for 41 days after injection through the automatic groundwater sampling described in Section 2.6.3. From each of the 500 mL ISCO samples collected during the tracer monitoring period, a 100 mL nontransparent HDPE bottle was filled to determine Uranine concentration. Bottles were kept in darkness and stored at −2 to −8 °C until analysis. Additionally, charcoal bags were installed at the spring to detect Uranine arrival. Three bags remained in place for 71 days after injection, while another six were replaced at intervals ranging from 15 to 36 days, allowing for an 8 to 21-day overlap between consecutive bags. Following retrieval, the bags were air-dried in darkness and subsequently packed in individual plastic bags to avoid cross-contamination. The analysis of Uranine in water samples and charcoal bags was conducted in the laboratories of the Institute of Applied Geosciences at KIT (Karlsruher Institut für Technologie, Germany). Water samples were measured at an alkaline pH to increase the fluorescence yield. The analysis was performed using a fluorescence spectrometer LS55 by Perkin Elmer with the synchronous scan method. The desired wavelength range is traversed synchronously with a constant wavelength difference between excitation wavelength and emission wavelength. The advantage of this method is the formation of clearly identifiable peaks for each fluorescent dye. The device allows to measure at two different voltages (650 V and 900 V) in order to set an optimum measurement range, with a limit of detection of 0.005 µg/L. At first, all samples were measured with a voltage of 900 V. When the tracer concentration was too high (out of range for this voltage), the voltage was set to 650 V. For sample preparation of the charcoal bags, 0.5 g ± 0.1 g of charcoal were weighted and filled in a centrifuge tube. Subsequently 5 mL of eluent (50% NaOH and 50% 2-propanol (> 99.8% purity, Carl Roth GmbH, Germany)) were added and mixed for 4 h at 60 rpm under dark conditions. The supernatant was then measured as described above for water samples. Charcoal samples were categorized as either “positive” or “negative” based on Uranine detection, while those showing uncertain (very weak) fluorescence peaks were labelled as “likely positive”.

2.7. Results

2.7.1. Geomorphological and structural analysis

The geomorphological survey confirmed that the entire western sector of the study area is affected by a deep-seated gravitational deformation (DSGD) located on the steep slope above Nadìa Spring (Fig. 2.2). This specific landform likely results from the lateral spreading of the cohesive and tectonically fractured units with strong mechanical contrast, such as ED units, over the underlying ductile terrains of the Ligurian Domain (Mariani and Zerboni, 2020; Pasuto and Soldati, 2013; Pasuto et al., 2022). At the margin of the N slab, failure surfaces are produced evolving into complex landslide movements with toppled and slipped masses of PAT Formation (M. Asinello area in Fig. 2.2). The field analysis in the area of the DSGD has revealed the presence of two main gravitational morpho-structure types that fall within two major groups: 1) topographic anomalies, such as scarps and counter-slope scarps, and 2) trenches. In particular, the gravitational trenches are up to 500 m long and 110 m wide and usually oriented parallel to the slope strike. These structures are preferentially developed along inherited discontinuities of the PAT Formation oriented NNW-SSE. The trenches fill deposit consists of silts, clayey silts and fine sands of few meters thickness.

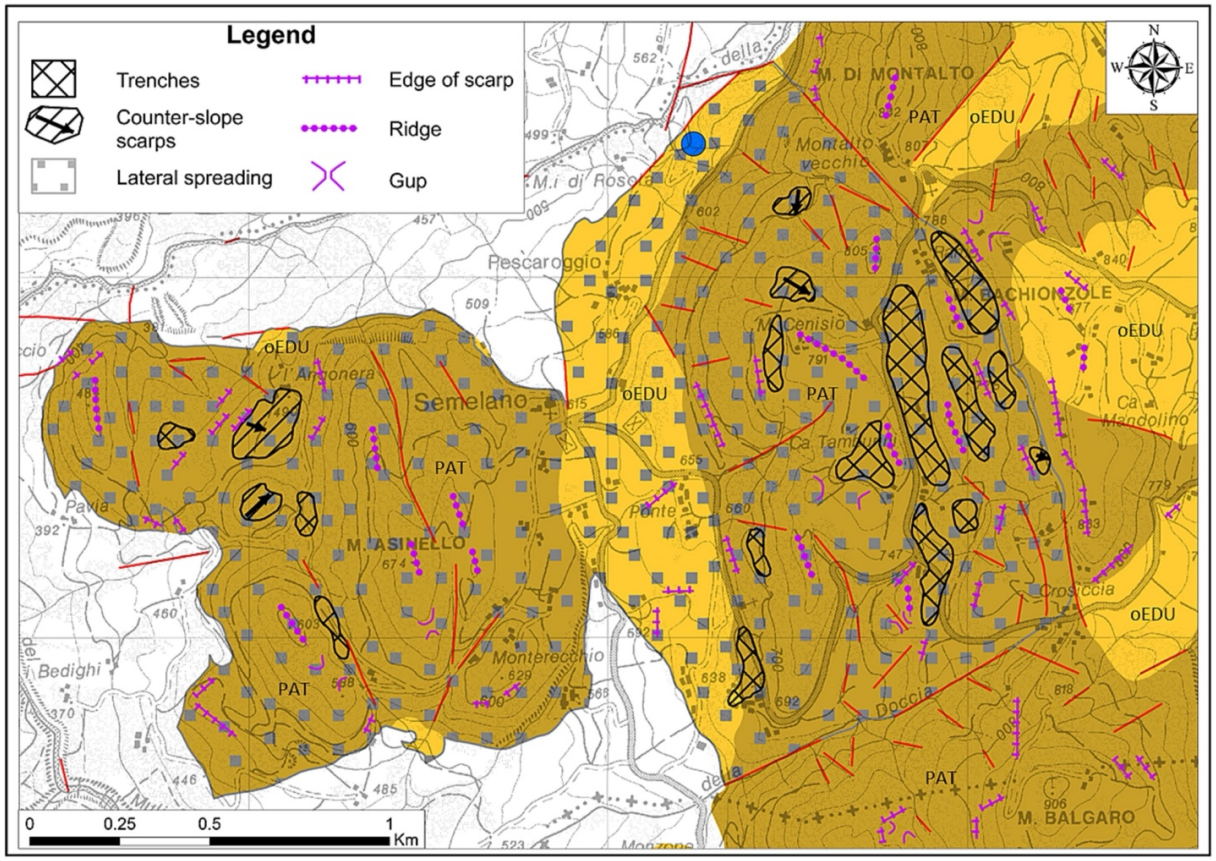

Fig. 2.2. Main geomorphological elements characterizing the N slab in the vicinity of Nadìa Spring. See Fig. 2.1 for the map location and the complete geological legend.

The field structural survey allowed the collection of over 600 observations of bedding, faults, and fractures/veins. The data show that bedding dips moderately to slightly eastward, northward, or southward, whereas faults and fractures/veins exhibit more variable orientations (Fig. 2.3a). The statistical analysis performed on the 160 fault data shows a dominant strike approximately oriented ENE-WSW (Gaussian curve n°1 in Fig. 2.3b), with a central value that deviates by approximately 12°. Orientation represented by the Gaussian curve n°5 can also be included in this set. These structures have an anti-Apennine orientation, parallel to the VLSS system.

Based on field observations, the ENE-WSW-striking faults are characterized by mature damage zones, in which interconnected shears creates an articulated fracturing network along the fault strike. Some of these faults show significant offsets juxtaposing the PAT Formation with other less permeable formations (see sections in Fig. 2.1c). A second main strike is oriented WNW-ESE (Gaussian curves n°2 in Fig. 2.3b), with a central value that deviates by about 10° from the preferred direction. A third main strike is oriented NNW-SSE (Gaussian curve n°3 in Fig. 2.3b), with a central value that deviates only 5° from the preferred direction. Structures pertaining to curves n°2 and 3 align with the Apennine orientation. These faults and fractures generally show single open surface and limited (or absent) damage zone. Finally, two subordinate strikes can be extracted from the statistical analysis, both oriented approximately NNE-SSW (Gaussians n°4 and n°6 in Fig. 2.3b).

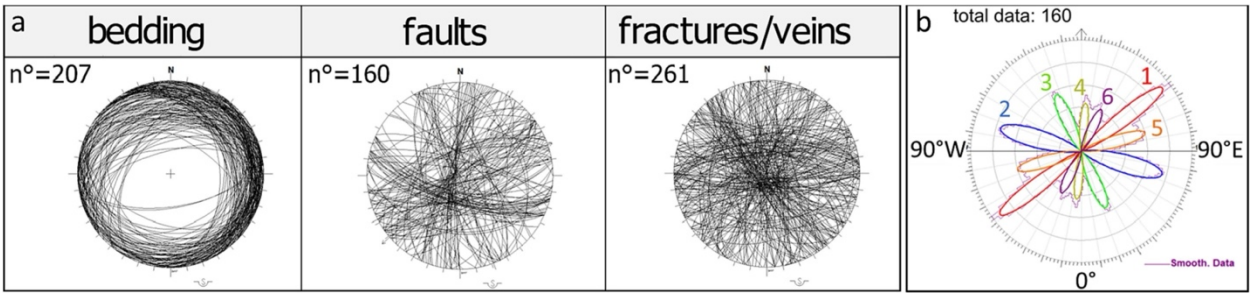

Fig. 2.3. Structural data: (a) stereographic projections (Schmidt net, lower hemisphere) of the main structural elements observed in the N slab during field surveys; (b) Rose diagrams (Daisy 3 version 5.40; Salvini et al., 1999) reporting the strike values of faults mapped in the study area. The red field (named 1) represents the dominant trend, while the purple field (named 6) is the least representative.

The optic and acoustic televiewer borehole logs performed nearby the N slab revealed fractures with decimetric apertures as deep as 61 to 71 m below ground surface (bgs), featuring irregular surfaces (see SM) most likely resulting from the chemical dissolution of the calcareous matrix of the Pantano arenites. The orientations of the open fractures align with the Apennine WNW-ESE and NNW-SSE directions identified for deformation structures in the N slab at the filed scale (i.e. Gaussians n° 2 and 3 in Fig. 2.3b).

2.7.2. Spring hydrographs

The spring hydrograph of the hydrologic year 2020-21 shows a rising limb since December 2020 (start of monitoring) reaching a discharge peak of 64 L/s at the beginning of March 2021 (Fig. 2.4). This is followed by a depletion limb down to a minimum of 42 L/s at the end of October 2021. The average yearly discharge is 54 L/s. The typical rising limb of the winter-spring recharge season is almost missing in the following year 2021-22. As a result, discharge variability along the year is limited compared to the preceding year, with maximum, minimum and average values of 48, 39, and 42 L/s, respectively. The available dataset for the year 2022-23 is limited to the first four months, from November 2022 to March 2023. Within this limited timespan, the average, minimum and maximum values are of 40, 38 and 43 L/s, respectively. It is worth noting that for the second consecutive year no evidence of a clear rising limb was registered during the recharge season.

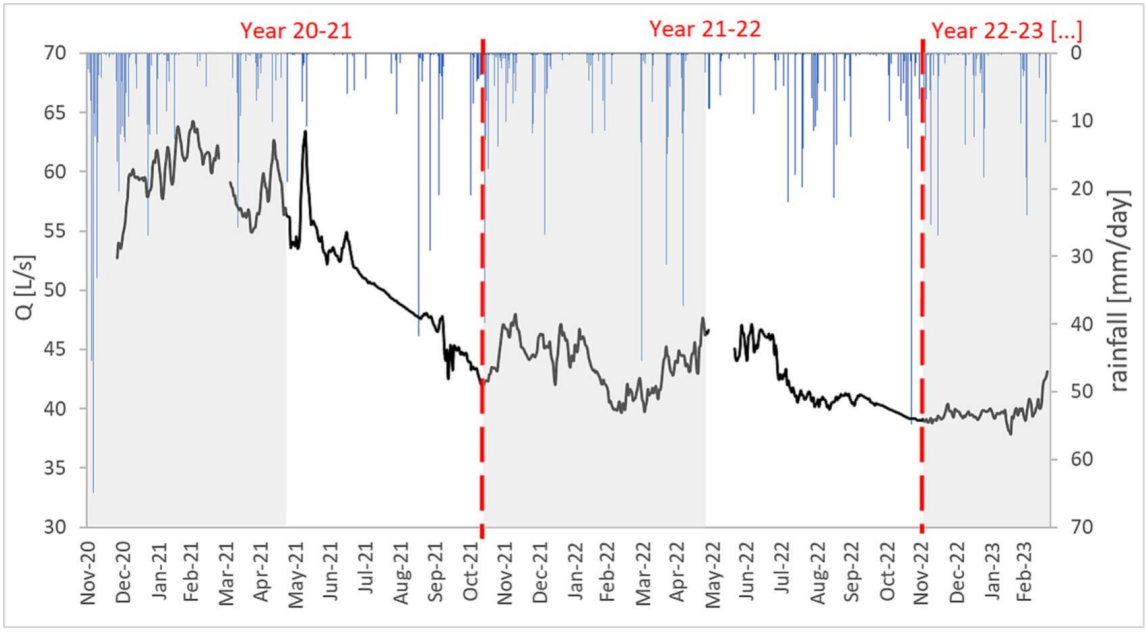

Fig. 2.4. Hydrograph of the total discharge of Nadìa Spring (including uptake and overflow) from December 2020 to March 2023. The hydrological years are indicated by red dashed lines. Daily precipitation from the Riola di Labante meteo-station is included for comparison. The typical Northern Apennines recharge season is shaded in grey.

Noticeable differences between the two complete yearly time series of 2020-21 and 2021-22 are observed in the maximum discharge values and yearly averages, showing a decrease of 16 and 12 L/s from 2020 to 21 to 2021-22, respectively. The difference is less pronounced (3 L/s) for minimum discharge values. The distinct discharge patterns observed in 2020-21 (higher flow) and 2021-22 (lower flow) are in line with the precipitation and air temperature trend of those two years (see SM), which suggest reduced aquifer recharge in 2021-22. The later year is also known to have been affected by a severe drought in the investigated region (ARPAE, 2023). The

hydrographs of the four hydrologic years from 1914 to 1918 show overall higher discharge values compared to the two more recent hydrographs of 2020-22 (Fig. 2.5a). The average discharge of the period 1914-18 is 92 L/s, which is almost twice the average value of 2020-22 (48 L/s). Moreover, the hydrographs from the past century show higher variability throughout the year, with peak discharge reaching up to 140 L/s and minimum values going down to 63 L/s. The differential between minimum and maximum discharge within a hydrologic year averaged 81 L/s at the beginning of the last century but reduced to 16 L/s in the more recent years. In the years 1915-16 and 1917-18, the winter-spring rising limb is less evident on the hydrograph compared to 1914-15 and 1916-17. This is in line with the precipitation trend monitored through those years, which appears to work as an effective recharge indicator during the time-span covered by the historical discharge monitoring (see SM).

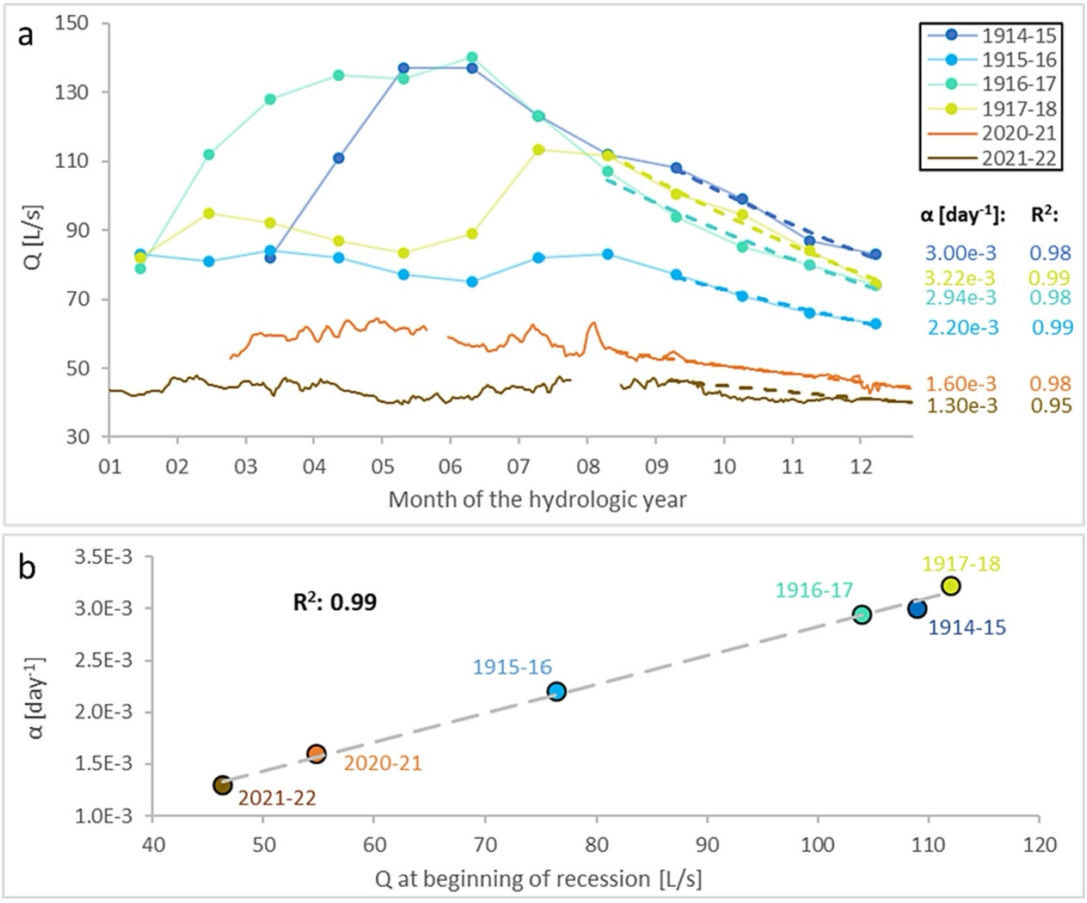

Fig. 2.5. Yearly hydrograph analysis: (a) historical (1914-18) and recent (2020-22) yearly hydrographs of Nadìa Spring. The x-axis represents months since the start of the hydrological years, with the first month varying between September and November based on the year. Historical hydrographs are based on monthly measurements, and since the precise monitoring date is unknown, discharge values were plotted on the 15th of each month. The exponential Maillet models used to fit the recession limb of the six hydrographs are represented with dashed lines; (b) linear relationship between the recession coefficient α and the spring discharge at the beginning of the recession season.

On all available hydrographs, a recession curve was identified starting in the 8th or 9th month of the hydrologic year (Fig. 2.5a). Despite a good fit between the recession curves and the exponential model of Maillet, with an R^2 always higher than 95%, the recession coefficient (α) shows slight albeit systematic differences among the years. The past century recorded higher values ranging between 3.2e-3 and 2.2e-3 day^{-1}, while recent years showed lower values ranging between 1.6e-3 and 1.3e-3 day^{-1}. A direct linear relationship was found between α and the spring discharge at the beginning of the recession curve (Fig. 2.5b).

2.7.3. Major ions and water stable isotopes

The major ion composition of spring water is similar through the different sampling years and seasons, showing a dominant Ca-Mg-HCO_3 hydrochemical facies (Fig. 2.6a), that is common to other springs in the Northern Apennines area, as reported by Hájek et al. (2021).

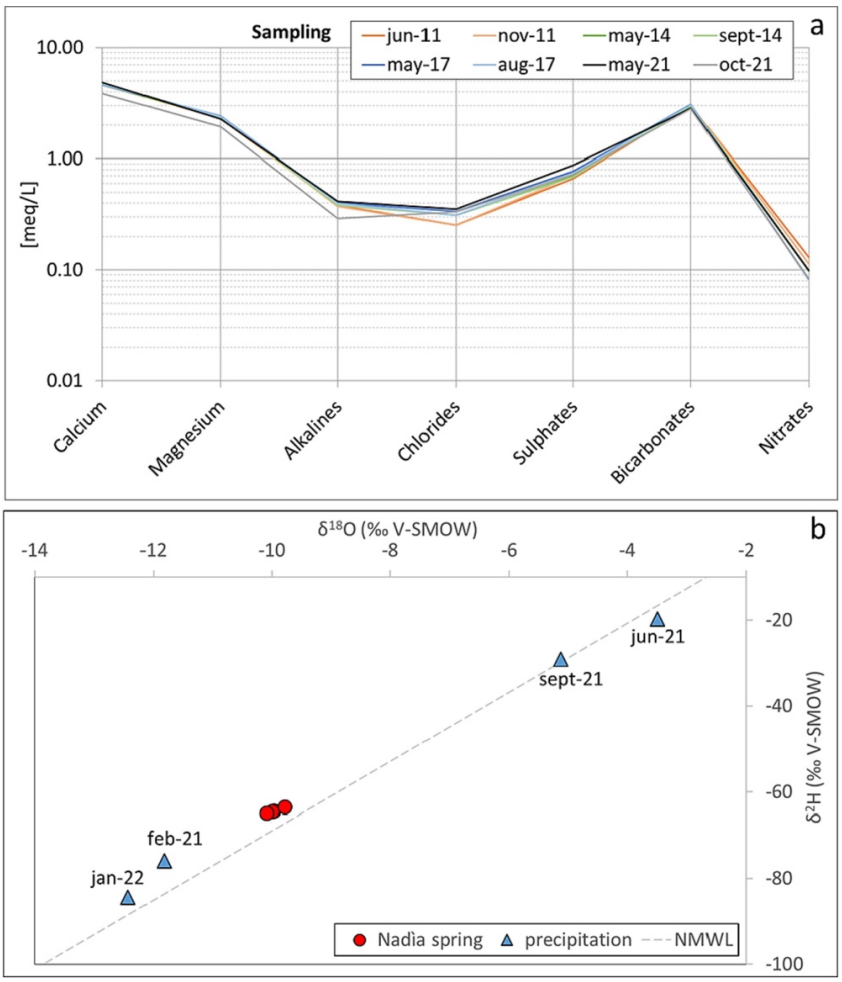

Fig. 2.6. Groundwater chemistry: (a) Schoeller diagram illustrating the major ion composition of spring water on a seasonal scale from 2011 to 2021; (b) seasonal water stable isotope composition of spring and precipitation samples collected between 2021 and 2022. The Northern-Italy Local Meteoric Water Line (NMWL) is represented by a dashed grey line.

The stable isotope composition of the four spring water samples shows a narrow range between −10.1 and − 9.8‰ for $\delta^{18}O$, and between −65.6 and − 63.6‰ for $\delta^{2}H$ (Fig. 2.6b). In contrast, rainwater collected in the spring recharge area exhibits much higher variability with values ranging from −12.4 to −3.5‰ for $\delta^{18}O$, and from −84.4 to −19.8‰ for $\delta^{2}H$. The most depleted rain samples were collected during the winter months (February 2021 and January 2022) whereas the more enriched samples correspond to June and September 2021. All the samples align along the Northern-Italy Local Meteoric Water Line (Giustini et al., 2016) with spring water being closer to the winter rain end-member. Together with the low variability in spring water isotopes for the period February 2021 to January 2022, this suggests a well-mixed water reservoir with higher contributions of recharge from winter precipitation.

2.7.4. Recharge-discharge time lag

The analysed time lags between recharge events and discharge indicators, ranging from 0 to 90 days, were divided into three main intervals considering the predefined R^2 thresholds of 0.3 and 0.6 (Fig. 2.7a): (I) strong correlation with Q ($R^2 > 0.6$) within the first 0 to 15 days of time lag, observed only during the high-flow period of 2020-21, indicating the arrival of newly infiltrated water through preferential flow paths; (II) weak correlations ($0.6 > R^2 > 0.3$) with Q and EC between 15 and 65 days of time lag, suggesting the arrival of newly infiltrated water through diffuse flow paths of varying lengths. Notably, a strong correlation with pH emerges at a 35-day time lag, exhibiting a 20-day delay compared to EC.

This observation implies that some acidification reactions may take place as direct recharge from precipitation moves through the extensive unsaturated zone. Indeed, previous literature has noted that a significant portion of the CO_2 found in groundwater originates from biological processes in the soil (Hartmann et al., 2014). It may then require several weeks for these reactions to cause a noticeable decrease in pH in spring water; (III) weak correlation with Q and an absence of correlation with EC and pH ($R^2 < 0.3$) from 55 to 90 days of time lag, indicating that the most delayed increases in discharge are likely induced by pressure transfer within the reservoir. It is important to note that the variability of EC and pH during the monitoring period was limited. EC ranges from 408 to 640 µS/cm with an average of 572 µS/cm and a standard deviation of 37 µS/cm, while pH varies between 7.7 and 8.4 with an average of 7.9 and a standard deviation of 0.2. This overall stability is consistent with the observations on the chemical and isotopic composition of spring water (see Section 2.7.3). In this context, even slight variations of the parameters may be useful to discriminate among different processes affecting the groundwater flow system.

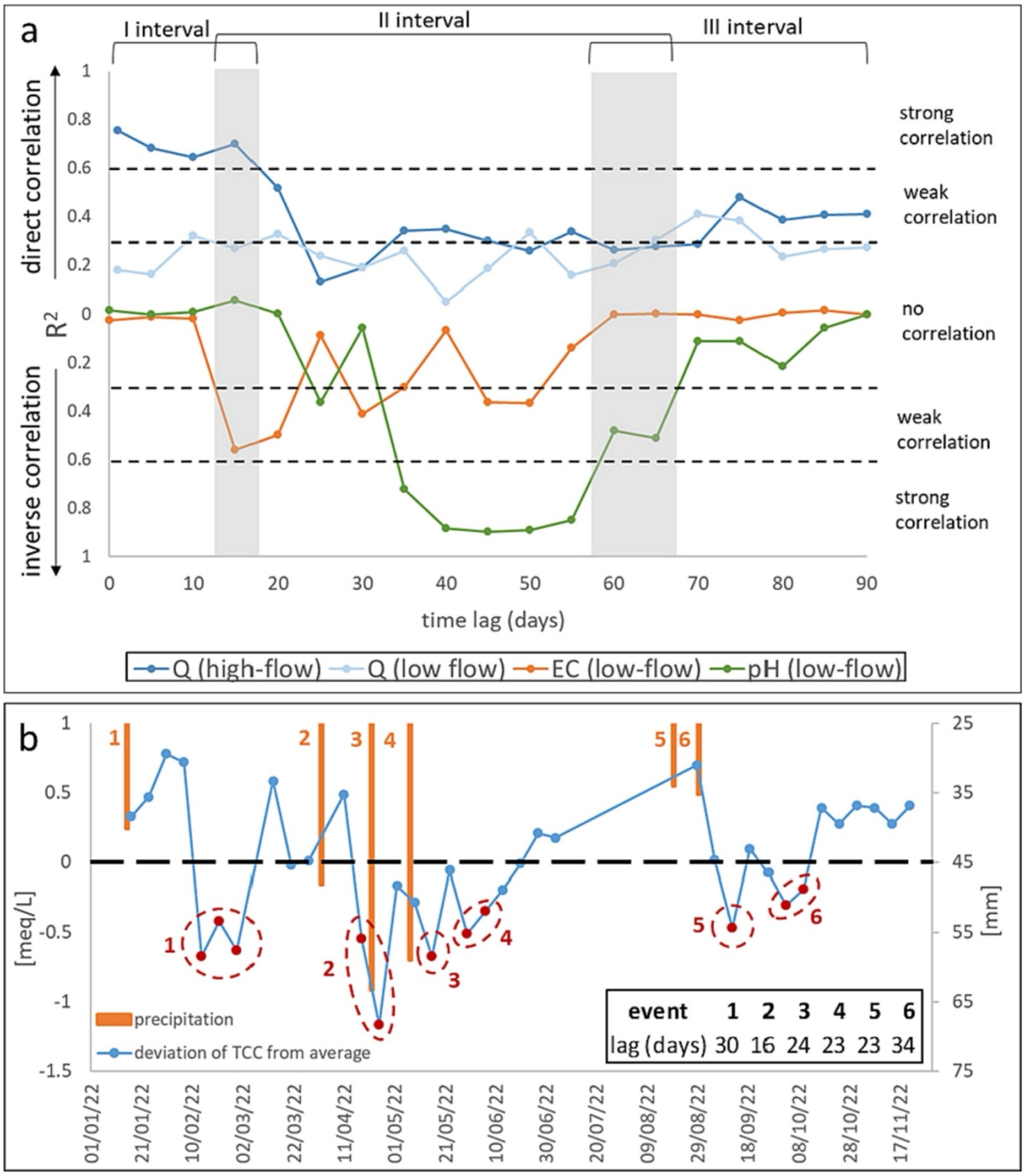

Fig. 2.7. Time lag analyses: (a) linear correlations between recharge and discharge indicators at increasing time lags. Dashed black lines indicate the different correlation thresholds. Grey bars denote partial overlaps between the three intervals identified by the analysis; (b) identification of time lags between precipitation events and decreases in TCC below the average of the monitoring period (5.8 meq/L). The dashed black line indicates a deviation of 0 from the average. Progressive numbers identify the main precipitation events and the associated dilution effect on spring water. The time lags for each event are summarized in the lower right corner.

Six precipitation events occurred during the TCC monitoring (Fig. 2.7b). Each of them induced an appreciable dilution on spring water, with variable time lags in the range of 16 to 34 days from the recharge event to the start of the dilution signal.

2.7.5. Artificial tracer test

The water samples occasionally exhibit peaks in Uranine concentration during the 41 days of sampling, ranging from 0.01 to 1.12 µg/L (Fig. 2.8). The earliest detections occurred 1 to 4 days following injection, with a peak value of 0.28 µg/L. Tracer arrival in this early interval was likely influenced by the relevant volume of water introduced during the tracer injection. Nevertheless, the result demonstrates the existence of rapid flowpaths between the injection point and the spring, with a maximum velocity of Uranine transfer in the range of 78 to 313 m/d (considering a planar distance of 313 m from injection to detection).

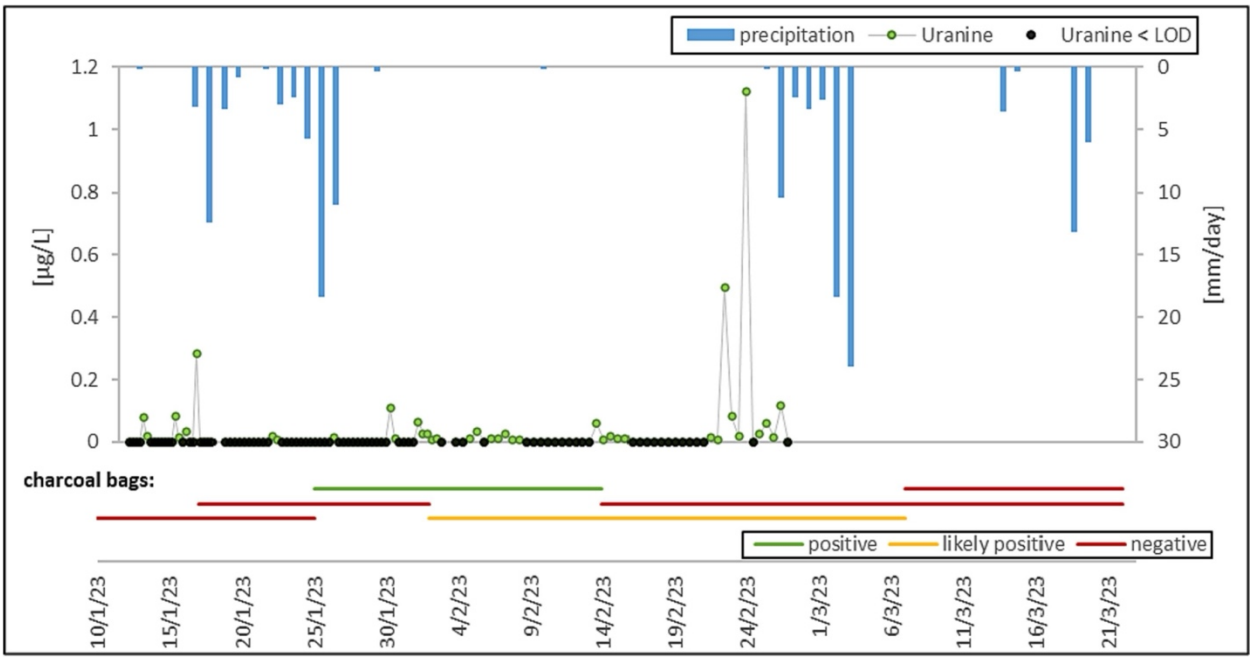

Fig. 2.8. Main results from the artificial tracer test. The concentration of Uranine measured in water samples are represented along with the information provided by charcoal bags. Concentrations below the Limit of Detection (LOD = 0.005) are represented as 0 for graphical purposes. The graph covers the tracer monitoring period from January 10th (day of injection) to March 22nd (collection of the last charcoal bag). Daily precipitation data from the Riola di Labante meteo-station are included for comparison.

The two highest concentration peaks were observed between February 21st and 23rd (42 to 44 days post-injection), with values of 0.5 and 1.1 µg/L, respectively. The primary recharge event preceding these peaks took place between January 21st and 25th, with a total amount of precipitation of 41 mm (i.e. > 25 mm in 5 days). The time lag between the recharge event and the two peaks is 27 to 33 days. The tracer transfer velocity associated with these peaks is between 12 and 9 m/d.

Throughout the tracer monitoring period, the spring discharge remained relatively stable, ranging from a minimum of 37.9 L/s to a maximum of 43.1 L/s, with an average of 39.8 L/s (see Fig. 2.4). Based on daily flow rates and detected tracer concentrations, it was estimated that

about 4.5 g of tracer were recovered, accounting for approximately 9 % of the total injected mass of 50 g. Of the 4.5 g recovered, 2.8 g reached the spring outlet in correspondence of the two main peaks of February 21st and 23rd. The small mass of tracer recovered in the first 41 days after injection can likely be explained assuming that some tracers have remained in the unsaturated zone and has been flushed out by subsequent meteoric events after the monitoring period ended. The evidence provided by charcoal bags largely align with water samples, confirming the arrival of Uranine between January 25th and February 14th, and suggesting a probable occurrence between February 2nd and March 7th, which coincides with the period of observation of the major peaks in water samples.

However, the negative result between February 14th and March 22nd appears inconsistent with the tracer detection in water samples. This discrepancy could be attributed to possible tracer desorption or biological degradation, which were previously hypothesized as reasons for decreased tracer concentration in charcoal that remains in water for an extended amount of time (Aley, 2019). The bag's total residence time was 36 days, extending up to 24 days after the arrival of the last recorded Uranine peaks. Eventually, the three bags left in place throughout the entire monitoring period (not shown in Fig. 2.8) were affected by significant background noise, which hindered the possible detection of Uranine trace on the charcoal.

2.8. Discussion

2.8.1. Factors enhancing the Nadìa Spring yield

The hydrological response of Nadìa Spring resembles that of many springs in the Northern Apennines that exhibit a rising discharge during winter and spring, followed by a declining discharge in summer and fall. The magnitude of the Nadìa Spring rising limb in each hydrological year depends on the amount of recharge during that year, with higher discharge peaks in years of greater recharge. This discharge response is typical of Northern Apennines springs due to their short groundwater flow paths, which make them responsive to local recharge patterns (Gargini et al., 2014). However, Nadìa Spring stands out with a unique base flow contribution of approximately 40 L/s at the end of the decreasing limb when most other Northern Apennine springs approach zero flow, leading to drinking water supply issues (Cervi et al., 2018).

A crucial factor that explains the increased yield of Nadìa Spring is the presence of a significant groundwater reservoir that supplies the spring. This is supported by the notably low Maillet recession coefficient α, averaging 2.4e-3 d^{-1} over the monitored years. In contrast, the dominant α values in the Northern Apennines region are typically one order of magnitude higher (Gargini et al., 2008), indicating smaller reservoirs (Tallaksen, 1995). Nadìa Spring is situated at

the lowest topographic elevation along the edge of the N slab, corresponding to the bottom elevation of the PAT Formation (see Fig. 2.1c). As a result, it serves as the most natural discharge point of the slab. Moreover, unlike the typical Northern Apennine setting where a large number of diffuse outlets are associated with one groundwater reservoir (Gargini et al., 2008), in this case, several factors have led to the concentration of drainage from the N slab into one primary discharge point which is Nadìa Spring. These factors are discussed in more detail in subsections 2.8.1.1 to 2.8.1.3 and include structural pattern of faults and fractures, the presence of slope instabilities, and karst dissolution.

2.8.1.1. Structural pattern

The anti-Apennine striking faults, aligned with the VLSS, are the most recurrent features in the area based on field data analysis. The primary and most continuous lineaments in the N slab follow this direction (Fig. 2.1b). These main structures likely constrain groundwater flow, as supported by the following observations: (1) some of the NE-SW structures create significant offsets, restricting the lateral continuity of the PAT aquifer (Fig. 2.1c); (2) Balocchi (2014) reported the presence of cataclasites on the major Anti-Apennine lineaments of the N slab (Fig. 2.1b), assigning them the role of flow barrier (Caine et al., 1996).

Apennine-oriented structures come second in terms of prevalence in the area. These are generally cut and displaced by the anti-Apennine-oriented faults (as visible in Fig. 2.3b and previously noted by Balocchi (2014). These structures, with their two primary strikes NNW-SSE and WNW-ESE, effectively “unlock” the rock mass within NE-SW “channels” delimited by anti-Apennine structures. Presumably, the Apennine striking structures serve as planes of weakness that enhance the rock mass's permeability, based on the following lines of evidence (discussed more in detail in the subsequent sections): (1) the development of a DSGS along Apennine-oriented planes of weakness (see Section 2.8.1.2); (2) the observation of karst dissolution along deep-seated Apennine-oriented structures in the borehole near the N slab (see Section 2.8.1.3). Additionally, the wide fracture chosen as injection points for the tracer experiment (see Section 2.7.5) also exhibit an Apennine strike (NNW-SSE), further confirming the presence of enlarged structures in that orientation. Finally, during the excavation of the drainage tunnel for spring uptake, which is oriented along the anti-Apennine direction, Vecchi (1920) reported groundwater inrush from fractures perpendicular to the tunnel's alignment, indicating an Apennine orientation.

As a result, the Apennine-oriented structures plausibly form the primary network for groundwater flow, facilitating the circulation of groundwater throughout the saturated part of the N slab. This circulation predominantly aligns with the anti-Apennine-oriented structures,

which mostly act as no-flow boundaries. Groundwater is consequently conveyed from the northeastern sector of the N slab towards Nadìa Spring.

2.8.1.2. Slope instabilities

The relaxation of stresses caused by the DSGS (classified as lateral spreading) along the edge of the N slab results in the formation of features like trenches and scarps/counter-scarps. These features can locally enhance the permeability of the unsaturated zone, allowing for concentrated recharge in the vicinity of the spring. Furthermore, it is highly probable that a localized drop in groundwater levels is associated with the observed increase in permeability in the DSGS area. This may lead to additional drainage from the surrounding regions towards the spring area. It is important to note that the morpho-structures related to lateral spreading align with Apennine-oriented faults and fractures (Fig. 2.2), which likely played a significant role in initiating and shaping the instability processes.

2.8.1.3. Rock dissolution

The chemical composition of groundwater suggests a significant interaction with a carbonate matrix, pointing to the likelihood of karst dissolution (Wijayanti and Dalmadi, 2021). This dissolution process could primarily impact either the calcitic cement/matrix of the calcarenite rock mass of PAT, or the limestone/dolostone clasts within the skeleton (the occurrence of non-negligible Mg content in the groundwater suggests the presence of dolomite in these clasts). Furthermore, there have been previous observations of travertine deposits at various spring outlets within the same aquifer lithology, as documented by Cantonati et al. (2016). This supports the hypothesis of an enrichment of $CaCO_3$ in the water during underground flow. Additionally, the discovery of wide discontinuities with apertures of up to 20 cm, identified at depths of 61 and 71 m bgs through televiewer borehole logging, provides further evidence of karst dissolution within the studied lithology. The borehole observations suggest that dissolution is primarily occurring along preexisting Apennine-oriented fractures. Karst dissolution is likely to increase the overall permeability of the aquifer and promote the development of preferential groundwater flow paths within the rock mass, as discussed further in Section 2.8.2.

2.8.2. Evidence of dual porosity in the N slab

The inferred occurrence of karst dissolution within the N slab is expected to trigger the development of a hierarchical groundwater flow system over time, which eventually results in a

more focused drainage of groundwater towards a limited number of larger discharge points (Hartmann et al., 2014; Worthington and Ford, 2009).

The findings from the analysis of recharge-discharge time lags suggest the existence of a dual porosity system connecting the recharge area to Nadìa Spring. This system consists of both fast-flow conduits and a diffuse fracture network. An additional contribution from matrix porosity, often observed in relatively young carbonate systems (Kresic and Stevanovic, 2010), cannot be definitively ruled out. However, information on matrix porosity in the investigated calcarenitic lithology of PAT is currently unavailable and should be the focus of further investigation efforts.

In the fast-flow system, which comprises enlarged fractures, newly infiltrated water is rapidly drained towards the spring (within 15 days after major recharge events, i.e. > 25 mm in 5 days). However, it is worth noting that these preferential flow contributions are likely minor (<10%), as indicated by results from the artificial tracer test. The fast-flow system appears to be active primarily during periods of high-flow hydrological conditions (monitoring year 2020-21), suggesting that the conduits become active when hydraulic head stands higher. Gradually, a signal from a more diffuse system becomes predominant during lower-flow conditions, resulting in variable time lags (between 15 and 65 days) for newly infiltrated water to reach the discharge outlet in response to major precipitation events. Over longer timescales (starting from 55 days of time lag), this same diffuse system appears to convey water stored in the reservoir through pressure transfer. Cationic composition data (TCC) during low-flow conditions support the estimated response times for newly infiltrated water through the diffuse drainage system following major precipitation events, with time lags ranging between 16 and 34 days.

Artificial tracing results also aligns with these response times, showing initial tracer arrival within a few days after injection, most likely due to activation of fast-flow circuits because of the large volume of water injected during the experiment. The later, more concentrated tracer arrival is consistent with the previously inferred transfer times of newly infiltrated water through the diffuse drainage system (between 27 and 33 days of time lag). Notably, the tracer transfer velocity associated with the diffuse drainage system (ranging from 12 to 9 m/d) falls within the range of values obtained experimentally by Vincenzi et al. (2014) for turbiditic sandstone aquifers characterized by diffuse groundwater flow networks (2 to 20 m/d). Conversely, the higher transfer velocity linked with fast-flow circuits (ranging from 313 to 78 m/d) more closely resembles the values observed by the same authors in a marly calcareous turbiditic aquifer affected by karst dissolution (94 m/d). These observations corroborate the hypothesis of a dual porosity system comprised of fast flowpaths associated with a diffuse fracture network.

The analysis of recent and historical hydrographs emphasizes once again the occurrence of a dual porosity system. The spring's recessive response observed over the past century (from 1914 to

2022) indicates progressively slower flow of recharge water as the discharge at the start of the recession limb decreases. In particular, the historical hydrographs are characterized by higher recession coefficients indicating faster flows between the recharge area and the spring, with larger flow variability observed throughout the hydrological year between the recharge and the recession seasons. This response is plausibly related with the existence of fast flow-paths connecting the recharge area to the spring, facilitating the transfer of newly infiltrated water as well as rapid responses to pressure changes. In more recent years (2020-2022 hydrographs), lower recession coefficients were observed in conjunction with reduced flow variability throughout the year. This is most likely attributable to groundwater flow occurring through slower circuits with a diffuse character.

2.8.3. Resilience to climate change

From various angles, Nadìa Spring exhibits remarkable stability and an inertia towards the year-to-year fluctuations in recharge factors. From a hydrological perspective, the minimum spring discharge values remain consistently stable throughout the recent years being apparently unaffected by annual variations in recharge. For instance, when comparing the hydrographs of 2020-21 and 2021-22, the latter shows only a minor decrease in the minimum annual discharge, even in the face of an exceptional drought during the recharge season. This implies that reductions in recharge primarily affect the peak phases of the yearly hydrograph but leave the minimum discharge almost unimpacted. This suggests significant resilience of the spring to individual dry years, ensuring it continues to provide an ecosystem service with a sufficient flow rate even in critical summer seasons.

From a geochemical perspective, the groundwater composition (i.e. major ions and stable isotopes) remains highly stable across seasons or even years, indicating a well-mixed aquifer reservoir supplying the spring. This is in contrast to heterogeneous media like real karst aquifers, which exhibit a strong hydrochemical variability over time (Sánchez et al., 2015). Thus, the observed chemical consistency further supports the hypothesis of a substantial contribution from a diffuse drainage system in recent years, as previously discussed in Section 2.8.2. Water isotopes additionally suggest that most recharge occurs during the winter-spring period when the combination of higher precipitation and lower temperature maximize the water's capacity to penetrate the unsaturated thickness of the system (Thornthwaite and Mather, 1957).

The rare opportunity to examine century-old hydrographs of the spring has allowed for notable observations regarding its interdecadal resilience in the face of discharge reductions caused by century-scale climate change. The significant decline in Nadìa Spring's discharge since the early 21st century, a trend also observed in other Mediterranean regions and attributed to

documented reductions in recharge season precipitation and snow-related parameters (e.g., Dragoni and Sukhija, 2008; Fiorillo et al., 2021), suggests a limited resilience of the spring to long-term recharge variations. However, the observed relationship between the initial discharge during the recession and the recession coefficient (Fig. 2.5b) indicates an increasing laminar capacity of the aquifer over time (i.e. decrease of discharge variability along one single year and increased stability of the minimum discharge values over different years).
This change should be linked to the previously inferred transition in recent years towards a more diffuse drainage system. This diffuse system is most likely located at lower altitude in the reservoir, so that the more dynamic fast-flowpaths are activated only when the hydraulic head in the aquifer is higher. As a result, future decreases in spring discharge due to reduced recharge may be less severe compared to the past, potentially enhancing the interdecadal spring's resilience to climate change.

2.9. Conclusions

A strategic spring resource in the Northern Apennines was explored due to its unique characteristics regarding discharge magnitude and consistency. This study employed an unprecedented combination of traditional geological and hydrogeological field investigations, continuous monitoring of recharge- and discharge-related indicators, an artificial tracer experiment, and an analysis of spring hydrographs dating back a century. These methods enabled us to unravel the factors contributing to the spring's distinctive features. The investigative approach presented here can serve as a valuable model for similar hydrogeological settings when studying and assessing local strategic groundwater discharge points.

In the case of Nadìa Spring, several factors influence the spring's response to recharge fluctuations. These include an extended groundwater reservoir supplying the spring, a complex network of fractures that constrain groundwater flow towards highly transmissive channels, a slab structure that triggers slope instability along its margins, and a high carbonate content in the rock mass favouring karst dissolution. This, in turn, facilitates active aquifer recharge in the occurrence of abundant precipitations during the winter-spring season and hierarchizes groundwater flow towards one main outlet. All these conditions favour an increased yield for the spring, as well as resilience to variations in recharge on an inter-annual scale. On the other hand, over several decades or centuries, the spring's discharge appears significantly affected by reduced recharge due to climate change. These long-term effects are particularly evident in terms of decreased peak discharge. Nevertheless, the capacity of the aquifer reservoir to store recharge water acts as a buffer mitigating the risk of an excessive decrease in spring discharge during future drought conditions.

The hydrodynamics of the spring indicate the presence of a dual porosity, characteristic of variably karstified systems, whereas karst dissolution is not commonly observed in arenitic aquifers. However, as hydraulic head and spring discharge decrease over time due to climate change-related discharge reductions, a significant portion of the fast-flow preferential system seems to deactivate gradually, possibly because of its higher elevation within the aquifer, which is gradually depleting. The primary spring discharge contribution today appears to originate from a diffuse drainage system, which likely constitutes the deeper portion of the aquifer. The dual porosity structure would then explain the different response observed in the spring one century ago compared to today.

A critical element that has allowed us to understand the spring's discharge response and draw conclusions about its resilience is the combination of a long-term monitoring of hydrological (including uptake and overflow) and hydrochemical parameters. Century-long spring discharge monitoring is a rare find in the existing literature and, in cases where it is available, as in the instance of Nadìa Spring, it allows unveiling the significant impacts of climate change on discharge. Another crucial aspect has been the continuous monitoring of spring discharge and chemistry during an exceptionally dry period spanning from 2021 to 2023. Such monitoring has emphasized the resilience of discharge in severely dry years, attributed to the drainage capacity of the diffuse fracture system. This effect might have gone unnoticed during less dry periods. Continuing the spring monitoring in the future will be essential to identify flow patterns under more variable atmospheric conditions, including variable discharge patterns over the hydrologic year.

In the future, it would be also beneficial to monitor additional strands of evidence, such as eco-hydrogeological indicators like endemic invertebrates or plant species, and the dendrochronology of trees situated at increasing distances from the spring. These could offer valuable insights into the long-term persistence of spring discharge and enhance our understanding of the spring's ecological significance. Relatively large springs like Nadìa often hold substantial ecosystem value. Understanding how discharge responds to climatic variations is a crucial step for managing and leveraging the ecosystem services provided by the spring, both in natural and economic terms.

While showing the importance of continuous spring discharge monitoring over time, this study also sheds light on a more general issue: while hydrologic monitoring networks for precipitation and surface water fluxes are well structured and operating in many areas of the world, a strong enhancement of such network is needed for springs in order to cope with the challenges of climate change, both in terms of water resources management and ecological preservation/valorisation of the spring environment.

Acknowledgements

The authors express their gratitude to the following students and researchers for their support in field and lab activities: Daniel De Luca, Laura Landi, Ernesto Pugliese, Benedetta Bellini, Francesca Stendardi and Nicholas Greggio. They also extend their acknowledgements to Alessandro Stefani and other employees of GruppoHera whose support made this investigation possible. Finally, they thank the two anonymous reviewers for their useful comments and corrections.

2.10. Supplementary Material

2.10.1. Coring and televiewer logging

Two boreholes were drilled between November and December 2021 in a location 7 km south of the Nadìa spring, in the same PAT aquifer Formation, where logistic conditions and land property rights were favourable for the drilling activities (Fig. 2.9).

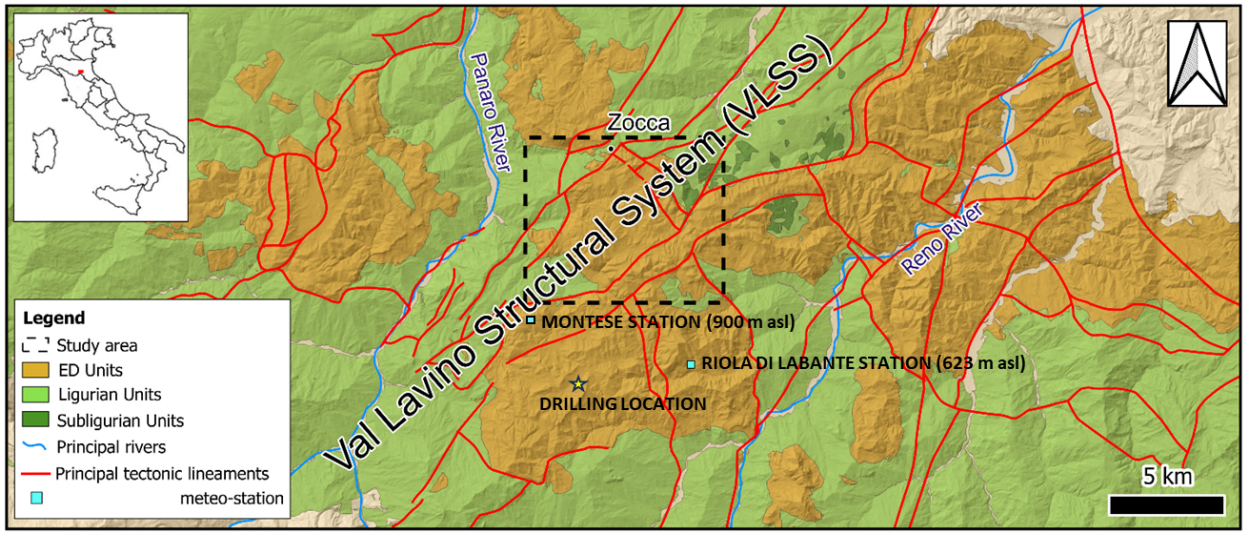

Fig. 2.9. An excerpt from Fig. 2.1a in the main text, displaying the chosen drilling location, as well as the Riola di Labante and Montese meteorological stations.

The locations of the two boreholes, namely ARP1 and ARP2, are at a ground altitude of 790 m asl and spaced apart of 10 m. The drilling of ARP1 was performed down to a depth of 80 m bgs using a wireline continuous coring system with single tube core barrel of 101 mm diameter that provided consistent, high core recovery of 90 to 100% in the hard rock intervals. For the purposes of this study, the cores were visually assessed in terms of aspect of fracture surfaces in order to detect evidences of rock dissolution. Borehole ARP2 was drilled down to a depth of 35 m bgs

using a core destruction probe with a 101 mm diameter. Acoustic and optical televiewer logs were performed along the uncased boreholes (50 to 80 m bgs in ARP1; 2 to 35 m bgs in ARP2) to observe the orientation and aperture of fractures. The primary structures of interest identified during the drilling investigation are fractures of decametric aperture at depths of 60-62 m bgs and 70-72 m bgs, with orientations of WNW-ESE and NNW-SSE. The surfaces of these structures exhibit significant irregularities at core inspection (Fig. 2.10).

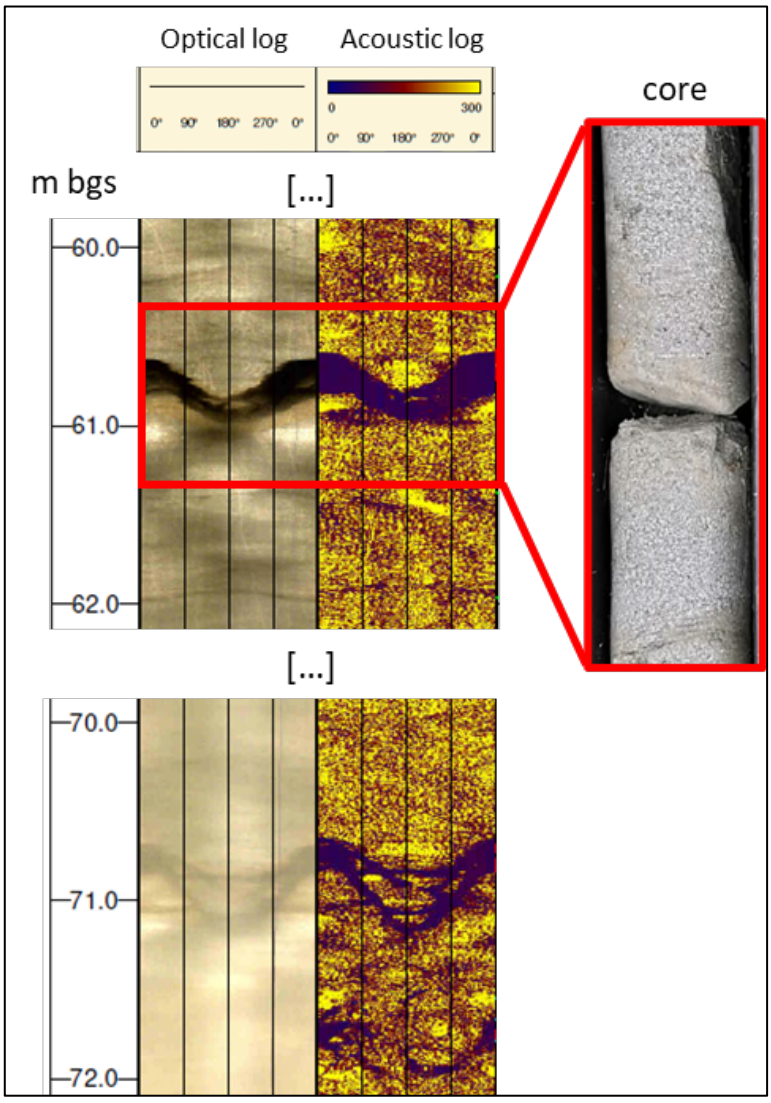

Fig. 2.10. Discontinuities of main interest identified through televiewer logging and core inspection.

2.10.2. Droughts in the Emilia Romagna Apennines

In Fig. 2.11, we present precipitation data from the past two decades obtained from two meteorological stations located in close proximity to the study area, namely Riola di Labante and

Montese (Fig. 2.9). The datasets include both the total annual precipitation and the precipitation during the recharge season, which spans from the beginning of the hydrological year to April.

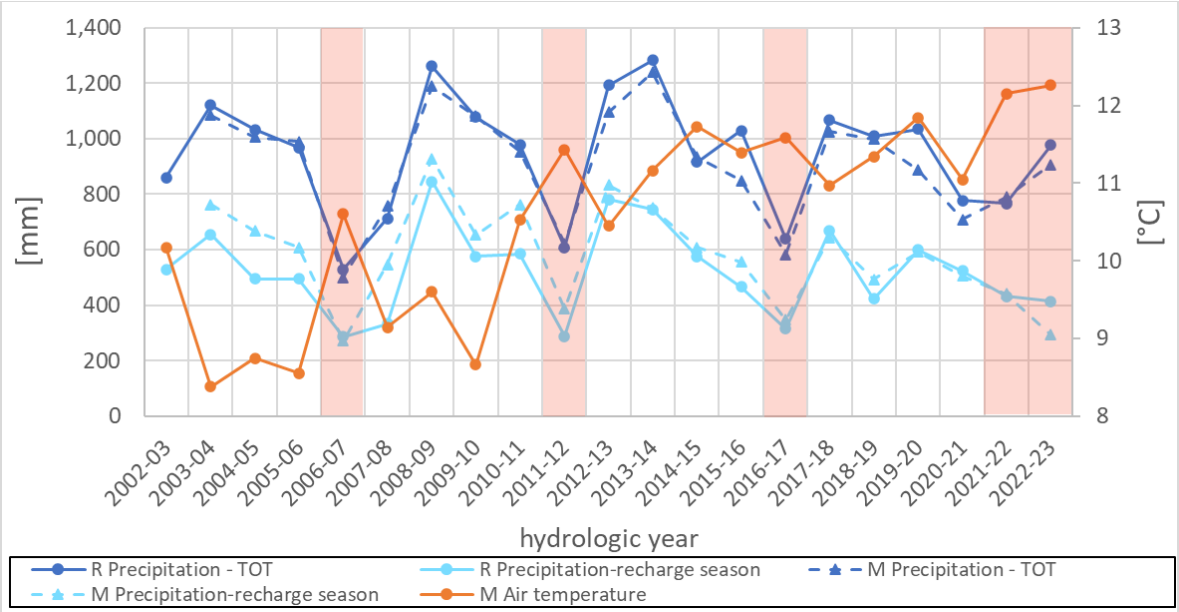

Fig. 2.11. Annual precipitation and mean annual air temperature in the area of the Nadìa spring. “R” and “M” indicate the Riola di Labante and Montese meteo-stations, respectively. “TOT” indicates the cumulated precipitation over the hydrologic year whereas “recharge season” indicates the cumulated precipitation from the beginning of the hydrologic year to April. Drought years are highlighted in red.

Riola di Labante station, as previously mentioned in the main text, serves as the most representative station for the N slab area due to its proximity and elevation (623 m asl). On the other hand, Montese station is positioned at a higher elevation compared to the study area's average (920 m asl). Notably, Montese provides additional data on air temperature for the period of interest (see the average annual air temperature in Fig. 2.11), which is not available from the Riola di Labante station.

Despite the differences in altitude, the total annual precipitation and recharge season precipitation have shown a similar pattern in both stations over the past two decades. Approximately every five years, we observe a convergence of low precipitation levels and unusually high air temperatures. The latter has the dual effect of increasing evapotranspiration and reducing snow-fall and -permanence on the ground. Such periods align with those previously identified at the regional level as drought periods (e.g. ARPAE, 2018, 2023). It's worth noting that the years 21-22 and 22-23 represent an extended period of drought, continuing at least until the spring of 23 when the monitoring for this study was concluded. The relatively high total annual rainfall reported in the graph for 22-23 is attributed to several events occurring during the late spring and summer, a season typically marked by dry conditions in the Norther Apennines (though outside the scope of this study's monitoring period).

2.10.3. Historical discharge and precipitation data

The historical monitoring data of spring discharge and precipitation collected by Vecchi (1920) are shown in Fig. 2.12. The discharge data represent discrete monthly measurements (the precise monitoring date is unknown). Precipitations represent the cumulated monthly amounts registered at the Montese meteorological station (Fig. 2.9), which was the only active station in the vicinity of the N slab during the time-span covered by the historical monitoring.

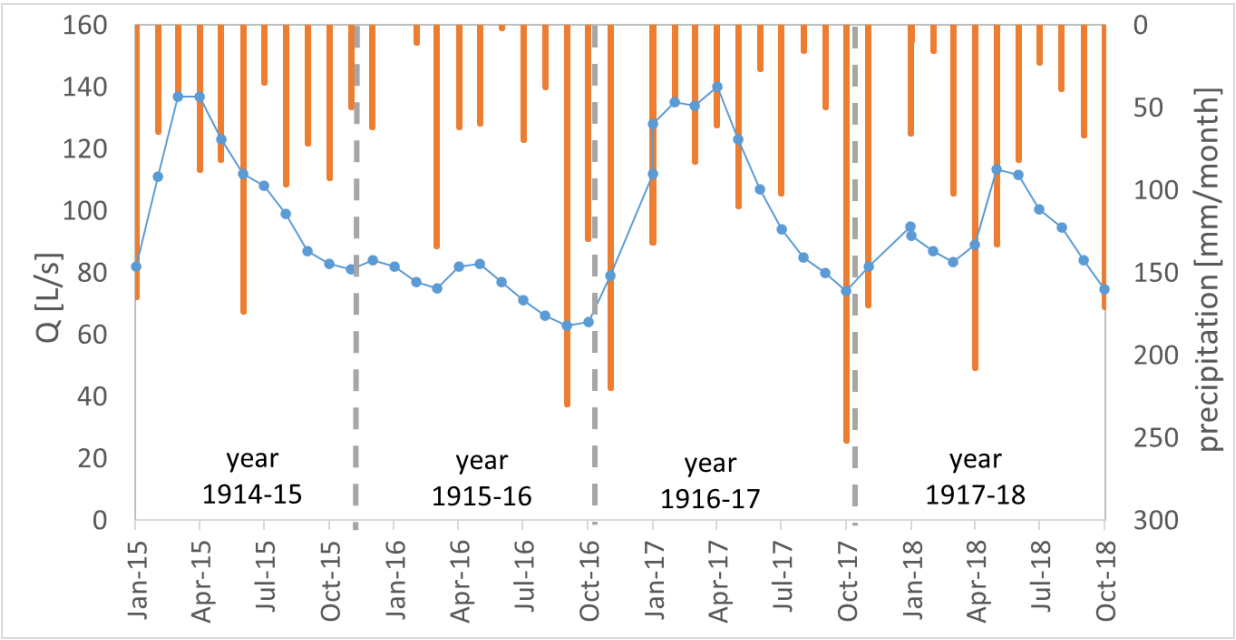

Fig. 2.12. Monthly discharge and monthly precipitation data from January 1915 to October 1918.

2.10.4. Correlation between annual precipitation and discharge over time

In Fig. 2.13, we illustrate the correlation between precipitation during the hydrological year or precipitation during the recharge season and the average discharge of the spring over the hydrological year (Q). This comparison was conducted using both historical and current monitoring data. Regarding historical data, only the three years from 1915 to 1918 are presented because we lack information to determine a consistent averaged discharge for the year 1914-15. As for recent data, the year 2022-23 is not represented for the same reason.

An estimation of the aquifer recharge variation for the historical monitoring period was not feasible due to the absence of temperature data for the beginning of the century. Nonetheless, a strong correlation between precipitation and spring discharge in the past is evident, suggesting that precipitation serves as an effective indicator (in relative terms) of recharge within a specific climatic context (in this case, that of the early century). However, in the present, precipitation values are higher than what would be expected if following the historical correlation.

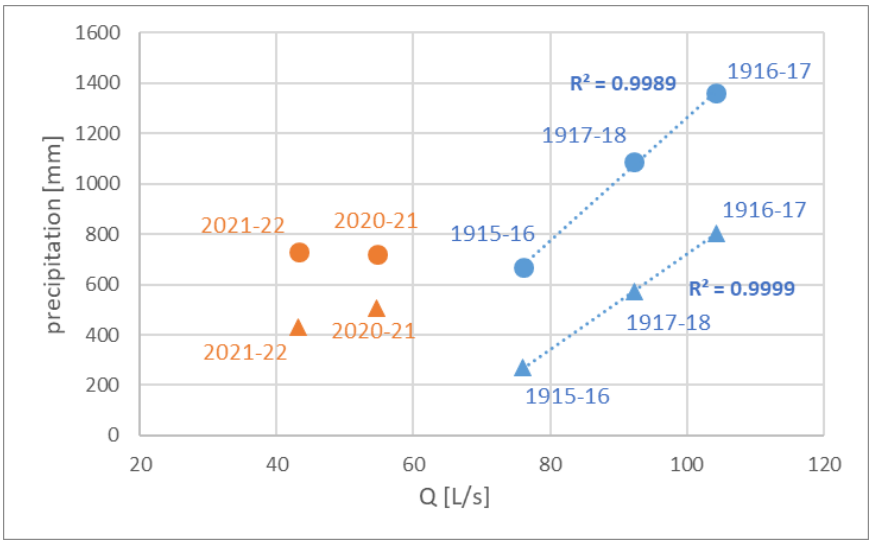

Fig. 2.13. Linear relationship between annual spring discharge and precipitation in the period 1915-18 and 2020-22. The circles represent the total precipitation over a hydrologic year whereas the triangles represent the precipitation of the recharge season.

Notable global changes, such as rising temperatures (resulting in increased evapotranspiration and decreased precipitation and snow cover) and shifts in precipitation patterns (with more frequent extreme events causing less effective for groundwater infiltration), have occurred since the past. This has created a different current climatic context compared to the past. Specifically, all the factors mentioned above, plausibly contribute to reduced recharge in the present compared to the past, resulting in lower discharge at the spring despite similar levels of precipitation. Therefore, relying solely on precipitation as a century-scale recharge indicator is not advisable, but it can be meaningful within a "homogeneous" climatic context.

It's worth noting that although the elevation of the past rain gauge (Montese station) and the present one (Riola di Labante station) differs (623 vs. 920 m asl), the analysis of the past two decades in Fig. 2.11 suggests that the recorded precipitation at both stations is similar. Hence, the observed difference between past and present conditions should not be attributed to variations in station elevation.

2.10.5. Liquid and solid precipitation

During the recent monitoring period of 2020-23, although there was no specific monitoring setup for solid precipitation near the study area, the research team diligently observed weather conditions between December 2020 and March 2023. Only two significant snowfall events were recorded during this timeframe - one at the end of December 2020 and another at the end of

January 2023. The limited occurrence of snowfall events led to the conclusion that they were insufficient for evaluating distinct spring discharge responses to solid versus liquid precipitation. To provide a more objective evaluation of solid precipitation during the monitoring period, major recharge events (i.e. precipitation > 25 mm in 5 days) were identified where the daily average air temperature was ≤ 0°C (considering the minimum air temperature among the 5 reference days for each event). Six such events were identified (Tab. 2.1), with two occurring during the hydrological year 20-21 (high flow period) and four during the hydrological years 21-22 and 22-23 (low flow period).

	major recharge event		P (sum of 5 days)	average daily T (min of 5 days)	ID
	first day	last day			
high flow	01/12/2020	05/12/2020	122.6	-2.4	1
	06/12/2020	10/12/2020	70.6	0.36	
	26/12/2020	30/12/2020	52.6	-2.7	2
	31/12/2020	04/01/2021	42.2	0.86	
	20/01/2021	24/01/2021	60.2	1.12	
	10/04/2021	14/04/2021	57.2	1.4	
	12/09/2021	16/09/2021	41.8	17.53	
	22/09/2021	26/09/2021	29.2	13.59	
	02/10/2021	06/10/2021	27.8	10.79	
low flow	01/11/2021	05/11/2021	29.2	5.14	
	11/11/2021	15/11/2021	59.8	7.21	
	05/01/2022	09/01/2022	40.2	-1.49	3
	31/03/2022	04/04/2022	48.2	1.44	
	20/04/2022	24/04/2022	63.4	5.47	
	05/05/2022	09/05/2022	59	8.4	
	18/08/2022	22/08/2022	34	15.76	
	28/08/2022	01/09/2022	35.2	16.13	
	21/11/2022	25/11/2022	59.4	2.31	
	01/12/2022	05/12/2022	30.4	0.61	
	06/12/2022	10/12/2022	31.4	2.33	
	11/12/2022	15/12/2022	30.4	-2.84	4
	20/01/2023	24/01/2023	29.8	-3.5	5
	01/03/2023	05/03/2023	45	-1.74	6

Tab. 2.1. List of the major recharge events registered during the monitoring period (precipitation > 25 mm in 5 days). The six events associated with an average daily air temperature < 0°C (minimum value of the 5-days interval) are highlighted in red and labeled with a progressive ID from 1 to 6.

These major recharge events were potentially associated with solid precipitation. Each of the six events underwent further analysis to determine if most of the precipitation occurred on days with a low average air temperature (≤ 2 °C): when at least 10 mm of precipitation occurred in a day with average air temperature < 2 °C, a “high probability” of snowfall was assigned to the 5-day recharge event. In the remaining cases, the events were labelled with a “low probability” of snowfall. This analysis led to the identification of three major recharge events with a "low

probability" of snowfall and three events with a "high probability" of snowfall (Tab. 2.2). The latter three events include the two already noted during the monitoring period (end of December 2020 and end of January 2023), plus an additional event at the end of December 2022. Importantly, the air temperature data used for the analysis originate from the Montese station, situated at a high elevation compared to Nadìa spring recharge area (see Section 2.10.2).

	ID	*days:*	*I*	*II*	*III*	*IV*	*V*	probability of snowfall
high flow	1	p	2.4	2.8	7	45.4	65	Low
		T	0.05	-2.4	-0.47	3.1	6.22	
	2	p	**16**		20.4	12	4.2	High
		T	**-1.47**	-2.7	2.03	2.78	0.63	
low flow	3	p	26.8	6	5.2	0.2	2	Low
		T	5.23	-1.24	-1.49	-0.97	-1.37	
	4	p	3.2			0.2	27	Low
		T	0.09	-2.4	-2.84	-1.82	3.78	
	5	p	0.2	3	2.4	5.8	**18.4**	High
		T	-2.99	-3.5	-2.54	-1.81	**0.36**	
	6	p	2.6	**18.4**	24			High
		T	-1.74	**0.02**	2.91	4.17	6.58	

Tab. 2.2. Detailed analysis of the six recharge events identified in Table 2.1. For each 5-day event, daily precipitations > 10 mm are highlighted in red, whereas daily averaged temperatures < 2 °C are highlighted in blue. When two such condition coexisted in the same day, values are further highlighted in bold.

This might have resulted in an underestimation of air temperatures compared to Nadìa recharge area. The three events identified with a high probability of snowfall align with the correlation analysis described in the main text, suggesting consistency with other precipitation events (see the correlation graphs in Section 2.10.6, where snowfall events are highlighted). This confirms the previously suggested impossibility of distinguishing between the effects of solid and liquid precipitation during the 20-23 monitoring period, where solid precipitation was notably scarce. Regarding the experimental data from historical monitoring (1914-18), we lack the necessary information to hypothetically differentiate between solid and liquid precipitation. Indeed, during this historical period, there was an absence of air temperature monitoring near the study area or any monitoring stations with geographical and topographical comparability to the studied zone.

Nonetheless, it is acknowledged that snowfall underwent variations between the two monitoring periods compared in this study. These variations, although imprecisely determinable for the investigated area, were previously observed in the study region (e.g., Diodato et al., 2019; Diodato et al., 2022). In particular, a decrease of snowfall and snow cover duration was registered during the XX century, contributing significantly to a general alteration of the climatic regime, as previously discussed in Section 2.10.4.

2.10.6. Linear correlations between recharge events and discharge indicators (Q, EC, pH)

Below are the linear correlation graphs used to derive the R^2 values for Fig. 2.7a in the main text. The methodology for correlation is described in Section 2.6.4 of the main text. Figs. 2.14 to 2.17 correspond to the indicator Q; Figs. 2.18 and 2.19 correspond to the indicator EC; Figs. 2.20 and 2.21 correspond to the indicator pH.

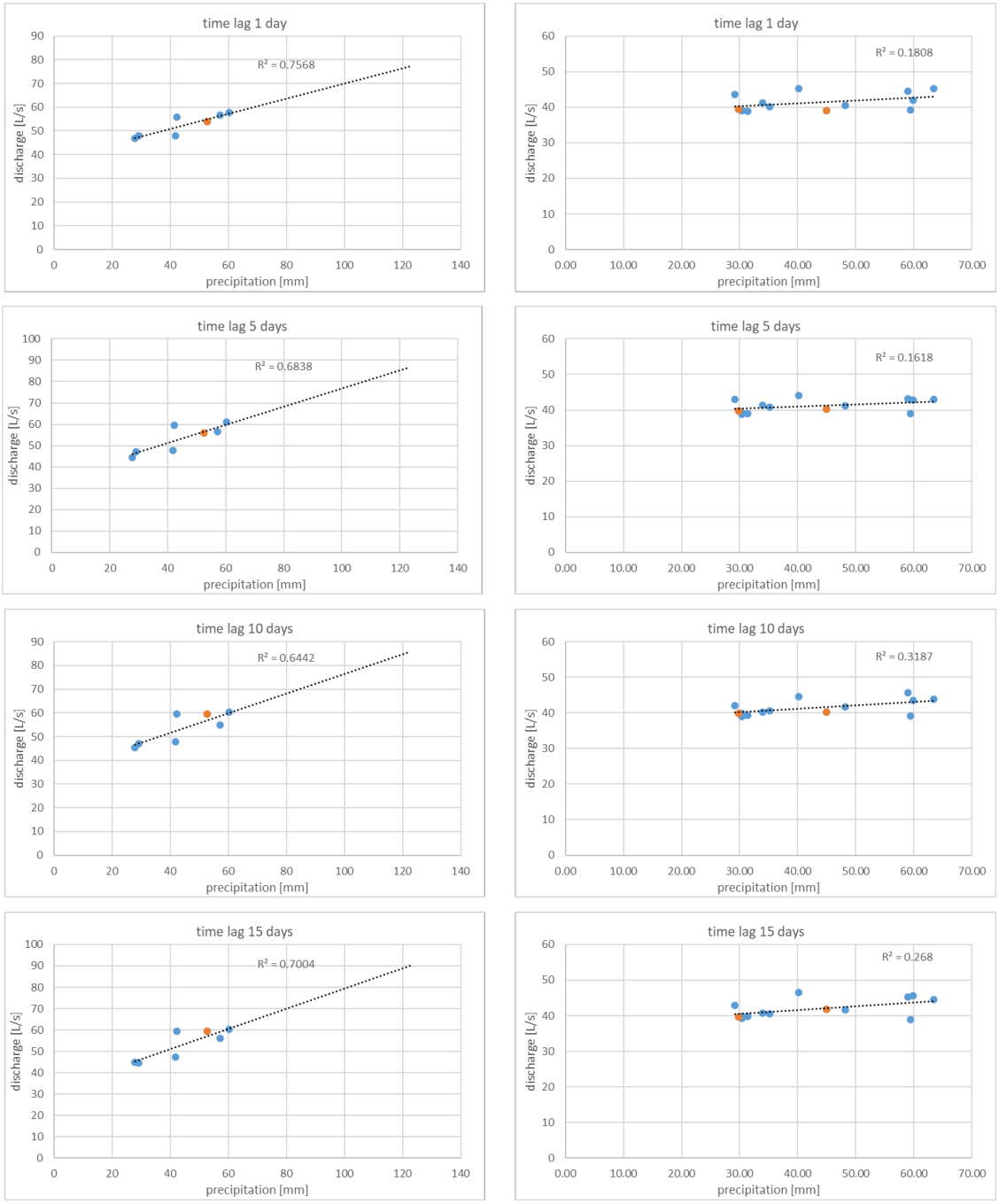

Fig. 2.14. Correlation graphs between precipitation (main recharge events) and Q, with increasing time lags from 1 to 15 days. Graphs on the right column represent the high flow period (hydrologic year 2020-21) while the graphs on the right refer to the low flow period (hydrologic years 2021-22 and 2022-23). The events associated to high snowfall probability are highlighted in orange.

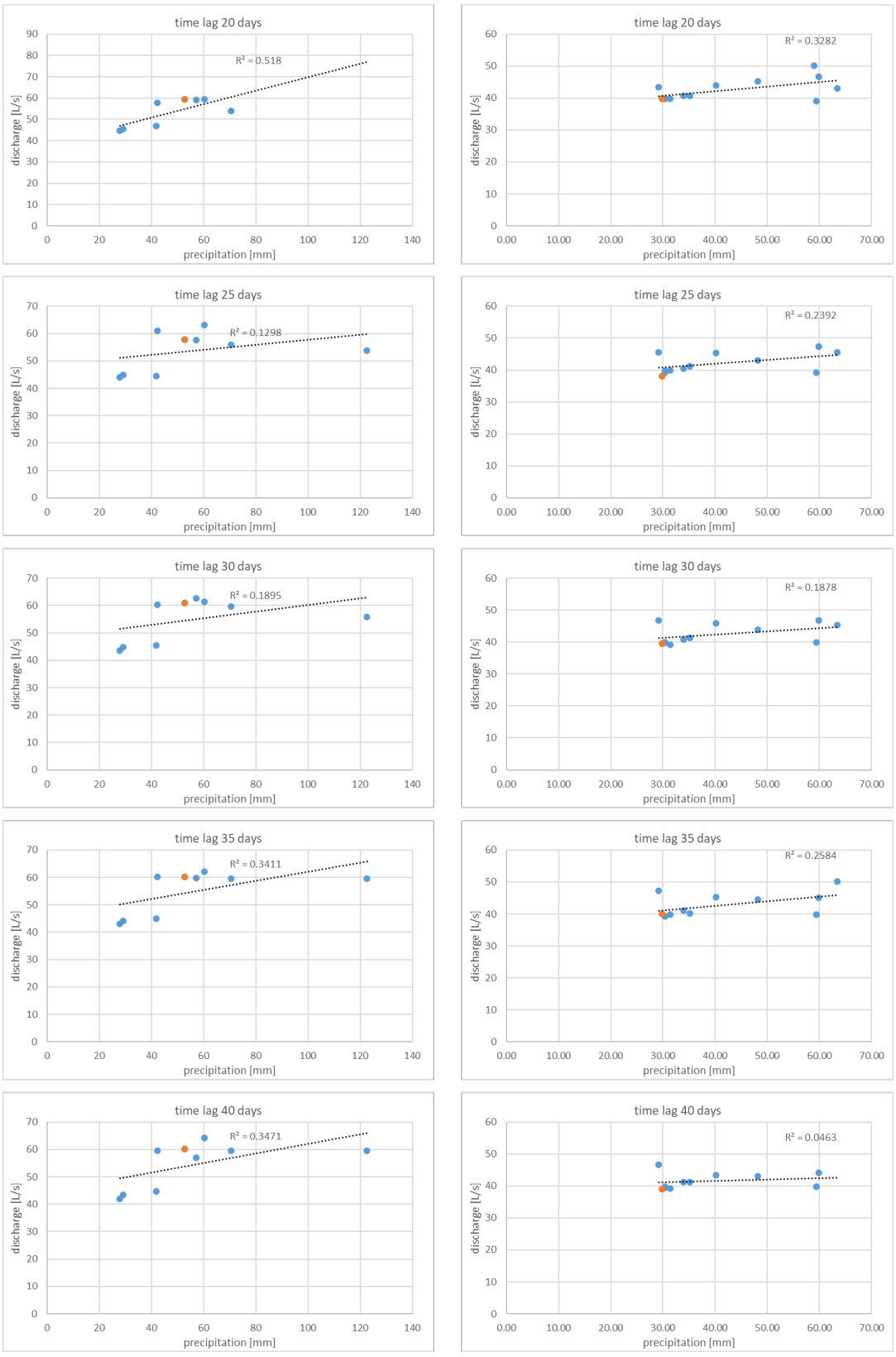

Fig. 2.15. Correlation graphs between precipitation (main recharge events) and Q, with increasing time lags from 20 to 40 days. Graphs on the right column represent the high flow period (hydrologic year 2020-21) while the graphs on the right refer to the low flow period (hydrologic years 2021-22 and 2022-23). The events associated to high snowfall probability are highlighted in orange.

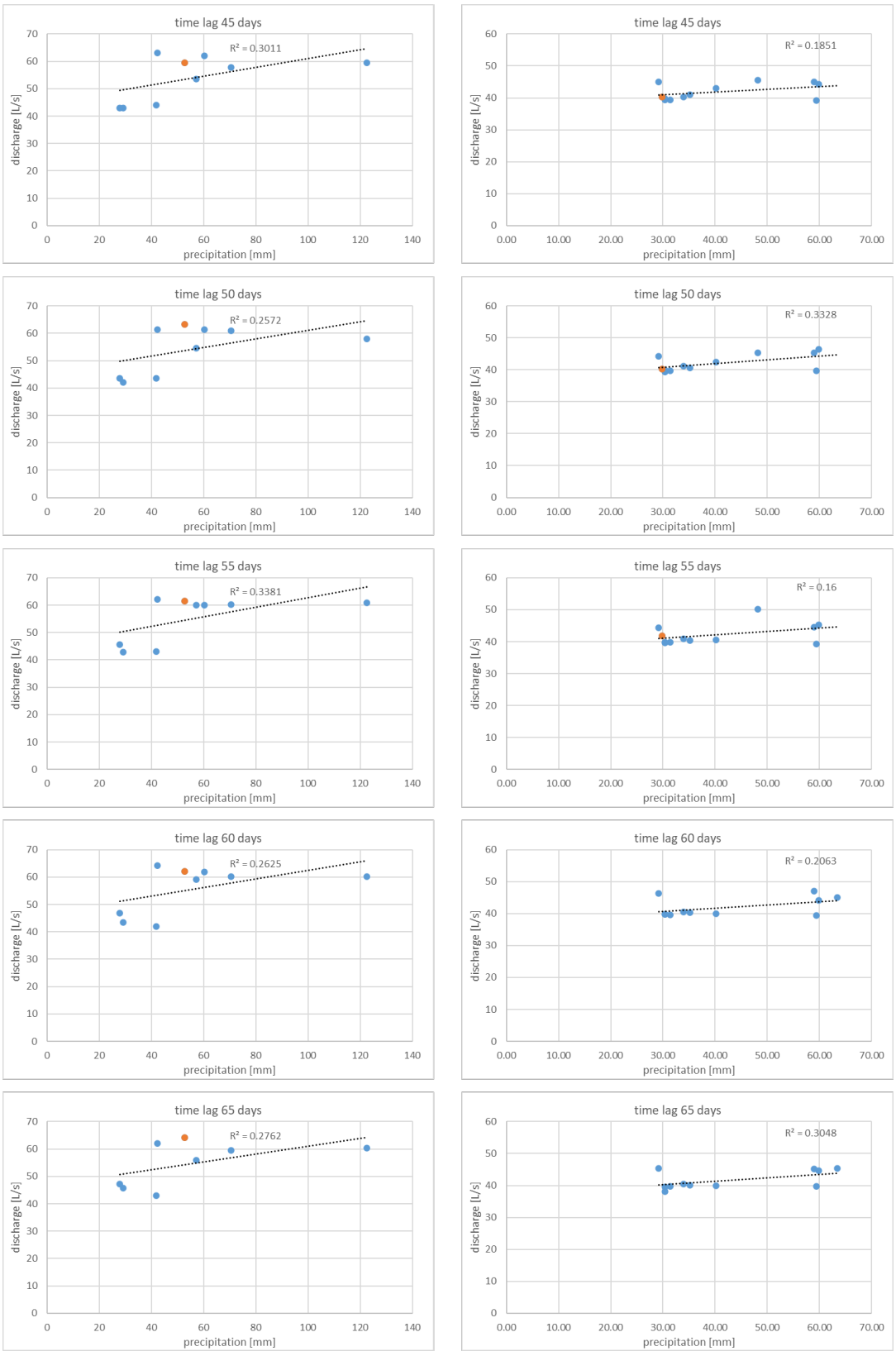

Fig. 2.16. Correlation graphs between precipitation (main recharge events) and Q, with increasing time lags from 45 to 65 days. Graphs on the right column represent the high flow period (hydrologic year 2020-21) while the graphs on the right refer to the low flow period (hydrologic years 2021-22 and 2022-23). The events associated to high snowfall probability are highlighted in orange.

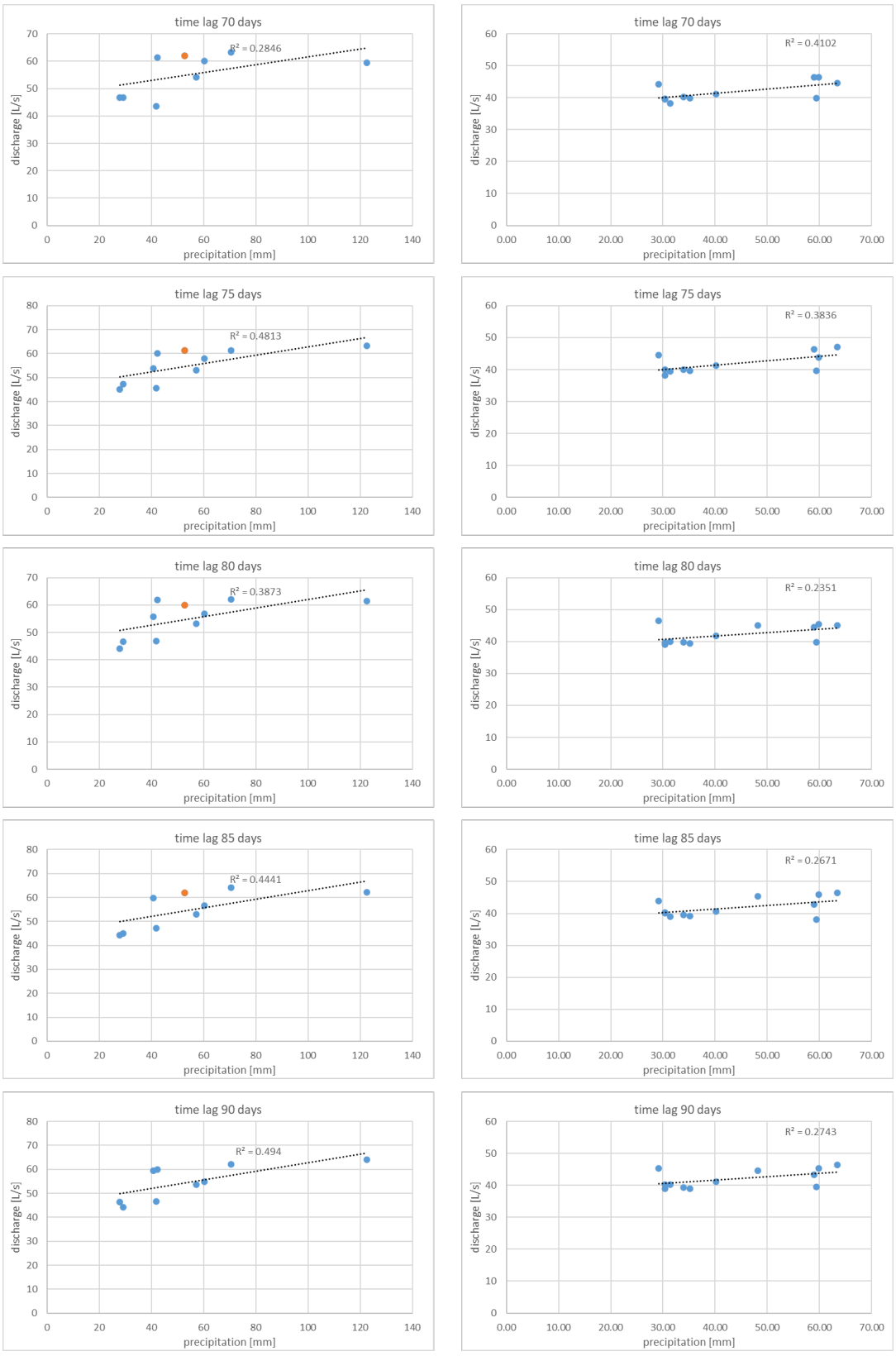

Fig. 2.17. Correlation graphs between precipitation (main recharge events) and Q, with increasing time lags from 50 to 90 days. Graphs on the right column represent the high flow period (hydrologic year 2020-21) while the graphs on the right refer to the low flow period (hydrologic years 2021-22 and 2022-23). The events associated to high snowfall probability are highlighted in orange.

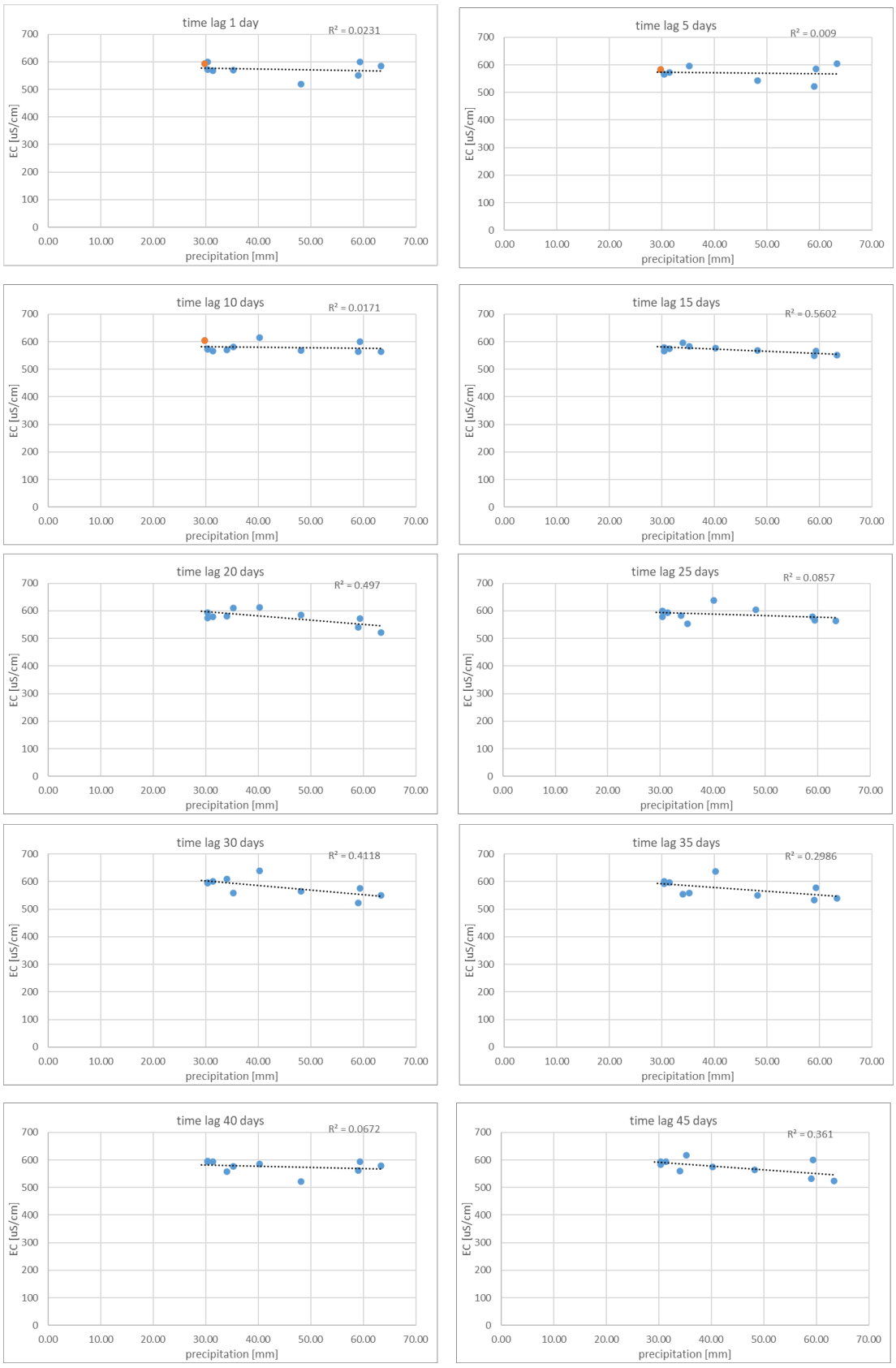

Fig. 2.18. Correlation graphs between precipitation (main recharge events) and EC, with increasing time lags from 1 to 45 days. All the graphs refer to the low flow period (hydrologic years 2021-22 and 2022-23). The events associated to high snowfall probability are highlighted in orange.

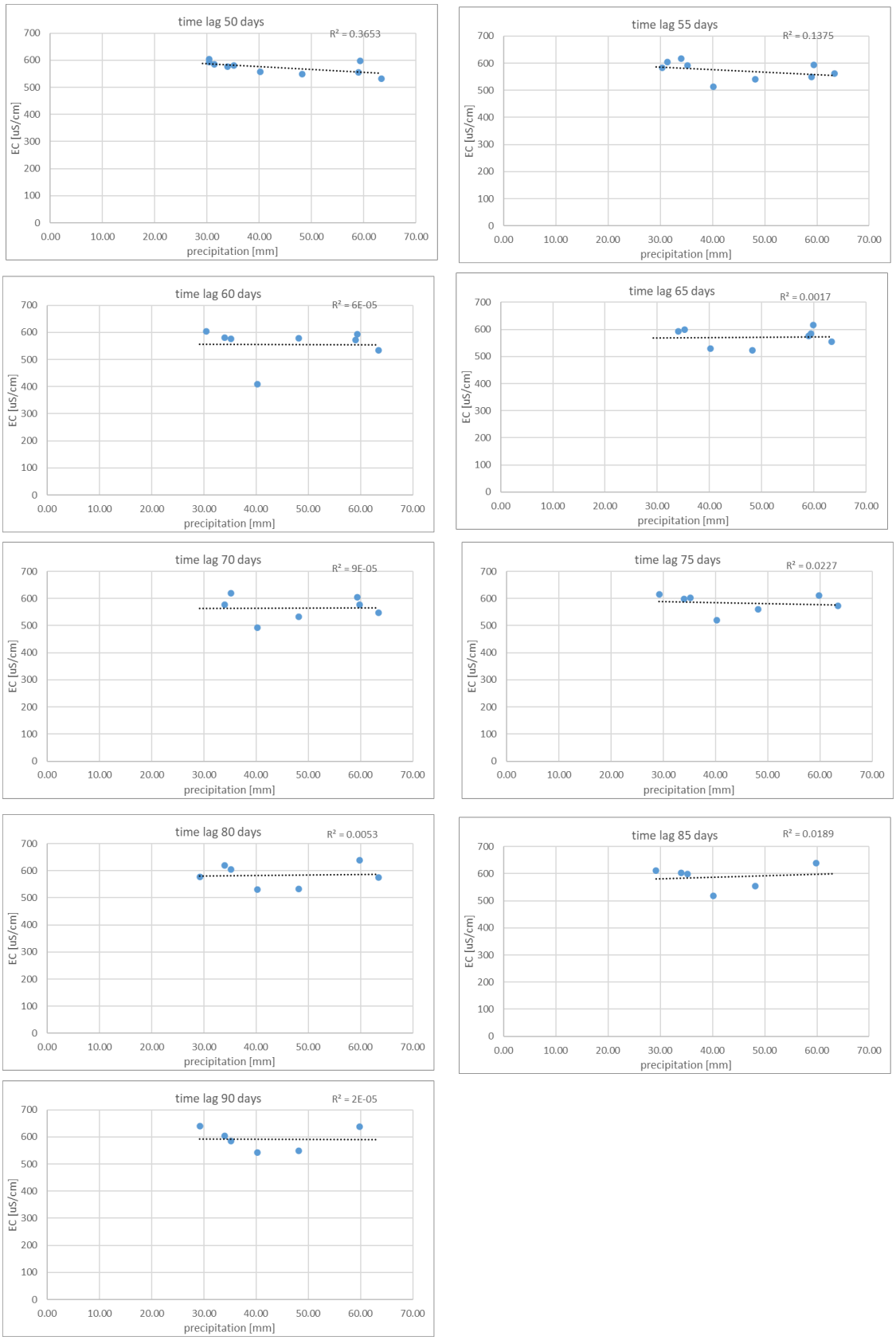

Fig. 2.19. Correlation graphs between precipitation (main recharge events) and EC, with increasing time lags from 50 to 90 days. All graphs refer to the low flow period (hydrologic years 2021-22 and 2022-23). The correlation dataset does not contain precipitation event associated with high probability of snowfall.

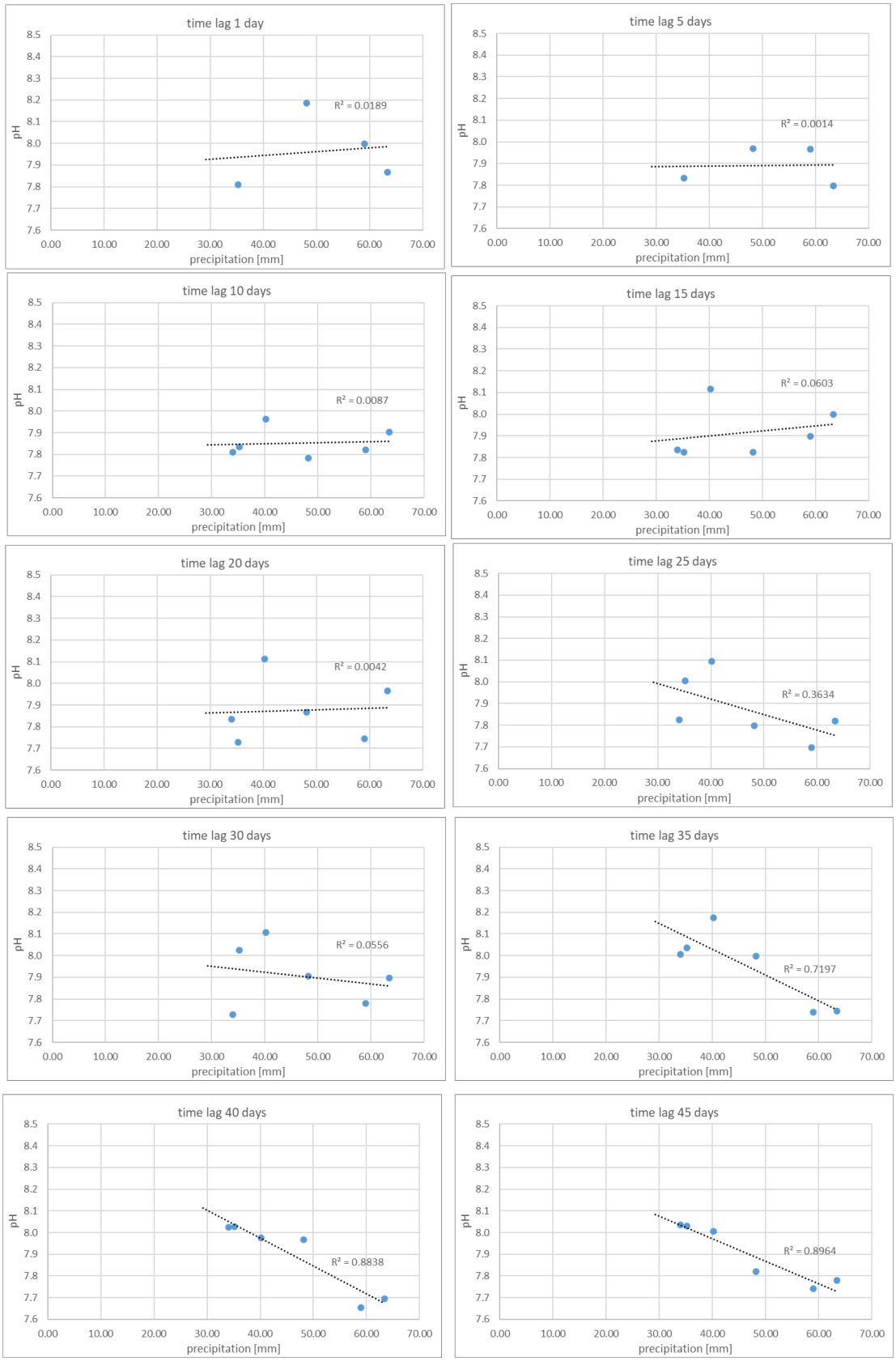

Fig. 2.20. Correlation graphs between precipitation (main recharge events) and pH, with increasing time lags from 1 to 45 days. All graphs refer to the low flow period (hydrologic years 2021-22 and 2022-23). The correlation dataset does not contain precipitation event associated with high probability of snowfall.

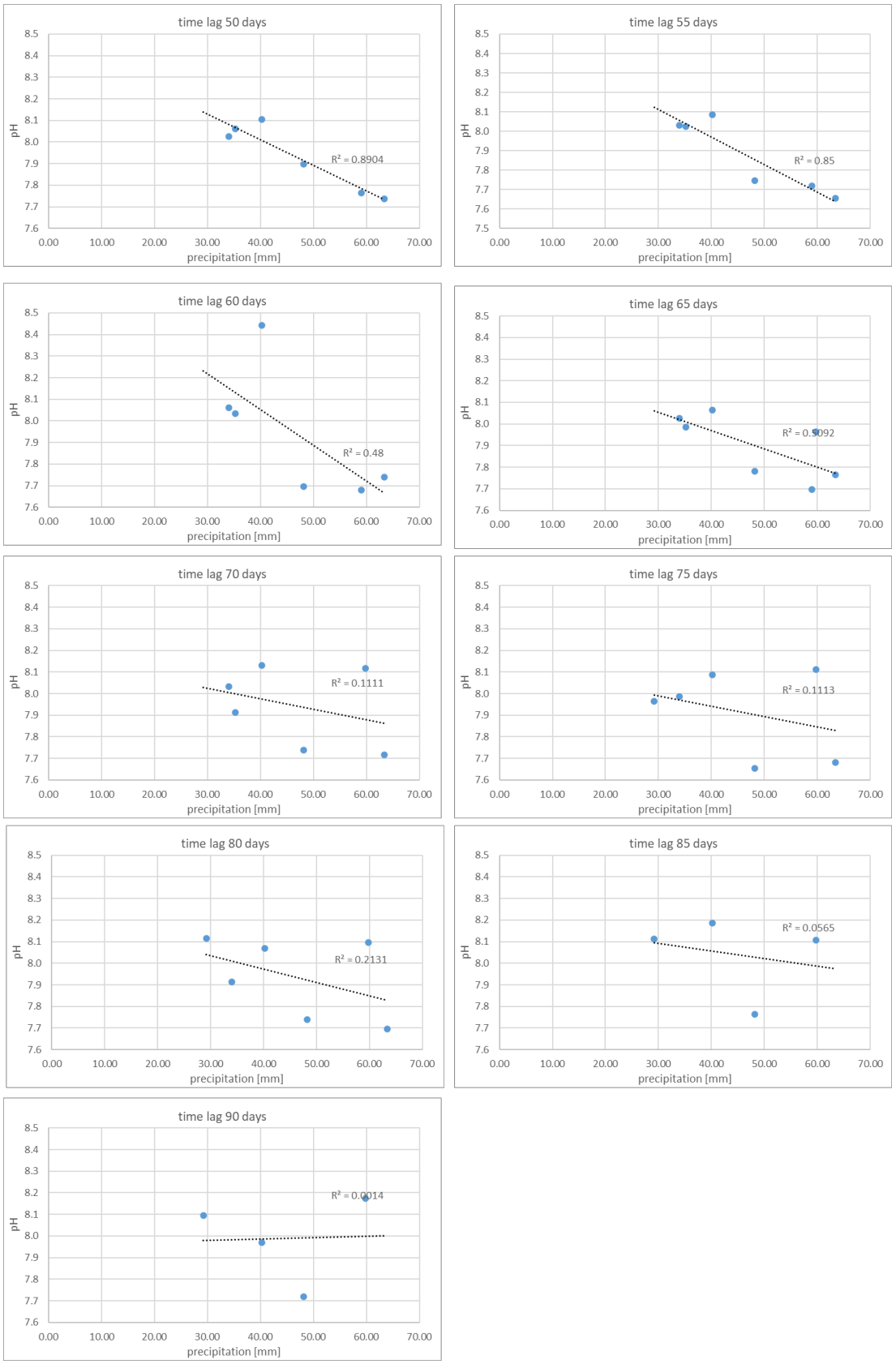

Fig. 2.21. Correlation graphs between precipitation (main recharge events) and pH, with increasing time lags from 50 to 90 days. All graphs refer to the low flow period (hydrologic years 2021-22 and 2022-23). The correlation dataset does not contain precipitation event associated with high probability of snowfall.

2.11. References

Abderrahman, W.A., 2005. Groundwater Management for Sustainable Development of Urban and Rural Areas in Extremely Arid Regions: A Case Study. International Journal of Water Resources Development, 21, 403-412.

Aley, T., 2019. The Ozark Underground Laboratory's Groundwater Tracing Handbook. Ozark Underground Laboratory.

Amanambu, A.C., Obarein, O.A., Mossa, J., Li, L., Ayeni, S.S., Balogun, O., Oyebamiji, A., Ochege, F.U., 2020. Groundwater system and climate change: Present status and future considerations. Journal of Hydrology, 589, 125163.

Amorosi, A., 1997. Miocene shallow-water deposits of the Northern Apennines: A stratigraphic marker across a dominantly turbidite foreland-basin succession. Geologie en Mijnbouw, 75, 295-307.

Amorosi, A., Spadafora, E., 1995. The upper Serravallian unconformity in the epi-Ligurian units of the Bologna Apennines, in: Polino, R., Sacchi, R. (Eds.), Rapporti Alpi-Appennino e guida alle escursioni, Peveragno, Cuneo, 69-86.

ARPAE, 2018. Rapporto idro-meteo-clima Emilia Romagna - rapporto annuale dati 2017 (Annual report of the idro-meteo-climatic data of the Emilia Romagna Region - year 2017). In Italian. ARPAE.

ARPAE, 2023. Rapporto idro-meteo-clima Emilia Romagna - rapporto annuale dati 2022 (Annual report of the idro-meteo-climatic data of the Emilia Romagna Region - year 2022). In Italian. ARPAE.

Atawneh, D.A., Cartwright, N., Bertone, E., 2021. Climate change and its impact on the projected values of groundwater recharge: A review. Journal of Hydrology, 601, 126602.

Azeez, N., West, L.J., Bottrell, S.H., 2015. Numerical simulation of spring hydrograph recession curves for evaluating behavior of the East Yorkshire chalk aquifer, in: Doctor, D.H., Land, L., Stephenson, J.B. (Eds.), 14th Sinkhole Conference. National Cave and Karst Research Institute, 05-09 Oct 2015, Rochester, Minnesota, 521-530.

Balocchi, P., 2014. Analisi macrostrutturale e mesostrutturale del Gruppo di Bismantova affiorante tra Zocca e Castel d'Aiano (Appennino modenese e bolognese). Atti della Società dei Naturalisti e Matematici di Modena 145, 27-42.

Boccaletti, M., Corti, G., Martelli, L., 2011. Recent and active tectonics of the external zone of the Northern Apennines (Italy). International Journal of Earth Sciences, 100, 1331-1348.

Boussinesq, J., 1904. Recherches théoriques sur l'écoulement des nappes d'eau infiltrées dans le sol et sur le débit des sources. Journal de mathématiques pures et appliquées, 10, 5-78.

Butscher, C., Huggenberger, P., 2009. Modeling the Temporal Variability of Karst Groundwater Vulnerability, with Implications for Climate Change. Environmental Science & Technology, 43, 1665-1669.

Caine, J.S., Evans, J.P., Forster, C.B., 1996. Fault zone architecture and permeability structure. Geology, 24, 1025-1028.

Caloiero, T., Caloiero, P., Frustaci, F., 2018. Long-term precipitation trend analysis in Europe and in the Mediterranean basin. Water and Environment Journal, 32, 433-445.

Campanale, C., Losacco, D., Triozzi, M., Massarelli, C., Uricchio, V.F., 2022. An Overall Perspective for the Study of Emerging Contaminants in Karst Aquifers. Resources, 11, 105.

Cantonati, M., Segadelli, S., Ogata, K., Tran, H., Sanders, D., Gerecke, R., Rott, E., Filippini, M., Gargini, A., Celico, F., 2016. A global review on ambient Limestone-Precipitating Springs (LPS): Hydrogeological setting, ecology, and conservation. Science of the Total Environment, 568, 624-637.

Cantonati, M., Stevens, L.E., Segadelli, S., Springer, A.E., Goldscheider, N., Celico, F., Filippini, M., Ogata, K., Gargini, A., 2020. Ecohydrogeology: The interdisciplinary convergence needed to improve the study and stewardship of springs and other groundwater-dependent habitats, biota, and ecosystems. Ecological Indicators, 110, 105803.

Capitani, M., 1997. Analisi mesostrutturale del sistema di deformazione trasversale della Val Lavino (Appennino settentrionale, Italia). Atti della Ticinese di Scienze della Terra, 99-110.

Carminati, E., Doglioni, C., 2012. Alps vs. Apennines: The paradigm of a tectonically asymmetric Earth. Earth-Science Reviews, 112, 67-96.

Cerino Abdin, E., Taddia, G., Gizzi, M., Lo Russo, S., 2021. Reliability of spring recession curve analysis as a function of the temporal resolution of the monitoring dataset. Environmental Earth Sciences, 80, 249.

Cervi, F., Corsini, A., Doveri, M., Mussi, M., Ronchetti, F., Tazioli, A., 2015. Characterizing the Recharge of Fractured Aquifers: A Case Study in a Flysch Rock Mass of the Northern Apennines (Italy), in: Lollino, G., Arattano, M., Rinaldi, M., Giustolisi, O., Marechal, J.-C., Grant, G.E. (Eds.), Engineering Geology for Society and Territory - Volume 3. Springer International Publishing, Cham, 563-567.

Cervi, F., Petronici, F., Castellarin, A., Marcaccio, M., Bertolini, A., Borgatti, L., 2018. Climate-change potential effects on the hydrological regime of freshwater springs in the Italian Northern Apennines. Science of the Total Environment, 622-623, 337-348.

Cibin, U., Spadafora, E., Zuffa, G.G., Castellarin, A., 2001. Continental collision history from arenites of episutural basins in the Northern Apennines, Italy. GSA Bulletin, 113, 4-19.

Conti, P., Cornamusini, G., Carmignani, L., 2020. An outline of the geology of the Northern Apennines (Italy), with Geological Map at 1:250,000 scale. Italian Journal of Geosciences.

Cuthbert, M.O., Taylor, R.G., Favreau, G., Todd, M.C., Shamsudduha, M., Villholth, K.G., MacDonald, A.M., Scanlon, B.R., Kotchoni, D.O.V., Vouillamoz, J.-M., Lawson, F.M.A., Adjomayi, P.A., Kashaigili, J., Seddon, D., Sorensen, J.P.R., Ebrahim, G.Y., Owor, M., Nyenje, P.M., Nazoumou, Y., Goni, I., Ousmane, B.I., Sibanda, T., Ascott, M.J., Macdonald, D.M.J., Agyekum, W., Koussoubé, Y., Wanke, H., Kim, H., Wada, Y., Lo, M.-H., Oki, T., Kukuric, N., 2019. Observed controls on resilience of groundwater to climate variability in sub-Saharan Africa. Nature, 572, 230-234.

De la Hera-Portillo, Á., López-Gutiérrez, J., Zorrilla-Miras, P., Mayor, B., López-Gunn, E., 2020. The Ecosystem Resilience Concept Applied to Hydrogeological Systems: A General Approach. Water, 12, 1824.

Dewandel, B., Lachassagne, P., Bakalowicz, M., Weng, P., Al-Malki, A., 2003. Evaluation of aquifer thickness by analysing recession hydrographs. Application to the Oman ophiolite hard-rock aquifer. Journal of Hydrology, 274, 248-269.

Diodato, N., Büntgen, U., Bellocchi, G., 2019. Mediterranean winter snowfall variability over the past millennium. International Journal of Climatology, 39, 384-394.

Diodato, N., Ljungqvist, F.C., Bellocchi, G., 2022. Empirical modelling of snow cover duration patterns in complex terrains of Italy. Theoretical and Applied Climatology, 147, 1195-1212.

Dore, M.H.I., 2005. Climate change and changes in global precipitation patterns: What do we know? Environment International, 31, 1167-1181.

Dragoni, W., Sukhija, B.S., 2008. Climate change and groundwater: a short review. Geological Society, London, Special Publications 288, 1-12.

Fiorillo, F., Leone, G., Pagnozzi, M., Esposito, L., 2021. Long-term trends in karst spring discharge and relation to climate factors and changes. Hydrogeology Journal, 29, 347-377.

Ford, D., Williams, P., 2007. Karst hydrogeology and geomorphology. Wiley, Chichester, UK.

Gargini, A., De Nardo, M.T., Piccinini, L., Segadelli, S., Vincenzi, V., 2014. Spring discharge and groundwater flow systems in sedimentary and ophiolitic hard rock aquifers: Experiences from Northern Apennines (Italy), in: J.M., S. (Ed.), Fractured Rock Hydrogeology. CRC Press, 129-143.

Gargini, A., Vincenzi, V., Piccinini, L., Zuppi, G., Canuti, P., 2008. Groundwater flow systems in turbidites of the Northern Apennines (Italy): natural discharge and high-speed railway tunnel drainage. Hydrogeology Journal, 16, 1577-1599.

Giustini, F., Brilli, M., Patera, A., 2016. Mapping oxygen stable isotopes of precipitation in Italy. Journal of Hydrology: Regional Studies, 8, 162-181.

Grönwall, J., Oduro-Kwarteng, S., 2018. Groundwater as a strategic resource for improved resilience: a case study from peri-urban Accra. Environmental Earth Sciences, 77, 1-13.

Hájek, M., Jiménez-Alfaro, B., Hájek, O., Brancaleoni, L., Cantonati, M., Carbognani, M., Dedić, A., Dítě, D., Gerdol, R., Hájková, P., Horsáková, V., Jansen, F., Kamberović, J., Kapfer, J., Kolari, T.H.M., Lamentowicz, M., Lazarević, P., Mašić, E., Moeslund, J.E., Pérez-Haase, A., Peterka, T., Petraglia, A., Pladevall-Izard, E., Plesková, Z., Segadelli, S., Semeniuk, Y., Singh, P., Šímová, A., Šmerdová, E., Tahvanainen, T., Tomaselli, M., Vystavna, Y., Biţă-Nicolae, C., Horsák, M., 2021. A European map of groundwater pH and calcium. Earth System Science, Data 13, 1089-1105.

Hartmann, A., Goldscheider, N., Wagener, T., Lange, J., Weiler, M., 2014. Karst water resources in a changing world: Review of hydrological modeling approaches. Reviews of Geophysics, 52, 218-242.

Herrera-Franco, G., Carrión-Mero, P., Aguilar-Aguilar, M., Morante-Carballo, F., Jaya-Montalvo, M., Morillo-Balsera, M.C., 2020. Groundwater Resilience Assessment in a Communal Coastal Aquifer System. The Case of Manglaralto in Santa Elena, Ecuador. Sustainability, 12, 8290.

Kačaroğlu, F., 1999. Review of Groundwater Pollution and Protection in Karst Areas. Water, Air, Soil Pollution, 113, 337-356.

Kresic, N., Stevanovic, Z., 2010. Groundwater hydrology of springs: engineering, theory, management, and sustainability. Butterworth-Heinemann, Oxford, UK.

Kruse, E., Eslamian, S., 2017. Groundwater management in drought conditions. Handbook of Drought and Water Scarcity, Management of Drought and Water Scarcity, 3, 275-282.

Kundzewicz, Z.W., Doli, P., 2009. Will groundwater ease freshwater stress under climate change? Hydrological Sciences Journal, 54, 665-675.

Lachassagne, P., 2008. Overview of the Hydrogeology of Hard Rock Aquifers: Applications for their Survey, Management, Modelling and Protection, in: Ahmed, S., Jayakumar, R., Salih, A. (Eds.), Groundwater Dynamics in Hard Rock Aquifers: Sustainable Management and Optimal Monitoring Network Design. Springer Netherlands, Dordrecht, 40-63.

Lachassagne, P., Wyns, R., Dewandel, B., 2011. The fracture permeability of Hard Rock Aquifers is due neither to tectonics, nor to unloading, but to weathering processes. Terra Nova, 23, 145-161.

Liesch, T., Wunsch, A., 2019. Aquifer responses to long-term climatic periodicities. Journal of Hydrology, 572, 226-242.

Lucci, P., Rossi, A., 2011. Speleologia e geositi carsici in Emilia-Romagna (Speleology and karst sites in the Emilia Romagna Region). In Italian. Federazione Speleologica Regionale dell'Emilia Romagna.

MacDonald, A., Bonsor, H., Calow, R., Taylor, R., Lapworth, D., Maurice, L., Tucker, J., O Dochartaigh, B., 2011. Groundwater resilience to climate change in Africa.

Maillet, E.T., 1905. Essais d'hydraulique souterraine & fluviale. A. Hermann, Paris.

Mariani, G.S., Zerboni, A., 2020. Surface Geomorphological Features of Deep-Seated Gravitational Slope Deformations: A Look to the Role of Lithostructure (N Apennines, Italy). Geosciences, 10, 334.

Medici, G., Lorenzi, V., Sbarbati, C., Manetta, M., Petitta, M., 2023. Structural Classification, Discharge Statistics, and Recession Analysis from the Springs of the Gran Sasso (Italy) Carbonate Aquifer; Comparison with Selected Analogues Worldwide. Sustainability, 15, 10125.

Meinzer, O.E., 1923. Outline of ground-water hydrology, with definitions, Water Supply Paper, 494. United States Geological Survey, Washington, D.C., 1-69.

Mézquita González, J.A., Comte, J.-C., Legchenko, A., Ofterdinger, U., Healy, D., 2021. Quantification of groundwater storage heterogeneity in weathered/fractured basement rock aquifers using electrical resistivity tomography: Sensitivity and uncertainty associated with petrophysical modelling. Journal of Hydrology, 593, 125637.

Mimi, Z.A., Assi, A., 2009. Intrinsic vulnerability, hazard and risk mapping for karst aquifers: A case study. Journal of Hydrology, 364, 298-310.

Nicholson, K.N., Neumann, K., Dowling, C., Gruver, J., Sherman, H., Sharma, S., 2018. An Assessment of Drinking Water Sources in Sagarmatha National Park (Mt Everest Region), Nepal. Mountain research and development, 38(4), 353-363.

Pasuto, A., Soldati, M., 2013. 7.25 Lateral Spreading, in: Shroder, J.F. (Ed.), Treatise on Geomorphology. Academic Press, San Diego, 239-248.

Pasuto, A., Soldati, M., Tecca, P.R., 2022. 5.10 - Lateral Spread: From Rock to Soil Spreading, in: Shroder, J.F. (Ed.), Treatise on Geomorphology (Second Edition). Academic Press, Oxford, 169-182.

Peña-Angulo, D., Vicente-Serrano, S.M., Domínguez-Castro, F., Lorenzo-Lacruz, J., Murphy, C., Hannaford, J., Allan, R.P., Tramblay, Y., Reig-Gracia, F., El Kenawy, A., 2022. The Complex and Spatially Diverse Patterns of Hydrological Droughts Across Europe. Water Resources Research, 58, e2022WR031976.

Petronici, F., Pujades, E., Jurado, A., Marcaccio, M., Borgatti, L., 2019. Numerical Modelling of the Mulino Delle Vene Aquifer (Northern Italy) as a Tool for Predicting the Hydrogeological System Behavior under Different Recharge Conditions. Water, 11, 2505.

Rakovec, O., Samaniego, L., Hari, V., Markonis, Y., Moravec, V., Thober, S., Hanel, M., Kumar, R., 2022. The 2018-2020 Multi-Year Drought Sets a New Benchmark in Europe. Earth's Future, 10, e2021EF002394.

Ram, R., Burg, A., Zappala, J.C., Yokochi, R., Yechieli, Y., Purtschert, R., Jiang, W., Lu, Z.-T., Mueller, P., Bernier, R., Adar, E.M., 2020. Identifying recharge processes into a vast “fossil” aquifer based on dynamic groundwater 81Kr age evolution. Journal of Hydrology, 587, 124946.

Riedel, T., Weber, T.K.D., 2020. Review: The influence of global change on Europe’s water cycle and groundwater recharge. Hydrogeology Journal, 28, 1939-1959.

Salvini, F., Billi, A., Wise, D.U., 1999. Strike-slip fault-propagation cleavage in carbonate rocks: the Mattinata Fault Zone, Southern Apennines, Italy. Journal of Structural Geology, 21, 1731-1749.

Sánchez, D., Barberá, J.A., Mudarra, M., Andreo, B., 2015. Hydrogeochemical tools applied to the study of carbonate aquifers: examples from some karst systems of Southern Spain. Environmental Earth Sciences, 74, 199-215.

Segadelli, S., Filippini, M., Monti, A., Celico, F., Gargini, A., 2021. Estimation of recharge in mountain hard-rock aquifers based on discrete spring discharge monitoring during base-flow recession. Hydrogeology Journal, 29, 949-961.

Segadelli, S., Vescovi, P., Ogata, K., Chelli, A., Zanini, A., Boschetti, T., Petrella, E., Toscani, L., Gargini, A., Celico, F., 2017. A conceptual hydrogeological model of ophiolitic aquifers (serpentinised peridotite): The test example of Mt. Prinzera (Northern Italy). Hydrological Processes, 31, 1058-1073.

Sharma, U.C., Sharma, V., 2006. Groundwater sustainability indicators for the Brahmaputra basin in the northeastern region of India. IAHS-AISH publication, 43-50.

Simsek, C., Elci, A., Gunduz, O., Erdogan, B., 2008. Hydrogeological and hydrogeochemical characterization of a karstic mountain region. Environmental Geology, 54, 291-308.

Stendardi, F., Viola, G., Vignaroli, G., 2023. Multiscale structural analysis of an Epiligurian wedge-top basin: insights into the syn- to post-orogenic evolution of the Northern Apennines accretionary wedge (Italy). International Journal of Earth Sciences, 112, 805-827.

Stevens, L.E., Aly, A.A., Arpin, S.M., Apostolova, I., Ashley, G.M., Barba, P.Q., Barquín, J., Beauger, A., Benaabidate, L., Bhat, S.U., Bouchaou, L., Cantonati, M., Carroll, T.M., Death, R., Dwire, K.A., Felippe, M.F., Fensham, R.J., Fryar, A.E., Garsaball, R.P.i., Gjoni, V., Glazier, D.S., Goldscheider, N., Gurrieri, J.T., Guðmundsdóttir, R., Guzman, A.R., Hájek, M., Hassel, K., Heartsill-Scalley, T., Herce, J.S.i., Hinterlang, D., Holway, J.H., Ilmonen, J., Jenness, J., Kapfer, J., Karaouzas, I., Knight, R.L., Kreiling, A.-K., Lameli, C.H., Ledbetter, J.D., Levine, N., Lyons, M.D., Mace, R.E., Mentzafou, A., Marle, P., Moosdorf, N., Norton, M.K., Pentecost, A., Pérez, G.G., Perla, B., Saber, A.A., Sada, D., Segadelli, S., Skaalsveen, K., Springer, A.E., Swanson, S.K., Schwartz, B.F., Sprouse, P., Tekere, M., Tobin, B.W., Tshibalo, E.A., Voldoire, O., 2022. The Ecological Integrity of Spring Ecosystems: A Global Review, in: DellaSala, D.A., Goldstein, M.I. (Eds.), Imperiled: The Encyclopedia of Conservation. Elsevier, Oxford, 436-451.

Sultan, M., Sturchio, N.C., Alsefry, S., Emil, M.K., Ahmed, M., Abdelmohsen, K., AbuAbdullah, M.M., Yan, E., Save, H., Alharbi, T., Othman, A., Chouinard, K., 2019. Assessment of age, origin, and sustainability of fossil aquifers: A geochemical and remote sensing-based approach. Journal of Hydrology, 576, 325-341.

Tague, C., Grant, G.E., 2004. A geological framework for interpreting the low-flow regimes of Cascade streams, Willamette River Basin, Oregon. Water Resources Research, 40.

Tallaksen, L.M., 1995. A review of baseflow recession analysis. Journal of Hydrology, 165, 349-370.

Tambe, S., Kharel, G., Arrawatia, M.L., Kulkarni, H., Mahamuni, K., Ganeriwala, A.K., 2012. Reviving Dying Springs: Climate Change Adaptation Experiments From the Sikkim Himalaya. Mountain Research and Development, 32, 62-72, 11.

Taylor, R.G., Scanlon, B., Döll, P., Rodell, M., van Beek, R., Wada, Y., Longuevergne, L., Leblanc, M., Famiglietti, J.S., Edmunds, M., Konikow, L., Green, T.R., Chen, J., Taniguchi, M., Bierkens, M.F.P., MacDonald, A., Fan, Y., Maxwell, R.M., Yechieli, Y., Gurdak, J.J., Allen, D.M., Shamsudduha, M., Hiscock, K., Yeh, P.J.F., Holman, I., Treidel, H., 2013. Ground water and climate change. Nature Climate Change, 3, 322-329.

Thornthwaite, C., Mather, J., 1957. Instructions and tables for computing potential evapotranspiration and the water balance, publications in climatology 10/3. Centerton: Drexel Institute of Technology.

Tsur, Y., 1990. The stabilization role of groundwater when surface water supplies are uncertain: The implications for groundwater development. Water Resources Research, 26, 811-818.

Vai, G.B., Martini, I.P., 2001. Anatomy of an Orogen: the Apennines and Adjacent Mediterranean Basins.

Vecchi, A., 1920. La sorgente di Rosola e la sua derivazione per l'acquedotto modenese (the Rosola spring and its uptake for the Modena aqueduct). In Italian, Giornale del Genio Civile. Genio Civile, Rome.

Vincenzi, V., Gargini, A., Goldscheider, N., Piccinini, L., 2014. Differential hydrogeological effects of draining tunnels through the northern Apennines, Italy. Rock Mechanics and Rock Engineering, 47, 947-965.

Weissinger, R., Philippi, T.E., Thoma, D., 2016. Linking climate to changing discharge at springs in Arches National Park, Utah, USA. Ecosphere, 7, e01491.

Wijayanti, P., Dalmadi, R., 2021. Hydrogeochemical and groundwater aggressiveness assessment in the epikarst aquifer: a spatial and temporal analysis. IOP Conference Series: Earth and Environmental Science, 683, 012141.

Worthington, S.R.H., Ford, D.C., 2009. Self-Organized Permeability in Carbonate Aquifers. Groundwater, 47, 326-336.

Zeydalinejad, N., 2023. An overview of the methods for evaluating the resilience of groundwater systems. MethodsX, 10, 102134.

2.12. Additional observations

As outlined in the preface to this second chapter, this post-article section presents detailed data concerning the frequency and severity of droughts in the Emilia-Romagna Apennines, with a particular focus on the catchment area of Nadìa Spring. It also examines the substantial reduction in Nadìa Spring's discharge observed today compared to 100 years ago, to which these droughts have significantly contributed.

2.12.1. Insights from the Montese rain gauge

The Montese rain gauge, which is highly representative of the precipitation over the Nadìa Spring catchment, provides a continuous historical dataset spanning nearly a century, from 1930 to the present. Additionally, data on rainfall for the period 1915-1919 were collected by Vecchi (1920), as previously mentioned. The graph in Fig. 2.22 focuses not on monthly cumulative precipitation but rather on the cumulative precipitation during the typical recharge period for aquifers, which spans from 1 November of one year to 31 May of the following year (Gargini et al., 2008; Segadelli et al., 2021). This period is identified as the key recharge period for groundwater due to the following reasons: (i) rainfall intensity is greater, especially during November-December and early spring season; (ii) temperatures are sufficiently low to minimise evapotranspiration; (iii) the soil remains moist, making it more effective in transferring direct recharge downward; and (iv) snowmelt during the early spring season is a key factor due to the high infiltration rate.

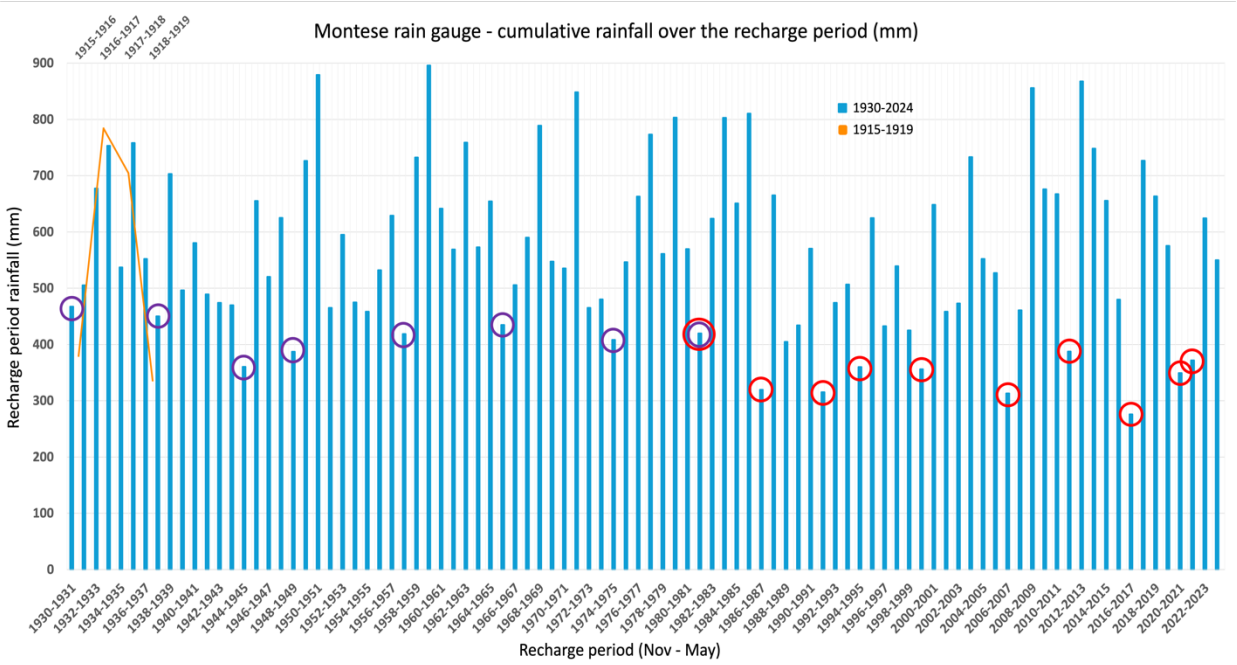

Fig. 2.22. Cumulative rainfall recorded by the Montese rain gauge over the recharge period (November-May). The orange line refers to the period 1915-1919, with the corresponding years displayed on the secondary horizontal axis at the top of the graph.

The 17 circular markers in Fig. 2.22 represent drought periods characterised by significantly low precipitation between November and May. Markers to the left of 1981-1982 are coloured purple, while those to the right are coloured red. For the drought specifically corresponding to 1981-1982, both markers are displayed.

The reason for adopting two different colours becomes apparent in Fig. 2.23, which highlights the interval of time between successive droughts.

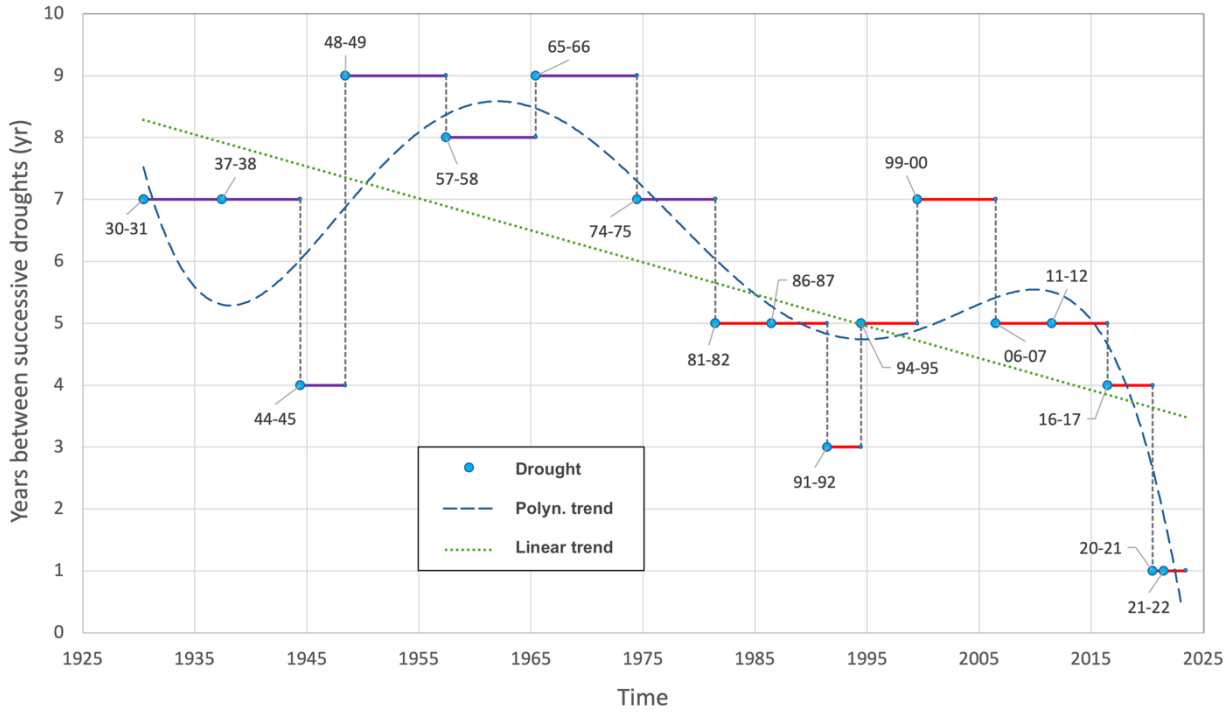

Fig. 2.23. Time intervals between successive drought events recorded by the Montese rain gauge. The horizontal bars share the same colours as the circular markers shown in Fig. 2.22, which enclose the corresponding periods. The polynomial trend was constructed using a degree 5 basis.

For instance, the gap between the droughts of 1931 and 1938 is 7 years, followed by another 7 years between 1938 and 1945. However, the interval between 1945 and 1949 is only 4 years, as indicated by the corresponding purple bar at 4 on the y-axis. Between 1931 and 1982, droughts occurred approximately every 7 to 8 years. In contrast, between 1982 and 2017, they became more frequent, occurring on average every 4 to 5 years.

Between the early 1980s and the first half of the 2010s, the frequency of water scarcity events in the Northern Apennines appeared to have stabilised at around five years. However, the Montese rain gauge recorded three drought events in just five years between 2017 and 2022, two of which (those of 2020-2021 and 2021-2022) occurred consecutively.

The graph shown in Fig. 2.24 is closely linked to the preceding one in Fig. 2.23. In this case, it displays the cumulative precipitation from 1 November of one year to 31 May of the following year, but only for the years corresponding to the droughts highlighted earlier. What stands out

in this figure, particularly with the support of the two trend lines, is that recharge period rainfall has been decreasing during drought years: from an average of approximately 420 mm between 1931 and 1982 to about 340 mm between 1987 and 2022, reflecting a 20% reduction.

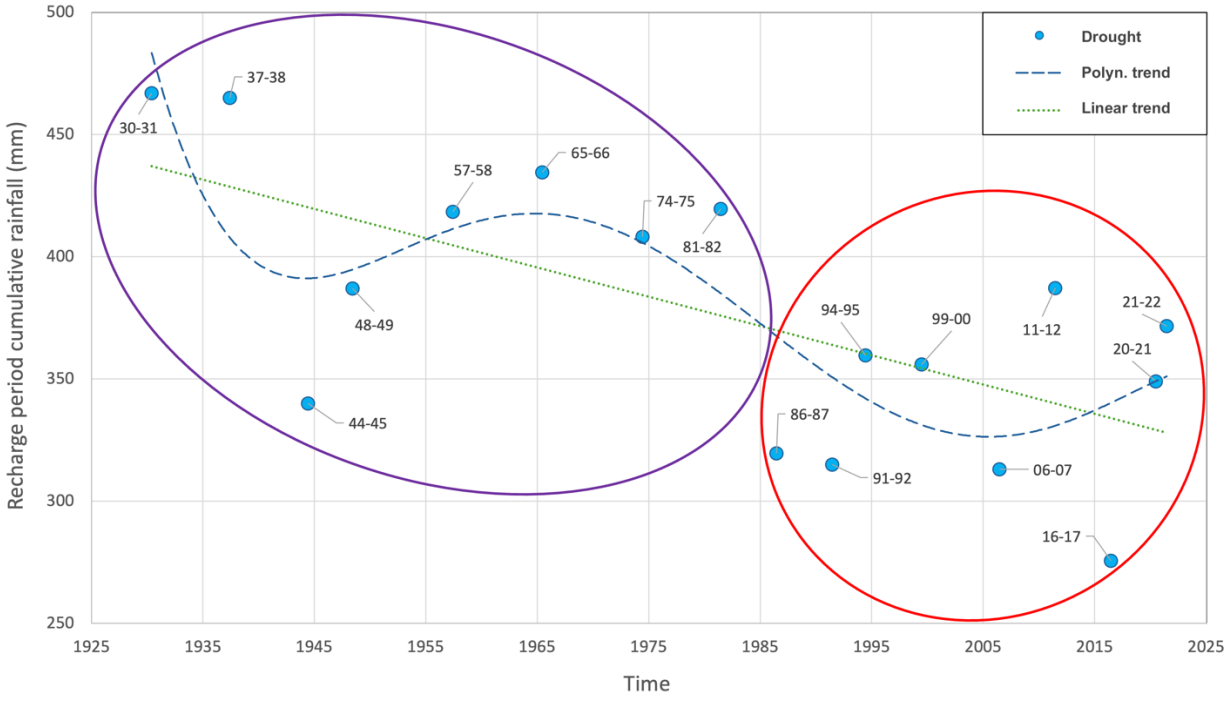

Fig. 2.24. Cumulative rainfall during the recharge period recorded by the Montese rain gauge, limited to droughts events. The two elliptical markers highlight a clear division in recharge period rainfall amounts during droughts occurring before and after the mid-1980s. The polynomial trend uses a degree 5 basis.

This graph further illustrates that droughts are not only occurring more frequently (Fig. 2.23) but are also becoming increasingly severe and critical, as precipitation during the recharge period continues to decline (Fig. 2.24). This deficit in liquid precipitation is further exacerbated by the decline in solid precipitation. In fact, in recent years, snowfall values have exhibited negative trends in both quantity (and consequently snow cover thickness) and permanence to the ground in the Northern Apennines (Diodato et al., 2022).

2.12.2. Nadìa Spring discharge reduction

As highlighted in Section 2.8.3, the reductions in recharge observed between 2020 and 2022 in the Nadìa Spring catchment primarily affected the peak phases of the yearly hydrograph, while leaving the minimum discharge largely unaffected (Fig. 2.5). This indicates significant resilience of the spring to individual dry years, maintaining a sufficient flow rate even during critical summer seasons. However, the notable decline in spring discharge since the early 21st century suggests limited resilience of Nadìa Spring to long-term recharge variations.

Figure 2.25 clearly illustrates this significant drop in the average discharge of Nadìa Spring over the past century. The comparison of mean monthly discharge between the periods 1915-1919 and 2020-2023 reveals a reduction in flow rate of approximately 40%, clearly reflecting the long-term increasing frequency and severity of droughts in the Northern Apennines, as highlighted in the preceding three figures (Figs. 2.22, 2.23, and 2.24).

2020-2023	1915-1919
54.56	90.00
59.32	91.00
61.18	97.30
61.61	103.10
56.87	108.30
58.28	106.70
56.26	98.30
52.72	90.50
49.88	83.90
48.00	78.25
46.15	77.10
43.41	72.90
Average:	
54.02 L/s	91.45 L/s

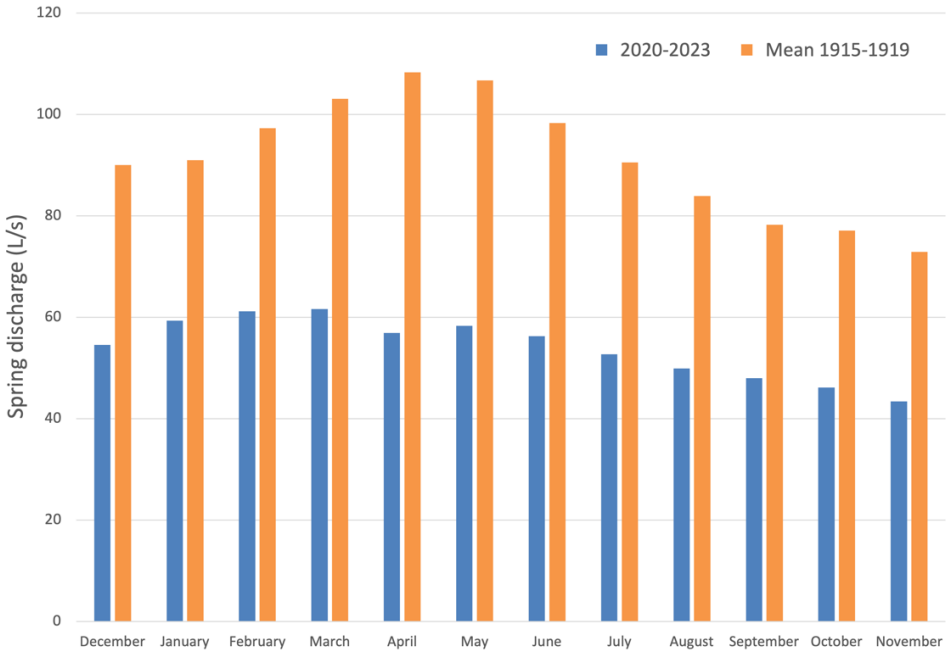

Fig. 2.25. Comparison between the 1915-1919 and 2020-2023 average monthly discharge of Nadìa Spring. The table on the left presents the values displayed in the graph on the right.

At the beginning of the 20th century, during 1915-1919, the spring exhibited an annual average discharge of roughly 91-92 L/s, while the average discharge between December 2020 and March 2023 has dropped to just 54 L/s. This change must be natural, as there have been no human-made alterations to both the aquifer conditions (e.g., pumping wells) and land use in the restricted catchment area of Nadìa Spring over the past 100 years.

Nevertheless, Fig. 2.5b reveals an increasing laminar capacity of the calcarenitic aquifer over time, characterised by a decrease in discharge variability within a single year and enhanced stability of minimum discharge values across different years. This evidence suggests that, despite the significant natural decline in Nadìa Spring's discharge over the past century, the spring demonstrates resilience to climate change, maintaining a consistent base flow and continuing to provide an ecosystem service with an adequate flow rate.

Chapter 3:

Assessing the long-term trend of spring discharge in a climate change hotspot area

3.1. Preface

The analyses summarised in the preceding chapter addressed the first scientific question of this PhD project, concentrating on quantifying the historical impact of climate change on spring discharge across the Apennines over the past century and evaluating the climatic resilience of a spring through a multidisciplinary approach. The next critical step involves a comprehensive investigation into the intricate relationship between recharge-related parameters and spring discharge, based on extensive historical time-series data, with the aim of projecting flow rates into the long-term future.

To support this endeavour, an extensive research phase was dedicated to identifying hydrological time series of spring discharge in the Apennines that met the following criteria: continuous monitoring spanning a century or nearly a century; spring catchments with no significant groundwater withdrawals, either deliberate or unintentional (e.g., due to tunnelling or mining), that could affect the discharge process; and relatively stable land use conditions within the catchment area, with no disturbances to the soil water or energy budget and the associated recharge processes. These criteria were vital for isolating the effects of global warming from other anthropogenic factors. Following this, an in-depth literature review was undertaken. Discharge data for two selected springs were provided by the water companies Acquedotto Pugliese and Acquedotto del Fiora, while analysis was conducted in collaboration with Alessandro Gargini and Maria Filippini. Antonio Navarra contributed to the assessment of future discharge using climate projections from regional atmospheric circulation models.

This chapter presents the multivariate statistical approach employed to assess the long-term trends in the discharge of Sanità and Ermicciolo Springs. The chapter consists of a paper published in the journal *Science of the Total Environment*: Casati, T.[1], Navarra, A[1, 2], Filippini, M.[1], Gargini, A.[1], 2024. Assessing the long-term trend of spring discharge in a climate change hotspot area, STOTEN, 957, 177498, ISSN 00489697, https://doi.org/10.1016/j.scitotenv.2024.177498.

[1] Department of Biological, Geological, and Environmental Sciences - BiGeA, Alma Mater Studiorum University of Bologna, via Zamboni 67, 40126, Bologna, Italy
[2] Fondazione Centro Euro-Mediterraneo sui Cambiamenti Climatici (Euro-Mediterranean Center on Climate Change), via Marco Biagi 5, 73100, Lecce, Italy

3.2. Highlights, Graphical abstract, and Keywords

- Long-term effects of climate change on spring discharge under a Mediterranean climate.
- Statistical correlation analyses between spring discharge and recharge-related data.
- Application of correlation factors to RCPs 4.5 and 8.5 future weather scenarios.
- Estimation of long-term spring discharge scenarios for the 2040-2070 period.
- A projected 9-11% decrease in flow rate is expected to affect the studied springs.

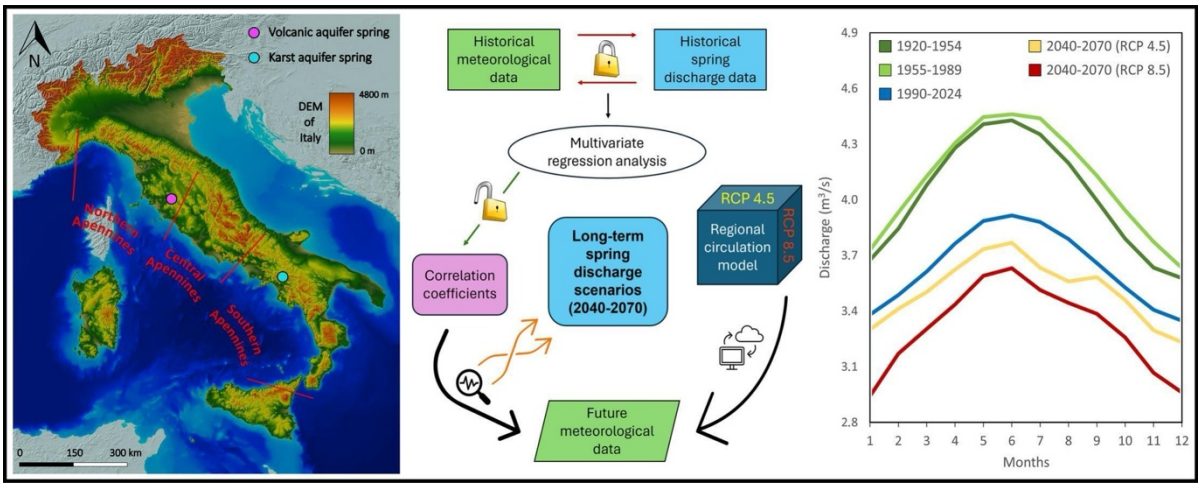

Spring discharge, Mediterranean region, Climate change, Multivariate statistics, Regional circulation model, Long-term discharge projections

3.3. Abstract

Global warming affects atmospheric and oceanic energy budgets, modifying the Earth's water cycle. The Mediterranean region is a critical zone for climate change due to a decrease in recharge and an increase in the frequency and severity of droughts over recent decades. While the impacts of possible emissions scenarios on surface water have been extensively studied, the effects on groundwater discharge remain uncertain at both global and local scales. The primary objective of this study is to predict the long-term effects of climate change on the discharge of two springs with extensive discharge records, located in distinctly different hydrogeological settings within the Mediterranean climate zone. Through multivariate statistical analyses on secular time-series, correlation factors were identified between the springs' historical discharge and recharge-related parameters representative of their catchment. Future climate projections from a Regional Circulation Model were used to estimate long-term discharge trends of the springs for the 2040-2070 period. The results indicate that the discharge of both springs, on a multi-decadal trend scale, could decrease by 9% to 11% by 2040-2070 compared to that of the past few decades. The

consistent negative trends observed across the two different hydrogeological settings suggest that the multi-decadal decline in spring discharge is more influenced by climatic factors than by specific hydrogeological features. This leads to the speculation that similar trends could be expected in other springs within Mediterranean-type climates worldwide. Future water shortages will significantly impact the hydrogeological contexts within these climates. Therefore, the long-term outcomes of this study are crucial for assisting water utility agencies in the sustainable management of groundwater resources, providing them with adequate time to plan and implement large-scale infrastructure projects over the coming decades.

3.4. Introduction

Global climate change is expected to have a significant impact on the water cycle. Extensive studies have been performed on the impact on atmospheric and surface branches of the cycle (Pekel et al., 2016; Trenberth et al., 2003), but comparatively less attention has been provided on the groundwater component. Comprehensive assessments of climate change effects on groundwater resources, particularly in regions encountering increasing qualitative and quantitative impacts on surface water (Secci et al., 2023), are needed given the crucial role of groundwater in providing key ecosystemic services. Climate change affects the recharge of groundwater and in turn the long-term average renewable groundwater resource. This impact arises from rising mean air temperature, shifts in mean precipitation, and modifications in precipitation typology and regime, with extreme regional variability of the effects (Caloiero et al., 2018; Kundzewicz and Döll, 2009). Mediterranean-type climates according to the Köppen-Geiger classification (Kottek et al., 2006) are among the areas of the planet most exposed to droughts, as demonstrated by various researchers (Alilou et al., 2022; Blake et al., 2010; Fiorillo and Guadagno, 2012; Garreaud et al., 2017; Scanlon et al., 2012; Van Loon et al., 2014). In particular, the Mediterranean region stands out as one of the hotspots for climate change, experiencing a rate of global warming that overcomes the global mean trend (Giorgi, 2006; Sivelle et al., 2021; Todaro et al., 2022). These critical factors are expected to have a major impact on groundwater recharge and its future availability.

Among other impacts, the declining discharge of springs has becoming more pronounced in recent decades, as a consequence of recurring droughts (Jeelani, 2008) and the associated shortage of recharge. This alarming trend emphasizes the vulnerability of groundwater to climate-induced alterations of the hydrologic cycle (Hao et al., 2006; Portoghese et al., 2013). In addition to the quantitative aspect, another significant threat to springs, particularly in karst settings (Kalhor et al., 2019), is aquifer pollution resulting from human activities associated with societal development and expansion in the context of a changing climate (García-Ruiz et al.,

2011). The infiltration of chemicals and various types of waste into the subsurface degrades groundwater quality and poses risks to both human and ecological health (Balaram et al., 2023). The exploitation of groundwater through the uptake of natural springs discharge is widely common (Simsek et al., 2008) as springs typically provide high-quality water (Nicholson et al., 2018). In the Mediterranean region, especially along the Apennine chain in Italy, spring water frequently serves as the primary source of potable water. Prominent urban centers, such as Rome and Naples, rely on springs to meet the demands of public aqueducts (Kresic and Stevanovic, 2009). Across the Italian peninsula, the effects of climate change on both the quantity and quality of spring discharge have been extensively studied in the southern (Allocca et al., 2014; Fiorillo et al., 2015b; Fiorillo and Guadagno, 2012; Leone et al., 2021; Polemio and Casarano, 2008) and central Apennines (Barbieri et al., 2023; Petitta et al., 2022; Sappa et al., 2018; Sappa et al., 2019). In recent years, these impacts have also been documented in the northern part of the mountain range (Filippini et al., 2024; Rotiroti et al., 2023; Secci et al., 2021).

The connection between recharge and spring discharge in the Mediterranean region, in relation to climate drivers, has been studied through various quantitative approaches, primarily to understand the impacts of climate change on spring flow and, in some cases, to estimate future discharge scenarios as well. These methods include the application of various types of models, such as rainfall-runoff hydrologic models (Cervi et al., 2018; Joigneaux et al., 2011), karst reservoir models (Cinkus et al., 2023; Fan et al., 2023), and multiple hydrogeological numerical models (Doummar et al., 2018; Gattinoni and Francani, 2010; Kovačič et al., 2020; Kovács and Stevanović, 2023). Other estimates of the recharge-discharge connection have been achieved with long-term time series statistical and correlation analyses on data extending back decades or centuries, such as the extensive discharge time series of Sanità Spring (Southern Italy) starting in 1883 (Diodato et al., 2017), the flow monitoring dataset of Fontaine de Vaucluse Spring (South-Eastern France) monitored since 1878 (Bonacci, 2007), or the discharge time series of Serino Spring group (Southern Italy) dating back to 1887 (Fiorillo et al., 2007). Alternative statistical methods were employed by Zhu et al. (2020), who studied the relationship between climatic variables and groundwater discharge using regression coefficients derived from multivariate regression analyses; and by Fiorillo et al. (2015b), who used the Rescaled Adjusted Partial Sums (RAPS) technique to examine the influence of a cyclic atmospheric circulation pattern, the North Atlantic Oscillation (NAO), on spring discharge. Furthermore, Artificial Intelligence (AI) techniques, such as those based on Artificial Neural Networks (ANN) (Smiatek et al., 2013; Wunsch et al., 2022), have been employed to investigate trends and fluctuations in recharge-discharge datasets, also in relation to climate change effects (Secci et al., 2023). Additional ANN studies (Di Nunno et al., 2021; Lambrakis et al., 2000) and studies based on multiple machine learning models (Granata et al., 2018) have focused on the potential for short and medium-term

forecasting of spring discharge. Lastly, other researchers have combined multiple methods to simulate spring discharge, such as ANN models with multilinear regression analyses (Gholami and Khaleghi, 2019), or random forest techniques with hydrogeological numerical models (Bouhafa et al., 2024). Although these studies are based on various types of analyses and different initial datasets – most of which do not extend further back than the 1990s – they share a common objective: analyzing the relationship between spring discharge and meteorological variables and/or recurring climate phenomena. Some studies pursue this aim solely to quantify the effects of climate change on the qualitative and quantitative status of groundwater, while others also seek to estimate short-term future discharge trends, sometimes using meteorological scenarios derived from General Circulation Models (GCMs).

To the best of our knowledge, none of the previous studies focus on long-term future discharge estimation, which is essential for allowing water utility agencies sufficient time to plan and implement large-scale infrastructure projects. By establishing long-term discharge relationships with recharge-related meteorological parameters based on extensive historical records (> 80 yr; Chen et al., 2004; Leone et al., 2021), there is a potential to project these relationships into the future, leveraging climate scenario data (i.e., General Circulation Models; Klaas et al., 2019; Shepherd et al., 2010) over similar multi-decadal spans. Moreover, all the previous studies considered the dynamics of single springs, missing a broader eye on the global effects of recharge reductions induced by climate change. The discharge dynamics of each spring are undeniably shaped by the features of its basin (Tóth et al., 2022). This complexity poses a challenge in gauging the impact of climate change beyond the boundaries of individual spring watersheds, e.g., extending to broader climatic zones. However, long-term spring discharge dynamics, spanning decades, are typically less tethered to the unique attributes of specific basins and more reflective of climate shifts within a given area (Hartmann et al., 2014; Zhong et al., 2016). Thus, assuming a broader applicability of future multi-decadal discharge trends, these could also aid in managing springs throughout a climatic zone lacking sufficiently extensive hydrogeological data for detailed analysis.

The present research focuses on the application of multivariate statistical analysis to extensive historical discharge records of two springs of the Apennine Mountain chain in Italy. ANN and hydrogeological modeling methods have had various successes in simulating/predicting discharge on relatively short time scales, but it is unclear if they represent a clear advantage for long-term projections based on climate scenarios spanning several decades. Therefore, in this first exploratory paper, we focus on well-tested multivariate regression techniques to assess the potential predictability of spring discharge. The Apennine Mountains are a highly representative example of a Mediterranean setting rich in groundwater discharge through springs, particularly in its southern and central sectors. Most groundwater in this region is stored in karst aquifers (De

Vita et al., 2012; Petitta and Tallini, 2002; Sappa et al., 2019). Nonetheless, aquifers with a significant yield are also found in other geological settings, related to volcanic and arenitic formations (Doveri et al., 2012; Filippini et al., 2024). The two investigated springs, namely Sanità (Cervialto Massif, Southern Apennines) and Ermicciolo (Amiata Volcano, Northern Apennines), are associated to watersheds that are affected by similar climatic variability typical of the Mediterranean-type climates, however situated in two very different hydrogeological settings, i.e., a carbonatic karstified massif and a fractured volcanic structure, respectively. For both springs, continuous discharge monitoring is available with at least monthly measurements, from the beginning of the 20th century and extending to the present day. The aim of the study is to identify the historical connection between spring discharge and recharge-related meteorological parameters from a multi-decadal perspective, to utilize this relationship in conjunction with future meteorological variables projected by GCMs to assess the multi-decadal discharge availability for the period 2040-2070.

3.5. Geological and hydrogeological settings

The Apennine Mountain chain is the backbone of the Italian peninsula and extends for about 1200 km in a NW-SE alignment, between Ligurian-Tyrrhenian Seas to the West, and Adriatic-Ionian Seas to the East. The chain is subdivided into Northern, Central and Southern Apennines (Fig. 3.1a). From a geological standpoint, Apennines are a Neogene accretionary fold-thrust belt that formed from the subduction between the African Plate below Eurasia within the Alpine System (Patacca et al., 1993). The structure of the chain presents a series of tectonic units thrusted over each other, subjected after the compressional phase to an extensional one with volcanic activity in the Tyrrhenian side (Carminati et al., 2010; Carminati et al., 2012).

The first of the two investigated springs, Sanità Spring, is situated nearby the village of Caposele in Campania Region (Southern Apennines) at an elevation of 417 m above sea level (asl) (40° 48’ 58.8” N, 15° 13’ 13.9” E) (Fig. 3.1b). Sanità Spring, with a mean annual discharge of 4.0 m^3/s, is considered the most significant spring draining the Cervialto Massif (peak elevation of 1809 m asl), one of the main Meso-Cenozoic carbonate platforms of the Central-Southern Apennines, acting as key groundwater reservoir (Allocca et al., 2014; Fiorillo et al., 2015b). The Cervialto Massif is composed of a series of limestone and limestone-dolomite (Late Triassic-Miocene) with a thickness ranging between 2500 and 3000 m (Fiorillo et al., 2021). Karst processes have transformed the morphology of the massif creating endorheic areas known as ‘polje’, surrounded by steep slopes of 35°-45° controlled by fault scarps, where recharge is concentrated, constituting almost the entire contribution area of Sanità Spring (Fiorillo et al., 2015a).

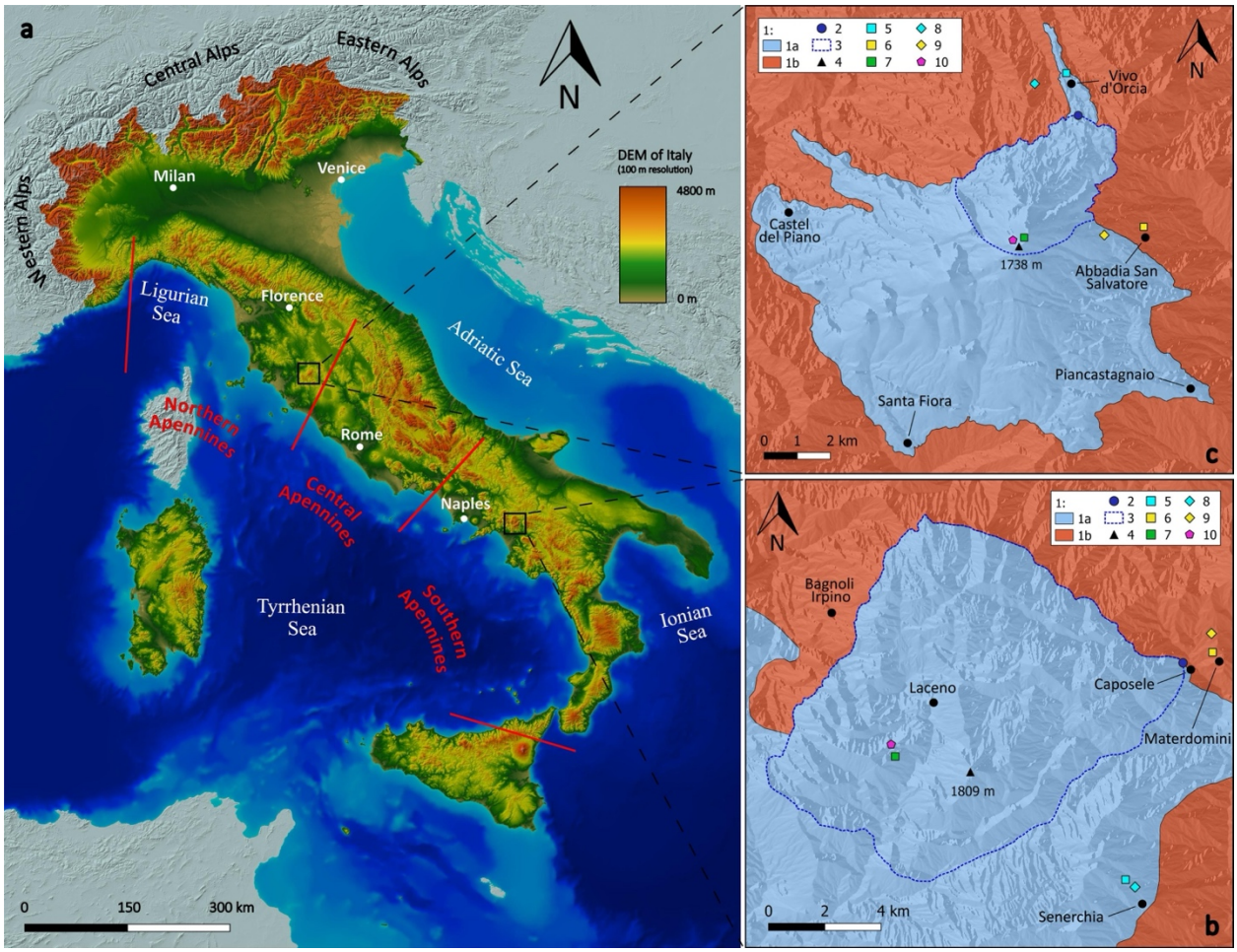

Fig. 3.1. Location of the two study areas in the Apennines Mountain chain: (a) 100 m resolution Digital Elevation Model (DEM) of Italy realized by the National Institute of Geophysics and Volcanology (INGV) (Tarquini et al., 2023), with indication of the Apennines subdivision into Northern, Central and Southern sectors; (b) 1. Geological formations; 1a. Karst aquifer; 1b. Aquitard units; 2. Sanità Spring; 3. Sanità Spring catchment; 4. Cervialto Massif peak; 5. "Senerchia" rain gauge; 6. "Materdomini" temperature gauge; 7. "Rifugio Laceno" snow gauge; 8. CMCC-CLM TLP chosen grid point; 9. CMCC-CLM 2 m °C chosen grid point; 10. ERA5 (HSR) snowfall chosen grid point; (c) 1. Geological formations; 1a. Volcanic aquifer; 1b. Aquitard units; 2. Ermicciolo Spring; 3. Ermicciolo Spring catchment; 4. Mount Amiata peak; 5. "Vivo d'Orcia" rain gauge; 6. "Abbadia San Salvatore" temperature gauge; 7. "Monte Amiata" snow gauge; 8. CMCC-CLM TLP chosen grid point; 9. CMCC-CLM 2 m °C chosen grid point; 10. ERA5 (HSR) snowfall chosen grid point.

The spring is of strategic significance to Southern Italy, particularly for the Puglia Region, which represents one of the areas with the lowest precipitation in the central Mediterranean region, receiving approximately 600 mm of annual precipitation. The water from Sanità Spring is conveyed through a 450 km long gravity-driven series of tunnels and bridges from the Campania Region to the southernmost part of Puglia since the 1930s (Fiorillo, 2009). The climate in Sanità Spring catchment area is Mediterranean and falls within the "Csa" category according to the Köppen-Geiger classification (Kottek et al., 2006). The average annual precipitation and

temperature at the mean elevation of the spring catchment are approximately 1500 mm and 12.1 °C (www.centrofunzionale.regione.campania.it).

The second spring of interest, Ermicciolo Spring, is situated along the northern slope of Mount Amiata, in the southern part of the Tuscany Region at an elevation of 1020 m asl (42° 55′ 25.8″ N; 11° 38′ 29.5″ E), approximately 100 km to the south-west of the Northern Apennines main divide (Fig. 3.1c). Ermicciolo Spring is one of the major springs in the Tuscany region, with a mean annual discharge of about 0.15 m^3/s and a maximum recorded flow rate of nearly 0.4 m^3/s. Mount Amiata (peak elevation of 1738 m asl), an extinct volcano, represents the youngest Quaternary volcanic edifice of the Tuscan Roman Magmatic Province (Frondini et al., 2009) and covers an outcropping surface of about 80 km^2. The evolution of the volcano is associated to the most recent Apenninic post-orogenic extensional phase that occurred between 300 ky and 190 ky, when several dacitic, rhyodacitic and olivine-latitic eruptions gave rise to the volcanic edifice (Bortolotti and Passerini, 1970). From a hydrogeological perspective, the volcanic structure is a fractured aquifer that can be broadly divided into two distinct groundwater flow systems separated by a dynamic groundwater divide located near the peak of the mountain (Fig. 3.1c; Doveri et al., 2012), with Ermicciolo Spring being fed by the northernmost system. Amiata aquifer stands as one of the crucial groundwater reservoirs for Southern Tuscany as it feeds major springs utilized by the local water company, providing drinkable water to the surrounding lowlands and coastal areas, which are characterized by lower precipitation, aquifer overdrafting, and groundwater salinization issues. The climate in the spring catchment is Mediterranean and categorized as “Csb” (Beck et al., 2023), with average annual precipitation and temperature of about 1200 mm and 10.6 °C (www.sir.toscana.it).

3.6. Materials and methods

3.6.1. Discharge monitoring

Measurements of the total discharge at Sanità Spring started in January 1920 (Fig. 3.2) when the Italian National Hydrographic Institute established a systematic monitoring. The spring is uptaken by the water company Acquedotto Pugliese S.p.A. (AQP) since the beginning of twentieth century (Fiorillo and Guadagno, 2012) with an artificial draining tunnel, characterized by several niches, along the discharge front at the base of the mountain slope. A portion of the spring discharge is released as overflow, providing ecological services to a local river. Originally, the discharge was quantified through a hydrometric reel along the main channel, with a monitoring frequency of two times per month (on the 2nd and 16th day of each month). Since their introduction in 1927, Venturi tubes have allowed for more frequent discharge measurements (Fiorillo et al., 2021). The monitoring system was further improved in 1980, when data acquisition became daily.

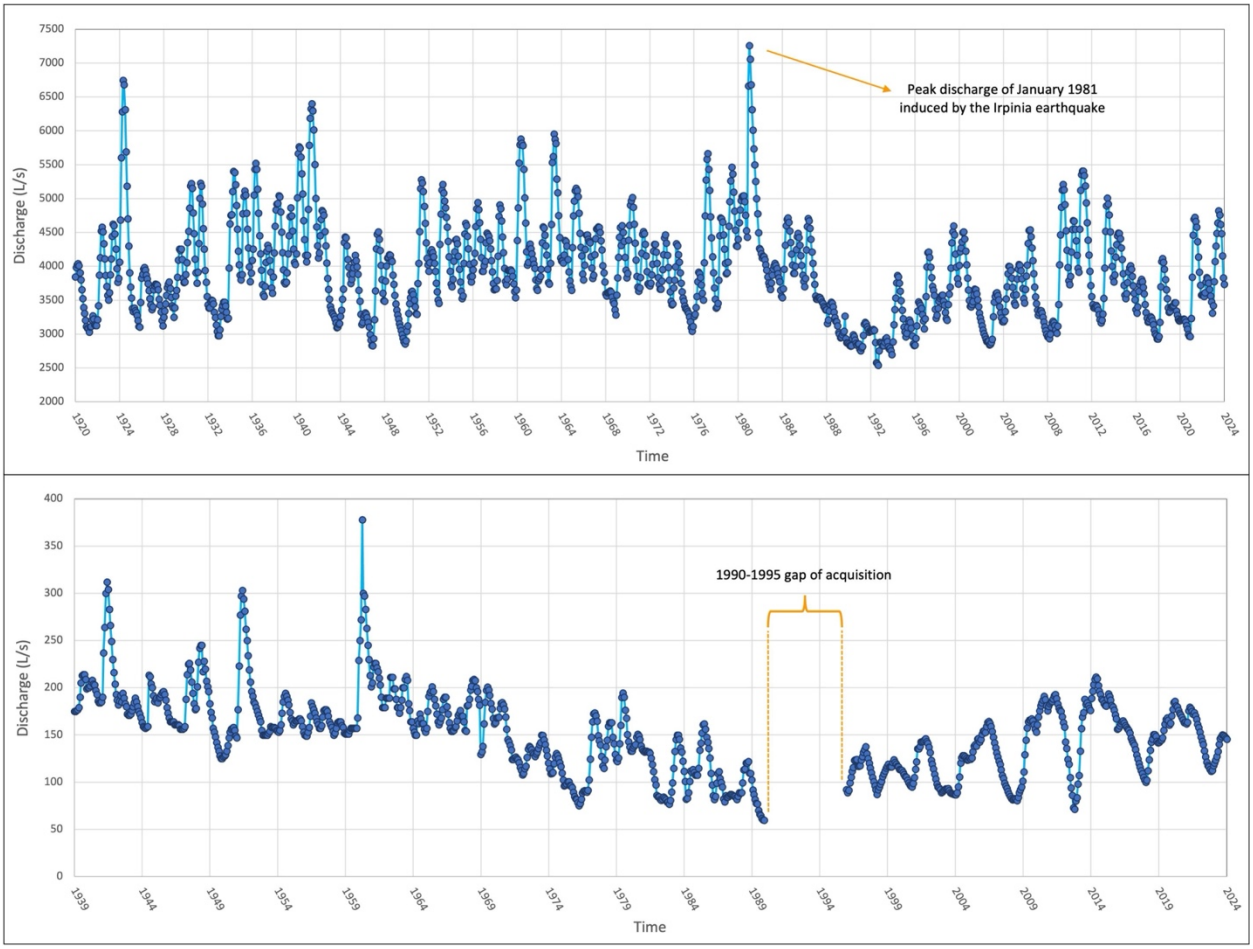

Fig. 3.2. Mean monthly discharge of Sanità (top) and Ermicciolo (bottom) Springs. The labels on the x-axis indicate January of each respective year.

Ermicciolo Spring is uptaken through a draining tunnel constructed between 1908 and 1914 (Parco Vivo, 2019 - https://www.parcovivo.it/sorgenti-del-monte-amiata/) on the north side of Mount Amiata aquifer complex. The tunnel is lined with concrete and connects three niches in the walls, enabling direct gravity drainage of groundwater from the aquifer's primary transmissive fractures. A portion of the spring discharge is withdrawn by the local water utility, Acquedotto del Fiora S.p.A. (AdF) (Doveri et al., 2012), while the excess overflows from the tunnel into a nearby stream. Total flow rate data are available from 1939 to nowadays, with a gap of acquisition from 1990 to 1995 inclusive (Fig. 3.2). Initially, flow rate monitoring was performed manually using stage measurements with a thin-wall weir, at a variable frequency of 2-3 times per month. Since the 1990s, an automatic contactless hydrometer has been installed, with a measurement frequency of four and a half hours (approximately 5 measurements per day).

The hydrographs in Fig. 3.2 represent monthly values, each averaged from all available single-shot measurements corresponding to that month.

3.6.2. Thermo-pluviometric and snowfall data

Monthly average air temperature and monthly cumulative precipitation data for the catchment area of the two investigated springs were obtained from local meteorological stations managed by regional authorities (Fig. 3.1), within the same time intervals covered by spring discharge monitoring. The stations used for Sanità Spring watershed are the “Senerchia” station for precipitation (approximately 600 m asl), and the “Materdomini” station for air temperature (550 m asl) (www.centrofunzionale.regione.campania.it). For Ermicciolo Spring catchment the “Vivo d'Orcia” station was considered for precipitation (about 842 m asl), while air temperature was acquired from the “Abbadia San Salvatore” station (855 m asl) (www.sir.toscana.it).

Precipitation time series at the selected stations were collected through non-heating rain gauges. Thus, their capacity to record snowfall precipitation is poor. Snowfall is a fundamental parameter for groundwater recharge in mountainous regions in terms either of snow depth or of permanence of snow to the ground (Halloran et al., 2023), as also put in evidence in the investigated sites (Doveri et al., 2012; Petitta et al., 2022). To avoid the risk of underestimating total precipitation in the springs' catchment area, it was decided to add the snowfall precipitation, as measured by local specific snow gauges, to the liquid precipitation recorded by conventional rain gauges. This approach has been recently adopted by other authors for hydrogeological budgeting of an Alpine area in Northern Italy (Stevenazzi et al., 2023). However, time series of direct measurements of snowfall in the investigated areas are available only for the most recent 30-40 yr, and can be found on the MeteoMont website (meteomont.carabinieri.it), a service for avalanche prevention and forecasting. Specifically, the available data include the number of days with snow-covered ground and the total snowfall within 24 h; for our study, only the daily snowfall data were collected and then aggregated into monthly cumulative totals. The snowfall stations “Rifugio Laceno” (1460 m asl) and “Monte Amiata” (1700 m asl) were selected as representative of Sanità and Ermicciolo Springs catchment, respectively (Fig. 3.1). In the former case, data are available from 1996 to the present, while in the latter from 1982.

Snowfall data from earlier decades were estimated by reconstructing them using the fifth version of ECMWF ReAnalysis (ERA5) data. Reanalyses combine historical observations with models to generate consistent time series of various atmospheric and ground variables at numerous grid points, with precise coordinates, centered and pertaining to a specific area (Tarek et al., 2020). Developed by the European Centre for Medium-Range Weather Forecasts (ECMWF), ERA5 provides hourly data, spanning from 1940 to 2023, for atmospheric, land-surface, and sea-state parameters, with a $\simeq$31 km horizontal resolution (Hersbach et al., 2020). For both case studies, monthly cumulative snowfall data were selected from the nearest ERA5 node to the local MeteoMont snow gauge. To achieve even better spatial resolution, the new dataset created by

Raffa et al. (2021) was also utilized, albeit covering only the period 1981-2023. This dataset is based on a dynamically downscaling over Italy of the ERA5 reanalysis, improving the horizontal resolution to approximately 2.2 km. Monthly cumulative snowfall data were picked from two nodes of the ERA5 dataset with High Spatial Resolution (HSR) (Fig. 3.1), chosen based on their distance to the two snow gauges pertaining to MeteoMont.

3.6.2.1. Past snowfall data reconstruction

In the time frame where ERA5 and ERA5 HSR datasets overlap (1981-2023), a linear regression analysis was performed to determine the coefficients linking the datasets. Through these coefficients, the ERA5 HSR time series was extended back to 1940. The same procedure was then applied between the extended ERA5 HSR and the local snow gauge time series to similarly reconstruct the MeteoMont snowfall data back to 1940. These steps were undertaken for both Sanità and Ermicciolo Springs catchment to obtain snowfall data with the highest possible spatial resolution and the longest possible temporal coverage. Once the snowfall data was reconstructed (Fig. 3.3) it was converted into Snow Water Equivalent (SWE).

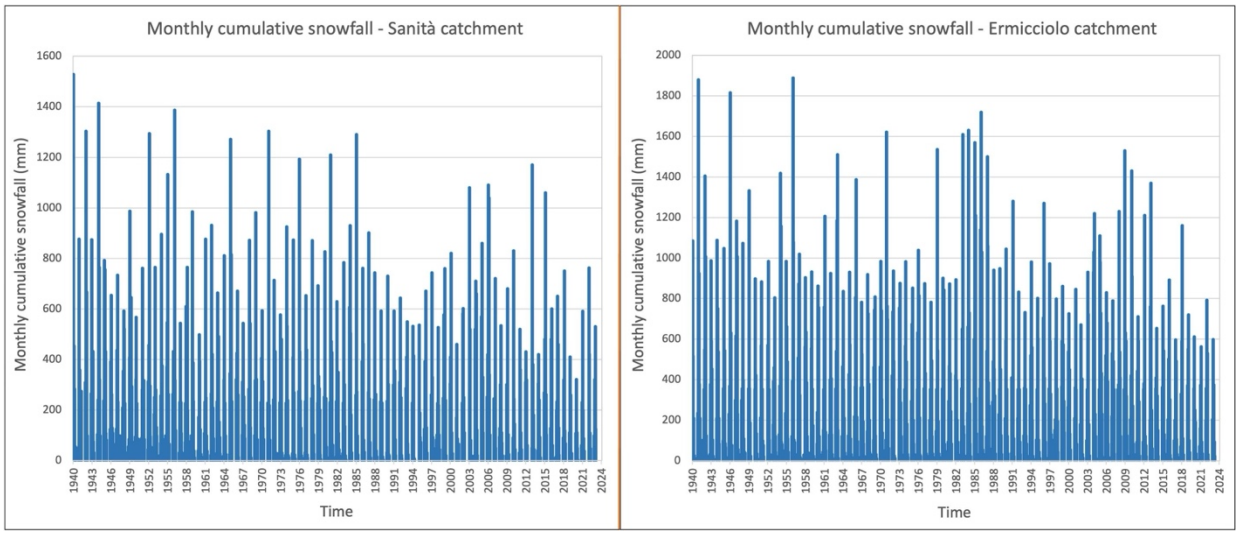

Fig. 3.3. MeteoMont monthly cumulative snowfall (1940-2023), partially reconstructed (1940-1996 for Sanità Spring and 1940-1982 for Ermicciolo Spring) using ERA reanalyses, pertaining to the contribution area of Sanità (left) and Ermicciolo (right) Springs.

Given that the initial data of the three datasets are provided on an hourly or, at most, daily basis, it can be assumed that the recorded snowfall data represent recently fallen and uncompacted snow. Consequently, a density of 100 kg/m^3 was used in converting snowfall precipitation to SWE (Mekis and Brown, 2010). Assuming a density of rainwater of 1000 kg/m^3, the data conversion was performed by a simple division by 10. The resulting data were added to the rainfall data. This process yielded a combined precipitation measure, referred to as the Total Liquid Precipitation

(TLP), which represents the aggregate contribution of both liquid and solid forms of precipitation, with the latter contributing to a lesser extent.

3.6.3. Combined statistical analysis of spring discharge and meteorological variables

To unravel the relationship between meteorological parameters and spring discharge, univariate and multivariate linear regression analyses (Gholami and Khaleghi, 2019; Zhou and Zhang, 2023) were conducted on historical meteorological data (cumulative TLP and average monthly air temperature) as independent variables, and on monthly discharge data as the dependent variable. Prior to regression analyses, all datasets underwent normalization using monthly mean and standard deviation values calculated from the whole dataset (1940-2023), a process commonly referred to as anomaly normalization (Brockwell and Davis, 2016). Specifically, each value in the dataset was transformed by subtracting the mean of the corresponding month and then dividing by the standard deviation calculated across the entire data population for that same month. Data normalization plays a crucial role in the analysis of time series with disparate units of measurement and numerical scales, ensuring fair comparisons among parameters (Montgomery et al., 2008).

As a first step, separate linear regressions were performed between the dependent variable (discharge) and each independent variable, TLP or air temperature (AirT), to analyse the individual relationships between these parameters and to identify possible variable-specific time lags to be considered in the subsequent multivariate analyses. Once the correlations among the individual variables were established, twelve different monthly lags, ranging from 1 to 12 months, were implemented in the linear regression. The time lag that yielded the highest R-value, indicating a stronger relationship between the parameters, was selected (Fig. 3.4).

The multivariate statistical analysis was performed using the Ordinary Least Squares (OLS) model from the Python statsmodels library (Seabold and Perktold, 2010). The OLS model is a commonly utilized linear regression technique that evaluates, through the estimation of Correlation Factors (CF), the relationship between a dependent variable and one or more independent variables by minimizing the sum of the squares of the differences between the observed and predicted values (Farahani et al., 2010; Hayes and Matthes, 2009). Additionally, the OLS model determines the uncertainty associated with the regression coefficients by estimating confidence intervals for these factors. The p-value, used to assess the significance of the relationship between variables, and the R-squared, which represents the proportion of variance in the dependent variable explained by the independent variables (Kutner et al., 2005; James et al., 2013), were also evaluated.

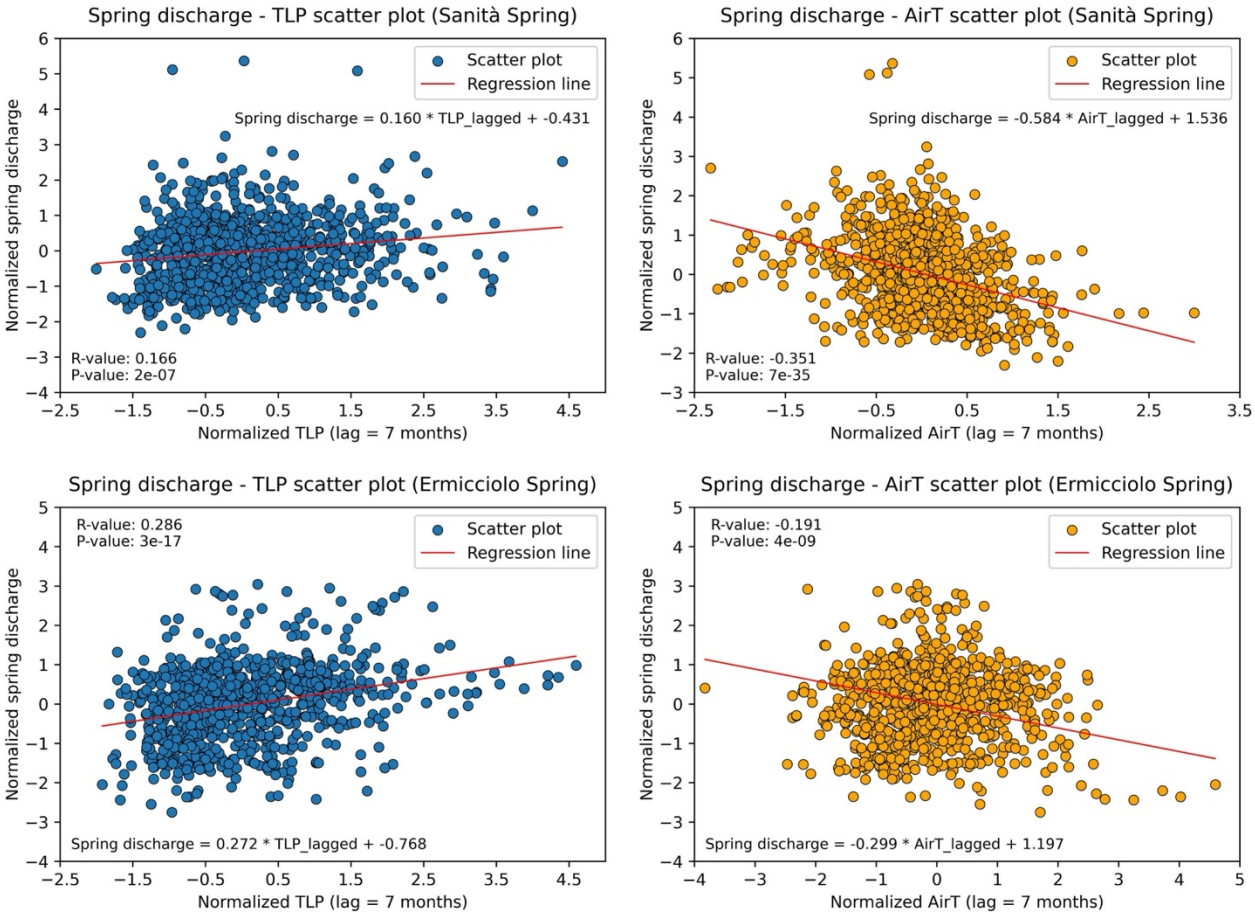

Fig. 3.4. Scatter plots resulting from the univariate linear regressions performed between the dependent variable (spring discharge) and the independent variables (TLP and AirT). For both case studies, the lag time that yields the best correlation (i.e., the highest R-value) with spring discharge is 7 months for both meteorological variables. The relatively modest R-values are due to noise in the data.

3.6.4. Estimation of future spring discharge

3.6.4.1. RCPs 4.5 and 8.5 climate projections

The Representative Concentration Pathways (RCPs), provided by the Intergovernmental Panel on Climate Change (IPCC, 2014), are climate scenarios, expressed in terms of greenhouse gas concentrations (Van Vuuren et al., 2011), that estimate emissions of greenhouse gasses (GHG) and air pollutants levels of 8.5, 6.0, 4.5 and 2.6 W/m^2, by the end of the century. These RCPs were estimated depending on both socio-economic development scenarios and the associated climate policies that will be implemented to reduce the production of GHG. For example, the RCP 4.5 scenario anticipates that emissions will be halved by 2080, while the RCP 8.5 scenario represents an estimate of emissions that will be reached by the end of the century if no additional efforts are made to constrain the generation of greenhouse gasses.

General Circulation Models (GCMs) using multiple emission scenarios (Klaas et al., 2019; Shepherd et al., 2010) represent the most advanced instruments for simulating the response of the global ocean-atmosphere system to climate changes (Shahgedanova et al., 2020). The RCPs are indeed employed in GCMs to estimate future meteorological variables. General Circulation Models require a downscaling process to represent the hydrogeological watershed-scale dynamics, which involves obtaining more detailed and localized information (Gudmundsson et al., 2012; Haylock et al., 2006). Ban et al. (2021) enhanced the downscaling capabilities of GCMs by providing climate data with a spatial resolution ranging from 1 to 3 km and an hourly temporal resolution. These improvements reduce associated errors and add value to the estimation of atmospheric variables at the local scale.

Each of the RCPs covers the 1850-2100 period and is reported at a 0.5 × 0.5° spatial resolution (approximately 40-55 km) (Van Vuuren et al., 2011). To achieve a better spatial resolution of the future climate scenarios, projections derived from the Euro-Mediterranean Center on Climate Change Foundation — Climate Model (CMCC-CM), elaborated with the RCPs 4.5 and 8.5, were utilized (Raffa et al., 2023). These estimates, which are available from January 2006 up to December 2070, were generated at approximately 2.2 km resolution through a dynamical downscaling process using the regional climate model “COSMO-CLM” (Consortium for Small-scale Modeling - Climate Limited-area Model) over Italy, allowing for the generation of highly detailed and comprehensive datasets of projected climatological data (Raffa et al., 2023). Just as for the ERA5 reanalyses data, these future projections over Italy were computed at numerous grid points, pertaining to a specific area. For this study, monthly data were selected for the variables “Total precipitation” and “2 m temperature”, covering each of the Sanità and Ermicciolo Springs catchments.

The variables were acquired from grid nodes based on their proximity to meteorological stations (Fig. 3.1), ensuring relevance to the collected historical thermo-pluviometric data. Furthermore, data were acquired for both RCPs 4.5 and 8.5, providing insights into both moderate and more extreme climate futures. Before using these meteorological projections, quality control was performed on the data. Considering the period spanning from January 2006 to December 2023, during which both the climate projections and the historical data from weather stations are available, a comparison was made to detect and correct any constant deviations of the scenarios from the actual historical data. The historical and forecasted meteorological time series were compared by means of simple subtractions. This process facilitated the verification of the presence of any deltas between each meteorological parameter.

3.6.4.2. Application of CF to weather scenarios

The regression equations and corresponding correlation factors obtained from the OLS models were applied to the two selected meteorological data outputs of the 4.5 and 8.5 future projections (2040-2070), previously normalized using the same approach described in Section 3.6.3 for past time series. The normalized future discharge dataset for Sanità and Ermicciolo Springs were then determined between January 2040 and December 2070, for both RCP 4.5 and RCP 8.5 scenarios. Subsequently, the projected discharges were denormalized by applying the reverse process described for normalization, using the same monthly means and standard deviations, in order to obtain the estimated spring discharge values for the period 2040-2070.

3.6.5. Multi-decadal hydrographs

With the aim of analysing the long-term trend of spring discharge, a multi-decadal cycle approach was used. Considering that at least 30 yr of data are required to appreciate climate trend (Livezey et al., 2007), the historical flow rate dataset of Sanità Spring was divided into three 35-yr subsets: 1920 to 1954, 1955 to 1989, and 1990 to 2024. As for Ermicciolo Spring, the historical discharge data were divided into three multi-decadal groups, with the oldest one spanning only 16 yr: 1939 to 1954, 1955 to 1989, and 1990 to 2024. The two most recent periods are consistent with that of Sanità Spring, thereby enabling a comparison between the multi-decadal discharge values of the two springs. In both cases, the historical discharge subsets were plotted along with standard deviation uncertainty bands around the mean, defined by adding/subtracting the standard deviation of the monthly spring discharge values for each multi-decadal group to the mean of those values. The projected discharge data of Sanità and Ermicciolo Springs were graphed alongside the historical data by creating two 30-yr groups for each spring, spanning from 2040 to 2070, respectively in relation to RCPs 4.5 and 8.5 scenarios. For the future discharge estimates, the uncertainty bands around the mean were derived from the flow rate values obtained through the lower and upper bounds of the coefficients' confidence intervals determined by the multivariate OLS models.

3.7. Results

3.7.1. Discharge time series

Sanità and Ermicciolo Springs have century-long continuous discharge monitoring dating back to January 1920 and 1939, respectively, and extending to the present. In Fig. 3.2, the last data point represented is that of January 2024 and the data are presented as monthly averages in accordance with the temporal scale used in the statistical analyses of the present study.

Sanità Spring hydrograph since 1920 (Fig. 3.2) exhibits an annual cyclic variation in relation to recharge, with the yearly peak discharge occurring between May and July, and the low flow period between November and December (Fig. 3.5). The average hydrological year for this spring, throughout the entire monitoring period, exhibits a discharge ranging from approximately 3.3 m^3/s to 5.4 m^3/s (Fig. 3.2), placing it within the second (II) class of Meinzer's (1923) spring discharge classification. Ermicciolo Spring hydrograph since 1939 (Fig. 3.2) shows a peak discharge during the same months as Sanità, while the low flow occurs slightly later, between January and February of the following year (Fig. 3.5). The average spring discharge of Ermicciolo fluctuates from roughly 90 L/s to 210 L/s (Fig. 3.2), placing it between the III and IV classes of Meinzer's classification. Notably, a decreasing trend in Ermicciolo Spring Meinzer's class is apparent when comparing the periods before and after the mid-1970s.

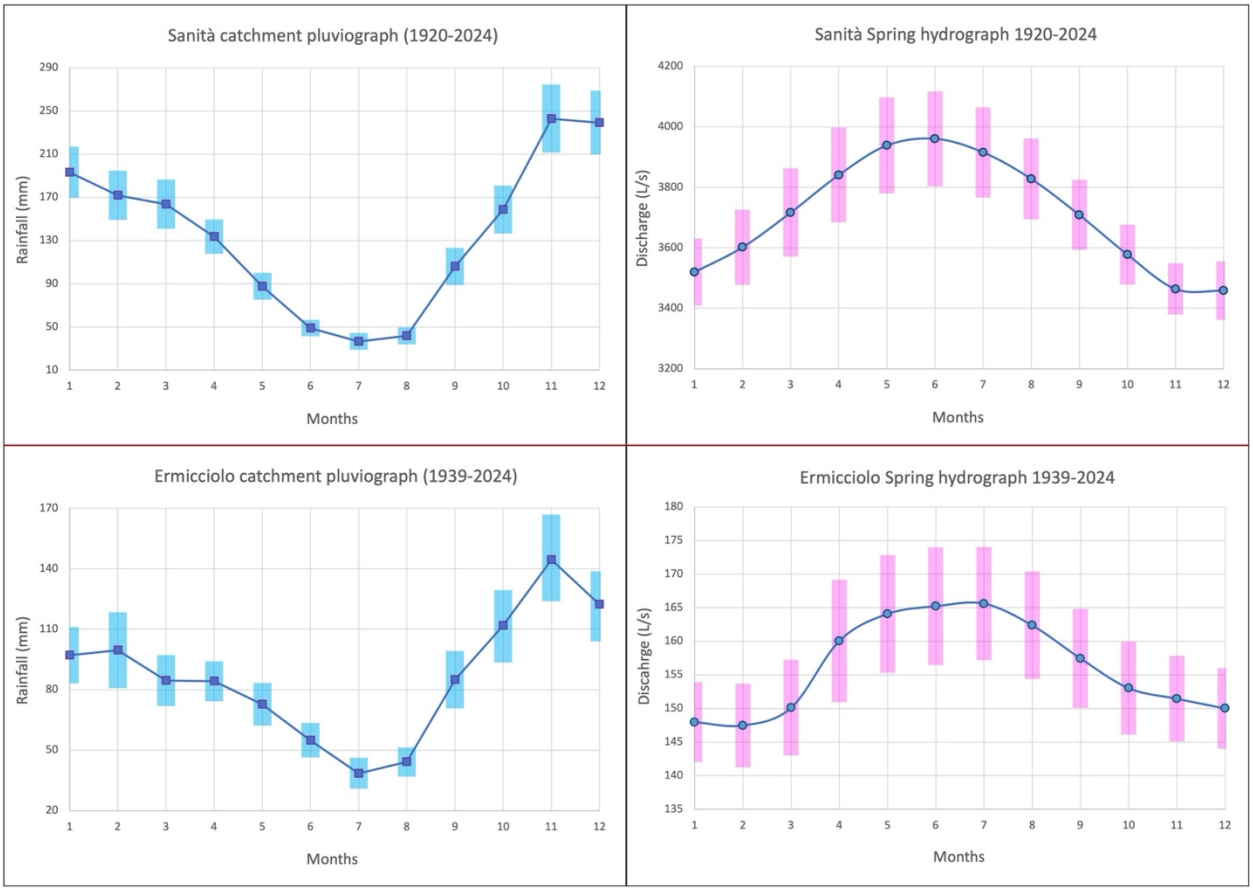

Fig. 3.5. Monthly mean rainfall of Sanità and Ermicciolo Springs reference rain gauges (on the left); monthly mean discharge of Sanità and Ermicciolo Springs (on the right). For each monthly mean value, the error bar represents the 95% confidence interval.

The secular discharge data of Sanità and Ermicciolo Springs have the potential to provide valuable insights into changes in water resource availability due to climate change effects, given (i) the length of the series, (ii) the systematic quality of the records and (iii) the absence of human-made alteration of the natural conditions of the aquifers, for the almost absence of pumping wells or

groundwater draining facilities (Doveri and Menichini, 2017; Leone et al., 2021). The only significant effect not attributed to natural recharge variations is linked to the major earthquake of November 23rd, 1980 (Surface wave Magnitude – Ms – 6.9, the Irpinia earthquake). With its epicentre located approximately 10 km southeast of Sanità Spring, the earthquake impacted the spring's discharge, leading to an extraordinary anomalous value of 7.32 m^3/s recorded on January 19th, 1981 (Fiorillo and Guadagno, 2012) (Fig. 3.2).

3.7.2. Regression analysis

Before conducting the linear regression analyses, we applied multiple tests to explore potential non-linear or threshold relationships between the variables. The results did not provide any significant evidence of these patterns (high p-value) in each of the four univariate cases, suggesting that the linear form of the model is appropriate for our datasets. The univariate linear regressions (Fig. 3.4) showed that, for Sanità and Ermicciolo Springs, discharge has the strongest negative correlation with the average AirT (R-value: −0.351 and −0.191, respectively) and the strongest positive correlation with cumulative TLP (R-value: 0.166 and 0.286, respectively) with a time lag of 7 months (Fig. 3.4), which is consistent from a physical standpoint as peak liquid precipitation (representing the majority of TLP) occurs in November, while peak discharge is observed in summer (Fig. 3.5). It is also logical that air temperature is more strongly correlated with spring discharge at the same lag time as TLP, since higher air temperatures increase evapotranspiration, thereby reducing the effectiveness of precipitation in recharging aquifers (Cardell et al., 2020). Thus, a time lag of 7 months was used in the subsequent multivariate analysis for AirT and TLP. The two variables registered 7 months in advance compared to discharge will be called “AirTLag7” and “TLPLag7” hereafter.

For both Sanità and Ermicciolo Springs, the multivariate analysis confirms a positive correlation between TLPLag7 and discharge (Q), and a negative correlation between AirTLag7 and discharge. Specifically, for the Sanità Spring, the OLS model produced the following equation (Eq. 3.1):

$$Q_{San} = +0.143 + 0.183 * TLP_{Lag7} - 0.544 * AirT_{Lag7} + \varepsilon \quad [3.1]$$

where “QSan” represents the dependent variable, which in this case is the predicted flow rate of Sanità Spring, the error term “ε” represents the difference between the observed value of the dependent variable and the value predicted by the linear regression model, and “TLPLag7” and “AirTLag7” are the independent variables.

The confidence intervals provided for the coefficients are calculated at the 95% confidence level. Specifically, for the TLPLag7 variable, the confidence interval bounds of the relative Correlation Factor (CF) are [+0.253, +0.113], resulting in an uncertainty margin of ±0.07; for AirTLag7, the CF

confidence interval bounds are [−0.414, −0.674], indicating a margin of error of ±0.13; for the intercept term the confidence interval bounds are [+0.213, +0.073], resulting in an uncertainty margin of ±0.07.

Similarly, for Ermicciolo Spring, the regression equation (Eq. 3.2) is as follows:

$$Q_{Erm} = -0.032 + 0.278*TLP_{Lag7} - 0.289*AirT_{Lag7} + \varepsilon \quad [3.2]$$

where “QErm” represents the predicted discharge of Ermicciolo Spring, “ϵ” is the error term, and “TLPLag7” and “AirTLag7” are the recharge-related independent variables.

The confidence intervals for the coefficients calculated at the 95 % confidence level are the following: for TLPLag7, the confidence interval bounds of its regression coefficient with the discharge are [+0.338, +0.218], resulting in an uncertainty margin of ±0.06; for the AirTLag7 variable, the CF confidence interval bounds are [−0.089, −0.489], indicating a margin of error of ±0.20; for the intercept term, finally, the confidence interval bounds are [+0.038, −0.102], resulting in an uncertainty margin of ±0.07.

Both models exhibit statistically significant results, as evidenced by the consistently low p-value, remaining below 1×10^{-4} in both case studies, indicating a high level of confidence in the observed relationships.

3.7.3. Future recharge-related meteorological parameters

Thanks to the comparison of climate projections with historical meteorological data for the 2006-2023 period, it was found that in both case studies, the historical precipitation aligns closely with both projections of the RCPs 4.5 and 8.5 scenarios, with a maximum monthly deviation of 15%. However, a systematic bias was found for the 2 m temperature leading to a deviation from historical data of 2 °C in the case of Sanità Spring catchment and 3 °C in the case of the Ermicciolo's one. These constant deviations were then used to adjust the entire historical series of future temperature projections.

Considering the adjusted RCPs 4.5 and 8.5 future data (2024-2070) and the historical values (1940-2023), it is evident that air temperature will experience a significant increase in the future, whereas total precipitation, which has shown a relatively increasing trend from the 1990s to the present, is projected to undergo a considerable decrease (Fig. 3.6).

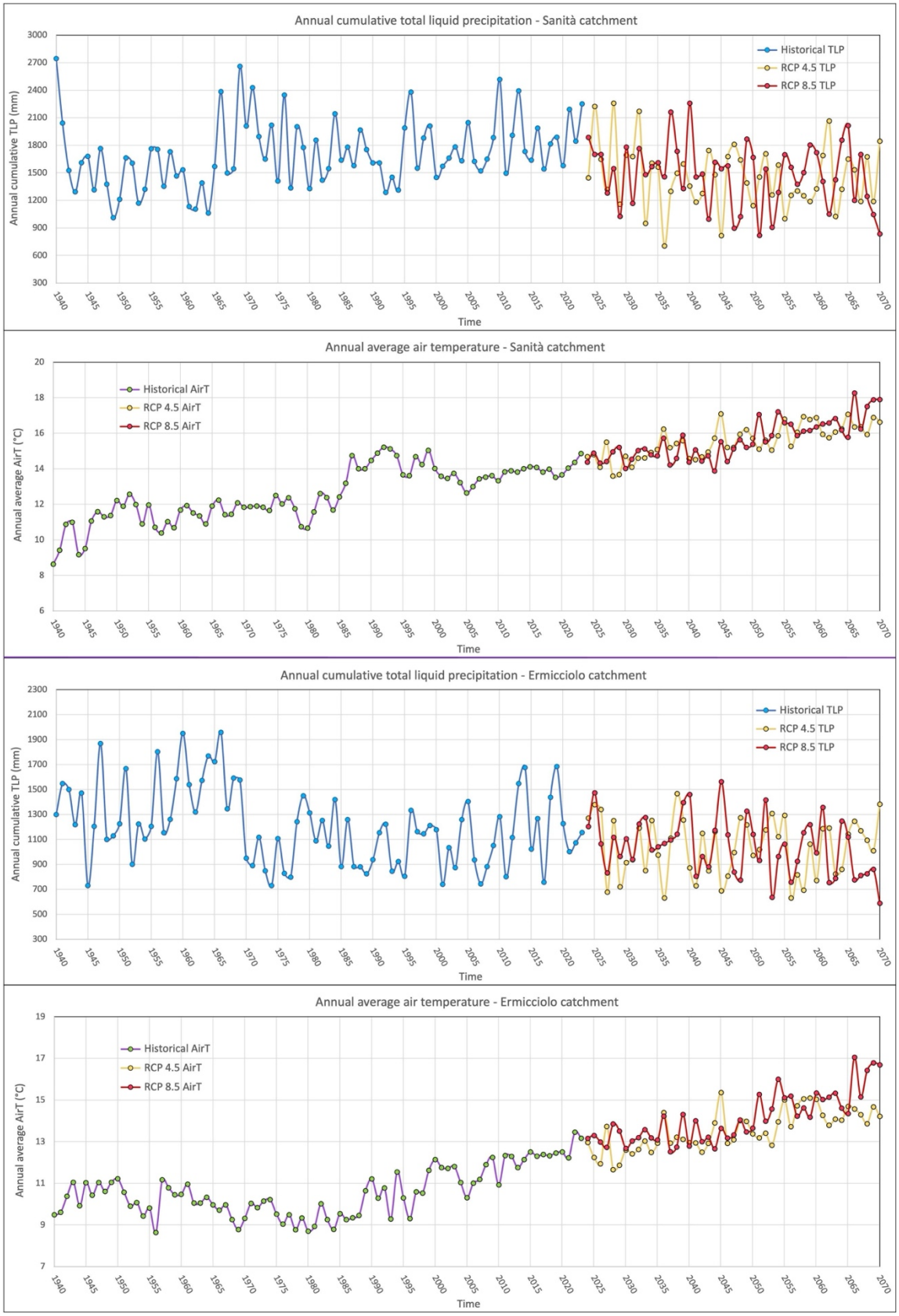

Fig. 3.6. Plots of annual cumulative TLP and mean annual AirT for the contribution area of Sanità (top) and Ermicciolo (bottom) Springs. Both historical data (1940-2023) and future projections of the RCPs 4.5 and 8.5 scenarios (2024-2070) are plotted on all graphs.

3.7.4. Multi-decadal spring discharge analysis

The multi-decadal analysis of Sanità Spring discharge data displays an average flow rate ranging from approximately 3580 to 4430 L/s during the oldest 1920-1954 historical band (Fig. 3.7), with a standard deviation uncertainty band that varies from 70 to 180 L/s both below and above the average value. The intermediate historical band (1955-1989) is characterized by the highest discharge and partially overlaps with the first band. It covers a range between 3820 and 4630 L/s, with an uncertainty band oscillating from 80 to 150 L/s indicating lower variability compared to the preceding period. The most recent historical band (1990-2024) shows an average discharge ranging from 3360 to 3920 L/s, with a standard deviation uncertainty band that fluctuates around the mean of 70-130 L/s, suggesting less variability in the data.

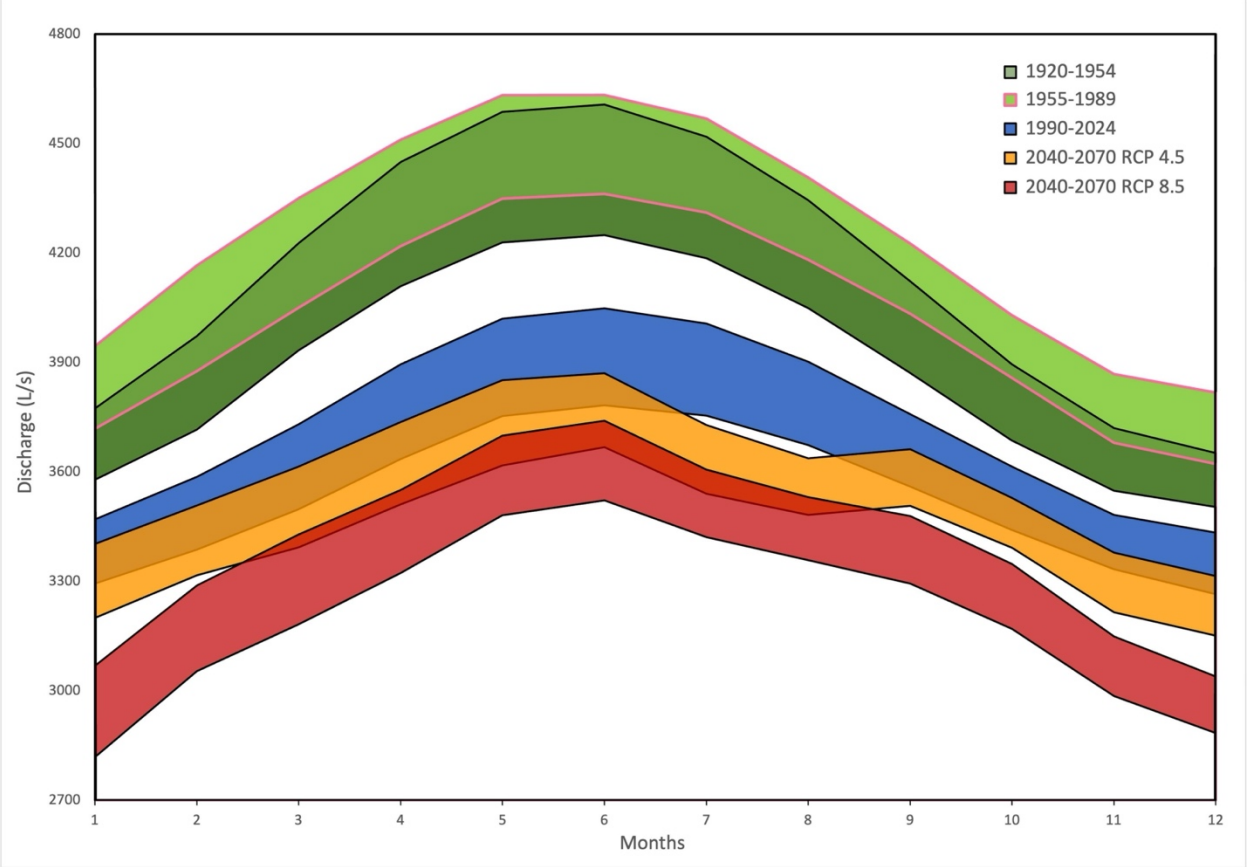

Fig. 3.7. Hydrographs of Sanità Spring based on the mean multi-decadal approach with uncertainty bands. Three bands are constructed using historical data, while the remaining two are built using the future discharge projections resulting from the multivariate statistical analysis performed on the Sanità dataset.

The uncertainty bands for the two future discharge scenarios (2040-2070) exhibit even lower variability, ranging from 60 to 120 L/s on both sides of the average value, giving them a narrower appearance. In the RCP 4.5 scenario an average discharge from 3220 to 3830 L/s is observed, with the band slightly intersecting that of the most recent 35-yr historical period. In the more

severe RCP 8.5 scenario, the average discharge varies from 2970 to 3630 L/s, showing a partial overlap with the values of the other future scenario.

Concerning Ermicciolo Spring, the three historical bands show a progressively lower average discharge moving from the two older periods to the most recent, with the following discharge ranges: 172-201 L/s (1939-1954), 135-157 L/s (1955-1989), and 131-147 L/s (1990-2024) (Fig. 3.8). The standard deviation uncertainty bands vary from 5 to 11 L/s in the first two cases and from 8 to 11 L/s in the third, suggesting an overall lower variability in the data population compared to Sanità Spring. Regarding the bands of the two future discharge scenarios (2040-2070), the average discharge ranges from 131 to 146 L/s in the RCP 4.5 scenario and from 116 to 131 L/s in the 8.5 scenario. In both cases, the data variability is very low, with bands oscillating of only 2-5 L/s around the mean. Additionally, a partial overlap exists among the two most recent historical bands and the future one related to the RCP 4.5 scenario.

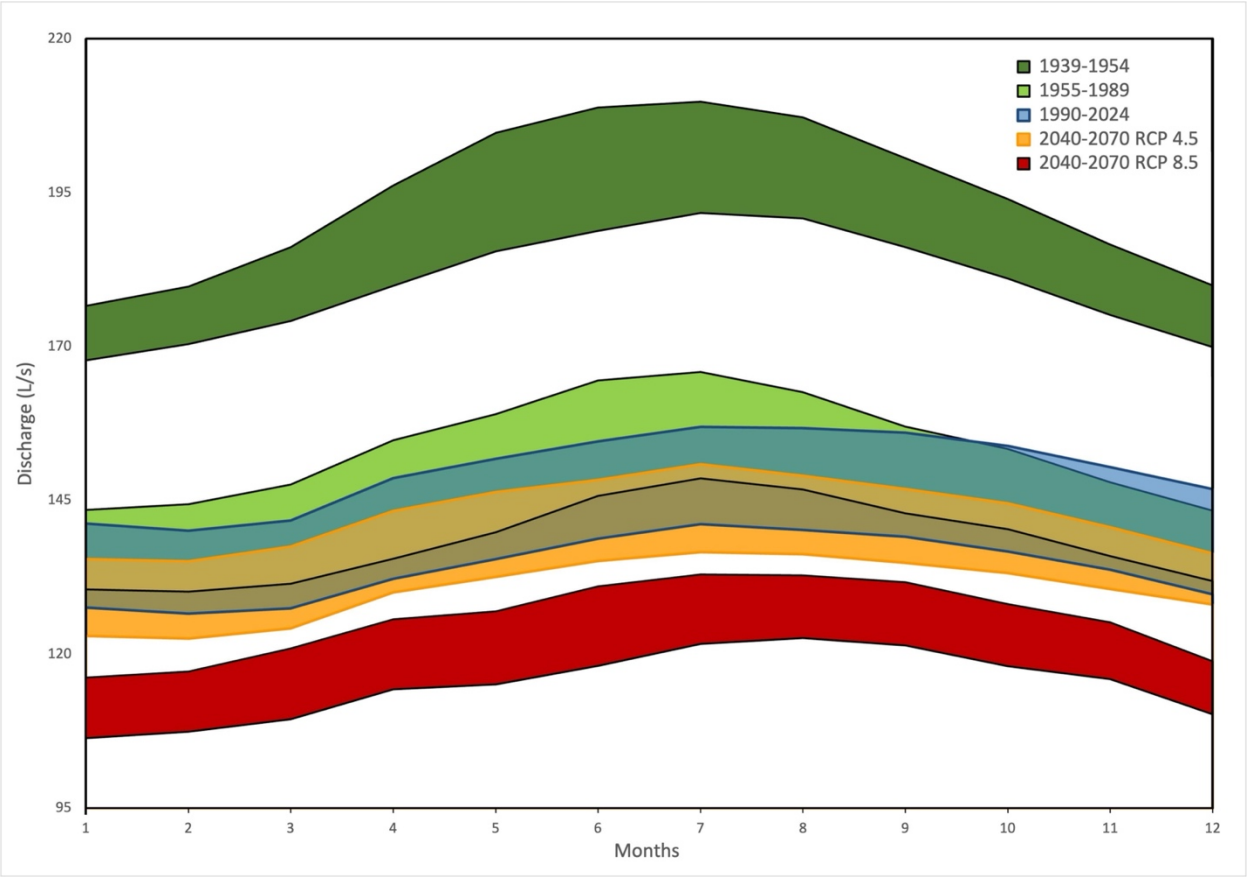

Fig. 3.8. Hydrographs of Ermicciolo Spring based on the mean multi-decadal approach with uncertainty bands. The division of discharge bands is the same as in Fig. 3.7.

3.8. Discussion

The hydrographs of the investigated springs (Fig. 3.2) provide insights into both the specific features of the hydrogeological setting, and the broader effects of climate change over the Apennines Mountain chain.

The flow rate of Sanità Spring indeed shows greater variability compared to that of Ermicciolo Spring. This difference is linked to the typical dynamics of a karst environment. Ermicciolo Spring, on the other hand, reflects the dynamics of a less heterogeneous fractured context (i.e. a volcanic aquifer) than the former, resulting in less discharge variability. However, univariate regression at both springs reveals a robust, inverse statistical correlation between AirT and monthly discharge, with a lag of 7 months. In contrast, the cumulative monthly TLP exhibits a statistically significant positive correlation with the discharge over the same time lag (Fig. 3.4). Surprisingly, the same time lag between the historical independent variables and historical spring discharge was found to characterize two rather different hydrogeological watersheds. Sanità Spring is fed by a karst system that is expected to show quicker discharge responses to precipitation compared to the lower permeability fractured volcanic aquifer feeding Ermicciolo Spring. Nonetheless, it appears that the extensive catchment associated to Sanità Spring can considerably delay the effects of direct recharge. The contribution area of the spring is 110 km^2 (Fiorillo and Doglioni, 2010), whereas Ermicciolo Spring catchment is one tenth the area, at around 13 km^2 (Doveri and Raco, 2021). For this reason, the similar TLP lag identified for the two watersheds is considered reasonable.

Regarding the effects of global warming on spring discharge along the Apennines, Fig. 3.2 indicates that climate change in the Mediterranean region has negatively affected the discharge availability of Sanità and Ermicciolo Springs over the past 3-4 decades. At the multi-decadal scale, negative consistent historical trends are indeed observed between the two springs, with the last 35-yr period exhibiting a decrease in discharge and reduced data variability in both case studies compared to the previous period (Fig. 3.7, 3.8). At Sanità Spring, the percentage discharge decreases between the most recent period, 1990-2024, and the intermediate period, 1955-1989, was a significant 12.5. In contrast, at Ermicciolo Spring, the reduction over the same periods was only 3.7%. The greater reduction in discharge at Sanità compared to Ermicciolo can likely be attributed to the Irpinia earthquake, which temporarily caused a substantial increase in discharge that partially depleted the aquifer in the following 3-4 yr. Moreover, previous research (Fiorillo and Guadagno, 2012) shows a discharge drop after 1986 in many springs in Southern Italy, plausibly related to climate change, which is consistent with the trend observed in Sanità Spring.

The expected rise in air temperatures in the Mediterranean region will result in increased evapotranspiration and consequent reduction of liquid precipitation recharging the aquifers (Cardell et al., 2020; Rosenberg et al., 1999; Yusoff et al., 2002). Moreover, there will be adverse effects on solid precipitation, as already observed in Italy in recent decades (Diodato et al., 2019; Diodato et al., 2022), with a shorter duration of snow permanence to the ground and a significant reduction in total snowfall (also confirmed in the two study areas, Fig. 3.3), further amplifying the groundwater recharge reduction. Additional critical factors that impair recharge must be considered, including the projected decrease in total precipitation associated with the RCPs 4.5 and 8.5 scenarios (Fig. 3.6), as well as the increased frequency of extreme precipitation events, which is expected to reduce the infiltration rate relative to the surface runoff rate.

Given the concerning future outlook for groundwater in the Mediterranean region, a multivariate OLS model was employed in both case studies to estimate future spring discharge. With this model, we sought to identify the regression coefficients linking recharge-related variables to spring discharge using nearly century-long historical datasets (1940-2023). Although climatic conditions are changing with increasing rates and variability in recent decades (Caloiero et al., 2018), the assumption underlying our study is that the processes by which meteorological factors affect spring discharge remain consistent when looking at a long-term trend. For this reason, using only the past decade or the past two to three decades (during which climate change has accelerated) for the multivariate analyses was not considered ideal for identifying the best long-term recharge-discharge relationships. As evidence of this, during the validation process of both the multiregression models, we tested the use of only these recent decades; however, the results showed lower statistical significance and much weaker correlations between the variables compared to those of the 1940-2023 data models, potentially leading to unreliable predictions.

Thanks to the correlation factors derived from the OLS 1940-2023 data models (Eq. 3.1, Eq. 3.2), it was possible to estimate the future discharge scenarios of Sanità and Ermicciolo Springs within the 2040-2070 period. The reconstructed discharge clearly exhibits a further decreasing trend compared to the historical dataset of both springs, with some differences in relation to the chosen RCP scenario. Under the RCP 4.5 scenario, the future discharge projections appear to show no excessive impairment in flow rate output compared to the most recent historical period (Fig. 3.7, Fig. 3.8). Indeed, the estimated decrease in discharge is only 3.0% for Sanità Spring and 0.1% for Ermicciolo Spring. Conversely, under the more severe RCP 8.5 scenario, characterized by higher greenhouse gas emissions, a further decrease in spring discharge is evident in the 2040-2070 time frame, with a percentage decrease of 8.6% relative to the 1990-2024 interval (19.9% when compared to the 1955-1989 period, characterized by the highest groundwater yield), at Sanità Spring, and a similar percentage decrease of 10.8% relative to the most recent 35-yr period (or even 33.3% when compared to the 1939-1954 time frame) at Ermicciolo Spring.

The results in terms of percentage associated with the RCP 8.5 scenario indicate that Sanità Spring could lose, over the 2040-2070 period, an average of 9.8 million m^3 of water/yr, when compared to the annual average discharge of the last 35 yr. Regarding Ermicciolo Spring, the future estimated discharge loss respect to the 1990-2024 interval amounts to almost 0.5 million m^3/yr, considering the same scenario. Analysing these losses in spring discharge and considering a daily water consumption per person of 220 L (Eurispes, 2023 - https://eurispes.eu/en/news/a-system-that-treads-water-the-condition-of-water-in-italy/), the average annual decrease in discharge at Sanità equates to the annual demand of a city with 122,000 inhabitants. Applying the same calculation to the results obtained for Ermicciolo Spring, the decrease in discharge would be sufficient to meet the water needs of a town of over 6000 inhabitants.

Given that long-term spring discharge dynamics, which span decades, tend to be less influenced by the specific characteristics of individual basins and more indicative of broader climate shifts within a region (Hartmann et al., 2014; Zhong et al., 2016), the similar multi-decadal downtrend in spring discharge forecasted through future climate factors for both Sanità and Ermicciolo Springs for the 2040-2070 period is likely extendable to other settings within Mediterranean-type climates.

The approach presented here offers new insights into the ability to estimate future trends in groundwater discharge. Recent studies in the literature have employed machine learning methods, particularly Artificial Neural Networks, as well as hydrogeological numerical models, to achieve the same objective of estimating future spring discharge. These studies have demonstrated the capability to accurately forecast spring discharge from weeks up to three months ahead (Granata et al., 2018) or even up to 12 months (Di Nunno et al., 2021). Some researchers have also managed to estimate annual peak and minimum spring discharge values up to the end of the current century using these methods (e.g., Doummar et al., 2018; Fan et al., 2023). However, both approaches present certain limitations. As highlighted by Cinkus et al. (2023) and Di Nunno et al. (2021), these methods require high temporal resolution data, ideally daily or at least bi-weekly measurements. Moreover, they struggle to reproduce long-term discharge values and extreme events, and are often time-consuming to run. The multivariate statistical analysis approach, although it may provide less accurate short-term forecasts compared to ANN-based systems (Gholami and Khaleghi, 2019), offers the advantage of making long-term discharge projections using only monthly resolution data, provided the analysis is applied to century-long datasets, as in the present research. This method allows for the estimation of expected long-term annual peak and minimum discharges for springs, as well as the generation of springs' hydrographs over a multi-decadal time span, depicting monthly discharge fluctuations in the mid-to-late 21st century (2040-2070).

3.9. Conclusion

Two strategic aqueduct springs, Sanità and Ermicciolo, located along the Apennines Mountain chain (Italy) in two distinct hydrogeological settings but under a similar Mediterranean-type climate, have been the focus of this work due to their rare, century-long historical record of discharge data. The study approach was based on the multivariate statistical correlation between spring discharge and recharge-related data (air temperature and total precipitation), representative of the springs' catchment area. The regression coefficients derived from the statistical analyses were then applied to projected meteorological data from the RCPs 4.5 and 8.5 future climate scenarios to estimate the long-term discharge trend for both Sanità and Ermicciolo Springs. Under the most severe emission scenario, a significant decrease in discharge is observed for both springs during the 2040-2070 period compared to the most recent historical one (1990-2024). The estimated percentage decrease in flow rate between these two periods is 8.6% at Sanità Spring and 10.8% at Ermicciolo Spring, corresponding to a reduction in discharge of 310 L/s and 15 L/s, respectively. It is important to note that these decreases will affect two springs that, due to climate change, are already experiencing a decline in discharge compared to previous decades. Past and future multi-decadal discharge reductions are consistent across two different hydrogeological settings, suggesting a greater influence from climatic drivers (common to both sites) as opposed to the specific hydrogeological features of the individual catchments. This allows us to speculate that the observed negative trends may also be valid in other springs within similar climatic contexts. There is a strong and widespread perception that water scarcity in the future will profoundly impact the Apennines, already facing water crises (Fiorillo et al., 2015b; Fiorillo and Guadagno, 2012). This has been confirmed in the northern part of the chain as well (Filippini et al., 2024), and most likely these negative effects will be extended to many major springs within similar Mediterranean-type climates. Therefore, for local public water supply companies, the results obtained in this work hold significant importance as they allow for proactive measures in addressing forthcoming water crises within their respective management areas, and possibly beyond. The methods applied in this study hold potential for application in other hydrogeological settings, contingent upon the availability of continuous secular datasets for both spring discharge and meteorological parameters.

Acknowledgements

The authors wish to express their gratitude to the public water supply companies Acquedotto Pugliese S.p.A. and Acquedotto del Fiora S.p.A., for granting access to the springs discharge data. Special thanks are directed to Gerardo Ventafridda and Massimo Bellatalla, who served as vital points of communication with the respective entities. Additional appreciation is extended to Acquedotto Pugliese S.p.A. for supporting this research as part of the first author's doctoral program, which included an internship period at the company's headquarters in Bari, Puglia Region. The authors also acknowledge Paola Mercogliano from CMCC for facilitating access to the future climate scenarios. This research was supported by the Fondo Sociale Europeo (FSE) with resources from the Recovery Assistance for Cohesion and the Territories of Europe (REACT-EU) program, through the Programma Operativo Nazionale (PON) of the Ministero dell'Istruzione, dell'Università e della Ricerca (MIUR) for doctoral reasearch in innovation and green topics, 37th PhD cycle.

3.10. References

Alilou, H., Oldham, C., McFarlane, D., Hipsey, M.R., 2022. A structured framework to interpret hydro-climatic and water quality trends in Mediterranean climate zones. Journal of Hydrology, 614, 128512.

Allocca, V., Manna, F., De Vita, P., 2014. Estimating annual groundwater recharge coefficient for karst aquifers of the southern Apennines (Italy). Hydrology and Earth System Sciences, 18(2), 803-817.

Balaram, V., Copia, L., Kumar, U.S., Miller, J., Chidambaram, S., 2023. Pollution of water resources and application of ICP-MS techniques for monitoring and management—A comprehensive review. Geosystems and Geoenvironment, 2(4), 100210.

Ban, N., Caillaud, C., Coppola, E., Pichelli, E., Sobolowski, S., Adinolfi, M., Ahrens, B., Alias, A., Anders, I., Bastin, S., Belušić, D., Berthou, S., Brisson, E., Cardoso, R.M., Chan, S.C., Christensen, O.B., Fernández, J., Fita, L., Frisius, T., Gašparac, G., Giorgi, F., Goergen, K., Haugen, J.E., Hodnebrog, O., Kartsios, S., Katragkou, E., Kendon, E.J., Keuler, K., Lavin-Gullon, A., Lenderink, G., Leutwyler, D., Lorenz, T., Maraun, D., Mercogliano, P., Milovac, J., Panitz, H.J., Raffa, M., Reca Remedio, A., Schär, C., Soares, P.M.M., Srnec, L., Marie Steensen, B., Stocchi, P., Tölle, M.H., Truhetz, H., Vergara-Temprado, J., De Vries, H., Warrach-Sagi, K., Wulfmeyer, V., Zander, M.J., 2021. The first multi-model ensemble of regional climate simulations at kilometer-scale resolution, part I: evaluation of precipitation. Climate Dynamics, 57, 275-302.

Barbieri, M., Barberio, M.D., Banzato, F., Billi, A., Boschetti, T., Franchini, S., Gori, F., Petitta, M., 2023. Climate change and its effect on groundwater quality. Environmental Geochemistry and Health, 45(4), 1133-1144.

Beck, H.E., McVicar, T.R., Vergopolan, N., Berg, A., Lutsko, N.J., Dufour, A., Zeng, Z., Jiang, X., van Dijk, A.I.J.M., Miralles, D.G., 2023. High resolution (1 km) Köppen-Geiger maps for 1901-2099 based on constrained CMIP6 projections. Scientific Data, 10(1), 724.

Blake, D., Mlisa, A., Hartnady, C., 2010. Large scale quantification of aquifer storage and volumes from the Peninsula and Skurweberg Formations in the southwestern Cape. Water SA, 36(2), 177-184.

Bonacci, O., 2007. Analysis of long-term (1878-2004) mean annual discharges of the karst spring Fontaine de Vaucluse (France). Acta Carsologica, 36(1), 151-156.

Bortolotti, V., Passerini, P., 1970. Magmatic activity. Sedimentary Geology, 4(3-4), 599-624.

Bouhafa, N., Sakarovitch, C., Lalague, L., Goulard, F., Pryet, A., 2024. Hybrid modeling of karstic springs: Error correction of conceptual reservoir models with machine learning. Water Supply, 24(5), 1559-1573.

Brockwell, P.J., Davis, R.A., 2016. Introduction to Time Series and Forecasting - Third Edition. Springer International Publishing, Cham, Switzerland.

Caloiero, T., Caloiero, P., Frustaci, F., 2018. Long-term precipitation trend analysis in Europe and in the Mediterranean basin. Water and Environment Journal, 32, 433-445.

Cardell, M.F., Amengual, A., Romero, R., Ramis, C., 2020. Future extremes of temperature and precipitation in Europe derived from a combination of dynamical and statistical approaches. International Journal of Climatology, 40(11), 4800-4827.

Carminati, E., Lustrino, M., Cuffaro, M., Doglioni, C., 2010. Tectonics, magmatism and geodynamics of Italy: What we know and what we imagine. Journal of the Virtual Explorer, 36.

Carminati, E., Lustrino, M., Doglioni, C., 2012. Geodynamic evolution of the central and western Mediterranean: Tectonics vs. igneous petrology constraints. Tectonophysics, 579, 173-192.

Cervi, F., Petronici, F., Castellarin, A., Marcaccio, M., Bertolini, A., Borgatti, L., 2018. Climate-change potential effects on the hydrological regime of freshwater springs in the Italian Northern Apennines. Science of The Total Environment, 622-623, 337-348.

Chen, Z., Grasby, S.E., Osadetz, K.G., 2004. Relation between climate variability and groundwater levels in the upper carbonate aquifer, southern Manitoba, Canada. Journal of Hydrology, 290(1-2), 43-62.

Cinkus, G., Wunsch, A., Mazzilli, N., Liesch, T., Chen, Z., Ravbar, N., Doummar, J., Fernández-Ortega, J., Barberá, J.A., Andreo, B., Goldscheider, N., Jourde, H., 2023. Comparison of artificial neural networks and reservoir models for simulating karst spring discharge on five test sites in the Alpine and Mediterranean regions. Hydrology and Earth System Sciences, 27(10), 1961-1985.

De Vita, P., Allocca, V., Manna, F., Fabbrocino, S., 2012. Coupled decadal variability of the North Atlantic Oscillation, regional rainfall and karst spring discharges in the Campania region (Southern Italy). Hydrology and Earth System Sciences, 16(5), 1389-1399.

Di Nunno, F., Granata, F., Gargano, R., de Marinis, G., 2021. Prediction of spring flows using nonlinear autoregressive exogenous (NARX) neural network models. Environmental Monitoring and Assessment, 193(6), 350.

Diodato, N., Bellocchi, G., Fiorillo, F., Ventafridda, G., 2017. Case study for investigating groundwater and the future of mountain spring discharges in Southern Italy. Journal of Mountain Science, 14(9), 1791-1800.

Diodato, N., Büntgen, U., Bellocchi, G., 2019. Mediterranean winter snowfall variability over the past millennium. International Journal of Climatology, 39(1), 384-394.

Diodato, N., Ljungqvist, F.C., Bellocchi, G., 2022. Empirical modelling of snow cover duration patterns in complex terrains of Italy. Theoretical and Applied Climatology, 147(3-4), 1195-1212.

Doummar, J., Hassan Kassem, A., Gurdak, J.J., 2018. Impact of historic and future climate on spring recharge and discharge based on an integrated numerical modelling approach: Application on a snow-governed semi-arid karst catchment area. Journal of Hydrology, 565, 636-649.

Doveri, M., Nisi, B., Cerrina Feroni, A., Ellero, A., Menichini, M., Lelli, M., Masetti, G., Da Prato, S., Principe, C., Raco, B., 2012. Geological, hydrodynamic and geochemical features of the volcanic aquifer of Monte Amiata (Tuscany, central Italy): an overview. Acta Vulcanologica, 23(1-2), 51-72.

Doveri, M., Menichini, M., 2017. Aspetti idrogeologici delle vulcaniti del Monte Amiata. In: Principe, C., Lavorini, G., Vezzoli, L., “Il Vulcano di Monte Amiata”, 255-265.

Doveri, M., Raco, B., 2021. Studio di approfondimento sulle caratteristiche quali-quantitative della risorsa idrica delle sorgenti di Santa Fiora - Monte Amiata. Accordo di Collaborazione Scientifica tra Acquedotto del Fiora (ADF) e Istituto di Geoscienze e Georisorse del Consiglio Nazionale delle Ricerche (IGG-CNR), unpublished technical report (in italian).

Eurispes, 2023. A system that treads water: the condition of water in Italy, [https://eurispes.eu/en/news/a-system-that-treads-water-the-condition-of-water-in-italy/]. Eurispes, Istituto di Studi Politici, Economici e Sociali. URL (accessed 2.29.24).

Fan, X., Goeppert, N., Goldscheider, N., 2023. Quantifying the historic and future response of karst spring discharge to climate variability and change at a snow-influenced temperate catchment in central Europe. Hydrogeology Journal, 31(8), 2213-2229.

Farahani, H.A., Rahiminezhad, A., Same, L., Immannezhad, K., 2010. A comparison of Partial Least Squares (PLS) and Ordinary Least Squares (OLS) regressions in predicting of couples mental health based on their communicational patterns. Procedia - Social and Behavioral Sciences, 5, 1459-1463.

Filippini, M., Segadelli, S., Dinelli, E., Failoni, M., Stumpp, C., Vignaroli, G., Casati, T., Tiboni, B., Gargini, A., 2024. Hydrogeological assessment of a major spring discharging from a calcarenitic aquifer with implications on resilience to climate change. Science of The Total Environment, 913, ISSN 0048-9697.

Fiorillo, F., Esposito, L., Guadagno, F.M., 2007. Analyses and forecast of water resources in an ultra-centenarian spring discharge series from Serino (Southern Italy). Journal of Hydrology, 336(1-2), 125-138.

Fiorillo, F., 2009. Spring hydrographs as indicators of droughts in a karst environment. Journal of Hydrology, 373, 290-301.

Fiorillo, F., Doglioni, A., 2010. The relation between karst spring discharge and rainfall by the cross-correlation analysis. Hydrogeology Journal, 18, 881-1895.

Fiorillo, F., Guadagno, F.M., 2012. Long karst spring discharge time series and droughts occurrence in Southern Italy. Environmental Earth Sciences, 65(8), 2273-2283.

Fiorillo, F., Pagnozzi, M., Ventafridda, G., 2015. A model to simulate recharge processes of karst massifs. Hydrological Processes, 29(10), 2301-2314.

Fiorillo, F., Petitta, M., Preziosi, E., Rusi, S., Esposito, L., Tallini, M., 2015. Long-term trend and fluctuations of karst spring discharge in a Mediterranean area (central-southern Italy). Environmental Earth Sciences, 74(1), 153-172.

Fiorillo, F., Leone, G., Pagnozzi, M., Esposito, L., 2021. Long-term trends in karst spring discharge and relation to climate factors and changes. Hydrogeology Journal, 29(1), 347-377.

Frondini, F., Caliro, S., Cardellini, C., Chiodini, G., Morgantini, N., 2009. Carbon dioxide degassing and thermal energy release in the Monte Amiata volcanic-geothermal area (Italy). Applied Geochemistry, 24(5), 860-875.

García-Ruiz, J.M., López-Moreno, J.I., Vicente-Serrano, S.M., Lasanta-Martínez, T., Beguería, S., 2011. Mediterranean water resources in a global change scenario. Earth-Science Reviews, 105(3-4), 121-139.

Garreaud, R.D., Alvarez-Garreton, C., Barichivich, J., Pablo Boisier, J., Christie, D., Galleguillos, M., LeQuesne, C., McPhee, J., Zambrano-Bigiarini, M., 2017. The 2010-2015 megadrought in central Chile: Impacts on regional hydroclimate and vegetation. Hydrology and Earth System Sciences, 21(12), 6307-6327.

Gattinoni, P., Francani, V., 2010. Depletion risk assessment of the Nossana Spring (Bergamo, Italy) based on the stochastic modeling of recharge. Hydrogeology Journal, 18, 325-337.

Gholami, V., Khaleghi, M.R., 2019. A comparative study of the performance of artificial neural network and multivariate regression in simulating springs discharge in the Caspian Southern Watersheds, Iran. Applied Water Science, 9(1), 9.

Giorgi, F., 2006. Climate change hot-spots. Geophysical Research Letters, 33, L08707.

Granata, F., Saroli, M., De Marinis, G., Gargano, R., 2018. Machine learning models for spring discharge forecasting. Geofluids, 2018, 8328167.

Gudmundsson, L., Bremnes, J.B., Haugen, J.E., Engen-Skaugen, T., 2012. Technical Note: Downscaling RCM precipitation to the station scale using statistical transformations – A comparison of methods. Hydrology and Earth System Sciences, 16(9), 3383-3390.

Halloran, L.J.S., Millwater, J., Hunkeler, D., Arnoux, M., 2023. Climate change impacts on groundwater discharge-dependent streamflow in an alpine headwater catchment. Science of the Total Environment, 902, 166009.

Hao, Y., Yeh, T., Hu, C., Wang, Y., Li, X., 2006. Karst groundwater management by defining protection zones based on regional geological structures and groundwater flow fields. Environmental Geology, 50, 415-422.

Hartmann, A., Goldscheider, N., Wagener, T., Lange, J., Weiler, M., 2014. Karst water resources in a changing world: review of hydrological modeling approaches. Reviews of Geophysics, 52(3), 218-242.

Hayes, A.F., Matthes, J., 2009. Computational Procedures for Probing Interactions in OLS and Logistic Regression: SPSS and SAS Implementations. Behavior Research Methods, 41, 924-936.

Haylock, M.R., Cawley, G.C., Harpham, C., Wilby, R.L., Goodess, C.M., 2006. Downscaling heavy precipitation over the United Kingdom: A comparison of dynamical and statistical methods and their future scenarios. International Journal of Climatology, 26(10), 1397-1415.

Hersbach, H., Bell, B., Berrisford, P., Hirahara, S., Horányi, A., Muñoz-Sabater, J., Nicolas, J., Peubey, C., Radu, R., Schepers, D., Simmons, A., Soci, C., Abdalla, S., Abellan, X., Balsamo, G., Bechtold, P., Biavati, G., Bidlot, J., Bonavita, M., De Chiara, G., Dahlgren, P., Dee, D., Diamantakis, M., Dragani, R., Flemming, J., Forbes, R., Fuentes, M., Geer, A., Haimberger, L., Healy, S., Hogan, R.J., Hólm, E., Janisková, M., Keeley, S., Laloyaux, P. Lopez, P., Lupu, C., Radnoti, G., de Rosnay, P., Rozum, I., Vamborg, F., Villaume, S., Thépaut, J.N., 2020. The ERA5 global reanalysis. Quarterly Journal of the Royal Meteorological Society, 146(730), 1999-2049.

IPCC, 2014. Climate Change 2014: Synthesis Report. Contribution of Working Groups I, II and III to the Fifth Assessment Report of the Intergovernmental Panel on Climate Change [Core Writing Team, R.K., Pachauri and L.A., Meyer (eds.)]. IPCC, Geneva, Switzerland, 151.

James, G., Witten, D., Hastie, T., Tibshirani, R., 2013. An Introduction to Statistical Learning with Applications in R. Springer, Berlin, Germany.

Jeelani, G., 2008. Aquifer response to regional climate variability in a part of Kashmir Himalaya in India. Hydrogeology Journal, 16, 1625-1633.

Joigneaux, E., Albéric, P., Pauwels, H., Pagé, C., Terray, L., Bruand, A., 2011. Impact of climate change on groundwater point discharge: Backflooding of karstic springs (Loiret, France). Hydrology and Earth System Sciences, 5(8), 2459-2470.

Kalhor, K., Ghasemizadeh, R., Rajic, L., Alshawabkeh, A., 2019. Assessment of groundwater quality and remediation in karst aquifers: A review. Groundwater for Sustainable Development, 8, 104-121.

Klaas, D.K.S.Y., Imteaz, M.A., Sudiayem, I., Klaas, E.M.E., Klaas, E.C.M., 2019. Coping with climate change in a tropical karst island: Assessment of groundwater resources under HadCM3-GCM scenarios and proposed adaptive strategies. Earth and Environmental Science, 239, 1-6.

Kottek, M., Grieser, J., Beck, C., Rudolf, B., Rubel, F., 2006. World map of the Köppen-Geiger climate classification updated. Meteorologische Zeitschrift, 15(3), 259-263.

Kovačič, G., Petrič, M., Ravbar, N., 2020. Evaluation and quantification of the effects of climate and vegetation cover change on karst water sources: case studies of two springs in South-Western Slovenia. Water (Switzerland), 12(11), 1-20.

Kovács, A., Stevanović, Z., 2023. A Combined Stochastic-Analytical Method for the Assessment of Climate Change Impact on Spring Discharge. Water (Switzerland), 15(4), 629.

Kresic, N., Stevanovic, Z., 2009. Groundwater Hydrology of Springs: Engineering, Theory, Management, and Sustainability. Elsevier, Rotterdam, Amsterdam.

Kundzewicz, Z.W., Döll, P., 2009. Will groundwater ease freshwater stress under climate change? Hydrological Sciences Journal, 54, 665-675.

Kutner, M.H., Nachtsheim, C.J., Neter, J., Li, W., 2005. Applied Linear Statistical Models - Fifth Edition. McGraw-Hill/Irwin, New York City, United States of America.

Lambrakis, N., Andreou, A.S., Polydoropoulos, P., Georgopoulos, E., Bountis, T., 2000. Nonlinear analysis and forecasting of a brackish karstic spring. Water Resources Research, 36(4), 875-884.

Leone, G., Pagnozzi, M., Catani, V., Ventafridda, G., Esposito, L., Fiorillo, F., 2021. A hundred years of Sanità Spring discharge measurements: trends and statistics for understanding water resource availability under climate change. Stochastic Environmental Research and Risk Assessment, 35(2), 345-370.

Livezey, R.E., Vinnikov, K.Y., Timofeyeva, M.M., Tinker, R., van den Dool, H.M., 2007. Estimation and extrapolation of climate normals and climatic trends. Journal of Applied Meteorology and Climatology, 46(11), 1759-1776.

Meinzer, O.E., 1923. Outline of groundwater hydrology with definitions. In: US Geological Survey Water-Supply Paper. 494, 48-54.

Mekis, É., Brown, R., 2010. Derivation of an adjustment factor map for the estimation of the water equivalent of snowfall from ruler measurements in Canada. Atmosphere - Ocean, 48(4), 284-293.

Montgomery, D.C., Jennings, C.L., Kulahci, M., 2008. Introduction to Time Series Analysis and Forecasting. John Wiley & Sons, Inc., Hoboken, United States of America.

Nicholson, K.N., Neumann, K., Dowling, C., Gruver, J., Sherman, H., Sharma, S., 2018. An Assessment of Drinking Water Sources in Sagarmatha National Park (Mt Everest Region), Nepal. Mountain research and development, 38(4), 353-363.

Parco Vivo, 2019. Sorgenti del Monte Amiata, [https://www.parcovivo.it/sorgenti-del-monte-amiata/]. Cooperativa di Comunità Parco Vivo. URL (accessed 12.06.23).

Patacca, E., Sartori, R., Scandone, P., 1993. Tyrrhenian Basin and Apennines. Kinematic evolution and related dynamic constraints. Recent evolution and seismicity of the Mediterranean region, 161-171.

Pekel, J.-F., Cottam, A., Gorelick, N., Belward, A.S., 2016. High-resolution mapping of global surface water and its long-term changes. Nature, 540(7633), 418-422.

Petitta, M., Tallini, M., 2002. Groundwater hydrodinamic of the Gran Sasso Massif (Abruzzi): New hydrological, hydrogeological and hydrochemical surveys (1994-2001). Bollettino della Societa Geologica Italiana, 121(3), 343-363.

Petitta, M., Banzato, F., Lorenzi, V., Matani, E., Sbarbati, C., 2022. Determining recharge distribution in fractured carbonate aquifers in central Italy using environmental isotopes: snowpack cover as an indicator for future availability of groundwater resources. Hydrogeology Journal, 30(5), 1619-1636.

Polemio, M., Casarano, D., 2008. Climate change, drought and groundwater availability in southern Italy. Geological Society Special Publication, 288, 39-51.

Portoghese, I., Bruno, E., Dumas, P., Guyennon, N., Hallegatte, S., Hourcade, J.-C. Nassopoulos, H., Pisacane, G., Struglia, M.V., Vurro, M., 2013. Impacts of Climate Change on Freshwater Bodies: Quantitative Aspects. In: Navarra, A., Tubiana, L. (eds) Regional Assessment of Climate Change in the Mediterranean. Advances in Global Change Research, vol 50. Springer, Dordrecht, Netherlands.

Raffa, M., Reder, A., Marras, G.F., Mancini, M., Scipione, G., Santini, M., Mercogliano, P., 2021. VHR-REA_IT dataset: Very high resolution dynamical downscaling of ERA5 reanalysis over Italy by COSMO-CLM. Data, 6(8), 88.

Raffa, M., Adinolfi, M., Reder, A., Marras, G.F., Mancini, M., Scipione, G., Santini, M., Mercogliano, P., 2023. Very High Resolution Projections over Italy under different CMIP5 IPCC scenarios. Scientific Data, 10(1), 238.

Rosenberg, N.J., Epstein, D.J., Wang, D., Vail, L., Srinivasan, R., Arnold, J.G., 1999. Possible impacts of global warming on the hydrology of the Ogallala aquifer region. Climatic Change, 42(4), 677-692.

Rotiroti, M., Sacchi, E., Caschetto, M., Zanotti, C., Fumagalli, L., Biasibetti, M., Bonomi, T., Leoni, B., 2023. Groundwater and surface water nitrate pollution in an intensively irrigated system: Sources, dynamics and adaptation to climate change. Journal of Hydrology, 623, 129868.

Sappa, G., Ferranti, F., Iacurto, S., De Filippi, F.M., 2018. Effects of climate change on groundwater feeding the Mazzoccolo and Capodacqua di Spigno Springs (Central Italy): First quantitative assessments. International Multidisciplinary Scientific GeoConference Surveying Geology and Mining Ecology Management, SGEM, 18(3.1), 219-226.

Sappa, G., De Filippi, F.M., Ferranti, F., Iacurto, S., 2019. Environmental issues and anthropic pressures in coastal aquifers: A case study in Southern Latium Region. Acque Sotterranee - Italian Journal of Groundwater, 8, 47-51.

Scanlon, B.R., Faunt, C.C., Longuevergne, L., Reedy, R.C., Alley, W.M., McGuire, V.L., McMahon, P.B., 2012. Groundwater depletion and sustainability of irrigation in the US High Plains and Central Valley. Proceedings of the National Academy of Sciences of the United States of America, 109(24), 9320-9325.

Seabold, S., Perktold, J., 2010. Statsmodels: Econometric and Modeling with Python. Proceedings of the 9th Python in Science Conference, Austin (United States of America), 28 June-3 July, 2010, 57-61.

Secci, D., Tanda, M.G., D'Oria, M., Todaro, V., Fagandini, C., 2021. Impacts of climate change on groundwater droughts by means of standardized indices and regional climate models. Journal of Hydrology, 603, 127154.

Secci, D., Tanda, M.G., D'Oria, M., Todaro, V., 2023. Artificial intelligence models to evaluate the impact of climate change on groundwater resources. Journal of Hydrology, 627, 130359, ISSN 0022-1694.

Shahgedanova, M., Adler, C., Gebrekirstos, A., Grau, H.R., Huggel, C., Marchant, R., Pepin, N., Vanacker, V., Viviroli, D., Vuille, M., 2020. Emptying Water Towers? Impacts of Future Climate and Glacier Change on River Discharge in the Northern Tien Shan, Central Asia. Mountain Research and Development, 41(2), 1-15.

Shepherd, A., Gill, K.M., Rood, S.B., 2010. Climate change and future flows of Rocky Mountain rivers: Converging forecasts from empirical trend projection and down-scaled global circulation modelling. Hydrological Processes, 24(26), 3864-3877.

Simsek, C., Elci, A., Gunduz, O., Erdogan, B., 2008. Hydrogeological and hydrogeochemical characterization of a karstic mountain region. Environmental Geology, 54, 291-308.

Sivelle, V., Jourde, H., Bittner, D., Mazzilli, N., Tramblay, Y., 2021. Assessment of the relative impacts of climate changes and anthropogenic forcing on spring discharge of a Mediterranean karst system. Journal of Hydrology, 598, 126396, ISSN 0022-1694.

Smiatek, G., Kaspar, S., Kunstmann, H., 2013. Hydrological climate change impact analysis for the Figeh spring near Damascus, Syria. Journal of Hydrometeorology, 14(2), 577-593.

Stevenazzi, S., Zuffetti, C., Camera, C.A.S., Lucchelli, A., Beretta, G.P., Bersezio, R., Masetti, M., 2023. Hydrogeological characteristics and water availability in the mountainous aquifer systems of Italian Central Alps: A regional scale approach. Journal of Environmental Management, 340, 117958.

Tarek, M., Brissette, F.P., Arsenault, R., 2020. Evaluation of the ERA5 reanalysis as a potential reference dataset for hydrological modelling over North America. Hydrology and Earth System Sciences, 24(5), 2527-2544.

Tarquini, S., Isola, I., Favalli, M., Battistini, A., Dotta, G., 2023. TINITALY, a digital elevation model of Italy with a 10 meters cell size (Version 1.1). Istituto Nazionale di Geofisica e Vulcanologia - National Institute of Geophysics and Volcanology (INGV), [https://tinitaly.pi.ingv.it/Download_Area1_1.html].

Todaro, V., D'Oria, M., Secci, D., Zanini, A., Tanda, M.G., 2022. Climate Change over the Mediterranean Region: Local Temperature and Precipitation Variations at Five Pilot Sites. Water (Switzerland), 14, 2499.

Tóth, Á., Kovács, S., Kovács, J., Mádl-Szőnyi, J., 2022. Springs regarded as hydraulic features and interpreted in the context of basin-scale groundwater flow. Journal of Hydrology, 610, 127907.

Trenberth, K.E., Dai, A., Rasmussen, R.M., Parsons, D.B., 2003. The changing character of precipitation. Bulletin of the American Meteorological Society, 84(9), 1205-1217+1161.

Van Loon, A.F., Tijdeman, E., Wanders, N., Van Lanen, H.A.J., Teuling, A.J., Uijlenhoet, R., 2014. How climate seasonality modifies drought duration and deficit. Journal of Geophysical Research, 119(8), 4640-4656.

Van Vuuren, D.P., Edmonds, J., Kainuma, M., Riahi, K., Thomson, A., Hibbard, K., Hurtt, G.C., Kram, T., Krey, V., Lamarque, J.-F., Masui, T., Meinshausen, M., Nakicenovic, N., Smith, S.J., Rose, S.K., 2011. The representative concentration pathways: an overview. Climate Change, 109(1), 5-31.

Wunsch, A., Liesch, T., Cinkus, G., Ravbar, N., Chen, Z., Mazzilli, N., Jourde, H., Goldscheider, N., 2022. Karst spring discharge modeling based on deep learning using spatially distributed input data. Hydrology and Earth System Sciences, 26(9), 2405-2430.

Yusoff, I., Hiscock, K.M., Conway, D., 2002. Simulation of the impacts of climate change on groundwater resources in eastern England. Geological Society Special Publication, 193, 325-344.

Zhong, Y., Hao, Y., Huo, X., Zhang, M., Duan, Q., Fan, Y., Liu, Y., Liu, Y., Yeh, T.J., 2016. A statistical model for karst spring discharge estimation under extensive groundwater development and extreme climate change. Hydrological Sciences Journal, 61(11), 2011-2023.

Zhou, R., Zhang, Y., 2023. Linear and nonlinear ensemble deep learning models for karst spring discharge forecasting. Journal of Hydrology, 627, 130394.

Zhu, R., Zheng, H., Croke, B.F.W., Jakeman, A.J., 2020. Quantifying climate contributions to changes in groundwater discharge for headwater catchments in a major Australian basin. Science of the Total Environment, 729, 138910.

3.11. Additional historical multi-decadal analyses

As introduced in Section 1.3.2 of this thesis, the discharge datasets for Verde Spring and Cassano Irpino and Serino Spring groups have proven useful, even though these springs were excluded from the more in-depth analyses performed using the multiregression method (Chapter 3) and the LSTM method (Chapter 4). In the following paragraphs, the complete discharge datasets for these springs will be presented, along with the results of the multi-decadal analysis conducted on their historical discharge to assess the pattern of flow rate.

3.11.1. Verde Spring (time span 1938-2005)

Verde Spring is characterised by a historical discharge dataset spanning 68 yr from January 1938 to December 2005 (Fig. 3.9). Despite several gaps in the dataset, the overall historical hydrograph exhibits a clear decreasing trend in discharge, with a more pronounced decline during the 1980s.

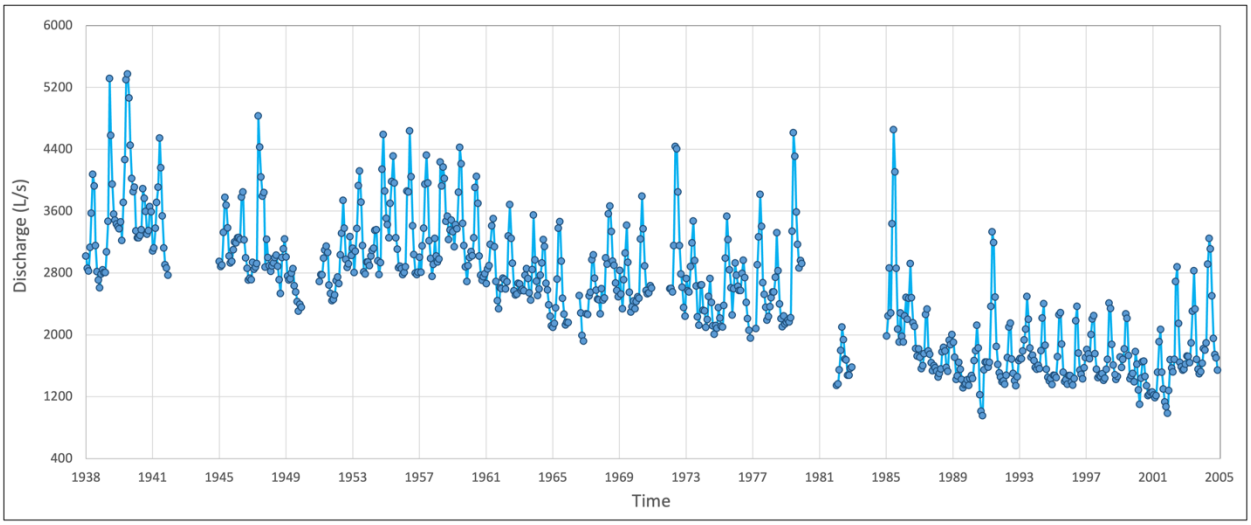

Fig. 3.9. Mean monthly discharge of Verde Spring. The x-axis labels indicate January of the respective year.

Given the availability of 68 yr of discharge data, the multi-decadal analysis in this case involved dividing the dataset into two parts, each 34 yr long: the first spanning from 1938 to 1971, and the second from 1972 to 2005 (Fig. 3.10).

Fig. 3.10 clearly shows that the older band is characterised by a significantly higher discharge compared to the more recent one. During the 1938-1971 period, Verde Spring exhibited an average discharge of approximately 2890 L/s, while in the 1972-2005 period, it recorded an average discharge of 1830 L/s, reflecting a decline of about 37%.

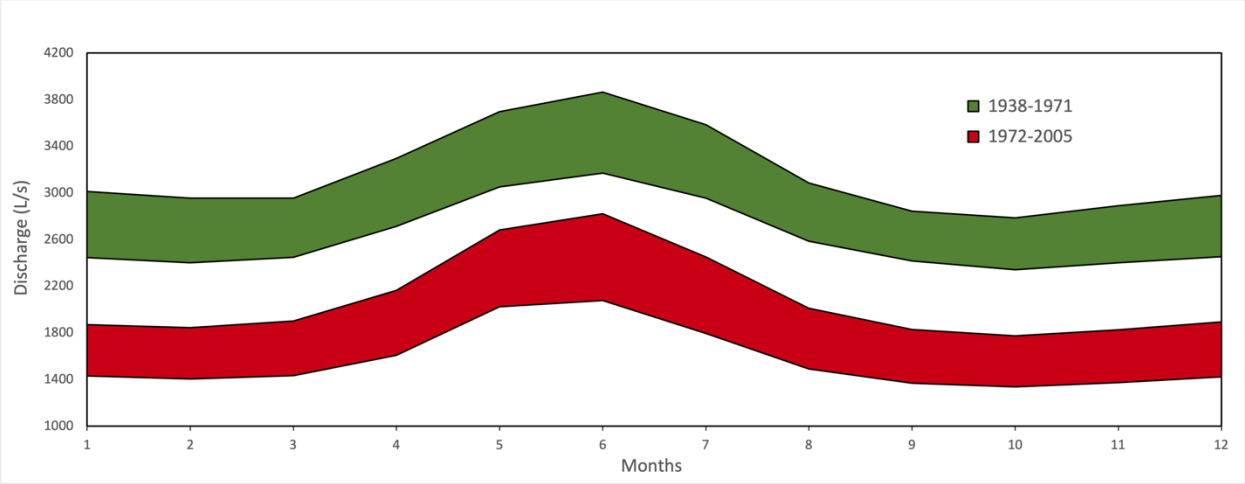

Fig. 3.10. Hydrographs of Verde Spring based on the multi-decadal approach with standard deviation uncertainty bands around the mean.

3.11.2. Cassano Irpino Spring group (time span 1965-2021)

Cassano Irpino Spring group has a historical discharge dataset spanning from January 1965 to December 2021 (Fig. 3.11), covering 56 yr. The dataset also shows a decline in discharge during the 1980s, which, however, reversed its trend from the early 2000s.

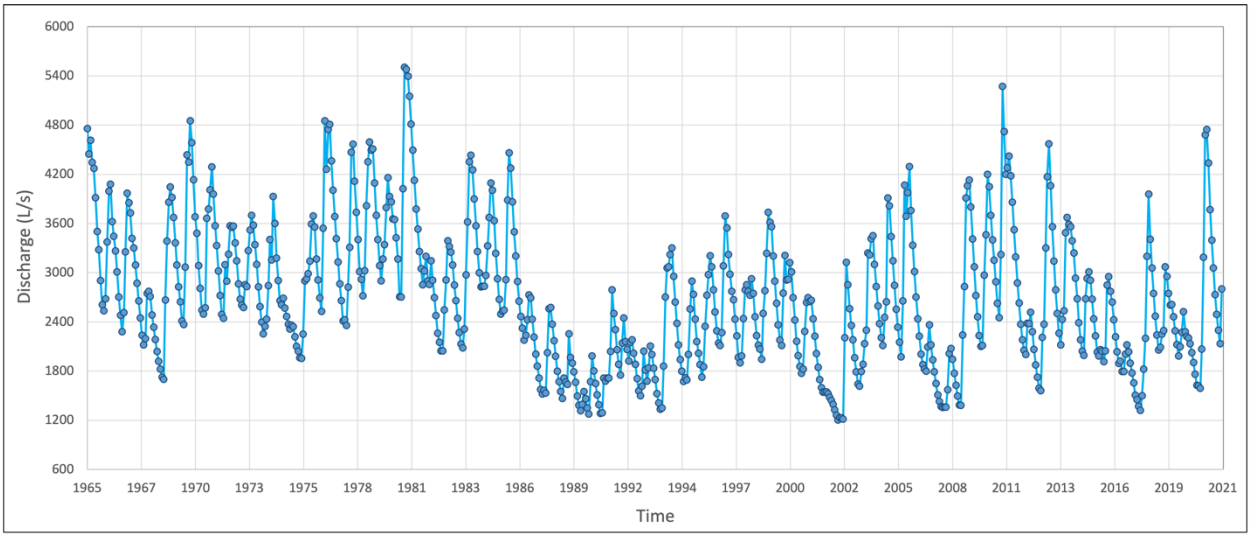

Fig. 3.11. Mean monthly discharge of Cassano Irpino Spring group.

Considering the availability of only 57 yr of data, the multi-decadal analysis was carried out by dividing the dataset into two periods of 29 yr each, both including the year 1993: the first from 1965 to 1993, and the second from 1993 to 2021 (Fig. 3.12).

Fig. 3.12 highlights that, in this case as well, the older period is characterised by a higher discharge compared to the more recent one. During the 1965-1993 period, Cassano Irpino Spring group

exhibited an average flow rate of roughly 3190 L/s, while in the 1993-2021 period, it recorded an average discharge of 2490 L/s, reflecting a decline of nearly 22%.

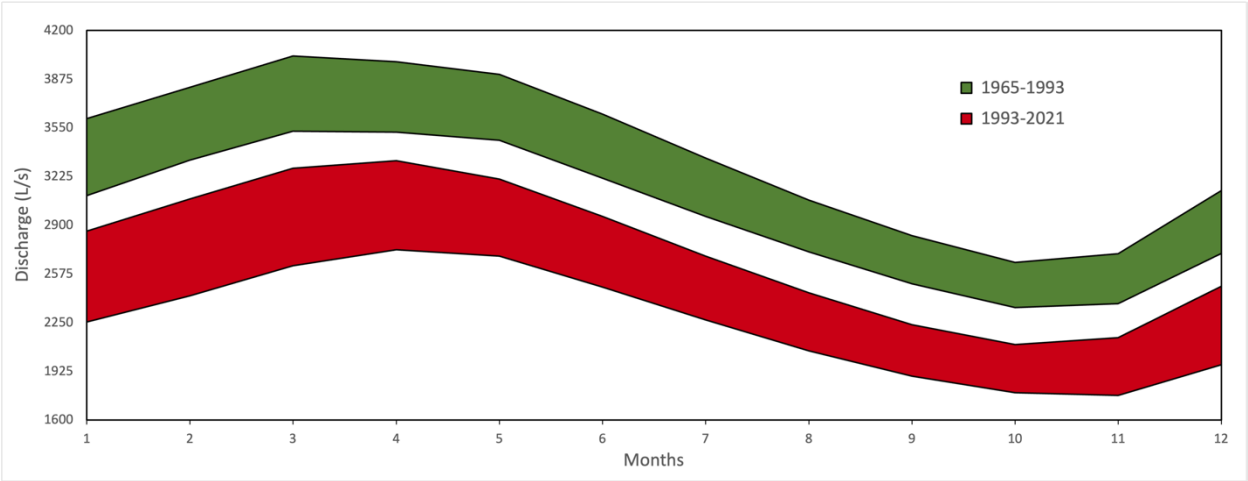

Fig. 3.12. Hydrographs of Cassano Irpino Spring group based on the multi-decadal approach with standard deviation uncertainty bands around the mean.

3.11.3. Serino Spring group (time span 1962-2019)

Serino Spring group is characterised by a historical discharge dataset spanning 58 yr from January 1962 to December 2019 (Fig. 3.13).

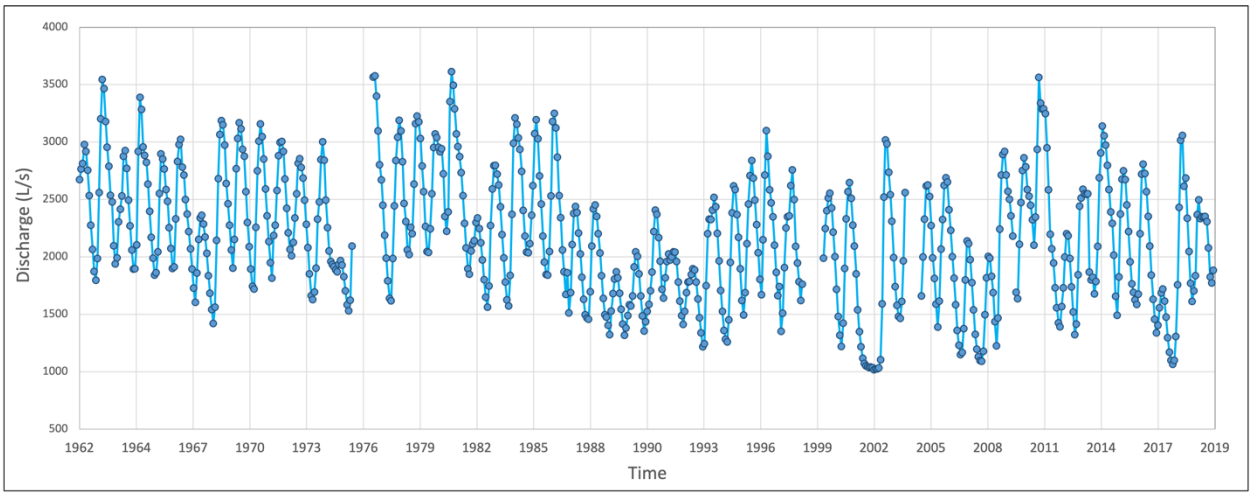

Fig. 3.13. Mean monthly discharge of Serino Irpino Spring group.

In this third case study as well, a significant decline in discharge also occurred during the 1980s. However, this trend reversed in the early 1990s. With 58 years of available data, the multi-decadal analysis was conducted by dividing the dataset into two periods of 29 yr each: the first covering the years 1962 to 1990, and the second spanning 1991 to 2019 (Fig. 3.14).

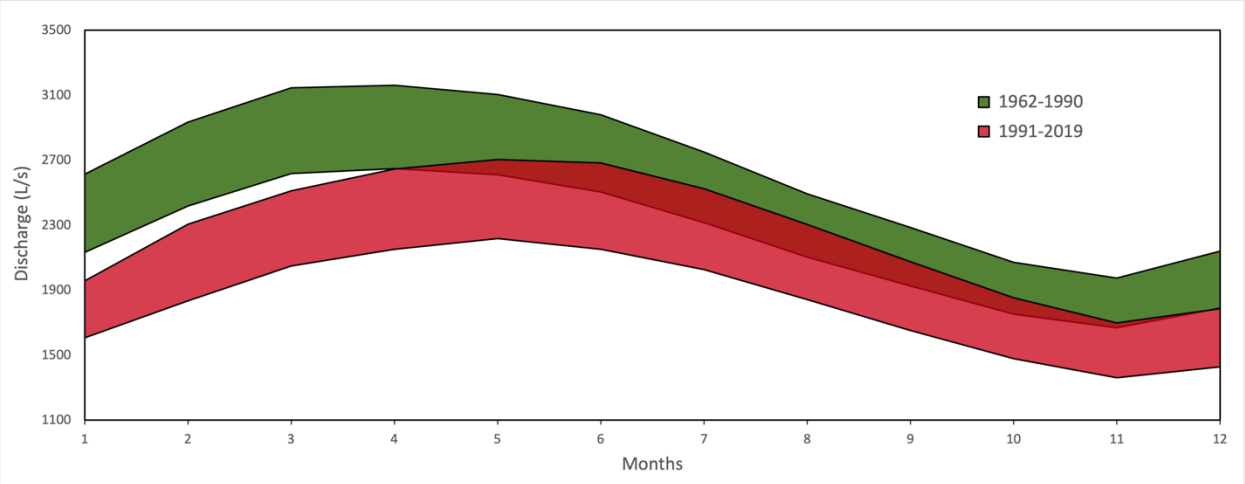

Fig. 3.14. Hydrographs of Serino Spring group based on the multi-decadal approach with standard deviation uncertainty bands around the mean.

Fig. 3.14 shows that the older period is characterised by a higher discharge compared to the more recent one, although less pronounced than in the previous two cases, partly due to the partial overlap of the two bands. During the 1962-1990 period, Serino Spring group exhibited an average discharge of approximately 2420 L/s, while in the 1991-2019 period, it recorded an average flow rate of roughly 2040 L/s, reflecting a decline of 16%.

A notable observation from the multi-decadal analysis of Serino Spring group is the shift in the peak discharge. In the older period, the yearly peak flow rate is observed between March and May, whereas in the more recent period, this peak occurs between April and June.

3.11.4. Historical discharge analysis conclusions

The findings from the multi-decadal analysis of historical discharge for Verde Spring and Cassano Irpino and Serino Spring groups confirm that water scarcity along the Apennines is profoundly impacting groundwater resources. All five springs analysed in this chapter, along with Nadìa Spring from the previous chapter, show flow rate declines. For obvious reasons related to the differing lengths and start and end years of the historical datasets, it was not possible to compare the same multi-decadal periods. Nonetheless, all the five springs exhibit a reduction in discharge in the more recent multi-decadal periods compared to the older ones. Notably, a significant decline for the springs occurred in the 1980s (Figs. 3.2, 3.9, 3.11, 3.13), after which they stabilised at lower average discharge rates. Regarding Cannucceto Spring, with flow rate data spanning only from 1979 to 2022 (44 yr), its dataset is too limited for reliable assessments of climate change effects. Nevertheless, it is the only studied spring showing a slight increase in discharge based on the linear trend (Fig. 1.9). To collectively present the historical hydrographs of all seven springs analysed in this thesis, Fig. 3.15 was created.

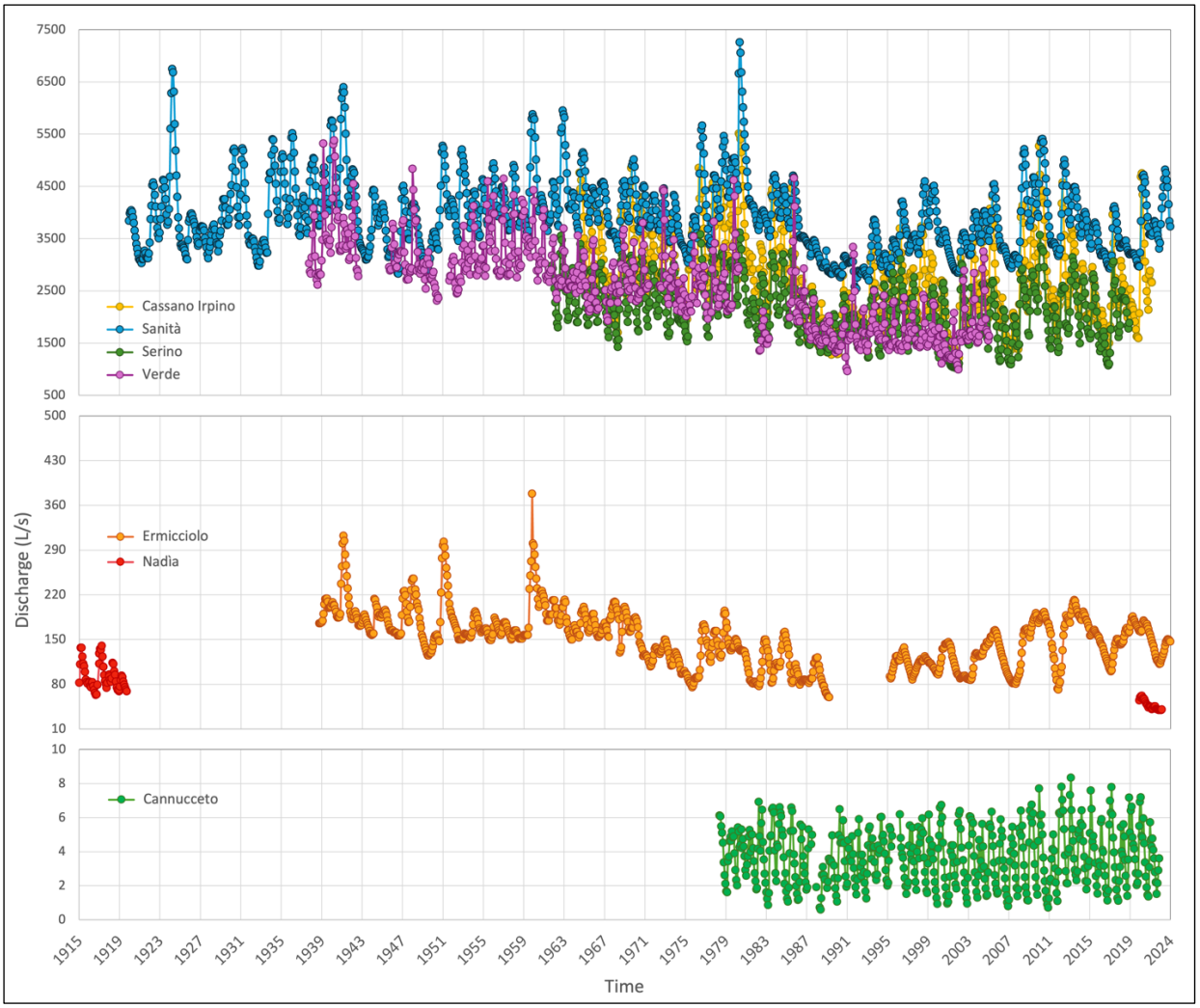

Fig. 3.15. Mean monthly spring discharge of: Cassano Irpino, Sanità, Serino, and Verde Springs at the top (Meinzer class II); Ermicciolo and Nadìa Springs in the middle (M. class IV); and Cannucceto Spring at the bottom (M. class V). The chart consists of three subgroups sharing the same axes but with different y-axis scales (0-10 L/s, 10-500 L/s, and 500-7500 L/s, labelled at 2, 70, and 1000 L/s intervals, respectively).

Figure 3.15 highlights the discharge decline experienced during the 1980s by all seven springs analysed along the Apennines (excluding Nadìa Spring, where this cannot be determined). This decline is evident from the first half of the 1980s for Sanità, Ermicciolo, Verde, Cassano Irpino, and Serino Springs, although it is difficult to rule out anthropogenic influences on the decrease for the latter three due to the reasons outlined in Section 1.3.2. In contrast, for Cannucceto Spring, the decline occurred in the second half, between 1987 and 1990, and is less pronounced compared to the other cases. The similar negative historical trends observed across the studied springs, all located along the Apennines within the same Mediterranean climate, coupled with the significant influence of climatic drivers on discharge, suggest that the future trends identified through multiregression analysis for Sanità and Ermicciolo Springs may also apply to many other springs within similar Mediterranean-type climates.

Chapter 4:

Long Short-Term Memory (LSTM) machine learning method for future spring discharge forecasting

4.1. Preface

The analyses detailed in the previous chapters have provided an overview of the effects of climate change on groundwater discharge processes along the Apennines, both in terms of the resilience of springs to climate modifications and the evaluation of future discharge trends, expressed as multi-decadal projections over the long term.

In detail, in Chapter 3, a linear regression statistical method was employed to identify long-term historical relationships between variables to be used in spring discharge forecasting. This method proved highly effective in capturing multi-decadal trends based on linear relationships, which predominantly govern the connection between discharge and recharge-related parameters. In contrast, this Chapter 4 focuses on a machine learning-based method, capable of capturing even non-linear relationships, for analysing the recharge-discharge connection thus enabling more accurate temporal predictions on a monthly basis.

Section 4.2 introduces the fundamental concepts of Machine Learning (ML), including key definitions, learning approaches, and algorithm structures, with a particular focus on the ML methodology adopted in this study: Long Short-Term Memory (LSTM). Following this introduction, the chapter explores the application of LSTM for assessing future projections of spring discharge, treated as the dependent variable. In this analysis, the independent variables comprise not only precipitation and atmospheric temperature but also the spring discharge from preceding months. Compared to the paper discussed in the previous chapter, extending the LSTM relationships into future projections required an iterative approach to predict discharge over time, month by month, by sequentially updating the dataset in the future.

The analyses summarised and presented here form the foundation for a forthcoming paper, to be submitted by the end of 2025, which will integrate and conclude the investigations conducted throughout this PhD project.

4.2. Machine Learning: a comprehensive introduction

4.2.1. Defining machine learning

Machine learning has revolutionised computer science, transforming how we solve problems and make decisions based on data analysis. Initially defined by Arthur Samuel (1959) as "the field of study that gives computers the ability to learn without being explicitly programmed", ML has evolved into a powerful tool. It enables systems to learn from extensive datasets and improve their performance over time without relying on hard-coded instructions. This shift, particularly with the advent of neural networks, has expanded our ability to address intricate challenges. Neural networks have unlocked new ways for machines to process and learn from data, allowing them to enhance their performance through experience (Jordan and Bishop, 2006).

The adaptability of machine learning is particularly valuable in scenarios where traditional rule-based programming proves inadequate. Indeed, ML models continuously refine their strategies by learning from new data, leading to more effective outcomes (Bhowmick and Hazarika, 2018). This adaptability has shown significant benefits in domains that rely on large datasets, such as medicine and astrophysics, where machine learning is able to identify patterns that would otherwise go unnoticed (Ball and Brunner, 2010). These advancements highlight ML's strength in handling high-dimensional data and extracting meaningful insights, making it indispensable across diverse scientific and commercial domains (Dal Seno, 2024).

Despite its widespread adoption in sectors such as finance, e-commerce, and healthcare, machine learning has seen slower integration into areas like civil protection, disaster response, territorial management, and the forecasting of natural parameters. This slower uptake clearly reflects the complexity of applying ML to real-world scenarios. The effectiveness of machine learning in these applications is often constrained by challenges such as incomplete or biased datasets, which can significantly hinder model performance. To ensure informed and equitable decision-making, it is essential to use datasets that are diverse, representative, and regularly updated (Gebru et al., 2018).

The private sector has been swift in embracing ML, leveraging it to enhance efficiency, foster innovation, and improve customer experiences. Industries such as finance and technology depend on ML to analyse vast datasets and inform strategic decisions, giving them a competitive advantage (Brynjolfsson and McAfee, 2017). However, the public sector faces unique hurdles, such as budgetary constraints, regulatory requirements, and the need to ensure equitable service delivery and ethical use of ML (Sun et al., 2019; Mikhaylov et al., 2018).

Nevertheless, in the field of applied geology, machine learning holds significant potential for landslide hazard assessment and, more broadly, for forecasting the response of natural systems

to complex combinations of pressures arising from climatic or anthropogenic origins. In summary, ML represents a transformative shift from traditional programming to flexible, data-driven learning. Its capacity to process complex datasets and extract meaningful insights has already reshaped many companies worldwide. However, its potential in the management of natural hazards remains underexplored. With appropriate frameworks and a strong emphasis on data quality and ethical application, ML could become a vital tool for improving preparedness, response, and resilience in the face of natural risks.

4.2.2. Machine Learning categories and algorithms

ML comprises four main approaches (Fig. 4.1), from which various algorithms emerge, enabling computers to extract knowledge from data and make data-driven decisions. These algorithms are grouped into a few key categories: supervised learning, unsupervised learning, reinforcement learning (Fig. 4.1), and semi-supervised learning, which represents a hybrid category.

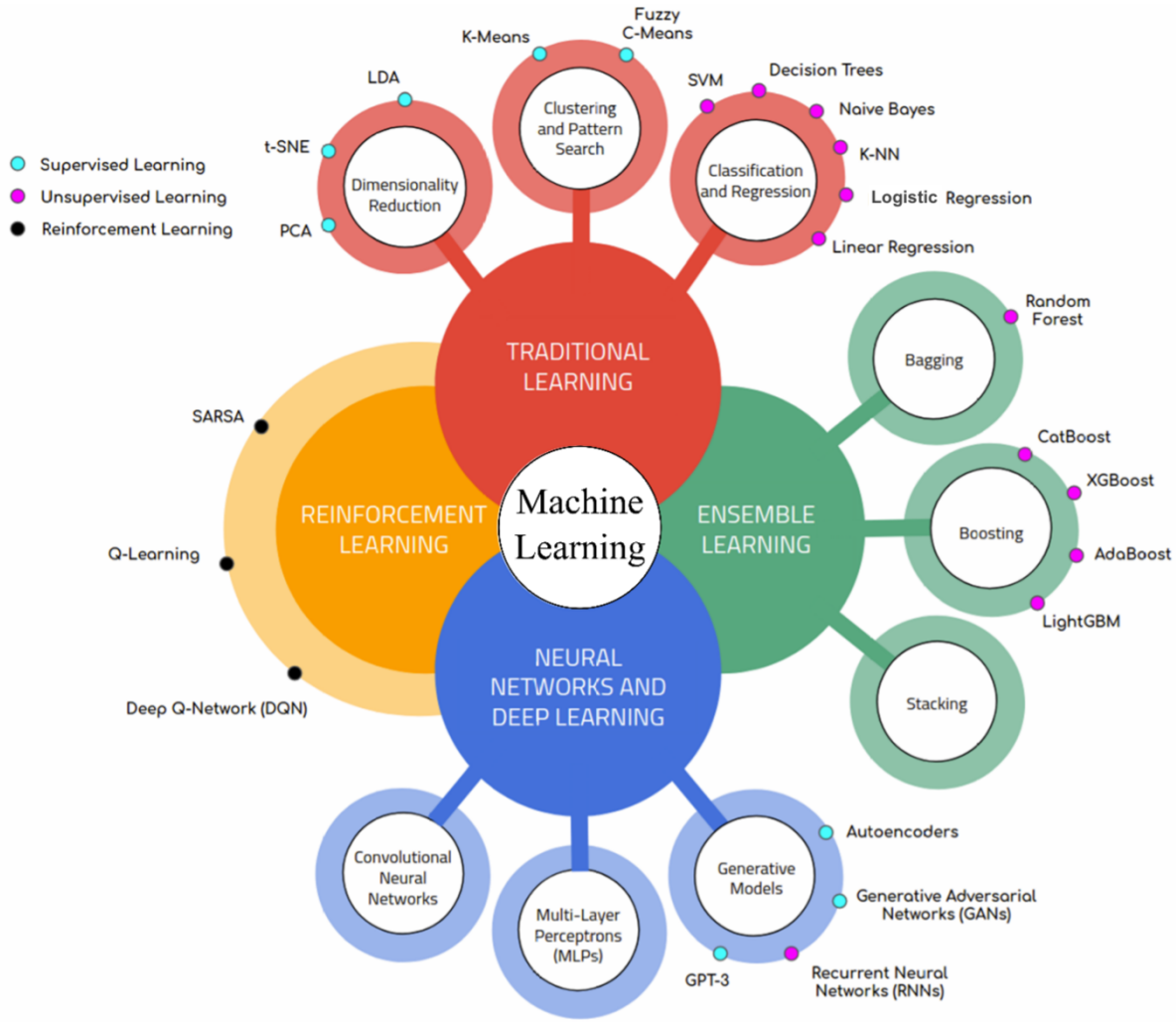

Fig. 4.1. Conceptual scheme of the four main ML approaches and their algorithms, organised into the three categories: Supervised, Unsupervised, and Reinforcement (Dal Seno, 2024).

Each category possesses distinct characteristics, advantages, and specific use cases, which depend on the type of data and the problem being addressed. ***Supervised learning*** relies on labelled data to train models, ***unsupervised learning*** identifies patterns in unlabelled data, and ***reinforcement learning*** trains models to optimise decisions by maximising cumulative rewards through interaction with an environment.

A common framework in ML comprises three key phases: training, validation, and testing. During training, the model learns patterns and adjusts its parameters to minimise errors. Validation fine-tunes the model and prevents overfitting by evaluating it on unseen data. Finally, testing measures the model's accuracy and generalisability using a separate dataset, ensuring its robustness for real-world applications. Additionally, before training, ML methods require the setting of hyperparameters, which are external configuration settings that control the learning process. Gaining an understanding of the main learning algorithms within the various categories is crucial for selecting the most suitable algorithm for a specific task and for building effective ML models capable of addressing a wide range of real-world problems (Dal Seno, 2024). Given the broader and more extensive practical application of *traditional learning* and *deep learning* in hydrogeology, this study chose to focus on these two approaches, leaving aside *reinforcement* and *ensemble learning* (Fig. 4.1).

4.2.2.1. Traditional learning algorithms

The following paragraphs will introduce the most widely used traditional learning algorithms in hydrogeology, focusing on *regression* for continuous predictions, *classification* for accurate data categorisation, and *clustering* for grouping similar data without predefined labels.

Linear regression is among the earliest and most easily interpretable algorithms in the field of ML. It establishes a relationship between input variables (features) and a continuous output variable by fitting a straight-line equation to the observed dataset (Seber and Lee, 2012). The basic form of linear regression (Eq. 4.1) can be expressed as:

$$y = \beta_0 + \beta_1 x_1 + \beta_2 x_2 + \ldots + \beta_n x_n + \varepsilon \qquad [4.1]$$

where y is the target variable, x_1, x_2, ..., x_n are the input features, β_0 is the intercept, β_1, β_2, ..., β_n are the coefficients, and ε is the error term (Draper and Smith, 1998). The algorithm aims to find the values of β that minimize the sum of squared residuals, which represent the differences between observed and predicted values. This is typically done using methods like Ordinary Least Squares or gradient descent (Murphy, 2012). Linear regression's strengths lie in its simplicity, interpretability, and computational efficiency. It is widely used across scientific fields for trend analysis (as in our case) and to understand relationships between variables (Kutner et al., 2004).

However, it assumes a linear relationship between variables and is sensitive to outliers. It may underperform on complex, non-linear relationships in data (Hastie et al., 2009).

Logistic regression is primarily designed for binary classification tasks. It estimates the probability that an instance belongs to a specific class by applying the logistic function to a linear combination of input features (Hosmer et al., 2013). The function σ (Eq. 4.2) is expressed as:

$$\sigma(z) = \frac{1}{(1 + e^{(-z)})} \quad [4.2]$$

where *z* is the linear combination of features: $z = \beta_0 + \beta_1 x_1 + \beta_2 x_2 + ... + \beta_n x_n$ and *e* denotes the base of the natural logarithm. Logistic regression seeks to determine the optimal values of β by maximising the likelihood of the observed data, typically achieved using techniques such as maximum likelihood estimation or gradient descent (Murphy, 2012). The model's capacity to generate probabilistic outputs makes it particularly valuable for forecasting in fields such as hydrology (Yu et al., 2019), hydrogeology (Sahour et al., 2022), risk analysis, and medical diagnostics (Menard, 2002). However, one limitation of logistic regression is its reliance on the assumption of linearity in the log-odds space (the logarithm of the odds of an event occurring), which may not model more complex relationships in the data (Bishop, 2006).

Decision trees are versatile machine learning algorithms commonly used for both classification and regression tasks, including hydrogeological applications, also for forecasting purposes (Mewes et al., 2020; Niraula et al., 2021). They create a predictive model by learning simple decision rules from data features (Quinlan, 1986). The structure of a decision tree resembles a flowchart (Fig. 4.2), branching from a root node based on feature-specific questions.

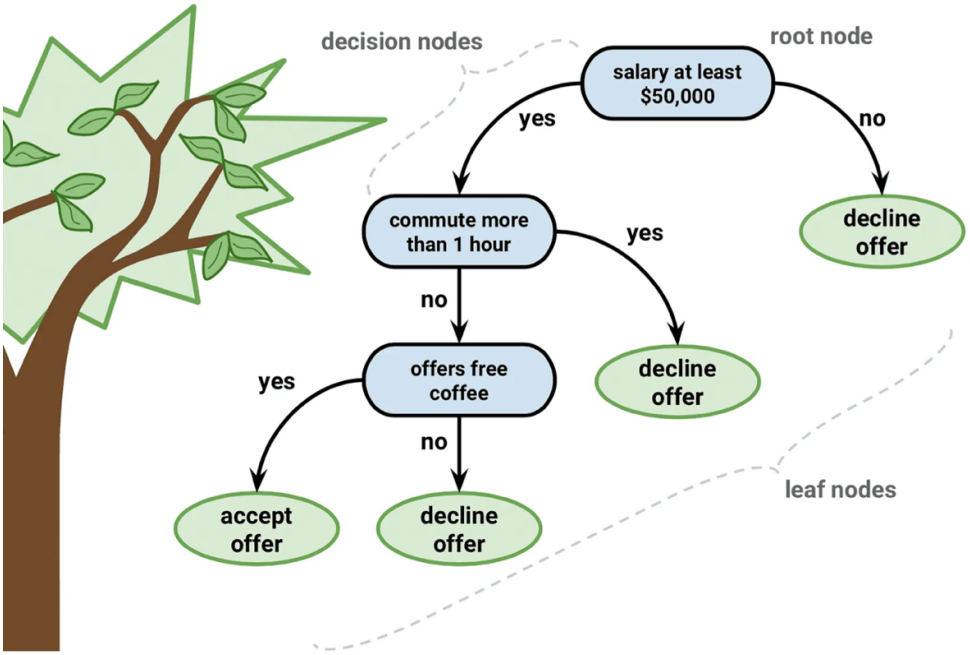

Fig. 4.2. Decision tree visualising whether to accept a job offer (GoPenAI, 2023, modified).

This process continues until reaching leaf nodes that provide final predictions. For example, a decision tree predicting whether it is advantageous to accept a new job offer might first consider the annual salary, then the commuting time, and so on. Tree construction follows a top-down approach, selecting the best feature to split the data by maximizing information gain or minimizing impurity (Breiman et al., 1984). This continues until a stopping criterion is met (e.g., max tree depth). Decision trees offer several advantages: they are interpretable, handle both numerical and categorical data, and perform automatic feature selection. They capture non-linear relationships and feature interactions (Loh, 2011). However, they can overfit if grown too deep, which can be mitigated by ensemble learning methods (Breiman, 2001).

Support Vector Machines (SVM) are powerful algorithms primarily employed for classification and regression problems. Renowned for their robust performance and solid theoretical underpinnings (Cortes and Vapnik, 1995), SVMs operate by identifying the optimal hyperplane that best separates classes within a high-dimensional space. For datasets that are linearly separable, SVM determines the hyperplane that maximises the margin between the classes. When the data is not linearly separable, SVM employs the "kernel trick" to project the data into a higher-dimensional space, enabling linear separation. Popular kernel functions include linear, polynomial, and radial basis functions (Schölkopf and Smola, 2002). The decision function (Eq. 4.3) for SVM classification is expressed as:

$$f(x) = sign(\Sigma_i \alpha_i y_i K(x, x_i) + b) \quad [4.3]$$

where α_i are the Lagrange multipliers, y_i are the class labels, K is the kernel function, x_i are the support vectors, and b is the bias term. SVMs are effective in high-dimensional feature spaces, especially when the number of features exceeds the number of samples. They provide a clear margin of separation, often resulting in better generalisation to unseen data. These algorithms are applied in areas such as text image analysis, spring discharge forecasting (Cheng et al., 2021; Zhou and Zhang, 2023), and bioinformatics (Ben-Hur et al., 2008). However, SVMs have notable limitations, including their inability to directly estimate probabilities and their sensitivity to the choice of kernel and hyperparameters. Furthermore, training SVMs on very large datasets can be computationally demanding.

K-means clustering is a core algorithm in unsupervised learning, widely utilised for tasks such as data partitioning and pattern recognition. It divides n observations into k clusters, assigning each observation to the cluster whose mean, or centroid, is closest (MacQueen, 1967). The algorithm operates in an iterative manner: it begins by randomly selecting k initial centroids, assigns each data point to the nearest centroid, recalculates the centroids based on the newly assigned points, and continues this process until convergence or until a predefined maximum number of

iterations is attained. This iterative approach minimises the Within-Cluster Sum of Squares (WCSS) (Eq. 4.4), which is mathematically defined as (Hartigan and Wong, 1979):

$$WCSS = \Sigma_i \Sigma_x //x - \mu_i//^2 \quad [4.4]$$

where x is a data point and μ_i is the centroid of cluster i. K-means is widely used across multiple fields due to its simplicity and scalability. In addition to hydrogeology (Kayhomayoon et al., 2022; Soleimani Motlagh et al., 2017), it has been applied to customer segmentation, image compression, and anomaly detection (Jain, 2010). Its ability to handle large datasets efficiently makes it particularly relevant in the era of big data. However, K-means also has its limitations: it requires the number of clusters (k) to be specified in advance, which can be challenging when the data structure is not well understood. Additionally, the algorithm is sensitive to the initial placement of centroids and assumes clusters are spherical, meaning they are evenly distributed around a central point, which may not accurately reflect the underlying data distribution (Arthur and Vassilvitskii, 2007).

4.2.2.2. Deep learning algorithms

Deep learning algorithms (Fig. 4.1) have transformed the field of machine learning, significantly advancing areas such as natural sciences, computer vision, and natural language processing. This shift in approach is defined using the key architecture of multi-layered Neural Networks (NNs), which can extract hierarchical features from data (LeCun et al., 2015). NNs takes inspiration from the neural architecture of the human brain. These systems are composed of interconnected layers of nodes, referred to as neurons, which process and transmit information (Rosenblatt, 1958). The most basic type of neural network is the feedforward network, where data flows in a single direction, from input to output, through one or more hidden layers. Each neuron applies a non-linear activation function to its inputs. Training a neural network involves optimising the weights of the connections between neurons to minimise the difference between predicted and actual outputs (LeCun et al., 1998). This is typically accomplished through backpropagation, a technique that calculates gradients in neural networks by propagating errors backward from the output to the input layers (Rumelhart et al., 1986). Moreover, the development of boosting algorithms, particularly AdaBoost (Freund and Schapire, 1997), which iteratively combines weak learners to form a strong predictor, further enhanced the field of ML and complemented neural network methods. The strength of neural networks lies in their capacity to approximate highly complex functions, making them powerful tools for addressing a wide range of machine learning challenges (Cybenko, 1989; Hornik, 1991).

The remarkable success of deep learning can be attributed to three primary factors: the availability of large datasets, enhanced computational resources, and innovative algorithmic advancements. Together, these developments have enabled the training of highly complex models that often surpass human performance in specific tasks (Goodfellow et al., 2016). In the field of applied geology, deep learning algorithms are increasingly utilised (Dal Seno, 2024); in hydrogeology, in particular, Convolutional Neural Networks (CNNs) and Recurrent Neural Networks (RNNs) are among the most employed (El Ansari et al., 2023; Piotrowska and Dąbrowska, 2024). For this reason, the following paragraphs will focus on these algorithms, with particular emphasis on Long Short-Term Memory (LSTM) networks, a specialised type of RNN widely used in trend analysis and forecasting tasks.

Convolutional Neural Networks (CNNs) are a class of neural networks designed to process grid-structured data, such as images. Drawing inspiration from the structure of the animal visual cortex, CNNs have revolutionised computer vision by learning hierarchical features directly from raw image data (LeCun et al., 1998). The training of a CNN typically involves two primary stages: feedforward and backpropagation. During the feedforward phase, input data is passed through several layers, including convolutional layers that apply trainable filters (kernels) to identify local patterns such as edges and textures. In the backpropagation phase, the model's predictions are compared to the actual targets, and a loss function (which represents error in terms of accuracy or predictive capability of the model) is used to compute the discrepancy. The calculated loss is then used to adjust the weights in the network, improving its predictive accuracy over successive iterations. Beyond the branch of applied geology, CNNs have achieved remarkable results in various computer vision tasks, often surpassing traditional approaches. Notably, CNNs have been widely applied in object detection and image classification, which are essential in the field of remote sensing. These applications extend to domains such as autonomous vehicles, medical image analysis, and satellite imagery interpretation. As CNN research advances, efforts are focused on improving their efficiency, enhancing interpretability, and addressing challenges such as generalisation to out-of-distribution samples (Dal Seno, 2024).

Recurrent Neural Networks (RNNs) are a type of neural network designed to handle sequential data, making them effective for applications such as hydrogeological and meteorological time series analysis, and natural language processing (Elman, 1990). What distinguishes RNNs is their ability to maintain a hidden state that stores information from previous time steps, allowing them to capture temporal dependencies within the data. In an RNN, the hidden state is updated at each time step using the current input and the hidden state from the previous step. This recurrent structure enables the network to retain a form of memory, making it useful for problems where the sequence of data points carries critical information (Mikolov et al., 2010). However, standard RNNs encounter difficulties when dealing with long-term dependencies due to the vanishing and

exploding gradient problems, which complicate the training of long sequences (Bengio et al., 1994). To address these challenges, more advanced RNN architectures were introduced, the most notable being Long Short-Term Memory (LSTM) networks.

Long Short-Term Memory (LSTM) networks are a specialised form of Recurrent Neural Networks developed to address the difficulties traditional RNNs face in handling long-term dependencies. Introduced in 1997, LSTMs have become a cornerstone for sequence modelling tasks that require the retention of information over extended timeframes. The primary innovation of LSTMs is the memory cell, which preserves its state across time steps. This memory is controlled by three gates (Fig. 4.3): the input gate determines which new information to store, the forget gate decides what to discard, and the output gate selects the information for the output (Hochreiter and Schmidhuber, 1997). This gating mechanism allows LSTMs to selectively store or forget information, enabling them to effectively capture long-term dependencies in sequential data. LSTMs have been successfully applied across a wide range of domains. In natural language processing, they have driven advancements in machine translation, text generation, and sentiment analysis (Sutskever et al., 2014). In time series analysis, they excel in tasks such as predicting stock prices and forecasting weather patterns (Graves, 2012). Despite their strengths, LSTMs are not without limitations. They can be computationally intensive to train, especially when working with long sequences, and often require substantial amounts of data to achieve optimal performance. To address some of these challenges, alternative architectures have been introduced to offer a more efficient approach for certain tasks (Cho et al., 2014).

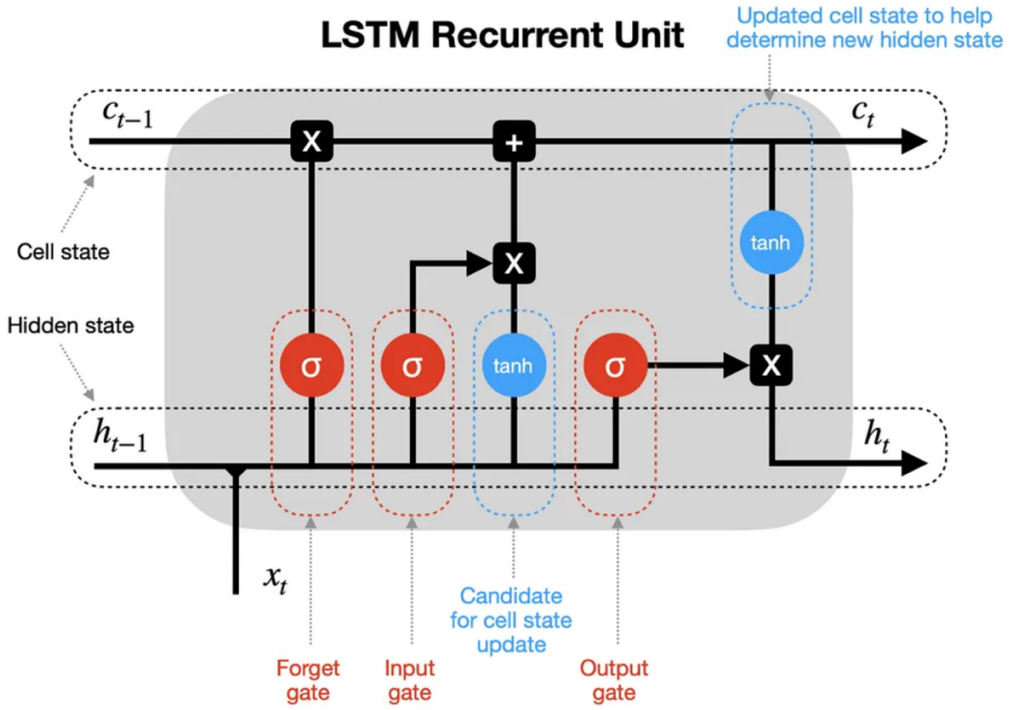

Fig. 4.3. Example of a general LSTM unit, illustrating the input, forget, and output gates along with the corresponding functions that govern their behaviour (Dobilas, 2022).

Delving deeper into the gating mechanism of an LSTM unit (Fig. 4.3): (i) The input gate determines which values from the input should be used to update the memory. A sigmoid function (σ) decides which values to allow through, outputting either 0 or 1, while a tanh function (hyperbolic tangent function) assigns weight to the values that pass through, determining their level of importance within a range of -1 to 1. (ii) The forget gate identifies which information should be discarded from the memory cell. This is governed by a sigmoid function (σ) that considers the previous state (h_{t-1}) and the current input (X_t), producing a value between 0 (to discard) and 1 (to retain) for each element in the previous cell state (C_{t-1}). (iii) The output gate determines the information to be output, based on the input and the memory of the block. A sigmoid function (σ) decides which values to pass through, outputting either 0 or 1, while a hyperbolic tangent function assigns weight to the passed values, determining their importance on a scale from -1 to 1. The output of the tanh function is then multiplied by the result of the sigmoid function (σ) to produce the final output (Dobilas, 2022).

4.2.2.2.1. LSTM application in hydrogeology

LSTM neural networks has become a transformative approach in applied geology, particularly in the geotechnical field of predicting rainfall-induced landslides (Dal Seno, 2024). Moreover, in recent years, LSTM has also emerged as a significant research method in hydrogeology, offering advanced tools to tackle the complexity of groundwater systems (Opoku et al., 2024; Zhang et al., 2024; Zhou et al., 2024). Traditional methods, such as statistical analysis and numerical models, have been instrumental in studying recharge-discharge dynamics and forecasting trends, but they struggle with non-linear relationships and high-dimensional datasets. ML techniques, particularly ANNs, excel in capturing these complexities, enabling more accurate predictions and deeper insights into groundwater behaviour. Indeed, as explained in the Chapter 3 of this thesis, ML has recently been utilised to address diverse hydrogeological challenges. Among these, some ML algorithms have demonstrated significant potential in forecasting short- and medium-term trends in spring discharge (Di Nunno et al., 2021; Gholami and Khaleghi, 2019; Granata et al., 2018), as well as uncovering long-term patterns in flow rate time series data (Secci et al., 2023). With increasing data availability, however, LSTM has emerged as the most prominent among ML algorithms in hydrogeological research, particularly for trend analysis and long-term spring discharge forecasting based on historical flow rate data (Zhang et al., 2024).

In the context of climate change, where the field of spring discharge prediction is becoming a central focus, Long Short-Term Memory (LSTM) neural networks, are increasingly emerging as powerful tools for modelling the complex relationships that govern spring dynamics.

Several studies have demonstrated the effectiveness of LSTM models in capturing the intricate temporal dependencies and partially non-linear behaviours of spring discharge:

Zhang et al. (2024) proposed a hybrid framework that incorporates variable screening, error suppression, hyperparameter optimisation, and decomposition-combination, relying on spring discharge data as input for the LSTM model. The authors' study focused on three karst springs located in Shanxi Province, in northeastern China. Their findings emphasised that hybrid models built solely around the dependent variable (flow rate) can outperform traditional methods based on meteorological data in short-term forecasting of spring discharge.

Similarly, Zhou and Zhang (2023) examined ensemble deep learning models integrating both linear and non-linear components to forecast daily discharge. The authors focused on Barton Spring group, located in Central Texas, USA, which discharge from a karstified carbonate aquifer. Their approach, which combined predictions from LSTM, Gated Recurrent Units (GRU), and One-Dimensional Convolutional Neural Networks (1D-CNN), demonstrated improved predictive accuracy and robust performance in short-term forecasting.

An et al. (2020) expanded the application of LSTM by incorporating time-frequency analysis to simulate spring discharge. The authors employed Singular Spectrum Analysis (SSA) and ensemble Empirical Mode Decomposition (EMD) to extract frequency and trend features. Their study, focused on Niangziguan Spring group, situated in eastern Shanxi Province (China), emphasised the advantages of integrating data pre-processing techniques with LSTM models to capture multi-scale temporal variations, thereby enhancing spring discharge predictions in karst systems characterised by high-frequency flow rate variability.

Song et al. (2022) examined spring discharge mechanism to attempt to predict spatial-temporal behaviours of karst springs, highlighting LSTM’s capability to model multi-hydrogeological processes, including precipitation, surface water runoff, infiltration, and groundwater flow. This study, also conducted on Niangziguan Spring group, which has been heavily impacted over the past 60 years, emphasised the importance of considering future scenarios of anthropogenic impacts when predicting short-term spring discharge.

Zhou et al. (2024) proposed a hybrid self-adaptive deep learning architecture for karst spring forecasting, focusing on Barton Spring group in Central Texas, USA. Their model combined Discrete Wavelet Transform (DWT), WaveNet, and LSTM to capture complex nonlinear patterns in karst systems, incorporating attention mechanisms and residual connections to improve prediction accuracy for short-term forecasts of up to 30 days.

Similarly, Pölz et al. (2024) compared the performance of Transformer and LSTM models in forecasting karst spring discharge using hourly data. The authors focused on three Austrian alpine springs discharging from a highly karstified limestone aquifer. Their results demonstrated that

Transformer models outperform LSTMs for springs with longer response times (ranging from weeks to months), whereas LSTMs are better suited for springs with shorter response times (from hours to days). An insightful contribution from these authors was the incorporation of past discharge itself as an independent variable.

Opoku et al. (2024) demonstrated the effectiveness of LSTM combined with Bayesian hyperparameter optimisation and a laboratory-based physical model simulating the spring discharge process. The study focused on Jinan Spring groups, located in midwestern Shandong Province, Northern China. The authors' findings revealed that integrating multiple techniques, including ML tools such as Bayesian optimisation and physically based approaches, significantly improved the short-term predictive accuracy of LSTM models.

Zhou and Zhang (2022) investigated the influence of deep learning model architecture on karst spring discharge prediction, comparing various machine learning models to determine the most effective for capturing spring dynamics. Focusing on Barton Spring group in Central Texas, USA, the authors evaluated the predictive performance of LSTM, GRU, and simple recurrent neural networks (RNNs). Increasing the input lag time interval for meteorological variables consistently improved discharge prediction accuracy during the test phase.

Meanwhile, Cheng et al. (2021) employed LSTM, Multi-Layer Perceptron (a widely used deep learning algorithm), and Support Vector Machine models to predict fluctuations in karst spring discharge. The authors focused on Longzici Spring, a karst spring located in Shanxi Province, North China. To compare the three ML methods, performance metrics such as mean squared error (MSE), mean absolute error (MAE), and root mean square error (RMSE) were utilised, as is standard practice in the field. The results demonstrated that LSTM proved to be the most effective ML method for accurately simulating and predicting karst spring discharge in the short-term future (ranging from days to weeks).

Together, these studies highlight the transformative potential of LSTM neural networks in capturing the complexity of aquifer system responses to climatic variables, enhancing the understanding of spring discharge processes, and forecasting them in the short term (hours to days) and medium term (weeks to a maximum of three months). By learning intricate temporal patterns and incorporating additional analytical techniques, LSTM models have made significant progress in tackling the challenges of spring flow rate forecasting. However, while LSTM excels at capturing long-term dependencies between variables, none of these studies has addressed long-term forecasting (years to decades), which is essential for water supply authorities to plan large-scale infrastructure and support aqueduct interconnections. The only study employing LSTM to predict a hydrogeological variable in the long-term future (up to 2095), while also incorporating future climatic data derived from RCP scenarios, is that of Secci et al. (2023).

However, this study focuses on hydraulic heads rather than spring discharge. Specifically, the authors investigated an area in the northern Tuscany Region (Italy), encompassing four river basins: Magra, Coastal Basins, Serchio, and part of the Arno.

The following sections of this chapter present a novel application of the LSTM machine learning method for predicting monthly spring discharge in the long-term future.

4.3. Materials and methods

Since the springs analysed in this chapter are the same as those examined in the previous one, their respective geological and hydrogeological settings will not be addressed here.

4.3.1. Sanità and Ermicciolo LSTM models

The data utilised in this chapter are the same as those employed for the multiregression statistical analysis presented in Chapter 3. These include spring discharge, thermo-pluviometric variables, and snowfall data for the catchment of Sanità Spring and Ermicciolo Spring. The methodologies for data collection and normalisation, the reconstruction of snowfall data back to January 1940, and the combination of rainfall and snowfall into Total Liquid Precipitation (TLP) are thoroughly explained in the previous chapter. The focus of this chapter is the application of a deep machine learning approach, specifically the LSTM neural network algorithm, to analyse the relationship between the independent variables and the dependent variable (spring discharge) and explore its significant predictive potential. For the predictions, the analysis will also rely on RCP 4.5 and RCP 8.5 climate projections, incorporating corrections for systematic bias, as used in the previous chapter.

For both case studies, a Python script implementing an LSTM neural network model was developed. The model was trained on one portion of the historical dataset, validated on another, and tested on the remaining portion to evaluate the relationships identified between the variables. Following the conventional percentage split for the three ML phases, 60-70% for training, 25-20% for validation, and 15-10% for testing, the division of the spring flow rate datasets for both springs is as follows:

Sanità Spring. The training phase included data up to December 1990, the validation phase covered data up to December 2010, and the testing phase extended to the end of the historical dataset (January 2024) (Fig. 4.4). For the training phase, the six-month period between December 1980 and May 1981 was excluded due the presence of the anomalous peak discharge induced by the Irpinia earthquake. Sanità Spring typically exhibits its seasonal high flow during summer (June-July, Fig. 3.5); however, in 1980 and 1981, this was observed in winter and spring instead. This anomaly affected the LSTM model's performance, making its exclusion necessary.

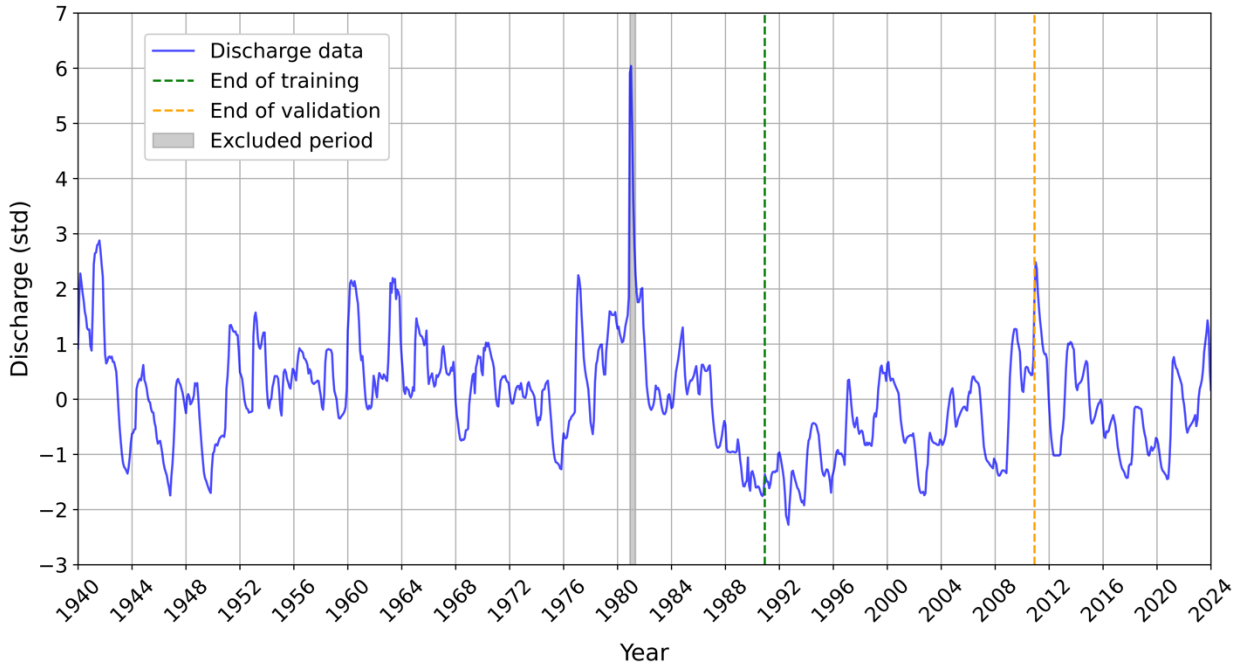

Fig. 4.4. Division of the Sanità Spring standardised discharge data into training, validation, and test phases. The six-month period excluded from the analysis is highlighted by a grey band.

Ermicciolo Spring. The training phase included data up to December 1999, the validation phase extended to June 2013, and the testing phase covered the remaining dataset (Fig. 4.5).

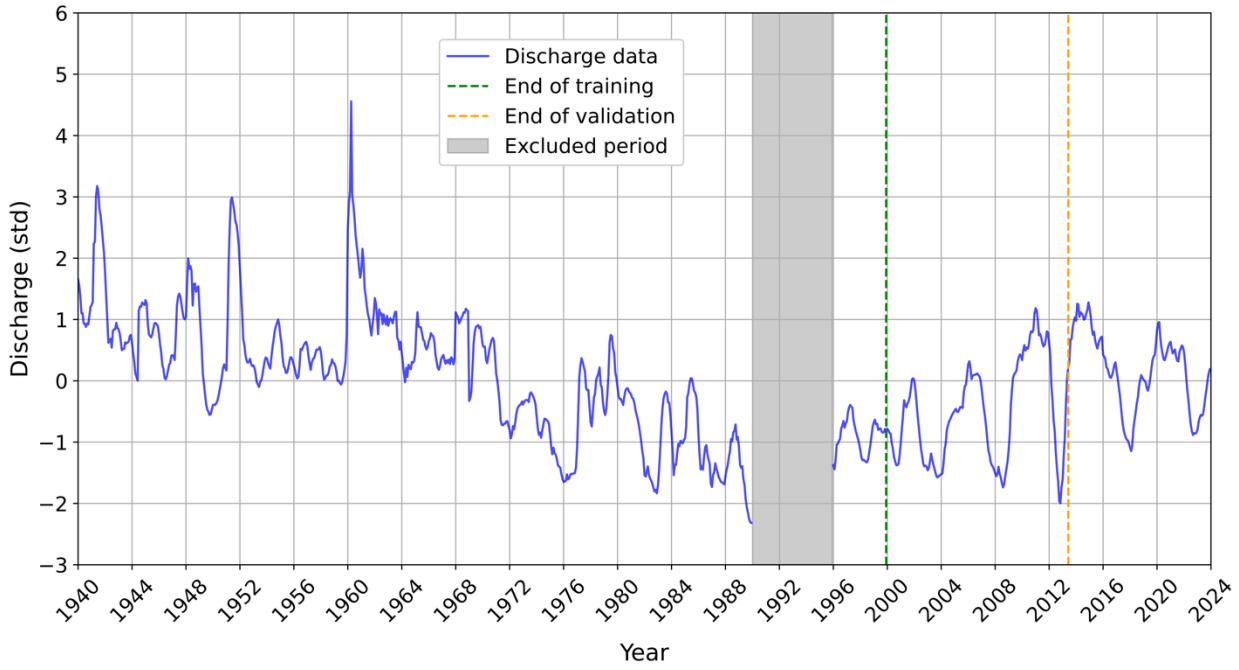

Fig. 4.5. Division of the Ermicciolo Spring standardised discharge data into training, validation, and test phases. The acquisition gap period is highlighted by a grey band.

The training phase excluded the gap in the discharge dataset from January 1990 to December 1995. Initially, the Ermicciolo model was trained using the same time frame as Sanità, excluding

1990 due to the gap. However, improved test performance was observed when the training phase included some post-gap data. This improvement was attributed to the cyclic drought patterns, spanning three to five years, which became more evident after January 1996. Extending the training phase enabled the model to better recognise and learn these cycles.

4.3.1.1. Determination of hyperparameters and lag time

After each iteration of both LSTM models, performance metrics such as MSE, MAE, and R^2 were thoroughly assessed by comparing predicted and observed values during the test phase. Key hyperparameters, including the number of epochs, batch size, LSTM units in the recurrent layer, and dense layer configuration, were also adjusted. Additionally, loss curves for the training and validation phases were monitored to evaluate performance. A brief description of these parameters is provided below for clearer understanding:

- An *epoch* represents one complete pass through the entire training dataset. Increasing the number of epochs can improve the LSTM model learning but may lead to overfitting if excessive. Overfitting occurs when a machine learning model learns the noise or random fluctuations in the training data instead of the underlying patterns, resulting in excellent performance on the training set but poor generalisation to unseen data (Goodfellow et al., 2016).

- The *batch size* defines the number of training examples processed at once. Smaller batch sizes often result in smoother convergence but may increase computational time (Bengio, 2012).

- The *LSTM units* are the number of memory cells in the LSTM layer. Higher numbers allow the model to capture more complex patterns but can increase the risk of overfitting and computational cost (Hochreiter and Schmidhuber, 1997).

- The *dense layers* are fully connected layers that aggregate learned features from preceding layers. The configuration of dense layers influences the model's ability to generalise its predictions (Hastie et al., 2009).

- The *loss curve* is a graphical representation of how the model's loss (error in terms of accuracy or predictive capability of the model) evolves during the training and validation phases. It provides insights into the model's learning process by showing whether the loss is decreasing, plateauing, or diverging. A steadily decreasing training loss with a stable or decreasing validation loss typically indicates effective learning. Conversely, a widening gap between training and validation loss may signal overfitting (Goodfellow et al., 2016).

The selection of the hyperparameters is crucial for assessing and improving model performance. As in the present work, this is typically achieved through trial and error, accompanied by the monitoring of metrics such as loss curves and MSE.

For both studies, the analysis began by examining the relationship between the meteorological independent variables and discharge. Monthly lags were applied exclusively to AirT and TLP variables to assess how their values in preceding months influence the current month's spring discharge. Various lag lengths were tested to determine the optimal value for the LSTM models. Unlike multivariate analysis, which considers only a single preceding month (corresponding to the lag) with the highest correlation among variables, the LSTM approach enables the analysis of temporal dependencies across all preceding months up to the maximum lag value.

The initial trials, implemented with diverse combinations of ML parameters and lags, produced unrealistic outputs, failing to capture the seasonal cycles characteristic of discharge patterns. This issue was further confirmed by loss curves that consistently displayed significant divergence between the training and validation phases (Fig. 4.6).

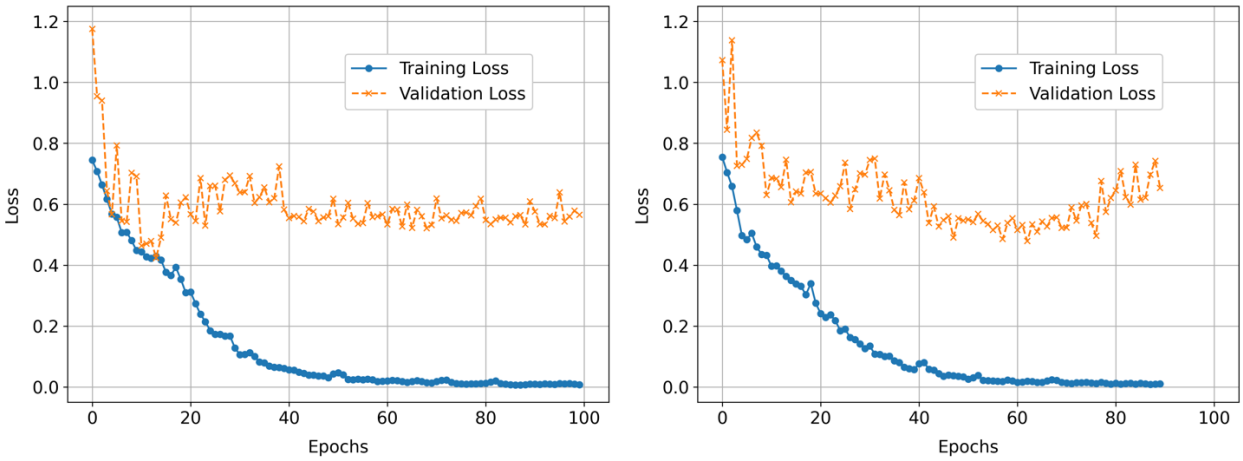

Fig. 4.6. Loss curves for two test cases conducted with the Sanità LSTM model (on the left) and the Ermicciolo LSTM model (on the right), where 100 and 90 epochs were used, respectively.

The specific test cases shown in Fig. 4.6 demonstrate poor generalisation capabilities by the models during training and validation. Indeed, in both graphs, while the training loss consistently decreases, stabilising at a low value, the validation loss plateaus or even increases in the case of the Ermicciolo model, also exhibiting significant oscillations. This indicates that the LSTM models continue to improve on the training data but fail to generalise to the validation set.

To address this issue, spring discharge from previous months was introduced as an additional independent variable, using the same lag as the two meteorological variables. This strategy, already employed by some authors (e.g., Pölz et al., 2024; Zhang et al., 2024), led to significant improvements: the loss curves showed better convergence (Fig. 4.7), and the predicted discharge during the test phase aligned closely with observed values (Fig. 4.8). Concerning the predicted spring discharge, it can be observed that in both cases, the respective standardised series starts with a certain delay from the vertical line marking the end of the validation. This is due to the lag time set in the models. During the test phase, the LSTM model requires the discharge values from

previous months (the number of which depends on the lag) to predict the discharge. For this reason, discharge predictions are not available for the initial months of the test phase, as the model cannot generate values until it has access to the specified number of preceding months determined by the lag. For instance, if the lag is 12, the LSTM model will begin predicting discharge from the thirteenth month of the test dataset.

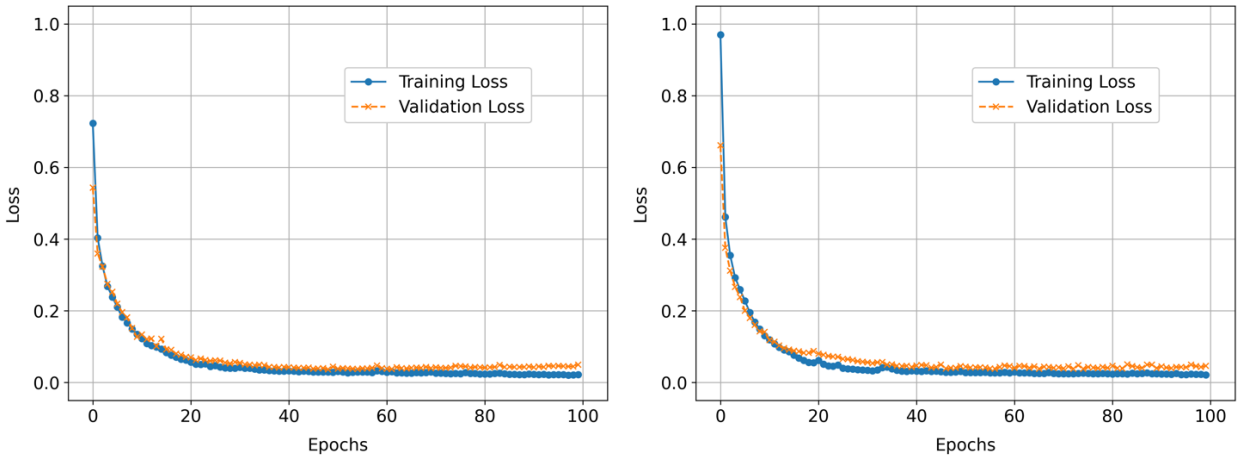

Fig. 4.7. Loss curves from the two best-performing LSTM models, with spring discharge included as an independent variable. Results for Sanità Spring are on the left, and for Ermicciolo Spring on the right.

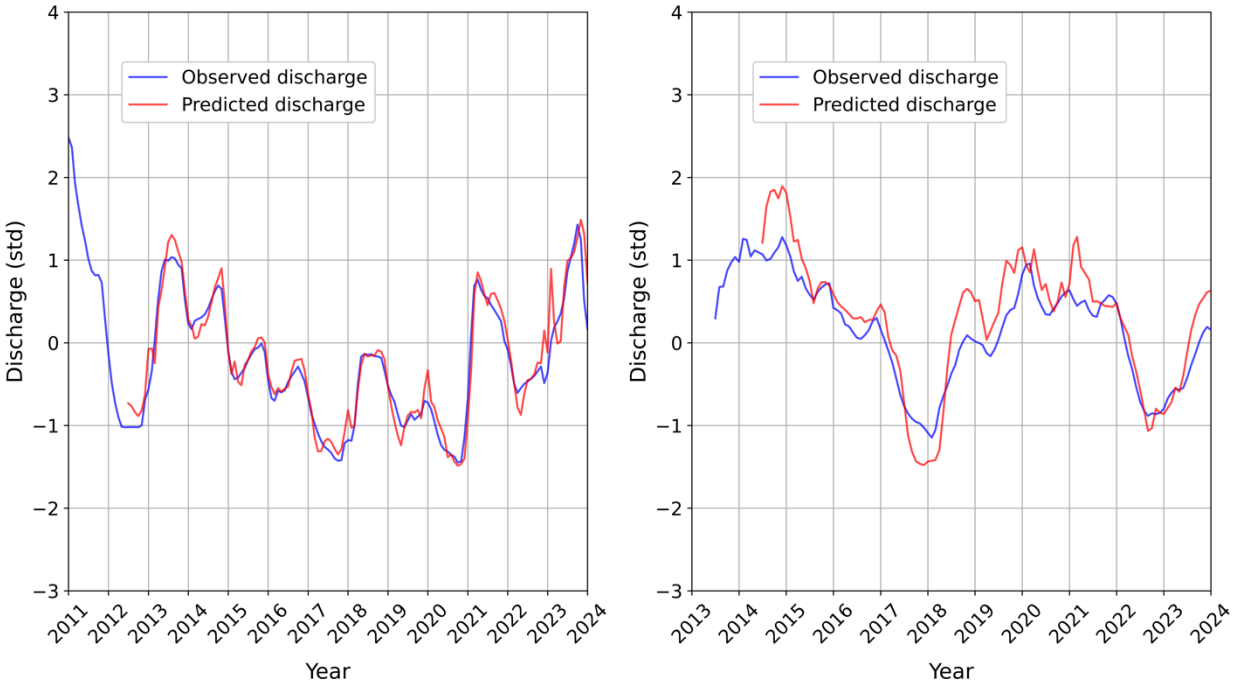

Fig. 4.8. Observed and predicted standardised spring discharge during the test phase from the two best-performing LSTM models, with discharge included as an independent variable. The results for Sanità Spring are shown on the left, while those for Ermicciolo Spring are displayed on the right.

The lag values that provided the best results were 18 months for Sanità Spring and 12 months for Ermicciolo Spring. By including discharge as an additional independent input variable, the

model was able to capture extended temporal dependencies, recognising that seasonal peaks and lows in spring discharge occur almost consistently every 11 to 13 months in both case studies; for Sanità Spring, given the larger extent of its catchment and aquifer, these patterns occasionally extend to as much as 18 months.

The best-performing models, identified after extensive experimentation with various parameter combinations, achieved an R^2 greater than 90% between predicted and observed values during the test phase, along with very low MSE and MAE values, indicating the robustness of the models. The hyperparameters that produced the optimised models are as follows:
For the Sanità Spring LSTM model: 100 epochs, although learning effectively concluded after approximately 70 epochs, as evident from the divergence between the validation loss and the training loss (Fig. 4.7); batch size of 32; 96 LSTM units in total (64 in the first LSTM layer and 32 in the second LSTM layer); and two dense layers (with 32 nodes in the first and 1 node in the second, used for the output data).
For the Ermicciolo Spring LSTM model: 100 epochs, although the learning process concluded after roughly 80 epochs, as observed from the divergence between the two loss curves (Fig. 4.7); batch size of 64; 96 LSTM units in total (64 in the first LSTM layer and 32 in the second LSTM layer), identical to the Sanità model; and two dense layers (with 32 nodes in the first and 1 node, for the output data, in the second), again mirroring the configuration of the Sanità model.

The selection of 100 epochs reflects an effort to provide sufficient training time for the models to converge without risking overfitting. Fig. 4.7 suggests that, while the two models were trained for 100 epochs, an early stopping mechanism could be introduced to truncate the training at the optimal point, further validating the suitability of the chosen epoch count. However, given the model's fast runtime (never exceeding 5 minutes), this was not deemed necessary.
The difference in batch size between the two LSTM models can be attributed to the varying characteristics of the datasets and the computational requirements associated with their respective patterns. Smaller batch sizes, such as 32, often facilitate more detailed updates to the model weights, which is beneficial for datasets with higher variability or more complex temporal dynamics, as is the case for a karst spring like Sanità. Conversely, the larger batch size of 64 for the Ermicciolo model enables more stable gradient updates, which can be advantageous for datasets with smoother temporal patterns or less variability.
The use of 96 LSTM units in total, distributed across two layers, aligns well with the complexity of the temporal dependencies inherent in spring discharging dynamics. The larger number of units in the first layer (64) allows the models to capture the broad temporal patterns and long-term dependencies, while the reduced number of units in the second layer (32) aids in refining and consolidating these representations for the test phase prediction task. This configuration

strikes a balance between model complexity and computational efficiency, avoiding overfitting while maintaining the capacity to learn nuanced patterns in the data.
The inclusion of two dense layers in both models represents a standard yet effective architecture for time series future assessment tasks. This configuration ensures that the model can extract meaningful features from the temporal patterns before producing the final test phase prediction, while maintaining a level of simplicity that avoids unnecessary computational overhead.

Overall, the selected hyperparameters were found to align well with the features of the analysed datasets and the aims of the study. The observed differences between the two LSTM models, particularly in batch size, underscore the importance of tailoring hyperparameter choices to the specific dynamics of each case study, reinforcing the robustness and adaptability of the LSTM neural network architecture.

4.3.1.2. Iterative forecasting of future monthly discharge

Indeed, with regard to discharge forecasting, the test phase represents only one part of the work commonly undertaken with ML methods, serving as a necessary step to verify the model's ability to capture temporal relationships and dependencies between variables. The objective of this study in terms of prediction, however, extends much further, aiming to estimate monthly discharge values in the long-term future by leveraging the seasonal and multi-year temporal relationships identified across the various datasets using the LSTM models.

After developing the two best-performing LSTM models, long-term flow rate forecasting was carried out using future TLP and AirT variables derived from the RCP 4.5 and RCP 8.5 climate projections as meteorological inputs. For discharge as an input variable, an iterative approach was employed, given that future spring discharge (the target variable) was obviously unavailable in the datasets. Leveraging the relationships learned by the LSTM models, future discharge was calculated step-by-step (starting from the most recent historical discharge data), with each predicted value being added iteratively to the projected dataset.

This approach allowed the model to incorporate relationships derived from historical data during the training and validation phases and apply them to future meteorological scenarios and iteratively predicted discharge, thereby producing monthly future discharge values. Naturally, once a temporal interval equivalent to the lag time set in the two LSTM models had elapsed, each model began predicting future discharge using previously predicted discharge values, which, while also future, had already been generated in earlier iterations.

4.4. Results

The two best-performing LSTM models generated future discharge outputs up to 2070 (Fig. 4.9 and Fig. 4.10) that accurately reflected overall trend and seasonal cycles consistent with historical data. Unlike Figs. 4.4 and 4.5, which display data from January 1940 to January 2024, Figs. 4.9 and 4.10 present the complete historical discharge datasets (beginning in 1920 for Sanità Spring and 1939 for Ermicciolo Spring) alongside future projections for both scenarios. The starting year of 1940 aligns with the availability of reconstructed snowfall data, as detailed in Chapter 3, and indeed also matches the starting date of the multivariate statistical analysis. Another key difference between Figs. 4.4 - 4.5 and Figs. 4.9 - 4.10 is that the former present standardised discharge data, whereas the latter display denormalised data, obtained using the same monthly means and standard deviations applied during the normalisation process.

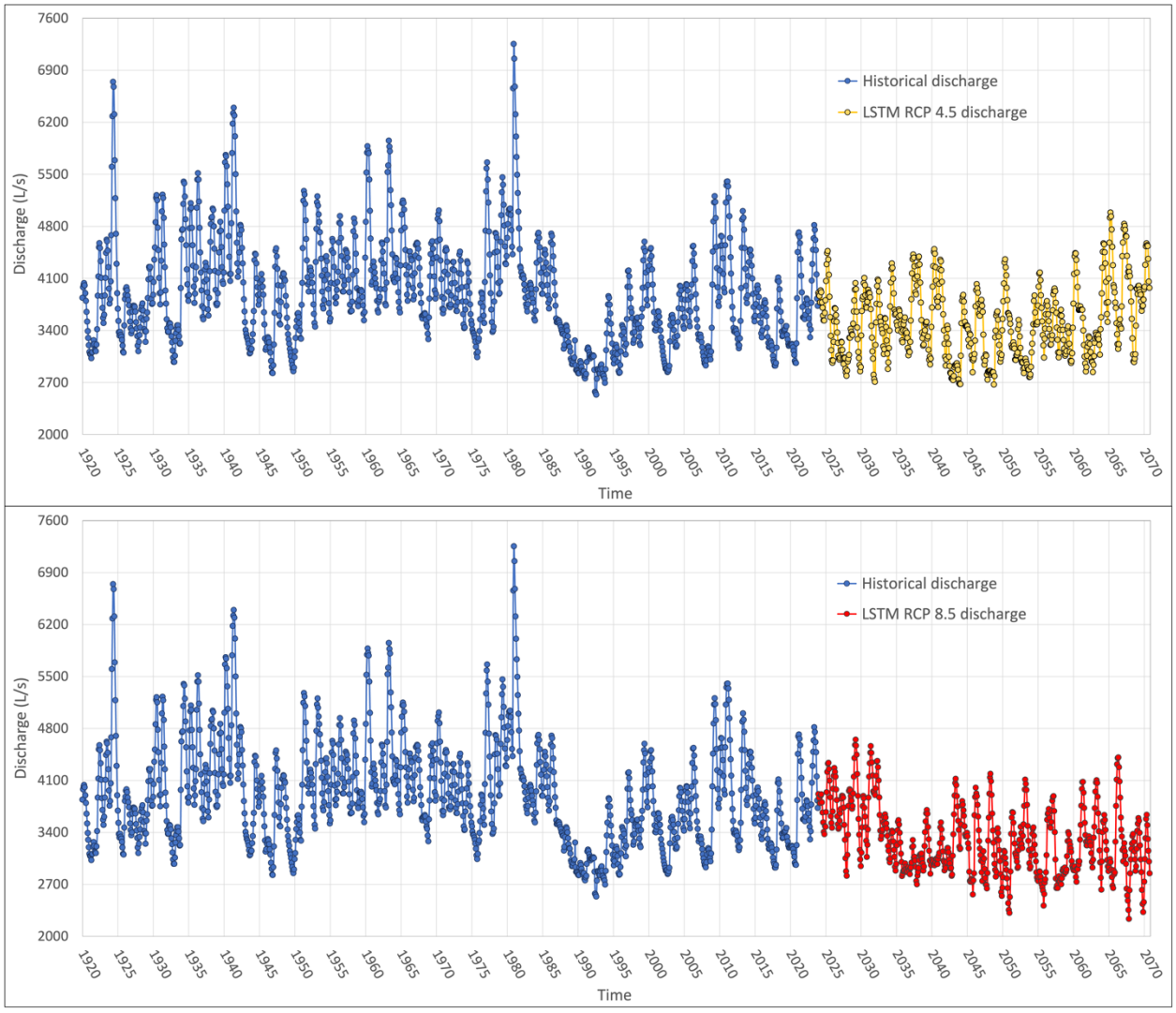

Fig. 4.9. Historical mean monthly discharge of Sanità Spring, followed by predicted mean monthly discharge under the RCP 4.5 scenario (top) and the RCP 8.5 scenario (bottom).

The results obtained for Sanità Spring under the RCP 4.5 scenario show a mean monthly discharge ranging from approximately 4980 to 2670 L/s, whereas under the more severe RCP 8.5 scenario, the mean monthly discharge ranges from about 4650 to 2230 L/s, which is considerably lower. A closer examination of Fig. 4.9 also reveals less variability in the predicted data, with both future series appearing slightly more "flattened" compared to the historical data, although the natural seasonality of peaks and troughs is preserved. Another relevant observation from the predicted historical series is that, under the RCP 4.5 scenario, prolonged intervals of low spring discharge, characteristic of extended recession periods, are absent. Notably, from 2060 onwards, an upward trend in the spring's discharge is also observed. In contrast, the more severe RCP 8.5 scenario reveals a prolonged low-flow period between 2032 and 2043, closely resembling the historical one observed between 1987 and 1997.

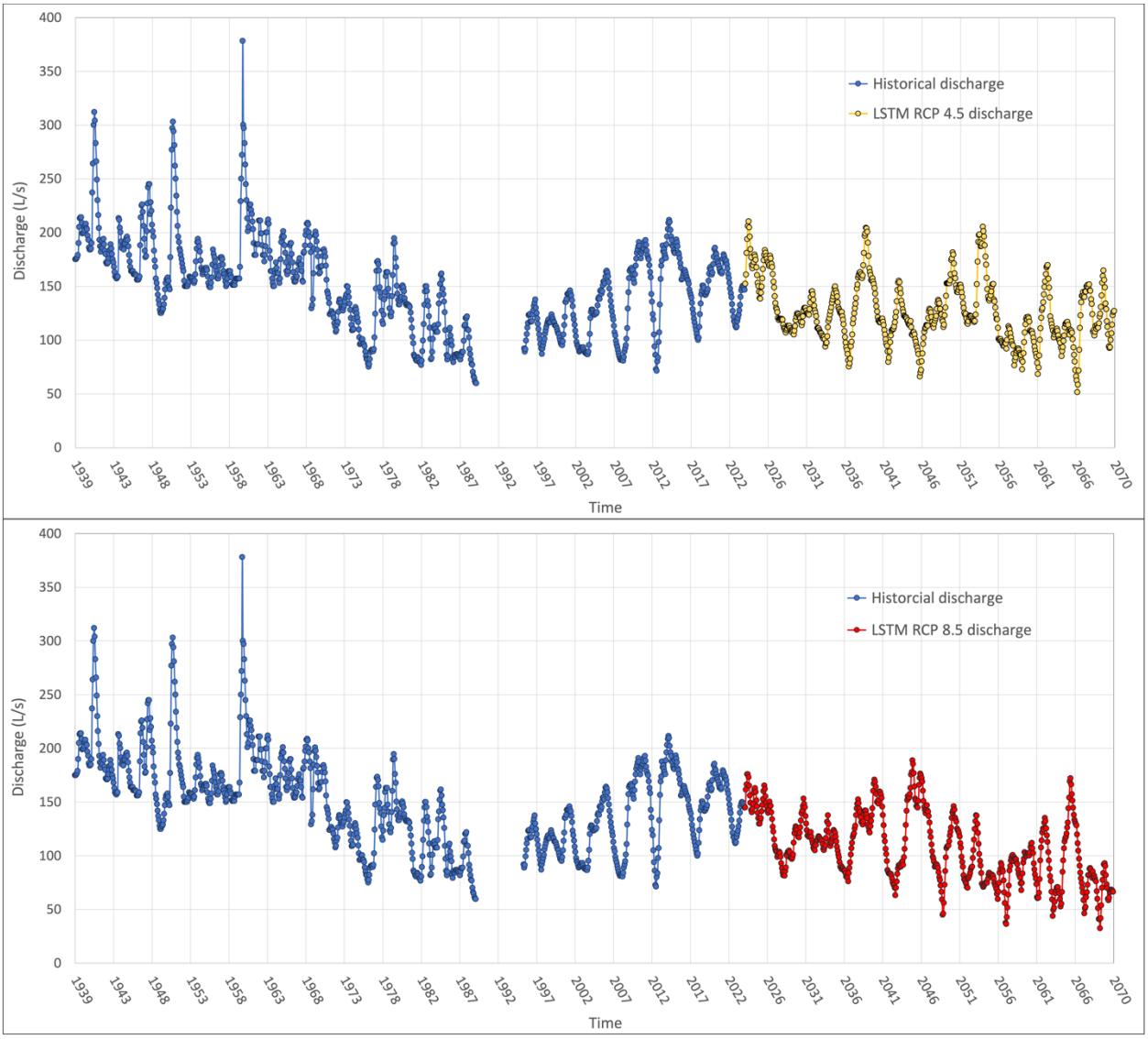

Fig. 4.10. Historical mean monthly discharge of Ermicciolo Spring, followed by predicted mean monthly discharge under the RCP 4.5 scenario (top) and the RCP 8.5 scenario (bottom).

The results for Ermicciolo Spring under the RCP 4.5 scenario indicate a mean monthly discharge ranging from roughly 210 to 51 L/s. In the more severe RCP 8.5 scenario, the mean monthly discharge ranges from about 189 to 33 L/s, which, as in the previous case, is considerably lower. Fig. 4.10 also shows that the model successfully captured triennial to quinquennial drought cycles, particularly evident in the historical data from 1996 onwards. A concerning observation regarding the long-term future is that, in both scenarios, from approximately 2050 onwards, these droughts begin to intensify both temporally (occurring more frequently) and in absolute terms (with increasingly lower discharge levels). Compared to the previous case, both scenarios exhibit a further declining trend in spring flow rate, especially under the RCP 8.5 scenario, where the predicted spring discharge frequently falls below 50 L/s.

To enable a comparison between the multi-decadal discharge derived from the Multivariate Statistical Analysis (MSA) presented in the previous chapter, two graphs were created: one for Sanità Spring (Fig. 4.11) and the other for Ermicciolo Spring (Fig. 4.12). These graphs plot, in addition to the historical data, the projected values obtained from both the MSA and LSTM methods. To avoid visual confusion, the spring discharge was plotted as a mean multi-decadal hydrograph without uncertainty bands, as their inclusion would cause numerous overlaps, making the graphs difficult to interpret. The multi-decadal hydrographs for the LSTM model results were constructed using only the 2040-2070 period, excluding the earlier portion of the predicted series (February 2024 to December 2039).

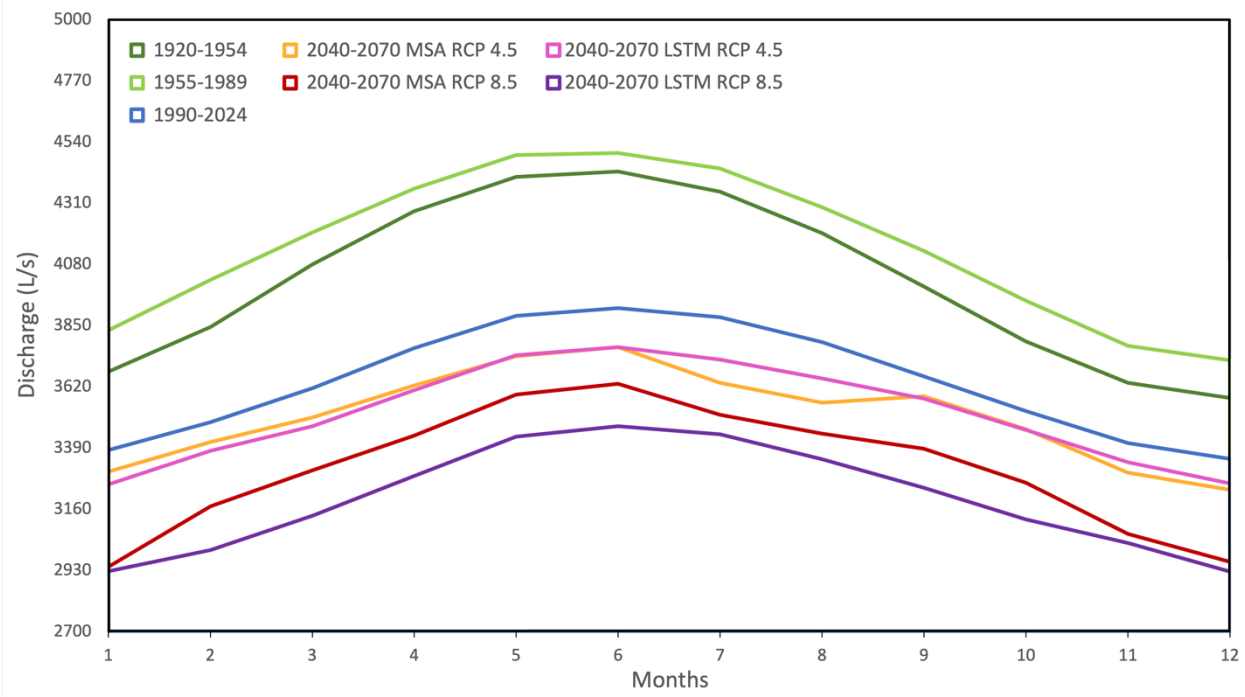

Fig. 4.11. Sanità Spring multi-decadal hydrographs, plotted without uncertainty bands. Three hydrographs depict historical data, while the remaining four illustrate future spring discharge projections derived from both the MSA and LSTM models.

Since the values in Fig. 4.11 are plotted without uncertainty bands, the maximum and minimum spring discharge values for the various multi-decadal periods (Tab. 4.1) are slightly different from those previously described in Section 3.7.4. The oldest historical hydrograph (1920-1954) shows an average flow rate ranging from approximately 4,430 to 3,580 L/s, the intermediate historical hydrograph (1955-1989) spans a range of 4,500 to 3,720 L/s, while the most recent historical hydrograph (1990-2024) exhibits an average spring discharge ranging from 3,920 to 3,350 L/s. Under the RCP 4.5 scenario of the MSA model, an average discharge ranging from 3,770 to 3,230 L/s is observed, whereas in the more severe RCP 8.5 scenario, the average spring discharge varies from 3,630 to 2,940 L/s. For the Sanità LSTM model, the RCP 4.5 scenario produces a flow rate ranging from roughly 3,770 to 3,250 L/s, while the RCP 8.5 scenario yields an average spring discharge covering a range of 3,470 to 2,920 L/s.

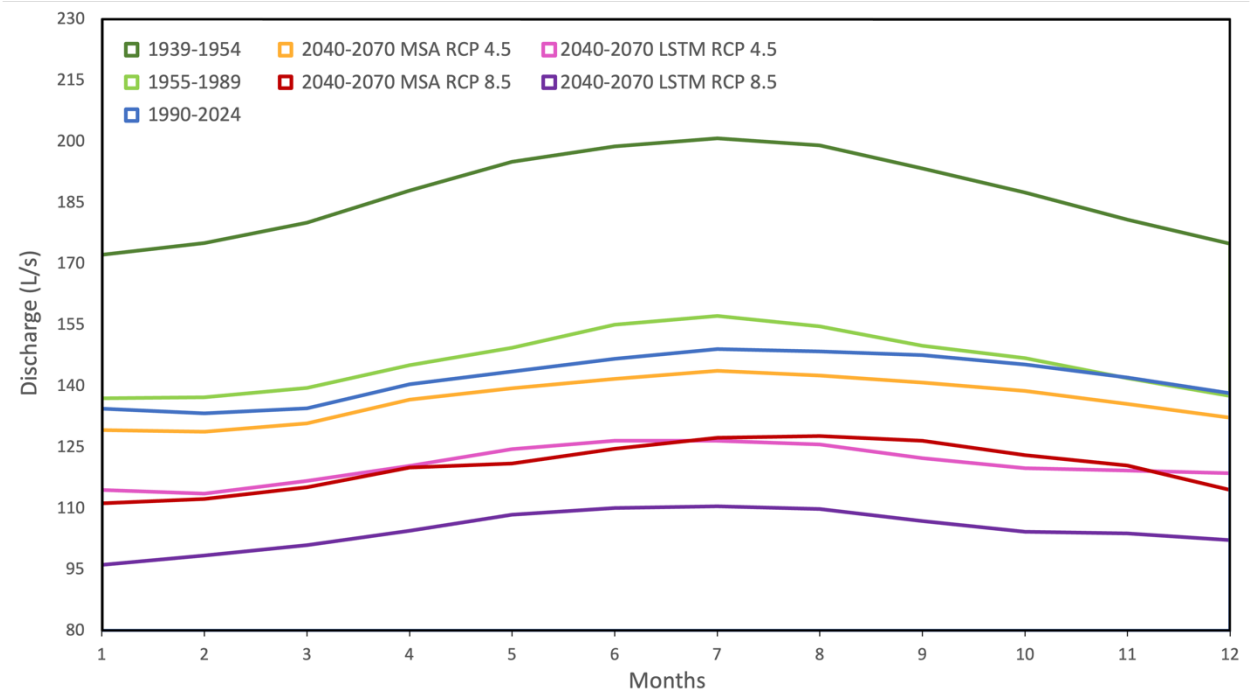

Fig. 4.12. Ermicciolo Spring multi-decadal hydrographs, plotted without uncertainty bands. Three hydrographs depict historical data, while the remaining four illustrate future spring discharge projections derived from both the MSA and LSTM models.

Under the RCP 4.5 scenario, the two methods produce very similar results (with a percentage deviation of less than 5%), with notable differences observed only during the summer months of July and August. In these months, the MSA method shows a slight drop in discharge, followed by a recovery in September, whereas the LSTM method does not exhibit this drop, as the discharge tends to decrease steadily until December, the month representing the seasonal low flow.

Under the RCP 8.5 scenario, although the discharge values predicted by the LSTM method in January and December are similar to those predicted by the MSA method, the generated

hydrographs display notable differences. In particular, the discharge predicted by the LSTM method is visibly lower than that obtained with the MSA method.

Similarly, the maximum and minimum spring discharge values for the multi-decadal hydrographs shown in Fig. 4.12 are reported below (and in Tab. 4.1). The oldest historical hydrograph (1939-1954) spans a range of 201 to 172 L/s, the intermediate historical hydrograph (1955-1989) shows an average flow rate ranging from approximately 157 to 137 L/s, and the most recent historical hydrograph (1990-2024) exhibits an average spring discharge ranging from 149 to 133 L/s. Under the RCP 4.5 scenario of the MSA model, an average discharge ranging from 144 to 129 L/s is observed, whereas in the more severe RCP 8.5 scenario, the average spring discharge varies from 128 to 111 L/s. For the Ermicciolo LSTM model, the RCP 4.5 scenario produces a flow rate ranging from approximately 127 to 114 L/s, while the RCP 8.5 scenario yields an average spring discharge covering a range of 111 to 96 L/s.

Under the RCP 4.5 scenario, the results produced by the two methods differ significantly. A noteworthy observation is that the hydrograph generated by the LSTM method under this scenario closely resembles that of the MSA method under the RCP 8.5 scenario, with a deviation of less than 3%. Under the RCP 8.5 scenario, the hydrographs produced by the two methods are also significantly different, with the discharge predicted by the LSTM method being considerably more severe than that predicted by the MSA method. As with Sanità Spring, the results of the LSTM under the most severe scenario show a greater reduction in discharge compared to those of the other method. However, in this case, the difference is even more pronounced, with a consistent discharge gap of approximately 13% between the two hydrographs.

4.5. Discussion and conclusive remarks

The analysis conducted, which aimed to understand the relationships between recharge-related variables and the discharge of two major springs using a machine learning method employed in Python, and to subsequently assess these relationships into the long-term future in order to predict their discharge, has confirmed for the two study areas the critical groundwater resource projections presented in the paper discussed in the previous chapter.

The ML method employed in this chapter was the Long Short-Term Memory (LSTM) neural network, which has recently been gaining prominence for modelling the complex relationships governing hydrogeological processes. During an initial exploratory phase, it became evident that incorporating discharge itself as an input variable was the optimal approach for developing two well-performing LSTM models. This approach is justified by the fact that the state of the aquifer reservoir, which directly influences the spring discharge in each month, is logically dependent on

its state in the preceding months. For instance, during a drought period, when the reservoir has significantly depleted, its replenishment does not solely depend on the amount of rainfall. This is because a deeper water table and a thicker unsaturated zone hinder efficient recharge, altering the dynamics of the system. The reservoir's state in each month indeed exerts a substantial influence on the discharge in the following months. The two optimised models, developed after testing various combinations of ML hyperparameters and lag times in the input dataset, achieved highly positive performance metrics. The lag times that provided the best results were 18 months for Sanità Spring and 12 months for Ermicciolo Spring, which is consistent with the seasonal, annual, and multi-annual cycles observed in the input parameters (particularly discharge itself) and their relationship with the dependent variable. Each lag, in fact, enables the model to analyse the seasonal and multi-year temporal dependencies between the dependent variable and all input variables across the preceding months, up to the maximum lag value.

Using the two best-performing LSTM models, it was possible to obtain long-term future discharge values by applying the identified relationships and temporal dependencies to the meteorological scenarios already adopted in Chapter 3, as well as to the discharge itself, which was iteratively predicted as part of a time-dependent autocorrelation process. This ML method not only allows for the estimation of spring hydrographs over a multi-decadal time span, depicting monthly discharge fluctuations at 2040-2070, as was already achieved with multiregression analysis, but also enables the estimation of monthly discharge expressed in absolute terms, rather than solely multi-decadal trends. Obviously, as the future discharge is calculated iteratively and used as an input variable for subsequent predictions, significant errors in the early stages of prediction could propagate over time, resulting in not fully reliable monthly absolute values. For this reason, accurate training, validation, and testing phases, conducted on extended datasets, are essential for constructing consistent LSTM models for long-term predictions.

Referring specifically to the results obtained with the LSTM method (Tab. 4.1): **under the RCP 4.5 scenario**, a decrease in discharge is observed for both springs during the 2040-2070 period compared to the most recent historical one (1990-2024). The estimated percentage decrease in flow rate between these two periods is 3.3% at Sanità Spring (3.5% with the MSA method) and 15.0% at Ermicciolo Spring (3.7% with MSA), corresponding to a reduction in discharge of 121 L/s (129 L/s with MSA) and 21 L/s (5 L/s with MSA), respectively. **Under the** more severe **RCP 8.5 scenario**, an even more pronounced and significant decrease is observed between the same multi-decadal periods. The estimated percentage decrease in flow rate between the 1990-2024 period and the 2040-2070 one is 12.1% at Sanità Spring (9.1% with the MSA method) and 26.3% at Ermicciolo Spring (15.2% with MSA), corresponding to a reduction in discharge of 442 L/s (329 L/s with MSA) and 37 L/s (22 L/s with MSA), respectively.

					Percentage declines in multi-decadal mean discharge (%)		
	Period (P)	Max L/s (P)	Min L/s (P)	Means L/s (P)	Rel. to 1st historical P	Rel. to 2nd historical P	Rel. to 3rd historical P
Sanità Spring	1920-1954	4428,0	3577,9	4022,0	-	-	-
	1955-1989	4497,8	3719,5	4142,1	-3,0	-	-
	1990-2024	3915,6	3349,0	3638,4	9,5	12,2	-
	MSA RCP 4.5	3768,8	3233,0	3509,5	12,7	15,3	3,5
	MSA RCP 8.5	3631,2	2943,2	3309,1	17,7	20,1	9,1
	LSTM RCP 4.5	3768,7	3252,6	3517,9	12,5	15,1	3,3
	LSTM RCP 8.5	3471,1	2924,7	3196,8	20,5	22,8	12,1
Ermicciolo Spring	1939-1954	200,8	172,2	187,1	-	-	-
	1955-1989	157,2	137,0	146,0	22,0	-	-
	1990-2024	149,0	133,3	142,0	24,1	2,7	-
	MSA RCP 4.5	143,7	128,8	136,7	26,9	6,3	3,7
	MSA RCP 8.5	127,7	111,3	120,3	35,7	17,6	15,2
	LSTM RCP 4.5	126,6	113,6	120,7	35,5	17,3	15,0
	LSTM RCP 8.5	110,5	96,1	104,7	44,1	28,3	26,3

2040-70

2040-70

Tab. 4.1. Maximum, minimum, and mean values for each multi-decadal hydrograph of Sanità Spring (Fig. 4.11) and Ermicciolo Spring (Fig. 4.12), including percentage declines in the multi-decadal mean discharge obtained using the two analytical methods (MSA and LSTM) under both future scenarios (RCPs 4.5 and 8.5) compared to all three historical multi-decadal periods.

The results obtained with the LSTM approach for Sanità Spring are consistent with those derived from the multivariate statistical approach. For Ermicciolo Spring, however, the LSTM method predicts a considerably greater reduction in spring discharge compared to the MSA method, approximately 2.5 times more severe. This may be attributed to the more pronounced and marked cyclicity in the historical discharge variations of Ermicciolo Spring compared to Sanità Spring, which are more challenging to capture using multivariate linear regression than with a machine learning method. Additionally, the six-year gap in Ermicciolo Spring's discharge dataset likely influences the MSA analysis but is less impactful on the LSTM method, which can mitigate this issue by capturing relationships between variables with longer and simultaneous lags over multiple months. For these reasons, concerning the discrepancy between MSA and LSTM results for Ermicciolo Spring, the findings obtained using the LSTM method are considered more reliable. In any case, there are clear indications to suggest that future groundwater shortages will pose significant challenges to water supply systems. For this reason, obtaining long-term discharge projections is crucial to alert water utility agencies and enable them to prepare in advance to implement proper adaptation measures.

4.6. References

An, L., Hao, Y., Yeh, T.-C.J., Liu, Y., Liu, W., Zhang, B., 2020. Simulation of karst spring discharge using a combination of time–frequency analysis methods and long short-term memory neural networks Journal of Hydrology, 589, 125320.

Arthur, D., Vassilvitskii, S., 2007. k-means++: The advantages of careful seeding. Proceedings of the Eighteenth Annual ACM-SIAM Symposium on Discrete Algorithms, 1027-1035.

Ball, N.M., Brunner, R.J., 2010. Data mining and machine learning in astronomy. International Journal of Modern Physics D, 19(07), 1049-1106.

Ben-Hur, A., Ong, C.S., Sonnenburg, S., Schölkopf, B., Rätsch, G., 2008. Support vector machines and kernels for computational biology. PLoS Computational Biology, 4(10), e1000173.

Bengio, Y., Simard, P., Frasconi, P., 1994. Learning Long-Term Dependencies with Gradient Descent is Difficult. IEEE Transactions on Neural Networks, 5(2), 157-166.

Bengio, Y., 2012. Practical recommendations for gradient-based training of deep architectures. In: Montavon, G., Orr, G.B., Müller, K.R. (Eds.), Neural Networks: Tricks of the Trade, 437-478. Springer, Berlin, Germany.

Bhowmick, A., Hazarika, S.M., 2018. Machine Learning for E-mail Spam Filtering: Review, Techniques and Trends.

Bishop, C.M., 2006. Pattern Recognition and Machine Learning. Springer.

Breiman, L., 2001. Random forests. Machine Learning, 45(1), 5-32.

Breiman, L., Friedman, J., Stone, C.J., Olshen, R.A., 1984. Classification and regression trees. CRC press.

Brynjolfsson, E., Mcafee, A., 2017. The Business of Artificial Intelligence. Harvard Business Review, 7, 3-11.

Cheng, S., Qiao, X., Shi, Y., Wang, D., 2021. Machine learning for predicting discharge fluctuation of a karst spring in North China. Acta Geophysica, 69(1), 257-270.

Cho, K., van Merrienboer, B., Gulcehre, C., Bahdanau, D., Bougares, F., Schwenk, H., Bengio, Y., 2014. Learning phrase representations using RNN encoder-decoder for statistical machine translation. Proceedings of the 2014 Conference on Empirical Methods in Natural Language Processing (EMNLP).

Cortes, C., Vapnik, V., 1995. Support-vector networks. Machine Learning, 20(3), 273-297.

Cybenko, G., 1989. Approximation by superpositions of a sigmoidal function. Mathematics of Control, Signals and Systems, 2(4), 303-314.

Dal Seno, N., 2024. Application of machine learning methods for landslide risk mitigation. PhD thesis, 37th PhD cycle, Alma Mater Studiorum - University of Bologna.

Di Nunno, F., Granata, F., Gargano, R., de Marinis, G., 2021. Prediction of spring flows using nonlinear autoregressive exogenous (NARX) neural network models. Environmental Monitoring and Assessment, 193(6), 350.

Dobilas, S., 2022. LSTM Recurrent Neural Networks - How to Teach a Network to Remember the Past. Published by the user in "Towards Data Science". https://towardsdatascience.com/lstm-recurrent-neural-networks-how-to-teach-a-network-to-remember-the-past-55e54c2ff22e. Medium, Human, stories & ideas. URL (accessed 11.26.24).

Draper, N.R., Smith, H., 1998. Applied Regression Analysis (3rd ed.). John Wiley & Sons.

El Ansari, R., El Bouhadioui, M., Aboutafail, M.O., Mejjad, N., Jamil, H., Jamal, E., Rissouni, Y., Zouiten, M., Boutracheh, H., Moumen, A., 2023. A review of Machine learning models and parameters for groundwater issues. ACM International Conference Proceeding Series, 54.

Elman, J.L., 1990. Finding structure in time. Cognitive Science, 14(2), 179-211.

Freund, Y., Schapire, R.E., 1997. A decision-theoretic generalization of on-line learning and an application to boosting. Journal of Computer and System Sciences, 55(1), 119-139.

Gebru, T., Morgenstern, J., Vecchione, B., Vaughan, J.W., Wallach, H., Daumé III, H., Crawford, K., 2018. Datasheets for datasets.

Gholami, V., Khaleghi, M.R., 2019. A comparative study of the performance of artificial neural network and multivariate regression in simulating springs discharge in the Caspian Southern Watersheds, Iran. Applied Water Science, 9(1), 9.

Goodfellow, I., Bengio, Y., Courville, A., 2016. Deep Learning. MIT Press.

GoPenAI, 2023. Decision Tree Algorithm - What are Decision Trees. Written by the user: "Abdul4code". https://blog.gopenai.com/decision-tree-algorithm-484ec33387f9. Medium, Human, stories & ideas. URL (accessed 11.24.24).

Granata, F., Saroli, M., De Marinis, G., Gargano, R., 2018. Machine learning models for spring discharge forecasting. Geofluids, 2018, 8328167.

Graves, A., 2012. Supervised Sequence Labelling with Recurrent Neural Networks. Springer.

Hartigan, J.A., Wong, M.A., 1979. Algorithm AS 136: A K-Means Clustering Algorithm. Journal of the Royal Statistical Society. Series C (Applied Statistics), 28(1), 100-108.

Hastie, T., Tibshirani, R., Friedman, J., 2009. The Elements of Statistical Learning: Data Mining, Inference, and Prediction. Springer.

Hochreiter, S., Schmidhuber, J., 1997. Long Short-Term Memory. Neural Computation, 9(8), 1735-1780.

Hornik, K., 1991. Approximation capabilities of multilayer feedforward networks. Neural Networks, 4(2), 251-257.

Hosmer, D.W., Lemeshow, S., Sturdivant, R.X., 2013. Applied Logistic Regression (3rd ed.). Wiley.

Jain, A.K., 2010. Data clustering: 50 years beyond K-means. Pattern Recognition Letters, 31(8), 651-666.

Jordan, M.I., Bishop, C.M., 1996. Neural networks. In A. Tucker (Ed.), CRC Handbook of Computer Science CRC Press.

Kayhomayoon, Z., Ghordoyee-Milan, S., Jaafari, A., Arya-Azar, N., Melesse, A.M., Kardan Moghaddam, H., 2022. How does a combination of numerical modeling, clustering, artificial intelligence, and evolutionary algorithms perform to predict regional groundwater levels? Computers and Electronics in Agriculture, 203, 107482.

Kutner, M.H., Nachtsheim, C.J., Neter, J., 2004. Applied Linear Regression Models. McGraw-Hill Irwin.

LeCun, Y., Bottou, L., Bengio, Y., Haffner, P., 1998. Gradient-based learning applied to document recognition. Proceedings of the IEEE, 86(11), 2278-2324.

LeCun, Y., Bengio, Y., Hinton, G.E., 2015. Deep learning. Nature, 521(7553), 436-444.

Loh, W.Y., 2011. Classification and regression trees. Wiley Interdisciplinary Reviews: Data Mining and Knowledge Discovery, 1(1), 14-23.

MacQueen, J., 1967. Some methods for classification and analysis of multivariate observations. Proceedings of the Fifth Berkeley Symposium on Mathematical Statistics and Probability, 1(14), 281-297.

Menard, S., 2002. Applied Logistic Regression Analysis (2nd ed.). Sage.

Mewes, B., Oppel, H., Marx, V., Hartmann, A., 2020. Information-Based Machine Learning for Tracer Signature Prediction in Karstic Environments. Water Resources Research, 56(2), e2018WR024558.

Mikhaylov, S.J., Esteve, M., Campion, A., 2018. Artificial intelligence for the public sector: opportunities and challenges of cross-sector collaboration. Philosophical Transactions of the Royal Society. A, 376:20170357.

Mikolov, T., Karafiát, M., Burget, L., Černocký, J., Khudanpur, S., 2010. Recurrent neural network-based language model. Interspeech, 2, 1045-1048.

Murphy, K.P., 2012. Machine Learning: A Probabilistic Perspective. MIT Press.

Niraula, R.R., Sharma, S., Pokharel, B.K., Paudel, U., 2021. Spatial prediction of spring locations in data poor region of Central Himalayas. Hydrology Research, 52(2), 492-505.

Opoku, P.A., Shu, L., Ansah-Narh, T., Kwaw, A.K., Niu, S., 2024. Prediction of karst spring discharge using LSTM with Bayesian optimisation hyperparameter tuning: A laboratory physical model approach. Modelling Earth Systems and Environment, 10(1), 1457-1482.

Piotrowska, J., Dąbrowska, D., 2024. Artificial intelligence methods in water systems research – a literature review. Geological Quarterly, 68(2), 68-19.

Pölz, A., Blaschke, A.P., Komma, J., Farnleitner, A.H., Derx, J., 2024. Transformer Versus LSTM: A Comparison of Deep Learning Models for Karst Spring Discharge Forecasting. Water Resources Research, 60(4), e2022WR032602.

Quinlan, J.R., 1986. Induction of decision trees. Machine Learning, 1(1), 81-106.

Rosenblatt, F., 1958. The Perceptron: A Probabilistic Model for Information Storage and Organization in the Brain. Psychological Review, 65(6), 386-408.

Rumelhart, D.E., Hinton, G.E., Williams, R.J., 1986. Learning representations by back-propagating errors. Nature, 323(6088), 533-536.

Sahour, H., Sultan, M., Abdellatif, B., Emil, M., Abotalib, Z., Abdelmohsen, K., Vazifedan, M., Mohammad, A.T., Hassan, S.M., Metwalli, M.R., El Bastawesy, M., 2022. Identification of shallow groundwater in arid lands using multi-sensor remote sensing data and machine learning algorithms. Journal of Hydrology, 614, 128509.

Samuel, A.L., 1959. Some Studies in Machine Learning Using the Game of Checkers. IBM Journal of Research and Development, 3(3), 210-229.

Schölkopf, B., Smola, A.J., 2002. Learning with kernels: Support vector machines, regularization, optimization, and beyond. MIT press.

Seber, G.A.F., Lee, A.J., 2012. Linear Regression Analysis. John Wiley & Sons.

Secci, D., Tanda, M.G., D'Oria, M., Todaro, V., 2023. Artificial intelligence models to evaluate the impact of climate change on groundwater resources. Journal of Hydrology, 627, 130359, ISSN 0022-1694.

Soleimani Motlagh, M., Ghasemieh, H., Talebi, A., Abdollahi, K., 2017. Identification and Analysis of Drought Propagation of Groundwater During Past and Future Periods. Water Resources Management, 31(1), 109-125.

Song, X., Hao, H., Liu, W., Wang, Q., An, L., Jim Yeh, T.-C., Hao, Y., 2022. Spatial-temporal behavior of precipitation driven karst spring discharge in a mountain terrain. Journal of Hydrology, 612, 128116.

Sun, T.Q., Medaglia, R., 2019. Mapping the challenges of Artificial Intelligence in the public sector: Evidence from public healthcare. Government Information Quarterly, 36(2), 368-383.

Sutskever, I., Vinyals, O., Le, Q.V., 2014. Sequence to sequence learning with neural networks. Advances in Neural Information Processing Systems, 27, 3104-3112.

Yu, K.-X., Qin, Y., Zhang, X., Hu, J., Sun, Q., 2019. Peak break-up water level and discharge forecast in the Inner Mongolia Reach of the Yellow River based on a binary logistic regression model. Taiwan Water Conservancy, 66(4), 9-17.

Zhang, W., Duan, L., Liu, T., Shi, Z., Shi, X., Chang, Y., Qu, S., Wang, G., 2024. A hybrid framework based on LSTM for predicting karst spring discharge using historical data. Journal of Hydrology, 633, 130946.

Zhou, R., Zhang, Y., 2022. On the role of the architecture for spring discharge prediction with deep learning approaches. Hydrological Processes, 36(10), e14737.

Zhou, R., Zhang, Y., 2023. Linear and nonlinear ensemble deep learning models for karst spring discharge forecasting. Journal of Hydrology, 627, 130394.

Zhou, R., Zhang, Y., Wang, Q., Jin, A., Shi, W., 2024. A hybrid self-adaptive DWT-WaveNet-LSTM deep learning architecture for karst spring forecasting. Journal of Hydrology, 634, 131128.

Chapter 5:

General conclusions

This PhD research primarily focused on the impacts of climate change on the discharge of springs located along the Apennine Mountain range and on the long-term projections of their flow rates. The reduction in spring discharge across the Italian peninsula, predominantly characterised by a Mediterranean climate, has become increasingly pronounced since the early 1980s, posing significant challenges for numerous water companies responsible for ensuring water supply to citizens. This decline is attributed to various factors, both directly and indirectly linked to the substantial rise in atmospheric temperatures: a significant increase in evapotranspiration, which reduces the effectiveness of precipitation in recharging aquifers; a shift in precipitation patterns, characterised by a higher frequency of intense events over shorter durations, leading to a greater proportion of surface runoff at the expense of direct or lateral recharge, alternating with prolonged droughts; and a reduction in snowfall, both in terms of total accumulation and the persistence of snow cover on the ground, which presents an even more critical scenario for groundwater resources. When these factors act in combination, the challenges to groundwater availability in the study region become starkly apparent.

The analyses conducted during this PhD project sought to provide insights into two primary research questions.

Question 1 - *What is the impact of global warming on spring discharge along the Apennines, and to what extent is it feasible to assess the resilience of springs to climate change?*

To address this question and establish a robust foundation for subsequent analyses of the quantitative impacts of global warming on spring discharge, with implications for resilience to climate change, a comprehensive approach was developed and implemented. This encompassed geological, hydrogeological, geochemical, isotopic, and tracer test analyses, along with discharge assessments based on recent data and data from a century ago, as detailed in Chapter 2, and long-term discharge analyses from a multi-decadal perspective, as outlined in Chapter 3.

In Chapter 2, the availability of a five-year spring discharge record dating back more than a century for Nadìa Spring, a major spring in the Northern Apennines situated in a largely natural watershed with minimal land use modifications, proved to be a critical asset for understanding the spring's response to climate variations and, as a secondary objective, for drawing conclusions about its long-term resilience to recharge reductions. The study of the historical precipitation over the spring catchment has revealed that, since the 1980s, drought events have become

increasingly frequent and severe. These reductions in precipitation, both solid and liquid, are directly reflected in spring discharge. In fact, a comparison of the average monthly discharge of Nadìa Spring between the periods 1915-1919 and 2020-2023 indicates a decrease in flow rate of approximately 40%. Despite this significant reduction, the spring exhibits a strong resilience on interdecadal timescales, maintaining a consistent base flow and ensuring the provision of an adequate discharge to support both public water supply and ecosystem services. The study presented in Chapter 2 has indeed also revealed that the comprehensive multidisciplinary investigation adopted can provide a detailed understanding of spring discharge dynamics, offering valuable insights into its long-term resilience to changes in recharge. The availability of data spanning several decades proves crucial not only for assessing the quantitative impacts of climate change on springs, but also for confirming the hypothesis of the presence of a dual-porosity system within the spring aquifer, characterised by fast-flow conduits and a diffuse fracture network. The fast-flow conduits are responsible for the aquifer's rapid responses during active recharge periods, whereas the diffuse network becomes dominant during hydrologic recession. This dual-porosity structure enables the spring to sustain a steady base flow despite fluctuations in recharge driven by increasing climate variability.

Regarding Chapter 3, the historical flow rate datasets of two major springs, Sanità (Cervialto Massif, Southern Apennines) and Ermicciolo (Amiata Mountain, Central Italy), dating back to January 1920 and 1939 respectively, have represented a valuable resource for assessing century-long discharge trends. The two datasets were ideally suited for this purpose not only due to the length of the discharge time series but also because of the systematic quality of the records and the absence of human-induced alterations to the natural conditions of the aquifers. Considering that at least 30 years of data are typically required to accurately assess climate trends, the historical flow rate datasets of Sanità and Ermicciolo Springs were divided into three multi-decadal subsets. The multi-decadal analysis of Sanità Spring discharge data reveals a mean hydrograph for the earliest historical subset (1920-1954) with an average flow rate ranging from approximately 3580 to 4430 L/s. The intermediate historical hydrograph (1955-1989) covers a range between 3820 and 4630 L/s and partially overlaps with that of the first subset, whereas the most recent historical hydrograph (1990-2024) indicates an average spring discharge ranging from 3360 to 3920 L/s, highlighting a notable flow rate decrease. For Ermicciolo Spring, the mean hydrographs for the three historical periods display a progressively declining average discharge, transitioning from the earliest two periods to the most recent. The corresponding discharge ranges are as follows: 172-201 L/s for 1939-1954, 135-157 L/s for 1955-1989, and 131-147 L/s for 1990-2024. Hence, at Sanità Spring, the discharge decreased by a significant 12.5% between the intermediate period, characterised by the highest discharge, and the most recent subset, which recorded the lowest spring discharge. Ermicciolo Spring exhibited a much greater reduction of

25.2% between the oldest period, which had the highest discharge, and the most recent period, which similarly represented the lowest discharge.

For an accurate quantification and assessment of spring discharge decline induced by climate change, it is essential to focus on springs with a very long historical discharge dataset, ideally exceeding 80 years. Relying on shorter historical records may lead to erroneous conclusions, as discussed in Chapter 1, Section 1.3.2. Long-term spring discharge dynamics, spanning decades, are generally less influenced by the specific characteristics of individual basins and more indicative of broader climate shifts within a region. Other springs analysed in Chapter 3, specifically the Verde Spring and the Cassano Irpino and Serino Spring groups, with relatively long historical discharge datasets (approximately 60 years), and situated in different settings but within the same Mediterranean climate, exhibit a multi-decadal historical discharge pattern similar to that of the Sanità and Ermicciolo Springs. Therefore, part of the study presented in Chapter 3 confirms and extends the findings already observed for Nadìa Spring in Chapter 2: spring discharge, compared to 100 years ago, has decreased across the entire Apennine range due to natural processes driven by global warming.

Question 2 - *Is it possible to estimate the long-term future discharge of springs based on long-term recharge-discharge relationships?*

To address this question and achieve a comprehensive understanding of the techniques most frequently used in hydrogeology to analyse the relationship between meteorological variables and spring flow rate, and to exploit this relationship to estimate future spring discharge, two conceptually similar yet methodologically distinct approaches were employed. These approaches included a Multiregression Statistical Analysis, as presented in Chapter 3, and a Long-Short Term Memory neural network analysis, as detailed in Chapter 4. Once the correlations between the variables involved were identified, in both cases these relationships were applied to the same projected meteorological variables (2024-2070) derived from the CMCC-CM regional circulation model, downscaled over Italy for the RCPs 4.5 and 8.5 scenarios. This process enabled the estimation of spring discharge projections in the long-term future.

Beginning with Chapter 3, the century-long discharge time series for Sanità and Ermicciolo Springs were analysed in conjunction with two meteorological variables: Total Liquid Precipitation (TLP), which encompasses both rainfall and snowfall contributions, and Air Temperature (AirT). The multivariate regression analysis demonstrated that, for both springs, discharge exhibits the strongest negative correlation with average AirT and the strongest positive correlation with cumulative TLP, with a time lag of seven months. This result aligns with physical expectations, as peak liquid precipitation (the predominant component of TLP) occurs in

November, whereas peak discharge is typically observed during the summer months. For the forecasting phase, we focused exclusively on the period 2040-2070, also to enable consistent multi-decadal comparisons with the trentennial periods defined for the historical spring discharge. For Sanità Spring, after applying the correlation factors derived from the MSA method to the future projections of TLP and AirT, a mean hydrograph with an average flow rate ranging from 3220 to 3830 L/s was produced under the RCP 4.5 scenario. In the more severe RCP 8.5 scenario, the hydrograph indicates a discharge range between 2970 and 3630 L/s. For Ermicciolo Spring, the mean hydrographs show an average discharge ranging from 131 to 146 L/s under the RCP 4.5 scenario and from 116 to 131 L/s under the RCP 8.5 scenario. Based on these results, it can be concluded that for both springs, with the MSA method, under the RCP 4.5 scenario, future discharge projections do not indicate significant impairment in flow rate output when compared to the most recent historical period. The estimated reduction in discharge is minimal, amounting to only 3.0% for Sanità Spring and 0.1% for Ermicciolo Spring. By contrast, under the more severe RCP 8.5 scenario, characterised by elevated greenhouse gas emissions, a more pronounced decline in spring discharge is observed during the 2040-2070 period. At Sanità Spring, the discharge is projected to decrease by 8.6% relative to the 1990-2024 period, while Ermicciolo Spring exhibits a comparable decline of 10.8% over the same interval. As previously discussed, long-term discharge is highly dependent on regional climate shifts. This is further evidenced by the similar percentage rates of flow rate decline observed in two hydrologically distinct springs. Consequently, the future multi-decadal downtrend identified for Sanità and Ermicciolo Springs is likely attainable for other springs within Mediterranean climate.

Regarding Chapter 4, the use of the LSTM machine learning method introduced a significant difference compared to the MSA method: the inclusion of spring discharge from previous months as an additional independent variable. This modification was implemented after initial testing with numerous combinations of ML hyperparameters revealed that adding spring discharge significantly improved the loss function outcomes and yielded highly positive performance metrics. Another notable improvement is that, by setting a lag time for an independent variable, the LSTM model analyses temporal dependencies with the dependent variable and all preceding months up to the maximum lag value. This contrasts with multiregression statistical analysis, which only accounts for relationships with the single preceding month corresponding to the specified lag. Once the best-performing models were identified, the optimal lag values were determined to be 18 months for Sanità Spring and 12 months for Ermicciolo Spring. These results align with the seasonal, annual, and multi-annual patterns observed in spring discharge. Indeed, by incorporating discharge as an independent variable, the models captured extended temporal dependencies, identifying that seasonal peaks and lows in spring discharge occur with near-consistent intervals of 11 to 13 months in both case studies. For Sanità Spring, due to the larger

size of its catchment and aquifer, these patterns sometimes extend up to 18 months. Despite the MSA method demonstrating significant relationships between meteorological variables and discharge up to a maximum lag of seven months, it was decided to use the same lag for the meteorological variables as for spring flow rate, as this configuration was not computationally demanding. The two optimal LSTM models were applied to the same future meteorological scenarios used in Chapter 3, generating future monthly discharge through an iterative approach. Specifically, for discharge as an input variable, since future spring discharge (the target variable) was not available in the datasets, it had to be calculated step-by-step, starting from the most recent historical data. Each predicted value was then sequentially incorporated into the projected dataset to enable subsequent predictions. To facilitate a comparison with the results of the MSA method, the discharge obtained through the LSTM method was also represented using mean hydrographs for the 2040-2070 period. The LSTM model projections for Sanità Spring produce mean hydrographs with an average discharge ranging from approximately 3,770 to 3,250 L/s under the RCP 4.5 scenario and from 3,470 to 2,920 L/s under the RCP 8.5 scenario. For Ermicciolo Spring, the LSTM model predicts a mean discharge of 127 to 114 L/s in the RCP 4.5 scenario and 111 to 96 L/s in the RCP 8.5 scenario.

While the results for Sanità Spring align closely with those obtained through the MSA method, the LSTM model projects a significantly sharper decline in discharge for Ermicciolo Spring, roughly 2.5 times greater than the MSA predictions. Beyond the differences in the results, all the findings from Chapters 3 and 4 underscore the importance of long-term spring discharge projections in addressing potential groundwater shortages, which are expected to pose significant challenges for water supply systems in the future. Unlike the vast majority of papers in the literature on this topic, which primarily focus on short-term predictions, this thesis emphasises the long-term future. Such long-term projections are crucial for providing water management agencies with the tools necessary to anticipate and mitigate future water scarcity through drought risk mitigation measures such as the construction of surface water reservoirs, the development of well fields in deeper aquifers, the implementation of aqueduct interconnections, and the repair and renewal of Italy's primary water supply networks.

The methodologies employed in this thesis enabled the quantification of the effects of climate change on spring discharge along the Apennines, the evaluation of their resilience to such changes, and the estimation of their long-term future flow rates, based on the previously identified recharge-discharge relationship.

General references

Abderrahman, W.A., 2005. Groundwater Management for Sustainable Development of Urban and Rural Areas in Extremely Arid Regions: A Case Study. International Journal of Water Resources Development, 21, 403-412.

Acocella, V., Funiciello, R., 2006. Transverse systems along the extensional Tyrrhenian margin of central Italy and their influence on volcanism. Tectonics, 25(2), TC2003.

Acquedotto Pugliese S.p.A., 2024. Siccità, riduzioni di pressione su tutta la rete per affrontare la crisi idrica. Comunicato Stampa - Comunicazione e Media, Bari, 21 October 2024.

Alexander, L.V., Zhang, X., Peterson, T.C., Caesar, J., Gleason, B., Klein Tank, A.M.G., Haylock, M., Collins, D., Trewin, B., Rahimzadeh, F., Tagipour, A., Rupa Kumar, K., Revadekar, J., Griffiths, G., Vincent, L., Stephenson, D.B., Burn, J., Aguilar, E., Brunet, M., Taylor, M., New, M., Zhai, P., Rusticucci, M., Vazquez-Aguirre, J.L., 2006. Global observed changes in daily climate extremes of temperature and precipitation. Journal of Geophysical Research Atmospheres, 111(5), D05109.

Aley, T., 2019. The Ozark Underground Laboratory's Groundwater Tracing Handbook. Ozark Underground Laboratory.

Alilou, H., Oldham, C., McFarlane, D., Hipsey, M.R., 2022. A structured framework to interpret hydro-climatic and water quality trends in Mediterranean climate zones. Journal of Hydrology, 614, 128512.

Allen, C.D., Macalady, A.K., Chenchouni, H., Bachelet, D., McDowell, N., Vennetier, M., Kitzberger, T., Rigling, A., Breshears, D.D., Hogg, E.H., Gonzalez, P., Fensham, R., 2010. Forest Ecology and Management, 259(4), pp. 660-684.

Allocca, V., Manna, F., De Vita, P., 2014. Estimating annual groundwater recharge coefficient for karst aquifers of the Southern Apennines (Italy). Hydrology and Earth System Sciences, 18(2), 803-817.

Amanambu, A.C., Obarein, O.A., Mossa, J., Li, L., Ayeni, S.S., Balogun, O., Oyebamiji, A., Ochege, F.U., 2020. Groundwater system and climate change: Present status and future considerations. Journal of Hydrology, 589, 125163.

Amorosi, A., 1997. Miocene shallow-water deposits of the northern Apennines: a stratigraphic marker across a dominantly turbidite foreland-basin succession. Geologie en Mijnbouw, Netherlands Journal of Geosciences, 75, 295-307.

Amorosi, A., Spadafora, E., 1995. The upper Serravallian unconformity in the epi-Ligurian units of the Bologna Apennines, in: Polino, R., Sacchi, R. (Eds.), Rapporti Alpi-Appennino e guida alle escursioni, Peveragno, Cuneo, 69-86.

An, L., Hao, Y., Yeh, T.-C.J., Liu, Y., Liu, W., Zhang, B., 2020. Simulation of karst spring discharge using a combination of time–frequency analysis methods and long short-term memory neural networks Journal of Hydrology, 589, 125320.

ARPAE, 2018. Rapporto idro-meteo-clima Emilia Romagna - rapporto annuale dati 2017 (Annual report of the idro-meteo-climatic data of the Emilia Romagna Region - year 2017). In Italian. ARPAE.

ARPAE, 2023. Rapporto idro-meteo-clima Emilia Romagna - rapporto annuale dati 2022 (Annual report of the idro-meteo-climatic data of the Emilia Romagna Region - year 2022). In Italian. ARPAE.

Arrhenius, S., 1896. On the Influence of Carbonic Acid in the Air upon the Temperature of the Ground. Philosophical Magazine and Journal of Science, 5(41), 237-276.

Arthur, D., Vassilvitskii, S., 2007. k-means++: The advantages of careful seeding. Proceedings of the Eighteenth Annual ACM-SIAM Symposium on Discrete Algorithms, 1027-1035.

Atawneh, D.A., Cartwright, N., Bertone, E., 2021. Climate change and its impact on the projected values of groundwater recharge: A review. Journal of Hydrology, 601, 126602.

Azeez, N., West, L.J., Bottrell, S.H., 2015. Numerical simulation of spring hydrograph recession curves for evaluating behavior of the East Yorkshire chalk aquifer, in: Doctor, D.H., Land, L., Stephenson, J.B. (Eds.), 14th Sinkhole Conference. National Cave and Karst Research Institute, 05-09 Oct 2015, Rochester, Minnesota, 521-530.

Balaram, V., Copia, L., Kumar, U.S., Miller, J., Chidambaram, S., 2023. Pollution of water resources and application of ICP-MS techniques for monitoring and management—A comprehensive review. Geosystems and Geoenvironment, 2(4), 100210.

Ball, N.M., Brunner, R.J., 2010. Data mining and machine learning in astronomy. International Journal of Modern Physics D, 19(07), 1049-1106.

Ban, N., Caillaud, C., Coppola, E., Pichelli, E., Sobolowski, S., Adinolfi, M., Ahrens, B., Alias, A., Anders, I., Bastin, S., Belušić, D., Berthou, S., Brisson, E., Cardoso, R.M., Chan, S.C., Christensen, O.B., Fernández, J., Fita, L., Frisius, T., Gašparac, G., Giorgi, F., Goergen, K., Haugen, J.E., Hodnebrog, O., Kartsios, S., Katragkou, E., Kendon, E.J., Keuler, K., Lavin-Gullon, A., Lenderink, G., Leutwyler, D., Lorenz, T., Maraun, D., Mercogliano, P., Milovac, J., Panitz, H.J., Raffa, M., Reca Remedio, A., Schär, C., Soares, P.M.M., Srnec, L., Marie Steensen, B., Stocchi, P., Tölle, M.H., Truhetz, H., Vergara-Temprado, J., De Vries, H., Warrach-Sagi, K., Wulfmeyer, V., Zander, M.J., 2021. The first multi-model ensemble of regional climate simulations at kilometer-scale resolution, part I: evaluation of precipitation. Climate Dynamics, 57, 275-302.

Balocchi, P., 2014. Analisi macrostrutturale e mesostrutturale del Gruppo di Bismantova affiorante tra Zocca e Castel d'Aiano (Appennino modenese e bolognese). Atti della Società dei Naturalisti e Matematici di Modena 145, 27-42.

Barbieri, M., Barberio, M.D., Banzato, F., Billi, A., Boschetti, T., Franchini, S., Gori, F., Petitta, M., 2023. Climate change and its effect on groundwater quality. Environmental Geochemistry and Health, 45(4), 1133-1144.

Beck, H.E., McVicar, T.R., Vergopolan, N., Berg, A., Lutsko, N.J., Dufour, A., Zeng, Z., Jiang, X., van Dijk, A.I.J.M., Miralles, D.G., 2023. High resolution (1 km) Köppen-Geiger maps for 1901-2099 based on constrained CMIP6 projections. Scientific Data, 10(1), 724.

Ben-Hur, A., Ong, C.S., Sonnenburg, S., Schölkopf, B., Rätsch, G., 2008. Support vector machines and kernels for computational biology. PLoS Computational Biology, 4(10), e1000173.

Bengio, Y., Simard, P., Frasconi, P., 1994. Learning Long-Term Dependencies with Gradient Descent is Difficult. IEEE Transactions on Neural Networks, 5(2), 157-166.

Bengio, Y., 2012. Practical recommendations for gradient-based training of deep architectures. In: Montavon, G., Orr, G.B., Müller, K.R. (Eds.), Neural Networks: Tricks of the Trade, 437-478. Springer, Berlin, Germany.

Bettelli, G., Boccaletti, M., Cibin, U., Panini, F., Poccianti, C., Rosselli, S., Sani, F., Catanzariti, R., Fioroni, C., Fornaciari, E., Fregni, P., Di Giulio, A., Benvenuti, M., Gasperini, P., Martelli, L., 2005. Note Illustrative della Carta Geologica d'Italia alla scala 1:50.000. Foglio 252 - Barberino di Mugello. A cura di Regione Toscana, ISPRA.

Bhowmick, A., Hazarika, S.M., 2018. Machine Learning for E-mail Spam Filtering: Review, Techniques and Trends.

Bishop, C.M., 2006. Pattern Recognition and Machine Learning. Springer.

Blake, D., Mlisa, A., Hartnady, C., 2010. Large scale quantification of aquifer storage and volumes from the Peninsula and Skurweberg Formations in the southwestern Cape. Water SA, Cape Town, 36(2), 177-184.

Boccaletti, M., Elter, P., Guazzone, G., 1971. Plate Tectonic Models for the Development of the Western Alps and Northern Apennines. Nature Physical Science, 234, 108-111.

Boccaletti, M., Conedera, C., Dainelli, P., Gočev, P., 1982. The recent (Miocene-Quaternary) regmatic system of the western Mediterranean Region: A New Model of Ensialic Geodynamic Evolution, in a Context of Plastic/Rigid Deformation. Journal of Petroleum Geology, 5(1), 31-49.

Boccaletti, M., Corti, G., Martelli, L., 2011. Recent and active tectonics of the external zone of the Northern Apennines (Italy). International Journal of Earth Sciences, 100, 1331-1348.

Bonacci, O., 2007. Analysis of long-term (1878-2004) mean annual discharges of the karst spring Fontaine de Vaucluse (France). Acta Carsologica, 36(1), 151-156.

Bortolotti, V., Passerini, P., 1970. Magmatic activity. Sedimentary Geology, 4(3-4), 599-624.

Bouhafa, N., Sakarovitch, C., Lalague, L., Goulard, F., Pryet, A., 2024. Hybrid modeling of karstic springs: Error correction of conceptual reservoir models with machine learning. Water Supply, 24(5), 1559-1573.

Boussinesq, J., 1904. Recherches théoriques sur l'écoulement des nappes d'eau infiltrées dans le sol et sur le débit des sources. Journal de mathématiques pures et appliquées, 10, 5-78.

Breiman, L., 2001. Random forests. Machine Learning, 45(1), 5-32.

Breiman, L., Friedman, J., Stone, C.J., Olshen, R.A., 1984. Classification and regression trees. CRC press.

Brockwell, P.J., Davis, R.A., 2016. Introduction to Time Series and Forecasting - Third Edition. Springer International Publishing, Cham, Switzerland.

Brynjolfsson, E., Mcafee, A., 2017. The Business of Artificial Intelligence. Harvard Business Review, 7, 3-11.

Bucci, F., Santangelo, M., Fongo, L., Alvioli, M., Cardinali, M., Melelli, L., Marchesini, I., 2022. A new digital lithological map of Italy at the 1:100000 scale for geomechanical modelling. Earth System Science Data, 14(9), 4129-4151.

Butscher, C., Huggenberger, P., 2009. Modeling the Temporal Variability of Karst Groundwater Vulnerability, with Implications for Climate Change. Environmental Science & Technology, 43, 1665-1669.

Caine, J.S., Evans, J.P., Forster, C.B., 1996. Fault zone architecture and permeability structure. Geology, 24, 1025-1028.

Caloiero, T., Caloiero, P., Frustaci, F., 2018. Long-term precipitation trend analysis in Europe and in the Mediterranean basin. Water and Environment Journal, 32, 433-445.

Campanale, C., Losacco, D., Triozzi, M., Massarelli, C., Uricchio, V.F., 2022. An Overall Perspective for the Study of Emerging Contaminants in Karst Aquifers. Resources, 11, 105.

Canora, F., Rizzo, G., Panariello, S., Sdao, F., 2019. Hydrogeology and hydrogeochemistry of the lauria mountains northern sector groundwater resources (basilicata, italy). Geofluids, 1-16.

Cantonati, M., Segadelli, S., Ogata, K., Tran, H., Sanders, D., Gerecke, R., Rott, E., Filippini, M., Gargini, A., Celico, F., 2016. A global review on ambient Limestone-Precipitating Springs (LPS): Hydrogeological setting, ecology, and conservation. Science of the Total Environment, 568, 624-637.

Cantonati, M., Stevens, L.E., Segadelli, S., Springer, A.E., Goldscheider, N., Celico, F., Filippini, M., Ogata, K., Gargini, A., 2020. Ecohydrogeology: The interdisciplinary convergence needed to improve the study and stewardship of springs and other groundwater-dependent habitats, biota, and ecosystems. Ecological Indicators, 110, 105803.

Capitani, M., 1997. Analisi mesostrutturale del sistema di deformazione trasversale della Val Lavino (Appennino settentrionale, Italia). Atti della Ticinese di Scienze della Terra, 99-110.

Cardell, M.F., Amengual, A., Romero, R., Ramis, C., 2020. Future extremes of temperature and precipitation in Europe derived from a combination of dynamical and statistical approaches. International Journal of Climatology, 40(11), 4800-4827.

Carmignani, L., Kligfield, R., 1990. Crustal extension in the northern Apennines: The transition from compression to extension in the Alpi Apuane Core Complex. Tectonics, 9(6), 1275-1303.

Carmignani, L., Decandia, F.A., Fantozzi, P.L., Lazzarotto, A., Liotta, D., Meccheri, M., 1994. Tertiary extensional tectonics in Tuscany (Northern Apennines, Italy). Tectonophysics, 238(1-4), 295-310, 313-315.

Carminati, E., Lustrino, M., Cuffaro, M., Doglioni, C., 2010. Tectonics, magmatism and geodynamics of Italy: What we know and what we imagine. Journal of the Virtual Explorer, 36.

Carminati, E., Lustrino, M., Doglioni, C., 2012. Geodynamic evolution of the central and western Mediterranean: Tectonics vs. igneous petrology constraints. Tectonophysics, 579, 173-192.

Carminati, E., Doglioni, C., 2012. Alps vs. Apennines: The paradigm of a tectonically asymmetric Earth. Earth-Science Reviews, 112, 67-96.

Celico, P., Russo, D., 1981. Studi idrogeologici sulla Piana del Dragone (Avellino). Bollettino della Società dei Naturalisti, 90, 37-50.

Cerino Abdin, E., Taddia, G., Gizzi, M., Lo Russo, S., 2021. Reliability of spring recession curve analysis as a function of the temporal resolution of the monitoring dataset. Environmental Earth Sciences, 80, 249.

Cervi, F., Corsini, A., Doveri, M., Mussi, M., Ronchetti, F., Tazioli, A., 2015. Characterizing the Recharge of Fractured Aquifers: A Case Study in a Flysch Rock Mass of the Northern Apennines (Italy), in: Lollino, G., Arattano, M., Rinaldi, M., Giustolisi, O., Marechal, J.-C., Grant, G.E. (Eds.), Engineering Geology for Society and Territory - Volume 3. Springer International Publishing, Cham, 563-567.

Cervi, F., Petronici, F., Castellarin, A., Marcaccio, M., Bertolini, A., Borgatti, L., 2018. Climate-change potential effects on the hydrological regime of freshwater springs in the Italian Northern Apennines. Science of the Total Environment, 622-623, 337-348.

Channell, J.E.T., Horváth, F., 1976. The African/Adriatic promontory as a palaeogeographical premise for alpine orogeny and plate movements in the Carpatho-Balkan region. Tectonophysics, 35(1-3), 71-101.

Chen, Z., Grasby, S.E., Osadetz, K.G., 2004. Relation between climate variability and groundwater levels in the upper carbonate aquifer, southern Manitoba, Canada. Journal of Hydrology, 290(1-2), 43-62.

Cheng, S., Qiao, X., Shi, Y., Wang, D., 2021. Machine learning for predicting discharge fluctuation of a karst spring in North China. Acta Geophysica, 69(1), 257-270.

Chiaudani, A., Di Curzio, D., Rusi, S., 2019. The snow and rainfall impact on the Verde Spring behavior: A statistical approach on hydrodynamic and hydrochemical daily time-series. Science of the Total Environment, 689, 481-493.

Cho, K., van Merrienboer, B., Gulcehre, C., Bahdanau, D., Bougares, F., Schwenk, H., Bengio, Y., 2014. Learning phrase representations using RNN encoder-decoder for statistical machine translation. Proceedings of the 2014 Conference on Empirical Methods in Natural Language Processing (EMNLP).

Cibin, U., Spadafora, E., Zuffa, G.G., Castellarin, A., 2001. Continental collision history from arenites of episutural basins in the Northern Apennines, Italy. GSA Bulletin, 113, 4-19.

Cinkus, G., Wunsch, A., Mazzilli, N., Liesch, T., Chen, Z., Ravbar, N., Doummar, J., Fernández-Ortega, J., Barberá, J.A., Andreo, B., Goldscheider, N., Jourde, H., 2023. Comparison of artificial neural networks and reservoir models for simulating karst spring discharge on five test sites in the Alpine and Mediterranean regions. Hydrology and Earth System Sciences, 27(10), 1961-1985.

Conti, P., Cornamusini, G., Carmignani, L., 2020. An outline of the geology of the Northern Apennines (Italy), with Geological Map at 1:250,000 scale. Italian Journal of Geosciences.

Coppola, L., Cotecchia, V., Lattanzio, M., Salvemini, A., Tadolini, T., Ventrella, N.A., 1989. Il gruppo di sorgenti di Cassano Irpino: regime idrologico ed analisi strutturale del bacino di alimentazione. Geologia Applicata e Idrogeologia, 24, 227-260.

Corniello, A., Ducci, D., Aquino, A., 2010. Hydrogeological map of the Monti Picentini Regional Park (Southern Italy) at 1: 50,000 scale. Bollettino di Geofisica Teorica ed Applicata, 51(4), 325-343, ISSN: 0006-6729.

Corriere della Sera, 2023. Acqua, italiani tra i più spreconi in Europa ma iniziano a cambiare le abitudini, [https://www.corriere.it/economia/consumi/23_marzo_21/acqua-italiani-piu-spreconi-europa-ma-iniziano-cambiare-abitudini-38103aaa-c7da-11ed-b48b-1072850ccecb.shtml]. Alessia Conzonato, Corriere della Sera, 'L'Economia - Risparmi, Mercati, Imprese', Milano, 21 March 2023.

Cortes, C., Vapnik, V., 1995. Support-vector networks. Machine Learning, 20(3), 273-297.

Cosentino, D., Cipollari, P., Marsili, P., Scrocca, D., 2010. Geology of the central Apennines: A regional review. Journal of the Virtual Explorer, 36.

Cuthbert, M.O., Taylor, R.G., Favreau, G., Todd, M.C., Shamsudduha, M., Villholth, K.G., MacDonald, A.M., Scanlon, B.R., Kotchoni, D.O.V., Vouillamoz, J.-M., Lawson, F.M.A., Adjomayi, P.A., Kashaigili, J., Seddon, D., Sorensen, J.P.R., Ebrahim, G.Y., Owor, M., Nyenje, P.M., Nazoumou, Y., Goni, I., Ousmane, B.I., Sibanda, T., Ascott, M.J., Macdonald, D.M.J., Agyekum, W., Koussoubé, Y., Wanke, H., Kim, H., Wada, Y., Lo, M.-H., Oki, T., Kukuric, N., 2019. Observed controls on resilience of groundwater to climate variability in sub-Saharan Africa. Nature, 572, 230-234.

Cybenko, G., 1989. Approximation by superpositions of a sigmoidal function. Mathematics of Control, Signals and Systems, 2(4), 303-314.

Dal Seno, N., 2024. Application of machine learning methods for landslide risk mitigation. PhD thesis, 37th PhD cycle, Alma Mater Studiorum - University of Bologna.

De la Hera-Portillo, Á., López-Gutiérrez, J., Zorrilla-Miras, P., Mayor, B., López-Gunn, E., 2020. The Ecosystem Resilience Concept Applied to Hydrogeological Systems: A General Approach. Water, 12, 1824.

De Vita, P., Allocca, V., Manna, F., Fabbrocino, S., 2012. Coupled decadal variability of the North Atlantic Oscillation, regional rainfall and karst spring discharges in the Campania region (Southern Italy). Hydrology and Earth System Sciences, 16(5), 1389-1399.

Dewandel, B., Lachassagne, P., Bakalowicz, M., Weng, P., Al-Malki, A., 2003. Evaluation of aquifer thickness by analysing recession hydrographs. Application to the Oman ophiolite hard-rock aquifer. Journal of Hydrology, 274, 248-269.

Di Curzio, D., Rusi, S., Di Giovanni, A., Ferretti, E., 2021. Evaluation of groundwater resources in minor plio-pleistocene arenaceous aquifers in central Italy. Hydrology, 8(3), 121.

Di Matteo, L., Dragoni, W., Maccari, D., Piacentini, S.M., 2016. A contribution to the definition of the ongoing climate change and its impacts on the water resources: The case of Monte Fumaiolo (Central Italy). Rendiconti Online Societa Geologica Italiana, 41, 46-49.

Di Nunno, F., Granata, F., Gargano, R., de Marinis, G., 2021. Prediction of spring flows using nonlinear autoregressive exogenous (NARX) neural network models. Environmental Monitoring and Assessment, 193(6), 350.

Diodato, N., Bellocchi, G., Fiorillo, F., Ventafridda, G., 2017. Case study for investigating groundwater and the future of mountain spring discharges in Southern Italy. Journal of Mountain Science, 14(9), 1791-1800.

Diodato, N., Büntgen, U., Bellocchi, G., 2019. Mediterranean winter snowfall variability over the past millennium. International Journal of Climatology, 39, 384-394.

Diodato, N., Ljungqvist, F.C., Fiorillo, F., Esposito, L., Ventafridda, G., Bellocchi, G., 2022. Climatic fingerprint of spring discharge depletion in the southern Italian Apennines from 1601 to 2020 CE. Environmental Research Communications, 4(12), 125011.

Diodato, N., Ljungqvist, F.C., Bellocchi, G., 2022. Empirical modelling of snow cover duration patterns in complex terrains of Italy. Theoretical and Applied Climatology, 147, 1195-1212.

Dobilas, S., 2022. LSTM Recurrent Neural Networks - How to Teach a Network to Remember the Past. Published by the user in "Towards Data Science". https://towardsdatascience.com/lstm-recurrent-neural-networks-how-to-teach-a-network-to-remember-the-past-55e54c2ff22e. Medium, Human, stories & ideas. URL (accessed 11.26.24).

Döll, P., Hoffmann-Dobrev, H., Portmann, F.T., Siebert, S., Eicker, A., Rodell, M., Strassberg, G., Scanlon, B.R., 2012. Impact of water withdrawals from groundwater and surface water on continental water storage variations. Journal of Geodynamics, 59-60, 143-156.

Dore, M.H.I., 2005. Climate change and changes in global precipitation patterns: What do we know? Environment International, 31, 1167-1181.

Doummar, J., Hassan Kassem, A., Gurdak, J.J., 2018. Impact of historic and future climate on spring recharge and discharge based on an integrated numerical modelling approach: Application on a snow-governed semi-arid karst catchment area. Journal of Hydrology, 565, 636-649.

Doveri, M., Nisi, B., Cerrina Feroni, A., Ellero, A., Menichini, M., Lelli, M., Masetti, G., Da Prato, S., Principe, C., Raco, B., 2012. Geological, hydrodynamic and geochemical features of the volcanic aquifer of Monte Amiata (Tuscany, central Italy): an overview. Acta Vulcanologica, 23(1-2), 51-72.

Doveri, M., Menichini, M., 2017. Aspetti idrogeologici delle vulcaniti del Monte Amiata. In: Principe, C., Lavorini, G., Vezzoli, L., “Il Vulcano di Monte Amiata”, 255-265.

Doveri, M., Raco, B., 2021. Studio di approfondimento sulle caratteristiche quali-quantitative della risorsa idrica delle sorgenti di Santa Fiora - Monte Amiata. Accordo di Collaborazione Scientifica tra Acquedotto del Fiora (ADF) e Istituto di Geoscienze e Georisorse del Consiglio Nazionale delle Ricerche (IGG-CNR), unpublished technical report (in italian).

Dragoni, W., Sukhija, B.S., 2008. Climate change and groundwater: a short review. Geological Society, London, Special Publications 288, 1-12.

Draper, N.R., Smith, H., 1998. Applied Regression Analysis (3rd ed.). John Wiley & Sons.

El Ansari, R., El Bouhadioui, M., Aboutafail, M.O., Mejjad, N., Jamil, H., Jamal, E., Rissouni, Y., Zouiten, M., Boutracheh, H., Moumen, A., 2023. A review of Machine learning models and parameters for groundwater issues. ACM International Conference Proceeding Series, 54.

Elman, J.L., 1990. Finding structure in time. Cognitive Science, 14(2), 179-211.

Essa, Y.H., Hirschi, M., Thiery, W., El-Kenawy, A.M., Yang, C., 2023. Drought characteristics in Mediterranean under future climate change. npj Climate and Atmospheric Science, 6(1), 133.

Eurispes, 2023. A system that treads water: the condition of water in Italy, [https://eurispes.eu/en/news/a-system-that-treads-water-the-condition-of-water-in-italy/]. Eurispes, Istituto di Studi Politici, Economici e Sociali. URL (accessed 2.29.24).

Fan, X., Goeppert, N., Goldscheider, N., 2023. Quantifying the historic and future response of karst spring discharge to climate variability and change at a snow-influenced temperate catchment in central Europe. Hydrogeology Journal, 31(8), 2213-2229.

Farahani, H.A., Rahiminezhad, A., Same, L., Immannezhad, K., 2010. A comparison of Partial Least Squares (PLS) and Ordinary Least Squares (OLS) regressions in predicting of couples mental health based on their communicational patterns. Procedia - Social and Behavioral Sciences, 5, 1459-1463.

Ferguson, G., Gleeson, T., 2012. Vulnerability of coastal aquifers to groundwater use and climate change. Nature Climate Change 2, 342-345.

Filippini, M., Segadelli, S., Dinelli, E., Failoni, M., Stumpp, C., Vignaroli, G., Casati, T., Tiboni, B., Gargini, A., 2024. Hydrogeological assessment of a major spring discharging from a calcarenitic aquifer with implications on resilience to climate change. Science of The Total Environment, 913, ISSN 0048-9697.

Fiorillo, F., Esposito, L., Guadagno, F.M., 2007. Analyses and forecast of water resources in an ultra-centenarian spring discharge series from Serino (Southern Italy). Journal of Hydrology, 336(1-2), 125-138.

Fiorillo, F., 2009. Spring hydrographs as indicators of droughts in a karst environment. Journal of Hydrology, 373, 290-301.

Fiorillo, F., Doglioni, A., 2010. The relation between karst spring discharge and rainfall by the cross-correlation analysis. Hydrogeology Journal, 18, 881-1895.

Fiorillo, F., Guadagno, F.M., 2012. Long karst spring discharge time series and droughts occurrence in Southern Italy. Environmental Earth Sciences, 65(8), 2273-2283.

Fiorillo, F., Pagnozzi, M., Ventafridda, G., 2015. A model to simulate recharge processes of karst massifs. Hydrological Processes, 29(10), 2301-2314.

Fiorillo, F., Petitta, M., Preziosi, E., Rusi, S., Esposito, L., Tallini, M., 2015. Long-term trend and fluctuations of karst spring discharge in a Mediterranean area (central-southern Italy). Environmental Earth Sciences, 74(1), 153-172.

Fiorillo, F., Esposito, L., Pagnozzi, M., Ciarcia, S., Testa, G., 2018. Karst springs of Apennines typified by upwelling flux. Acque Sotterranee - Italian Journal of Groundwater, 7(4), 21-30.

Fiorillo, F., Leone, G., Pagnozzi, M., Esposito, L., 2021. Long-term trends in karst spring discharge and relation to climate factors and changes. Hydrogeology Journal, 29(1), 347-377.

Ford, D., Williams, P., 2007. Karst hydrogeology and geomorphology. Wiley, Chichester, UK.

Fourier, J.B.J., 1824. Remarques générales sur les temperatures du globe terrestre et des espaces planétaires. Annales de Chimie et de Physique (Paris), deuxième série, 27, 136-167.

Fourier, J.B.J., 1827. Mémoire sur les températures du globe terrestre et des espaces planétaires. Mémoires de l'Académie des Sciences, deuxième série, 7, 569-604.

Freund, Y., Schapire, R.E., 1997. A decision-theoretic generalization of on-line learning and an application to boosting. Journal of Computer and System Sciences, 55(1), 119-139.

Frondini, F., Caliro, S., Cardellini, C., Chiodini, G., Morgantini, N., 2009. Carbon dioxide degassing and thermal energy release in the Monte Amiata volcanic-geothermal area (Italy). Applied Geochemistry, 24(5), 860-875.

Gaba E., 2009 (licensed under GFDL/CC-BY-SA). Italy topographic map. Sources of data: SRTM30 Plus, NGDC World Data Bank II, UN Cartographic section, and regions boundaries created from File.svg by NordNordWest.

Gandelli, S., 2022. La rete idrica italiana è un colabrodo: il 36% dell'acqua viene persa lungo il tragitto [Italy's water supply network is highly inefficient, with 36% of water lost along its distribution routes]. Fonti d'acqua dolce, Geopop.

García-Ruiz, J.M., López-Moreno, J.I., Vicente-Serrano, S.M., Lasanta-Martínez, T., Beguería, S., 2011. Mediterranean water resources in a global change scenario. Earth-Science Reviews, 105(3-4), 121-139.

Gargini, A., De Nardo, M.T., Piccinini, L., Segadelli, S., Vincenzi, V., 2014. Spring discharge and groundwater flow systems in sedimentary and ophiolitic hard rock aquifers: Experiences from Northern Apennines (Italy), in: J.M., S. (Ed.), Fractured Rock Hydrogeology. CRC Press, 129-143.

Gargini, A., Vincenzi, V., Piccinini, L., Zuppi, G., Canuti, P., 2008. Groundwater flow systems in turbidites of the Northern Apennines (Italy): natural discharge and high-speed railway tunnel drainage. Hydrogeology Journal, 16, 1577-1599.

Garreaud, R.D., Alvarez-Garreton, C., Barichivich, J., Pablo Boisier, J., Christie, D., Galleguillos, M., LeQuesne, C., McPhee, J., Zambrano-Bigiarini, M., 2017. The 2010-2015 megadrought in central Chile: Impacts on regional hydroclimate and vegetation. Hydrology and Earth System Sciences, 21(12), 6307-6327.

Gattinoni, P., Francani, V., 2010. Depletion risk assessment of the Nossana Spring (Bergamo, Italy) based on the stochastic modeling of recharge. Hydrogeology Journal, 18, 325-337.

Gebru, T., Morgenstern, J., Vecchione, B., Vaughan, J.W., Wallach, H., Daumé III, H., Crawford, K., 2018. Datasheets for datasets.

Gentilucci, M., Pambianchi, G., 2022. Prediction of Snowmelt Days Using Binary Logistic Regression in the Umbria-Marche Apennines (Central Italy). Water (Switzerland), 14(9), 1495.

Gholami, V., Khaleghi, M.R., 2019. A comparative study of the performance of artificial neural network and multivariate regression in simulating springs discharge in the Caspian Southern Watersheds, Iran. Applied Water Science, 9(1), 9.

Giorgi, F., 2006. Climate change hot-spots. Geophysical Research Letters, 33, L08707.

Giorgi, F., Lionello, P., 2008. Climate change projections for the Mediterranean region. Global and Planetary Change, 63(2-3), 90-104.

Giustini, F., Brilli, M., Patera, A., 2016. Mapping oxygen stable isotopes of precipitation in Italy. Journal of Hydrology: Regional Studies, 8, 162-181.

Goodfellow, I., Bengio, Y., Courville, A., 2016. Deep Learning. MIT Press.

GoPenAI, 2023. Decision Tree Algorithm - What are Decision Trees. Written by the user: "Abdul4code". https://blog.gopenai.com/decision-tree-algorithm-484ec33387f9. Medium, Human, stories & ideas. URL (accessed 11.24.24).

Granata, F., Saroli, M., De Marinis, G., Gargano, R., 2018. Machine learning models for spring discharge forecasting. Geofluids, 2018, 8328167.

Graves, A., 2012. Supervised Sequence Labelling with Recurrent Neural Networks. Springer.

Grimaldi, S., Leone, D., Summa, G., 2008. Studio sui caratteri idrogeologici, idrogeochimici e quantitativi della principale sorgente del massiccio del M.te Pollino: Sorgente del Mercure (Basilicata, Italia Meridionale) [Hydrogeological, hydrogeochemical and quantitave features of the main spring of the mount Pollino massif: The Mercure Spring (Baslicata, Southern Italy)]. Rendiconti Online Societa Geologica Italiana, 3(2), 458-459.

Grönwall, J., Oduro-Kwarteng, S., 2018. Groundwater as a strategic resource for improved resilience: a case study from peri-urban Accra. Environmental Earth Sciences, 77, 1-13.

Gudmundsson, L., Bremnes, J.B., Haugen, J.E., Engen-Skaugen, T., 2012. Technical Note: Downscaling RCM precipitation to the station scale using statistical transformations – A comparison of methods. Hydrology and Earth System Sciences, 16(9), 3383-3390.

Hájek, M., Jiménez-Alfaro, B., Hájek, O., Brancaleoni, L., Cantonati, M., Carbognani, M., Dedić, A., Dítě, D., Gerdol, R., Hájková, P., Horsáková, V., Jansen, F., Kamberović, J., Kapfer, J., Kolari, T.H.M., Lamentowicz, M., Lazarević, P., Mašić, E., Moeslund, J.E., Pérez-Haase, A., Peterka, T., Petraglia, A., Pladevall-Izard, E., Plesková, Z., Segadelli, S., Semeniuk, Y., Singh, P., Šímová, A., Šmerdová, E., Tahvanainen, T., Tomaselli, M., Vystavna, Y., Biţă-Nicolae, C., Horsák, M., 2021. A European map of groundwater pH and calcium. Earth System Science, Data 13, 1089-1105.

Halder, S., Sahoo, S., Hazra, T., Debsarkar, A., 2024. Studies on Impacts of Land Use/Land Cover Changes on Groundwater Resources: A Critical Review. Environmental Science and Engineering, Part F2387, 143-170.

Halloran, L.J.S., Millwater, J., Hunkeler, D., Arnoux, M., 2023. Climate change impacts on groundwater discharge-dependent streamflow in an alpine headwater catchment. Science of the Total Environment, 902, 166009.

Hao, Y., Yeh, T., Hu, C., Wang, Y., Li, X., 2006. Karst groundwater management by defining protection zones based on regional geological structures and groundwater flow fields. Environmental Geology, 50, 415-422.

Hartigan, J.A., Wong, M.A., 1979. Algorithm AS 136: A K-Means Clustering Algorithm. Journal of the Royal Statistical Society. Series C (Applied Statistics), 28(1), 100-108.

Hartmann, A., Goldscheider, N., Wagener, T., Lange, J., Weiler, M., 2014. Karst water resources in a changing world: Review of hydrological modeling approaches. Reviews of Geophysics, 52, 218-242.

Hastie, T., Tibshirani, R., Friedman, J., 2009. The Elements of Statistical Learning: Data Mining, Inference, and Prediction. Springer.

Hayes, A.F., Matthes, J., 2009. Computational Procedures for Probing Interactions in OLS and Logistic Regression: SPSS and SAS Implementations. Behavior Research Methods, 41, 924-936.

Haylock, M.R., Cawley, G.C., Harpham, C., Wilby, R.L., Goodess, C.M., 2006. Downscaling heavy precipitation over the United Kingdom: A comparison of dynamical and statistical methods and their future scenarios. International Journal of Climatology, 26(10), 1397-1415.

Herrera-Franco, G., Carrión-Mero, P., Aguilar-Aguilar, M., Morante-Carballo, F., Jaya-Montalvo, M., Morillo-Balsera, M.C., 2020. Groundwater Resilience Assessment in a Communal Coastal Aquifer System. The Case of Manglaralto in Santa Elena, Ecuador. Sustainability, 12, 8290.

Hersbach, H., Bell, B., Berrisford, P., Hirahara, S., Horányi, A., Muñoz-Sabater, J., Nicolas, J., Peubey, C., Radu, R., Schepers, D., Simmons, A., Soci, C., Abdalla, S., Abellan, X., Balsamo, G., Bechtold, P., Biavati, G., Bidlot, J., Bonavita, M., De Chiara, G., Dahlgren, P., Dee, D., Diamantakis, M., Dragani, R., Flemming, J., Forbes, R., Fuentes, M., Geer, A., Haimberger, L., Healy, S., Hogan, R.J., Hólm, E., Janisková, M., Keeley, S., Laloyaux, P. Lopez, P., Lupu, C., Radnoti, G., de Rosnay, P., Rozum, I., Vamborg, F., Villaume, S., Thépaut, J.N., 2020. The ERA5 global reanalysis. Quarterly Journal of the Royal Meteorological Society, 146(730), 1999-2049.

Hochreiter, S., Schmidhuber, J., 1997. Long Short-Term Memory. Neural Computation, 9(8), 1735-1780.

Hornik, K., 1991. Approximation capabilities of multilayer feedforward networks. Neural Networks, 4(2), 251-257.

Hosmer, D.W., Lemeshow, S., Sturdivant, R.X., 2013. Applied Logistic Regression (3rd ed.). Wiley.

Il Manifesto, 2024. Siccità e condutture colabrodo, l'Abruzzo in emergenza idrica, [https://ilmanifesto.it/siccita-e-condutture-colabrodo-labruzzo-in-emergenza-idrica]. Serena Giannico, Il Manifesto, Chieti, 21 July 2024.

Il Messaggero, 2024. Emergenza idrica, sorgenti al collasso. Tavolo in Prefettura, [https://www.primopianomolise.it/attualita/136823/emergenza-idrica-sorgenti-al-collasso-tavolo-in-prefettura/]. 'Primo Piano Molise' in Il Manifesto, Campobasso, 10 July 2024.

IPCC, 2014. Climate Change 2014: Synthesis Report. Contribution of Working Groups I, II and III to the Fifth Assessment Report of the Intergovernmental Panel on Climate Change [Core Writing Team, R.K., Pachauri and L.A., Meyer (eds.)]. IPCC, Geneva, Switzerland, 151.

IPCC, 2023. Climate Change 2023: Synthesis Report. Contribution of Working Groups I, II and III to the Sixth Assessment Report of the Intergovernmental Panel on Climate Change [Core Writing Team, H. Lee and J. Romero (eds.)]. Geneva, Switzerland, 35-115.

ISPRA, 2020. Le risorse idriche nel contesto geologico del territorio italiano. Disponibilità, grandi dighe, rischi geologici, opportunità. Istituto Superiore per la Protezione e la Ricerca Ambientale, Rapporti 323/2020, ISBN 978-88-448-1011-5.

Istat, 2022. Le statistiche dell'Istat sull'acqua, anni 2019-2022. Statistiche Report, Istituto nazionale di STATistica, 21-3-22. https://www.istat.it/it/files/2022/03/REPORTACQUA2022.pdf.

Jain, A.K., 2010. Data clustering: 50 years beyond K-means. Pattern Recognition Letters, 31(8), 651-666.

James, G., Witten, D., Hastie, T., Tibshirani, R., 2013. An Introduction to Statistical Learning with Applications in R. Springer, Berlin, Germany.

Jeelani, G., 2008. Aquifer response to regional climate variability in a part of Kashmir Himalaya in India. Hydrogeology Journal, 16, 1625-1633.

Joigneaux, E., Albéric, P., Pauwels, H., Pagé, C., Terray, L., Bruand, A., 2011. Impact of climate change on groundwater point discharge: Backflooding of karstic springs (Loiret, France). Hydrology and Earth System Sciences, 5(8), 2459-2470.

Jordan, M.I., Bishop, C.M., 1996. Neural networks. In A. Tucker (Ed.), CRC Handbook of Computer Science CRC Press.

Kačaroğlu, F., 1999. Review of Groundwater Pollution and Protection in Karst Areas. Water, Air, Soil Pollution, 113, 337-356.

Kalhor, K., Ghasemizadeh, R., Rajic, L., Alshawabkeh, A., 2019. Assessment of groundwater quality and remediation in karst aquifers: A review. Groundwater for Sustainable Development, 8, 104-121.

Kayhomayoon, Z., Ghordoyee-Milan, S., Jaafari, A., Arya-Azar, N., Melesse, A.M., Kardan Moghaddam, H., 2022. How does a combination of numerical modeling, clustering, artificial intelligence, and evolutionary algorithms perform to predict regional groundwater levels? Computers and Electronics in Agriculture, 203, 107482.

Klaas, D.K.S.Y., Imteaz, M.A., Sudiayem, I., Klaas, E.M.E., Klaas, E.C.M., 2019. Coping with climate change in a tropical karst island: Assessment of groundwater resources under HadCM3-GCM scenarios and proposed adaptive strategies. Earth and Environmental Science, 239, 1-6.

Kottek, M., Grieser, J., Beck, C., Rudolf, B., Rubel, F., 2006. World map of the Köppen-Geiger climate classification updated. Meteorologische Zeitschrift, 15(3), 259-263.

Kovačič, G., Petrič, M., Ravbar, N., 2020. Evaluation and quantification of the effects of climate and vegetation cover change on karst water sources: case studies of two springs in South-Western Slovenia. Water (Switzerland), 12(11), 1-20.

Kovács, A., Stevanović, Z., 2023. A Combined Stochastic-Analytical Method for the Assessment of Climate Change Impact on Spring Discharge. Water (Switzerland), 15(4), 629.

Kresic, N., Stevanovic, Z., 2010. Groundwater hydrology of springs: engineering, theory, management, and sustainability. Butterworth-Heinemann, Oxford, UK.

Kruse, E., Eslamian, S., 2017. Groundwater management in drought conditions. Handbook of Drought and Water Scarcity, Management of Drought and Water Scarcity, 3, 275-282.

Kundzewicz, Z.W., Döll, P., 2009. Will groundwater ease freshwater stress under climate change? Hydrological Sciences Journal, 54, 665-675.

Kutner, M.H., Nachtsheim, C.J., Neter, J., Li, W., 2005. Applied Linear Statistical Models - Fifth Edition. McGraw-Hill/Irwin, New York City, United States of America.

Lachassagne, P., 2008. Overview of the Hydrogeology of Hard Rock Aquifers: Applications for their Survey, Management, Modelling and Protection, in: Ahmed, S., Jayakumar, R., Salih, A. (Eds.), Groundwater Dynamics in Hard Rock Aquifers: Sustainable Management and Optimal Monitoring Network Design. Springer Netherlands, Dordrecht, 40-63.

Lachassagne, P., Wyns, R., Dewandel, B., 2011. The fracture permeability of Hard Rock Aquifers is due neither to tectonics, nor to unloading, but to weathering processes. Terra Nova, 23, 145-161.

Lambrakis, N., Andreou, A.S., Polydoropoulos, P., Georgopoulos, E., Bountis, T., 2000. Nonlinear analysis and forecasting of a brackish karstic spring. Water Resources Research, 36(4), 875-884.

LeCun, Y., Bottou, L., Bengio, Y., Haffner, P., 1998. Gradient-based learning applied to document recognition. Proceedings of the IEEE, 86(11), 2278-2324.

LeCun, Y., Bengio, Y., Hinton, G.E., 2015. Deep learning. Nature, 521(7553), 436-444.

Leone, G., Pagnozzi, M., Catani, V., Ventafridda, G., Esposito, L., Fiorillo, F., 2021. A hundred years of Sanità Spring discharge measurements: trends and statistics for understanding water resource availability under climate change. Stochastic Environmental Research and Risk Assessment, 35(2), 345-370.

Liesch, T., Wunsch, A., 2019. Aquifer responses to long-term climatic periodicities. Journal of Hydrology, 572, 226-242.

Livezey, R.E., Vinnikov, K.Y., Timofeyeva, M.M., Tinker, R., van den Dool, H.M., 2007. Estimation and extrapolation of climate normals and climatic trends. Journal of Applied Meteorology and Climatology, 46(11), 1759-1776.

Loh, W.Y., 2011. Classification and regression trees. Wiley Interdisciplinary Reviews: Data Mining and Knowledge Discovery, 1(1), 14-23.

Lucci, P., Rossi, A., 2011. Speleologia e geositi carsici in Emilia-Romagna (Speleology and karst sites in the Emilia Romagna Region). In Italian. Federazione Speleologica Regionale dell'Emilia Romagna.

MacDonald, A., Bonsor, H., Calow, R., Taylor, R., Lapworth, D., Maurice, L., Tucker, J., O Dochartaigh, B., 2011. Groundwater resilience to climate change in Africa.

MacQueen, J., 1967. Some methods for classification and analysis of multivariate observations. Proceedings of the Fifth Berkeley Symposium on Mathematical Statistics and Probability, 1(14), 281-297.

Magi, F., Doveri, M., Menichini, M., Minissale, A., Vaselli, O., 2019. Groundwater response to local climate variability: hydrogeological and isotopic evidences from the Mt. Amiata volcanic aquifer (Tuscany, central Italy). Rendiconti Lincei, 30(1), 125-136.

Maillet, E.T., 1905. Essais d'hydraulique souterraine & fluviale. A. Hermann, Paris.

Mariani, G.S., Zerboni, A., 2020. Surface Geomorphological Features of Deep-Seated Gravitational Slope Deformations: A Look to the Role of Lithostructure (N Apennines, Italy). Geosciences, 10, 334.

Marroni, M., Monechi, S., Perilli, N., Principi, G., Treves, B., 1992. Late Cretaceous flysch deposits of the Northern Apennines, Italy: age of inception of orogenesis-controlled sedimentation. Cretaceous Research, 13(5-6), 487-504.

Medici, G., Lorenzi, V., Sbarbati, C., Manetta, M., Petitta, M., 2023. Structural Classification, Discharge Statistics, and Recession Analysis from the Springs of the Gran Sasso (Italy) Carbonate Aquifer; Comparison with Selected Analogues Worldwide. Sustainability, 15, 10125.

Meinzer, O.E., 1923. Outline of groundwater hydrology with definitions. In: US Geological Survey Water-Supply Paper. 494, 48-54.

Mekis, É., Brown, R., 2010. Derivation of an adjustment factor map for the estimation of the water equivalent of snowfall from ruler measurements in Canada. Atmosphere - Ocean, 48(4), 284-293.

Menard, S., 2002. Applied Logistic Regression Analysis (2nd ed.). Sage.

Mewes, B., Oppel, H., Marx, V., Hartmann, A., 2020. Information-Based Machine Learning for Tracer Signature Prediction in Karstic Environments. Water Resources Research, 56(2), e2018WR024558.

Mézquita González, J.A., Comte, J.-C., Legchenko, A., Ofterdinger, U., Healy, D., 2021. Quantification of groundwater storage heterogeneity in weathered/fractured basement rock aquifers using electrical resistivity tomography: Sensitivity and uncertainty associated with petrophysical modelling. Journal of Hydrology, 593, 125637.

Mikhaylov, S.J., Esteve, M., Campion, A., 2018. Artificial intelligence for the public sector: opportunities and challenges of cross-sector collaboration. Philosophical Transactions of the Royal Society. A, 376:20170357.

Mikolov, T., Karafiát, M., Burget, L., Černocký, J., Khudanpur, S., 2010. Recurrent neural network-based language model. Interspeech, 2, 1045-1048.

Mimi, Z.A., Assi, A., 2009. Intrinsic vulnerability, hazard and risk mapping for karst aquifers: A case study. Journal of Hydrology, 364, 298-310.

Mirgol, B., Dieppois, B., Northey, J., Eden, J., Jarlan, L., Khabba, S., Le Page, M., Mahe, G., 2024. Future changes in agrometeorological extremes in the southern Mediterranean region: When and where will they affect croplands and wheatlands? Agricultural and Forest Meteorology, 358, 110232.

Molli, G., 2008. Northern Apennine-Corsica orogenic system: An updated overview. Geological Society Special Publication, 298, 413-442.

Montgomery, D.C., Jennings, C.L., Kulahci, M., 2008. Introduction to Time Series Analysis and Forecasting. John Wiley & Sons, Inc., Hoboken, United States of America.

Murphy, K.P., 2012. Machine Learning: A Probabilistic Perspective. MIT Press.

Nanni, T., Rusi, S., 2003. Idrogeologia del massiccio carbonatico della montagna della Majella (Appennino centrale) [Hydrogeology of the Montagna della Majella carbonate massif (Central Apennines - Italy)]. Bollettino della Società Geologica Italiana, 122, 173-202.

Navarra, A., Philander, G., 2016. Weathering global climate change. World Scientific Series on Asia-Pacific Weather and Climate, 7, 305-312.

Nicholson, K.N., Neumann, K., Dowling, C., Gruver, J., Sherman, H., Sharma, S., 2018. An Assessment of Drinking Water Sources in Sagarmatha National Park (Mt Everest Region), Nepal. Mountain research and development, 38(4), 353-363.

Niraula, R.R., Sharma, S., Pokharel, B.K., Paudel, U., 2021. Spatial prediction of spring locations in data poor region of Central Himalayas. Hydrology Research, 52(2), 492-505.

Oksana, T., Dmytro, G., 2021. Earth's Water Distribution. In: Leal Filho, W., Azul, A.M., Brandli, L., Lange Salvia, A., Wall, T. (Eds), Clean Water and Sanitation. Encyclopedia of the UN Sustainable Development Goals. Springer, Cham, Switzerland.

Opoku, P.A., Shu, L., Ansah-Narh, T., Kwaw, A.K., Niu, S., 2024. Prediction of karst spring discharge using LSTM with Bayesian optimisation hyperparameter tuning: A laboratory physical model approach. Modelling Earth Systems and Environment, 10(1), 1457-1482.

Pagnozzi, M., Fiorillo, F., Esposito, L., Leone, G., 2019. Hydrological features of endorheic areas in southern Italy. Italian Journal of Engineering Geology and Environment, Special Issue 1, 85-91.

Parco Vivo, 2019. Sorgenti del Monte Amiata, [https://www.parcovivo.it/sorgenti-del-monte-amiata/]. Cooperativa di Comunità Parco Vivo. URL (accessed 12.06.23).

Pasuto, A., Soldati, M., 2013. 7.25 Lateral Spreading, in: Shroder, J.F. (Ed.), Treatise on Geomorphology. Academic Press, San Diego, 239-248.

Pasuto, A., Soldati, M., Tecca, P.R., 2022. 5.10 - Lateral Spread: From Rock to Soil Spreading, in: Shroder, J.F. (Ed.), Treatise on Geomorphology (Second Edition). Academic Press, Oxford, 169-182.

Patacca, E., Sartori, R., Scandone, P., 1993. Tyrrhenian Basin and Apennines. Kinematic evolution and related dynamic constraints. Recent evolution and seismicity of the Mediterranean region, 161-171.

Patacca, E., Scandone, P., 2007. Geology of the Southern Apennines. Bollettino della Società Geologica Italiana, Supplemento, 7, 75-119.

Pekel, J.-F., Cottam, A., Gorelick, N., Belward, A.S., 2016. High-resolution mapping of global surface water and its long-term changes. Nature, 540(7633), 418-422.

Peña-Angulo, D., Vicente-Serrano, S.M., Domínguez-Castro, F., Lorenzo-Lacruz, J., Murphy, C., Hannaford, J., Allan, R.P., Tramblay, Y., Reig-Gracia, F., El Kenawy, A., 2022. The Complex and Spatially Diverse Patterns of Hydrological Droughts Across Europe. Water Resources Research, 58, e2022WR031976.

Petitta, M., Tallini, M., 2002. Groundwater hydrodinamic of the Gran Sasso Massif (Abruzzi): New hydrological, hydrogeological and hydrochemical surveys (1994-2001). Bollettino della Societa Geologica Italiana, 121(3), 343-363.

Petitta, M., Banzato, F., Lorenzi, V., Matani, E., Sbarbati, C., 2022. Determining recharge distribution in fractured carbonate aquifers in central Italy using environmental isotopes: snowpack cover as an indicator for future availability of groundwater resources. Hydrogeology Journal, 30(5), 1619-1636.

Petronici, F., Pujades, E., Jurado, A., Marcaccio, M., Borgatti, L., 2019. Numerical modelling of the Mulino Delle Vene Aquifer (Northern Italy) as a tool for predicting the hydrogeological system behavior under different recharge conditions. Water (Switzerland), 11(12), 2505.

Piotrowska, J., Dąbrowska, D., 2024. Artificial intelligence methods in water systems research – a literature review. Geological Quarterly, 68(2), 68-19.

Polemio, M., Casarano, D., 2008. Climate change, drought and groundwater availability in southern Italy. Geological Society Special Publication, 288, 39-51.

Pölz, A., Blaschke, A.P., Komma, J., Farnleitner, A.H., Derx, J., 2024. Transformer Versus LSTM: A Comparison of Deep Learning Models for Karst Spring Discharge Forecasting. Water Resources Research, 60(4), e2022WR032602.

Portoghese, I., Bruno, E., Dumas, P., Guyennon, N., Hallegatte, S., Hourcade, J.-C. Nassopoulos, H., Pisacane, G., Struglia, M.V., Vurro, M., 2013. Impacts of Climate Change on Freshwater Bodies: Quantitative Aspects. In: Navarra, A., Tubiana, L. (eds) Regional Assessment of Climate Change in the Mediterranean. Advances in Global Change Research, vol 50. Springer, Dordrecht, Netherlands.

Quinlan, J.R., 1986. Induction of decision trees. Machine Learning, 1(1), 81-106.

Raffa, M., Reder, A., Marras, G.F., Mancini, M., Scipione, G., Santini, M., Mercogliano, P., 2021. VHR-REA_IT dataset: Very high resolution dynamical downscaling of ERA5 reanalysis over Italy by COSMO-CLM. Data, 6(8), 88.

Raffa, M., Adinolfi, M., Reder, A., Marras, G.F., Mancini, M., Scipione, G., Santini, M., Mercogliano, P., 2023. Very High Resolution Projections over Italy under different CMIP5 IPCC scenarios. Scientific Data, 10(1), 238.

Rakovec, O., Samaniego, L., Hari, V., Markonis, Y., Moravec, V., Thober, S., Hanel, M., Kumar, R., 2022. The 2018-2020 Multi-Year Drought Sets a New Benchmark in Europe. Earth's Future, 10, e2021EF002394.

Ram, R., Burg, A., Zappala, J.C., Yokochi, R., Yechieli, Y., Purtschert, R., Jiang, W., Lu, Z.-T., Mueller, P., Bernier, R., Adar, E.M., 2020. Identifying recharge processes into a vast “fossil” aquifer based on dynamic groundwater 81Kr age evolution. Journal of Hydrology, 587, 124946.

Riedel, T., Weber, T.K.D., 2020. Review: The influence of global change on Europe’s water cycle and groundwater recharge. Hydrogeology Journal, 28, 1939-1959.

Rosenberg, N.J., Epstein, D.J., Wang, D., Vail, L., Srinivasan, R., Arnold, J.G., 1999. Possible impacts of global warming on the hydrology of the Ogallala aquifer region. Climatic Change, 42(4), 677-692.

Rosenblatt, F., 1958. The Perceptron: A Probabilistic Model for Information Storage and Organization in the Brain. Psychological Review, 65(6), 386-408.

Rotiroti, M., Sacchi, E., Caschetto, M., Zanotti, C., Fumagalli, L., Biasibetti, M., Bonomi, T., Leoni, B., 2023. Groundwater and surface water nitrate pollution in an intensively irrigated system: Sources, dynamics and adaptation to climate change. Journal of Hydrology, 623, 129868.

Rumelhart, D.E., Hinton, G.E., Williams, R.J., 1986. Learning representations by back-propagating errors. Nature, 323(6088), 533-536.

Sahour, H., Sultan, M., Abdellatif, B., Emil, M., Abotalib, Z., Abdelmohsen, K., Vazifedan, M., Mohammad, A.T., Hassan, S.M., Metwalli, M.R., El Bastawesy, M., 2022. Identification of shallow groundwater in arid lands using multi-sensor remote sensing data and machine learning algorithms. Journal of Hydrology, 614, 128509.

Salvini, F., Billi, A., Wise, D.U., 1999. Strike-slip fault-propagation cleavage in carbonate rocks: the Mattinata Fault Zone, Southern Apennines, Italy. Journal of Structural Geology, 21, 1731-1749.

Samuel, A.L., 1959. Some Studies in Machine Learning Using the Game of Checkers. IBM Journal of Research and Development, 3(3), 210-229.

Sánchez, D., Barberá, J.A., Mudarra, M., Andreo, B., 2015. Hydrogeochemical tools applied to the study of carbonate aquifers: examples from some karst systems of Southern Spain. Environmental Earth Sciences, 74, 199-215.

Sappa, G., Ferranti, F., Iacurto, S., De Filippi, F.M., 2018. Effects of climate change on groundwater feeding the Mazzoccolo and Capodacqua di Spigno Springs (Central Italy): First quantitative assessments. International Multidisciplinary Scientific GeoConference Surveying Geology and Mining Ecology Management, SGEM, 18(3.1), 219-226.

Sappa, G., De Filippi, F.M., Ferranti, F., Iacurto, S., 2019. Environmental issues and anthropic pressures in coastal aquifers: A case study in Southern Latium Region. Acque Sotterranee - Italian Journal of Groundwater, 8, 47-51.

Scanlon, B.R., Faunt, C.C., Longuevergne, L., Reedy, R.C., Alley, W.M., McGuire, V.L., McMahon, P.B., 2012. Groundwater depletion and sustainability of irrigation in the US High Plains and Central Valley. Proceedings of the National Academy of Sciences of the United States of America, 109(24), 9320-9325.

Schölkopf, B., Smola, A.J., 2002. Learning with kernels: Support vector machines, regularization, optimization, and beyond. MIT press.

Scoccimarro, E., Navarra, A., 2022. Precipitation and temperature extremes in a changing climate. Hydrometeorological Extreme Events and Public Health, Chapter 2, 3-25. John Wiley & Sons, Inc., New York, United States of America.

Seabold, S., Perktold, J., 2010. Statsmodels: Econometric and Modeling with Python. Proceedings of the 9th Python in Science Conference, Austin (United States of America), 28 June-3 July, 2010, 57-61.

Seber, G.A.F., Lee, A.J., 2012. Linear Regression Analysis. John Wiley & Sons.

Secci, D., Tanda, M.G., D'Oria, M., Todaro, V., Fagandini, C., 2021. Impacts of climate change on groundwater droughts by means of standardized indices and regional climate models. Journal of Hydrology, 603, 127154.

Secci, D., Tanda, M.G., D'Oria, M., Todaro, V., 2023. Artificial intelligence models to evaluate the impact of climate change on groundwater resources. Journal of Hydrology, 627, 130359, ISSN 0022-1694.

Segadelli, S., Filippini, M., Monti, A., Celico, F., Gargini, A., 2021. Estimation of recharge in mountain hard-rock aquifers based on discrete spring discharge monitoring during base-flow recession. Hydrogeology Journal, 29, 949-961.

Segadelli, S., Vescovi, P., Ogata, K., Chelli, A., Zanini, A., Boschetti, T., Petrella, E., Toscani, L., Gargini, A., Celico, F., 2017. A conceptual hydrogeological model of ophiolitic aquifers (serpentinised peridotite): The test example of Mt. Prinzera (Northern Italy). Hydrological Processes, 31, 1058-1073.

Shahgedanova, M., Adler, C., Gebrekirstos, A., Grau, H.R., Huggel, C., Marchant, R., Pepin, N., Vanacker, V., Viviroli, D., Vuille, M., 2020. Emptying Water Towers? Impacts of Future Climate and Glacier Change on River Discharge in the Northern Tien Shan, Central Asia. Mountain Research and Development, 41(2), 1-15.

Sharma, U.C., Sharma, V., 2006. Groundwater sustainability indicators for the Brahmaputra basin in the northeastern region of India. IAHS-AISH publication, 43-50.

Shepherd, A., Gill, K.M., Rood, S.B., 2010. Climate change and future flows of Rocky Mountain rivers: Converging forecasts from empirical trend projection and down-scaled global circulation modelling. Hydrological Processes, 24(26), 3864-3877.

Simsek, C., Elci, A., Gunduz, O., Erdogan, B., 2008. Hydrogeological and hydrogeochemical characterization of a karstic mountain region. Environmental Geology, 54, 291-308.

Sivelle, V., Jourde, H., Bittner, D., Mazzilli, N., Tramblay, Y., 2021. Assessment of the relative impacts of climate changes and anthropogenic forcing on spring discharge of a Mediterranean karst system. Journal of Hydrology, 598, 126396, ISSN 0022-1694.

Small, C., Nicholls, R.J., 2003. A global analysis of human settlement in coastal zones. Journal of Coastal Research, 19, 584-599.

Smiatek, G., Kaspar, S., Kunstmann, H., 2013. Hydrological climate change impact analysis for the Figeh spring near Damascus, Syria. Journal of Hydrometeorology, 14(2), 577-593.

Soleimani Motlagh, M., Ghasemieh, H., Talebi, A., Abdollahi, K., 2017. Identification and Analysis of Drought Propagation of Groundwater During Past and Future Periods. Water Resources Management, 31(1), 109-125.

Song, X., Hao, H., Liu, W., Wang, Q., An, L., Jim Yeh, T.-C., Hao, Y., 2022. Spatial-temporal behavior of precipitation driven karst spring discharge in a mountain terrain. Journal of Hydrology, 612, 128116.

Stendardi, F., Viola, G., Vignaroli, G., 2023. Multiscale structural analysis of an Epiligurian wedge-top basin: insights into the syn- to post-orogenic evolution of the Northern Apennines accretionary wedge (Italy). International Journal of Earth Sciences, 112, 805-827.

Stevenazzi, S., Zuffetti, C., Camera, C.A.S., Lucchelli, A., Beretta, G.P., Bersezio, R., Masetti, M., 2023. Hydrogeological characteristics and water availability in the mountainous aquifer systems of Italian Central Alps: A regional scale approach. Journal of Environmental Management, 340, 117958.

Stevens, L.E., Aly, A.A., Arpin, S.M., Apostolova, I., Ashley, G.M., Barba, P.Q., Barquín, J., Beauger, A., Benaabidate, L., Bhat, S.U., Bouchaou, L., Cantonati, M., Carroll, T.M., Death, R., Dwire, K.A., Felippe, M.F., Fensham, R.J., Fryar, A.E., Garsaball, R.P.i., Gjoni, V., Glazier, D.S., Goldscheider, N., Gurrieri, J.T., Guðmundsdóttir, R., Guzman, A.R., Hájek, M., Hassel, K., Heartsill-Scalley, T., Herce, J.S.i., Hinterlang, D., Holway, J.H., Ilmonen, J., Jenness, J., Kapfer, J., Karaouzas, I., Knight, R.L., Kreiling, A.-K., Lameli, C.H., Ledbetter, J.D., Levine, N., Lyons, M.D., Mace, R.E., Mentzafou, A., Marle, P., Moosdorf, N., Norton, M.K., Pentecost, A., Pérez, G.G., Perla, B., Saber, A.A., Sada, D., Segadelli, S., Skaalsveen, K., Springer, A.E., Swanson, S.K., Schwartz, B.F., Sprouse, P., Tekere, M., Tobin, B.W., Tshibalo, E.A., Voldoire, O., 2022. The Ecological Integrity of Spring Ecosystems: A Global Review, in: DellaSala, D.A., Goldstein, M.I. (Eds.), Imperiled: The Encyclopedia of Conservation. Elsevier, Oxford, 436-451.

Stone, A., Lanzoni, M., Smedley, P., 2019. Groundwater resources: past, present, and future. In: Dadson, S.J., Garrick, D.E., Penning-Rowsell, E.C., Hall, J.W., Hope, R., Hughes, J. (Eds.), Water Science, Policy, and Management: A Global Challenge, 29-54. John Wiley & Sons, Inc., New York, United States of America.

Sultan, M., Sturchio, N.C., Alsefry, S., Emil, M.K., Ahmed, M., Abdelmohsen, K., AbuAbdullah, M.M., Yan, E., Save, H., Alharbi, T., Othman, A., Chouinard, K., 2019. Assessment of age, origin, and sustainability of fossil aquifers: A geochemical and remote sensing-based approach. Journal of Hydrology, 576, 325-341.

Sun, T.Q., Medaglia, R., 2019. Mapping the challenges of Artificial Intelligence in the public sector: Evidence from public healthcare. Government Information Quarterly, 36(2), 368-383.

Sutskever, I., Vinyals, O., Le, Q.V., 2014. Sequence to sequence learning with neural networks. Advances in Neural Information Processing Systems, 27, 3104-3112.

Tague, C., Grant, G.E., 2004. A geological framework for interpreting the low-flow regimes of Cascade streams, Willamette River Basin, Oregon. Water Resources Research, 40.

Tallaksen, L.M., 1995. A review of baseflow recession analysis. Journal of Hydrology, 165, 349-370.

Tambe, S., Kharel, G., Arrawatia, M.L., Kulkarni, H., Mahamuni, K., Ganeriwala, A.K., 2012. Reviving Dying Springs: Climate Change Adaptation Experiments From the Sikkim Himalaya. Mountain Research and Development, 32, 62-72, 11.

Tarek, M., Brissette, F.P., Arsenault, R., 2020. Evaluation of the ERA5 reanalysis as a potential reference dataset for hydrological modelling over North America. Hydrology and Earth System Sciences, 24(5), 2527-2544.

Tarquini, S., Isola, I., Favalli, M., Battistini, A., Dotta, G., 2023. TINITALY, a digital elevation model of Italy with a 10 meters cell size (Version 1.1). Istituto Nazionale di Geofisica e Vulcanologia - National Institute of Geophysics and Volcanology (INGV), [https://tinitaly.pi.ingv.it/Download_Area1_1.html].

Taylor, R.G., Scanlon, B., Döll, P., Rodell, M., Van Beek, R., Wada, Y., Longuevergne, L., Leblanc, M., Famiglietti, J.S., Edmunds, M., Konikow, L., Green, T.R., Chen, J., Taniguchi, M., Bierkens, M.F.P., Macdonald, A., Fan, Y., Maxwell, R.M., Yechieli, Y., Gurdak, J.J., Allen, D.M., Shamsudduha, M., Hiscock, K., Yeh, P.J.-F., Holman, I., Treidel, H., 2013. Ground water and climate change. Nature Climate Change, 3(4), 322-329.

Tazioli, A., Colombani, N., Palpacelli, S., Mastrocicco, M., Nanni, T., 2020. Monitoring and modelling interactions between the montagna dei fiori aquifer and the castellano stream (Central Apennines, Italy). Water (Switzerland), 12(4), 973.

Thornthwaite, C., Mather, J., 1957. Instructions and tables for computing potential evapotranspiration and the water balance, publications in climatology 10/3. Centerton: Drexel Institute of Technology.

Todaro, V., D'Oria, M., Secci, D., Zanini, A., Tanda, M.G., 2022. Climate Change over the Mediterranean Region: Local Temperature and Precipitation Variations at Five Pilot Sites. Water (Switzerland), 14, 2499.

Tóth, Á., Kovács, S., Kovács, J., Mádl-Szőnyi, J., 2022. Springs regarded as hydraulic features and interpreted in the context of basin-scale groundwater flow. Journal of Hydrology, 610, 127907.

Tozzi, M., De Corso, S., Antonucci, A., Di Luzio, E., Lenci, F., Scrocca, D., 1999. Assetto geologico della Montagnola di Frosolone. Geologica Romana, 35, 89-109.

Trenberth, K.E., Dai, A., Rasmussen, R.M., Parsons, D.B., 2003. The changing character of precipitation. Bulletin of the American Meteorological Society, 84(9), 1205-1217+1161.

Troll, C., Paffen, K.H., 1963. Jahreszeitenklimate der Erde. In: Rodenwaldt, E., Jusak, H.J. (Hrsg): Weltkarten zur Klimakunde, 7-28, Berlin.

Tsur, Y., 1990. The stabilization role of groundwater when surface water supplies are uncertain: The implications for groundwater development. Water Resources Research, 26, 811-818.

UniBo and RER for Gruppo Hera, 2023. Progettazione idrogeologica, basata su indagini in situ, monitoraggio e modellazione numerica, di scenari di ottimizzazione/potenziamento della captazione di acque sotterranee nei punti di prelievo hera di Tolè (Comune di Vergato) e Arpolli (Comuni di Gaggio Montano e Montese) e di analisi della vulnerabilità idrogeologica del sistema sorgentizio Acquaretto-Vergatello (Comune di Castel d'Aiano). Final Report by UniBo and RER (Regione Emilia-Romagna) for the Scientific Collaboration with Gruppo Hera, authored by: Gargini, A., Filippini, M., Landi, L., Casati, T., Segadelli, S., 31 January 2023.

Vai, G.B., Martini, I.P., 2001. Anatomy of an Orogen: the Apennines and Adjacent Mediterranean Basins.

Van Loon, A.F., Tijdeman, E., Wanders, N., Van Lanen, H.A.J., Teuling, A.J., Uijlenhoet, R., 2014. How climate seasonality modifies drought duration and deficit. Journal of Geophysical Research, 119(8), 4640-4656.

Van Vuuren, D.P., Edmonds, J., Kainuma, M., Riahi, K., Thomson, A., Hibbard, K., Hurtt, G.C., Kram, T., Krey, V., Lamarque, J.-F., Masui, T., Meinshausen, M., Nakicenovic, N., Smith, S.J., Rose, S.K., 2011. The representative concentration pathways: an overview. Climate Change, 109(1), 5-31.

Vecchi, A., 1920. La sorgente di Rosola e la sua derivazione per l'acquedotto modenese (the Rosola spring and its uptake for the Modena aqueduct). In: Italian, Giornale del Genio Civile. Genio Civile, Rome.

Vincenzi, V., Gargini, A., Goldscheider, N., Piccinini, L., 2014. Differential hydrogeological effects of draining tunnels through the northern Apennines, Italy. Rock Mechanics and Rock Engineering, 47, 947-965.

Wada, Y., 2016. Modeling Groundwater Depletion at Regional and Global Scales: Present State and Future Prospects. Surveys in Geophysics, 37, 419-451.

Weissinger, R., Philippi, T.E., Thoma, D., 2016. Linking climate to changing discharge at springs in Arches National Park, Utah, USA. Ecosphere, 7, e01491.

Wijayanti, P., Dalmadi, R., 2021. Hydrogeochemical and groundwater aggressiveness assessment in the epikarst aquifer: a spatial and temporal analysis. IOP Conference Series: Earth and Environmental Science, 683, 012141.

Worthington, S.R.H., Ford, D.C., 2009. Self-Organized Permeability in Carbonate Aquifers. Groundwater, 47, 326-336.

Wunsch, A., Liesch, T., Cinkus, G., Ravbar, N., Chen, Z., Mazzilli, N., Jourde, H., Goldscheider, N., 2022. Karst spring discharge modeling based on deep learning using spatially distributed input data. Hydrology and Earth System Sciences, 26(9), 2405-2430.

Xanke, J., Liesch, T., 2022. Quantification and possible causes of declining groundwater resources in the Euro-Mediterranean region from 2003 to 2020. Hydrogeology Journal, 30, 379-400.

Yu, K.-X., Qin, Y., Zhang, X., Hu, J., Sun, Q., 2019. Peak break-up water level and discharge forecast in the Inner Mongolia Reach of the Yellow River based on a binary logistic regression model. Taiwan Water Conservancy, 66(4), 9-17.

Yusoff, I., Hiscock, K.M., Conway, D., 2002. Simulation of the impacts of climate change on groundwater resources in eastern England. Geological Society Special Publication, 193, 325-344.

Zeydalinejad, N., 2023. An overview of the methods for evaluating the resilience of groundwater systems. MethodsX, 10, 102134.

Zhang, W., Duan, L., Liu, T., Shi, Z., Shi, X., Chang, Y., Qu, S., Wang, G., 2024. A hybrid framework based on LSTM for predicting karst spring discharge using historical data. Journal of Hydrology, 633, 130946.

Zhong, Y., Hao, Y., Huo, X., Zhang, M., Duan, Q., Fan, Y., Liu, Y., Liu, Y., Yeh, T.J., 2016. A statistical model for karst spring discharge estimation under extensive groundwater development and extreme climate change. Hydrological Sciences Journal, 61(11), 2011-2023.

Zhou, R., Zhang, Y., 2022. On the role of the architecture for spring discharge prediction with deep learning approaches. Hydrological Processes, 36(10), e14737.

Zhou, R., Zhang, Y., 2023. Linear and nonlinear ensemble deep learning models for karst spring discharge forecasting. Journal of Hydrology, 627, 130394.

Zhou, R., Zhang, Y., Wang, Q., Jin, A., Shi, W., 2024. A hybrid self-adaptive DWT-WaveNet-LSTM deep learning architecture for karst spring forecasting. Journal of Hydrology, 634, 131128.

Zhu, R., Zheng, H., Croke, B.F.W., Jakeman, A.J., 2020. Quantifying climate contributions to changes in groundwater discharge for headwater catchments in a major Australian basin. Science of the Total Environment, 729, 138910.

Acknowledgments

At the end of this journey, I would like to take a moment to thank all the people who made it possible by supporting and encouraging me whenever I needed it.

Firstly, I would like to thank Dr. Ehsan Kamali Maskooni, who had originally secured this PhD research spot. Without his decision to decline the doctoral position, I wouldn't be writing these acknowledgements today — sometimes, coming second is all it takes. I would then like to thank my main supervisor, Alessandro Gargini, who (almost) always believed in me, from the day Ehsan stepped down onwards, of course. Jokes aside, Alessandro has been a constant source of unwavering support throughout these years, both within and beyond the University, helping me through difficult moments and encouraging me not to give up. I would also like to extend my gratitude to my two co-supervisors, Maria Filippini and Antonio Navarra, who, during my PhD journey, always provided stimulating and constructive ideas and discussions. The support and guidance of these three mentors allowed me to learn, grow, and transform what could have been merely a "job" into a genuine passion.

I would also like to express my heartfelt thanks to my friends and research colleagues Nicola, Laura, Matteo, Ernesto, Alessandro, and Rodolfo for the memorable moments we shared both within and beyond the University.

I wish to extend my sincere gratitude to Abramo, the university's porter, who greeted me with a smile every morning and was always available and willing to help.

Furthermore, I am grateful to Nico Goldscheider, who supervised me during my research period in Karlsruhe, for his invaluable guidance and warm hospitality. I would also like to thank Yanina, Mohammad, Julia, and Jiawen, who, during my time abroad, ensured I never felt alone.

Outside the academic world, I am deeply thankful to my girlfriend, Matilde, who has been and continues to be my haven, for her unfailing support in my decision to undertake this journey and throughout both the easier and more challenging moments.

I would like to thank my parents, Marco and Costanza, and my brother Andrea, for their lifelong guidance and support, and for always believing in me. I am also grateful to my grandmother, Maria Pia, and to all the relatives from both my family and Matilde's who have supported me along the way. A special thank you goes to my wonderful sister-in-law, Ylenia, and to my newborn niece, Vittoria, who has brought immense joy into our lives.

Last but not least, I want to thank my "TuttaLaNotte" and "Irriducibili" friends from Scarperia for always backing and motivating me, even though they never, or almost never, had any idea what I was actually doing for my PhD.

Borsa di dottorato del Programma Operativo Nazionale Ricerca e Innovazione 2014-2020 (CCI 2014IT16M2OP005), risorse FSE REACT-EU, Azione IV.4 "Dottorati e contratti di ricerca su tematiche dell'innovazione" e Azione IV.5 "Dottorati su tematiche Green. CUP: J35F21003370006